

NASA TECHNICAL NOTE



NASA TN D-6617

c.1



LOAN COPY: RE
AFWL (DO
KIRTLAND AFI

NASA TN D-6617

ELECTROSTATIC-PROBE MEASUREMENTS
OF PLASMA PARAMETERS FOR
TWO REENTRY FLIGHT EXPERIMENTS
AT 25 000 FEET PER SECOND

by W. Linwood Jones, Jr., and Aubrey E. Cross
Langley Research Center
Hampton, Va. 23365





0133161

1. Report No. NASA TN D-6617	2. Government Accession No.	3. Recipient's Catalog No.	
4. Title and Subtitle ELECTROSTATIC-PROBE MEASUREMENTS OF PLASMA PARAMETERS FOR TWO REENTRY FLIGHT EXPERIMENTS AT 25 000 FEET PER SECOND		5. Report Date February 1972	
		6. Performing Organization Code	
7. Author(s) W. Linwood Jones, Jr., and Aubrey E. Cross		8. Performing Organization Report No. L-7984	
9. Performing Organization Name and Address NASA Langley Research Center Hampton, Va. 23365		10. Work Unit No. 115-21-01-01	
		11. Contract or Grant No.	
12. Sponsoring Agency Name and Address National Aeronautics and Space Administration Washington, D.C. 20546		13. Type of Report and Period Covered Technical Note	
		14. Sponsoring Agency Code	
15. Supplementary Notes With appendix B by Lorraine F. Satchell and appendix C by William L. Weaver. Part of the information presented herein was included in a dissertation, "Probe Measurements of Electron Density Profiles During a Blunt-Body Reentry" by W. Linwood Jones, Jr., presented in partial fulfillment of the requirements for the degree of Doctor of Philosophy in Electrical Engineering, Virginia Polytechnic Institute and State University, Blacksburg, Virginia, June 1971.			
16. Abstract Unique plasma diagnostic measurements at high altitudes from two geometrically similar blunt-body reentry spacecraft using electrostatic probe rakes are presented. The probes measured the positive-ion density profiles (shape and magnitude) during the two flights. The probe measurements were made at eight discrete points (1 cm to 7 cm) from the vehicle surface in the aft flow field of the spacecraft over the altitude range of 85.3 to 53.3 km (280 000 to 175 000 ft) with measured densities of 10^8 to 10^{12} electrons/cm ³ , respectively. Maximum reentry velocity for each spacecraft was approximately 7620 meters/second (25 000 ft/sec). In the first flight experiment, water was periodically injected into a flow field which was contaminated by ablation products from the spacecraft nose region. The nonablative nose of the second spacecraft thereby minimized flow-field contamination. Comparisons of the probe-measured density profiles with theoretical calculations are presented with discussion as to the probable cause of significant disagreement. Also discussed are the correlation of probe measurements with vehicle angle-of-attack motions and the good high-altitude agreement between electron densities inferred from the probe measurements, VHF antenna measurements, and microwave reflectometer diagnostic measurements.			
17. Key Words (Suggested by Author(s)) Reentry communications; plasma diagnostics; electrostatic (Langmuir) probes; blackout alleviation; microwave reflectometer; body motions; electron concentration		18. Distribution Statement Unclassified - Unlimited	
19. Security Classif. (of this report) Unclassified	20. Security Classif. (of this page) Unclassified	21. No. of Pages 129	22. Price* \$3.00

CONTENTS

	Page
SUMMARY	1
INTRODUCTION	1
SYMBOLS	2
EXPERIMENT DESCRIPTION	6
Flight Objectives	6
Launch Vehicles	6
Payloads	7
Electrostatic Probe System	8
RAM C-I Water-Injection System	12
RAM C-II Microwave Reflectometer System	12
VHF System	13
ELECTROSTATIC PROBE THEORY	13
FLIGHT DATA RESULTS AND DISCUSSION	14
Measured Electrostatic Probe Ion Currents	14
Thermocouple Probe Results	15
Electron Densities Inferred by Electrostatic Probe	15
Effects of Ablation Impurities on Electron Density	16
Effects of Vehicle Angle-of-Attack Perturbations on Electron Density	16
Effects of Water Injection on Electron Density	17
Microwave Reflectometer Measurements	18
VHF Antenna Measurements	18
Comparison of Inferred Electron Densities for the RAM-C Flights	19
Comparison of Theoretical and Experimental Electron Density Profiles	19
CONCLUSIONS	21
APPENDIX A – ELECTROSTATIC PROBE THEORY	22
Flowing Plasmas	22
Directed Flow Parallel to Probe	23
Directed Flow Normal to Probe	26
Interpretation of RAM-C Fixed-Bias Electrostatic Probe Data	29
Sample Calculation	29
APPENDIX B – ELECTROSTATIC-PROBE AUTOMATIC DATA REDUCTION PROCEDURE AND LISTINGS	31

	Page
APPENDIX C – ANALYSIS OF SPACECRAFT MOTIONS AND WIND ANGLES . . .	56
Determination of Wind Angles	56
Summary of Wind-Angle Analysis	58
REFERENCES	59
TABLES	62
FIGURES	67

ELECTROSTATIC-PROBE MEASUREMENTS OF PLASMA PARAMETERS
FOR TWO REENTRY FLIGHT EXPERIMENTS AT
25 000 FEET PER SECOND*

By W. Linwood Jones, Jr., and Aubrey E. Cross
Langley Research Center

SUMMARY

Unique plasma diagnostic measurements at high altitudes from two geometrically similar blunt-body reentry spacecraft using electrostatic probe rakes are presented. The probes measured the positive-ion density profiles (shape and magnitude) during the two flights. The probe measurements were made at eight discrete points (1 cm to 7 cm) from the vehicle surface in the aft flow field of the spacecraft over the altitude range of 85.3 to 53.3 km (280 000 to 175 000 ft) with measured densities of 10^8 to 10^{12} electrons/cm³, respectively. Maximum reentry velocity for each spacecraft was approximately 7620 meters/second (25 000 ft/sec).

In the first flight experiment, water was periodically injected into a flow field which was contaminated by ablation products from the spacecraft nose region. The nonablative nose of the second spacecraft thereby minimized flow-field contamination.

Comparisons of the probe-measured density profiles with theoretical calculations are presented with discussion as to the probable cause of significant disagreement. Also discussed are the correlation of probe measurements with vehicle angle-of-attack motions and the good high-altitude agreement between electron densities inferred from the probe measurements, VHF antenna measurements, and microwave reflectometer diagnostic measurements.

INTRODUCTION

The plasma sheath (ionized gas) which envelops a spacecraft during entry into an atmosphere can disrupt radio communications and cause "radio blackout." This phenomenon has received much attention (refs. 1 and 2) from both the U.S. Department of Defense and the National Aeronautics and Space Administration because of the serious problems

* Part of the information presented herein was included in a dissertation, "Probe Measurements of Electron Density Profiles During a Blunt-Body Reentry" by W. Linwood Jones, Jr., presented in partial fulfillment of the requirements for the degree of Doctor of Philosophy in Electrical Engineering, Virginia Polytechnic Institute and State University, Blacksburg, Virginia, June 1971.

that it causes for mission planners. For instance, in manned flight missions there is a significant increase in the complexity of such onboard systems as navigation, guidance, and control due to the reduction of ground systems support during critical blackout periods. In other instances, provisions for onboard data storage and delayed playback, or even a recoverable package, may be required for data retrieval after blackout. Also, terminal-phase systems such as altimeters, landing radars, homing devices, and electronic countermeasures may be compromised for lack of real-time signal transmission. Consequently, a requirement exists for a fundamental understanding of the reentry plasma sheath and its interaction with spacecraft electromagnetic systems.

A project called "Radio Attenuation Measurements (RAM)" has been conducted at Langley Research Center where flow-field plasma characteristics and the resulting attenuation of propagating electromagnetic waves have been investigated both experimentally and theoretically. (See ref. 3.) Experiments have been performed in both ground facilities and on reentry flights to determine radio-frequency plasma attenuation and flow-field electron density and collision-frequency distribution.

This report presents electron density profiles (absolute magnitude and shape) inferred from electrostatic probe measurements during two blunt-body reentries at 7620 meters/second (25 000 ft/sec). A rake of eight negatively biased probes, located near the aft section of each spacecraft, collected positive ion current out to a normal distance of 7 cm (2.75 in.) and over an altitude range of 85.3 km (280 000 ft) to 53.3 km (175 000 ft). In addition, inferred electron densities are presented from VHF antenna measurements during both flights and from microwave reflectometer measurements during the second flight. Comparisons are made between the experimentally derived electron densities and theoretically calculated values to assess the validity of present plasma flow-field models. Also the effects on electron density profiles of material injection (during the first flight) and spacecraft motions are discussed.

Also included in this report are a discussion of electrostatic probe theory in appendix A, a description of the probe-data-reduction procedure and a listing of RAM C-I and C-II current and inferred density as a function of altitude and time for all probes in appendix B by Lorraine F. Satchell, and an analysis of spacecraft motions and wind angles in appendix C by William L. Weaver.

SYMBOLS

Values are given in both SI and U.S. Customary Units. The measurements and calculations in the text and appendix A were made in SI Units; those in appendixes B and C, in U.S. Customary Units.

A	current, amperes; also projected area of probe, cm ²
A _n	accelerometer-measured accelerations (normal)
a	radius of probe sheath, R _p + d _s , cm
a _y , a _n	accelerometer-measured accelerations due to aerodynamic force along Y-axis (tangential) and negative Z-axis (normal)
D	body nose diameter, cm
d _s	sheath thickness, cm
e	magnitude of electronic charge, 1.5921 × 10 ⁻¹⁹ coulomb
H	ratio of modified potential energy to kinetic energy, $\frac{\chi_p}{1 + S^2}$
H _l	lateral angular momentum
H _t	total angular momentum
H _X	roll angular momentum (about X-axis), I _X p
I, I ₊	positive ion current collected by a probe, amperes
I _d	directed current into probe, nev _f (2R _p L), amperes
I _l	lateral moment of inertia, $\frac{I_Y + I_Z}{2}$
I _n	normalized probe current, $\frac{I_+}{I_r}$
I _r	random ion current calculated for a probe, $\frac{nev_+}{4}(2\pi R_p L)$, amperes
I _X , I _Y , I _Z	moments of inertia about spacecraft axes, kg-m ²
J _i	saturation positive ion current density, 0.4nev ₊ , amperes-cm ⁻²
k	Boltzmann's constant, 1.38044 × 10 ⁻²³ joule-K ⁻¹

L	probe length, cm
\vec{L}	angular impulse
M	ion mass, g
N_e	electron density, electrons-cm ⁻³
n	electron density, electrons-cm ⁻³ , or ion density, ions-cm ⁻³
p,q,r	rotation rates about X-axis (roll), Y-axis (pitch), and Z-axis (yaw), rad-sec ⁻¹
R	modified normalized probe current, $\frac{I_n}{\sqrt{1 + S^2}}$, amperes
R_p	probe radius, cm
r_a	radius at which particles will just be collected, cm
S	ion speed ratio, $\frac{v_f}{v_+}$
T_e	mean electron temperature, K
V	probe potential, volts; also spacecraft velocity or wind axis
V'	absolute magnitude of applied probe bias, volts
V_O	initial energy of ion entering sheath, $\frac{kT_e}{e}$, joule-coulomb ⁻¹
V_∞	plasma potential, volts
v_+	random thermal velocity of ions entering sheath, $\sqrt{\frac{8kT_e}{\pi M}}$, cm-sec ⁻¹
v_f	normal component of flow velocity, cm-sec ⁻¹
v_{flow}	flow velocity of ion flux past probe, cm-sec ⁻¹
X,Y,Z	spacecraft body-axis system
x	distance from nose along body axis, cm

y	distance from body along normal to body surface, cm
α, β, η	wind angles: angle of attack, sideslip angle, total wind angle, deg
γ	ratio of probe-sheath radius to probe radius, $\frac{a}{R_p}$
ϵ	permittivity of free space
$ \Delta\eta $	absolute variation in total wind angle
Θ	inverted form of the Child-Langmuir 3/2-power law, $\frac{\text{volts}^{3/2}}{\text{ampere}}$
θ	precession cone half-angle; also angle between flow velocity and probe axis, deg
λ_D	Debye length, $\frac{\epsilon_0 k T_e}{e^2 n}$, cm
ν_b	precession frequency of vector ω_l about body axis
ν_H	precession frequency of X-axis about angular momentum vector
ρ	charge density
ϕ	angular coordinate for payload referenced to electrostatic probe rake, deg
χ_p	normalized potential difference between probe and plasma, $\frac{e(V - V_\infty)}{kT_e}$
ω_l	lateral angular velocity, $\sqrt{q^2 + r^2}$, rad-sec ⁻¹

Subscripts:

cr	critical
o	initial

An arrow over a symbol denotes a vector.

EXPERIMENT DESCRIPTION

Three flight experiments were conducted in the medium velocity (7620 meters/second (25 000 ft/sec)) reentry region to obtain quantitative measurements of plasma parameters about a hemisphere-cone body and to test radio-attenuation alleviation techniques. Only the first two flights are discussed herein, since the analysis of probe data for the third flight is incomplete. (Descriptions of the third flight and the preliminary probe results are found in refs. 4 and 5.) This section provides a brief description of the flight objectives, launch vehicles, and payload experiments. A description of the electrostatic probe system is given which includes the mechanical construction of the probe rake, the electronic circuitry, characteristics of the circuit components, and data format. Also described briefly are other plasma diagnostic experiment systems onboard the respective payloads.

Flight Objectives

The primary objectives of the first flight (RAM C-I) were to test the effectiveness of water injection as an alleviation technique and to establish the operational system injection parameters (mass flow, penetration distance, and injection orifice size and location) necessary to achieve a required level of signal recovery. During this flight, electrostatic probes were the principal diagnostic instrumentation for assessing the plasma alleviation. In the second flight (RAM C-II), the primary objective was to measure the electron density time and altitude histories at several locations along the spacecraft using microwave reflectometers and electrostatic probes. Flight details are discussed in reference 6 for RAM C-I and in reference 7 for RAM C-II.

Launch Vehicles

Similar four-stage solid-fuel Scout vehicles were used to launch the RAM C-I and C-II payloads from the NASA Wallops Island Station in Virginia. The two Scout vehicles designated S-159 and S-168, ready for launching, are shown in the composite photograph of figure 1. Pertinent vehicle-payload identification and launch information are given in the following table:

Designation		Launch	
Scout	Payload	Date	Time, GMT
S-159	RAM C-I	10-19-67	17:33:00
S-168	RAM C-II	8-22-68	15:16:00

Approximate staging sequencing applicable to the RAM C-I and C-II launch vehicles and payloads with important events is shown in figure 2(b). The launch vehicles transported their respective payloads to apogees greater than 220.5 km (720 000 ft) before propelling them back into the earth's atmosphere. To minimize lateral rotations and trajectory dispersion during the thrusting of the fourth-stage motor which was unguided, the motor and spacecraft were spin-stabilized just prior to motor ignition. Tip-off moments produced by the separation of the expended fourth-stage motor at an altitude of about 113 km (370 000 ft) caused coning of the spacecraft and a resulting oscillatory relative wind angle. The earth-relative reentry flight-path angle was a nominal -15° , and both payloads reached their maximum velocities at an altitude of 67.0 km (220 000 ft). Some pertinent dynamic characteristics for each payload are given in the following table:

Payload	Spin rate		Maximum velocity		Total wind angle over probe data period, deg
	rad/sec	rps	m/sec	ft/sec	
RAM C-I	18.5	2.95	7670	25 165	5.0
RAM C-II	19.1	3.04	7678	25 193	4.0

The reentry data periods occurred just north of Bermuda as shown in the RAM C-II ground track. (See fig. 2(a).) The RAM C-I and C-II payloads flew nearly identical reentry trajectories, as indicated in figure 3 and in table I; and for this reason, the RAM C-I trajectory was used in the data reduction for both flights. Although the use of the RAM C-I trajectory produced approximately a 365.8-meter (1200-ft) bias error in the altitude for all RAM C-II probe data, this procedure introduced negligible errors in the inferred electron and ion densities.

Payloads

The payload geometries were essentially identical and are shown in figure 4. Each payload consisted of an approximately 15-cm (6-in.) radius hemispherical nose followed by a 9° half-angle cone and had an overall length of about 130 cm (51 in.). The physical characteristics of each payload are given in the following table:

Payload	Nose material	Nose diameter		Body length		Weight before launch		Afterbody material
		cm	in.	cm	in.	kg	lb	
RAM C-I	NARMCO 4028 (Phenolic-graphite charring ablator)	31.90	12.56	130.25	51.28	121.1	267.0	Teflon
RAM C-II	Beryllium nose cap*	30.48	12.00	129.54	51.00	121.8	268.5	Teflon

* Ejected at time of electrostatic-probe retraction.

RAM C-I had a phenolic-graphite charring ablator on the hemispherical nose, whereas the nose of RAM C-II was covered by a beryllium-cap heat sink. Since RAM C-I was primarily a material-injection experiment, the ability to maintain the integrity of the injection orifices during the ablation period was mandatory; therefore, the phenolic-graphite material was selected. (See ref. 8; RAM-CA designation is synonymous with RAM C-I.) An analysis of a sample of the NARMCO 4028 used to fabricate the heat shield showed that it contained about 1100 $\mu\text{g/g}$ sodium. The analysis was incapable of detecting potassium, if present, at less than 3600 $\mu\text{g/g}$ which means that the ablator could have contained up to 4700 $\mu\text{g/g}$ of alkali. The beryllium nose cap and the teflon were found to be free of any significant amounts of alkaline impurities. For a sample of teflon, the analysis showed the alkali content to be less than 5 $\mu\text{g/g}$. Thus, during the RAM C-I reentry, the ablation of the nose fed easily ionizable alkali metals into the flow-field boundary layer. Since the primary objective of the RAM C-II flight was plasma flow-field diagnostics, the nonablative beryllium cap was selected to keep the flow field free of ablative contaminants so that a comparison could be made of measured plasma characteristics with pure-air theoretical calculations. The beryllium cap was ejected at an altitude of 56.4 km (185 000 ft) prior to the surface melting, and thus exposed a teflon-covered nose. For both flights, the effects of teflon ablation from the afterbodies are believed to be negligible at altitudes above 56.4 km (185 000 ft) (refs. 7 and 9) since the teflon had a low-alkali-metal contamination level; also, the ablation rates there were much less than those for the nose.

The location of the electrostatic and thermocouple probe rakes, the various radio-frequency antennas (diagnostic and instrumentation) on both payloads, and the water-injection orifices on the RAM C-I payload are shown in figure 5. Table II gives exact coordinate location and position of the various system sensors for both payloads.

Electrostatic Probe System

Design philosophy. - Realistic predictions of the electromagnetic wave attenuation to be experienced during atmospheric entry are dependent upon several factors, the foremost of which is the physical nature of the plasma itself. The requirement for accurate knowledge of gas composition is more stringent for an analysis of this problem than for other reentry problems such as heat transfer or aerodynamic flow. The reason for this requirement is that the free electrons, which control the electrical conductivity of the gas, are a trace species and, as such, require a comprehensive nonequilibrium flow-field analysis including finite-rate chemistry to determine the degree of gas ionization. For example, approximately 40 finite-rate chemical kinetic reactions involving 11 plasma species (free electrons, molecular and atomic ions, molecules, and atoms) must be considered in theoretical calculations of electron concentration. In addition, the dominant chemical kinetic process is dependent upon the velocity and body shape of the reentering spacecraft.

Moreover, calculations are more difficult to perform as one moves aft from the stagnation region because not only is a complete understanding of the local gas conditions required, but also of the entire gas history from the shock-entry point of each streamline to the location of interest.

The objective of the RAM-C electrostatic probe experiment for both flights was to determine experimentally the electron density profiles in the aft flow field in order to assess the validity of the theoretical calculations and to provide experimental data upon which to improve the analytical model used. The design of the RAM-C electrostatic probe system and the calibration testing in ground plasma facilities are discussed in detail in reference 4.

Configuration of electrostatic probe rakes on RAM C-I and C-II. - A photograph of the electrostatic probe rake is shown in figure 6(a); and the exterior configuration, a sectional view of the leading edge, and standoff dimensions of the ion collectors are shown in figure 6(b). Each of the iridium ion collectors extended 0.0254 cm (0.010 in.) beyond the wedge-shaped beryllium oxide leading edge of the rake. The two larger iridium pieces, one on each side of the rake, were electrically common and served as electron collectors. Iridium was chosen as the probe collector material because of its high melting temperature, high electronic work function, and negligible oxidation property. The beryllium oxide leading-edge material was a high-temperature insulator which mechanically and electrically separated the ion collectors and the electron collectors. The beryllium oxide leading edge was a 60° wedge with a leading-edge radius of 0.0254 cm (0.010 in.) and was inclined at an angle of 45° with respect to the payload surface. The main body of the probe was constructed of a phenolic fiber-glass ablation material.

Probe circuitry. - A fixed bias of -5.0 volts, referenced to the electron collectors, was applied simultaneously to all ion collectors to attract positive ions. Figure 7 gives a schematic drawing of the probe electronic system on both the RAM C-I and RAM C-II payloads. As each probe continuously collected plasma current, the mechanical commutator sampled the voltage developed across the probe load resistors and calibrate resistors and fed the signals to the logarithmic amplifier at the rate of 300 samples per second. The voltage developed across the probe load resistor was converted by the logarithmic amplifier to drive a telemetry subcarrier oscillator. A photograph of typical flight components is shown in figure 8.

For the RAM C-I experiment, the output of the logarithmic amplifier was connected single-ended to the input of the subcarrier oscillator; whereas on the RAM C-II experiment the output of the amplifier was connected to a differential-input subcarrier oscillator. This modification in the electronic system was made to correct an anomaly which occurred during the RAM C-I flight. The occurrence of the anomaly was ascertained during the onboard calibration of the logarithmic amplifier. The problem presented itself at an alti-

tude of about 67.0 km (220 000 ft) when the logarithmic amplifier output including all calibrate levels unexpectedly went to zero. During water injection, the amplifier returned to normal operation; however, after the injection stopped, the output returned to zero. Approximately 3 seconds later at 61.0 km (200 000 ft), the amplifier returned to normal and continued so for the remainder of the flight. The anomaly was analyzed and it could be reproduced in the laboratory by connecting a -1.85-volt potential between the electron collector and the payload ground. It is surmised that during the flight the electron collectors and the spacecraft metallic skin assumed different floating potentials in the plasma. This condition caused the internal input diodes of the logarithmic amplifier to conduct and thereby reduced the amplifier output to zero. The differential connection used on the RAM C-II system corrected the situation by effectively adding a large resistance (10 megohms) in series with this unwanted potential and thus prevented the diodes from conducting.

Logarithmic amplifier.- The solid-state logarithmic amplifier was developed specifically for the electrostatic probe experiments. The device was a low-level input, adjustable high gain, chopper-stabilized dc amplifier which converted a differential high-impedance input into a differential low-impedance output. Figure 9(a) shows the dynamic (commutated at 300 samples/sec) input-output voltage characteristics of the amplifiers used for flight. As can be seen from the figure, the device provided an output proportional to the logarithm of the input voltage for greater than a three-decade range. The amplifier gain was adjusted so that the voltage developed by an input current from the probes of at least 10^{-6} ampere, across the load resistor of 400 ohms, would be on the reasonably linear section of the characteristic curve. The maximum input current was 10^{-3} ampere and the minimum current value was determined by system noise (approximately 5×10^{-7} ampere for the RAM C-I experiment and 10^{-7} ampere for the RAM C-II experiment). The amplifier characteristics shown in figure 9(a) were obtained just prior to flight by calibrating the entire probe system as installed in the spacecraft. This calibration technique used a range of known resistances that were externally connected in sequence across the biased probe electrodes and thereby simulated a range of plasma currents. This calibration should not be confused with the onboard calibration the main purpose of which was to provide certain pulse levels in each data frame for automatic data reduction requirements.

Since the signal to the amplifier was commutated at 300 samples per second, good dynamic response was needed to reproduce the input accurately. Figure 9(b) shows a typical pulse-response curve of the amplifiers. With a delay time of less than 100 microseconds and rise and fall times of less than 75 microseconds each, the response was sufficient for data samples of approximately 3 milliseconds duration. For data-reduction purposes, only the center 50 percent of the pulse width was used.

Probe-experiment characteristics and data format. - The format used for electrostatic probe information from the logarithmic amplifier output, including currents from the probes and from the calibrates, is presented in figure 10. Shown in figure 10 is one complete data frame which has a duration of 100 milliseconds. There are five calibrate levels for each frame, which correspond to currents of 0.1, 1.0, 10.0, 100.0, and 1000.0 microamperes. Between the calibrate sequences are three consecutive samplings of the eight ion collectors. One profile measurement represents about 26.4 milliseconds or about 8 percent of a complete payload roll motion. The sampling rate of 300 samples per second was selected so that at least two data formats would be completed during the off time of the water-addition cycling system on RAM C-I. The same sampling rate was maintained for the RAM C-II experiment.

Thermocouple probes. - On both of the RAM-C payloads, a rake of thermocouples was located diametrically opposite the electrostatic probe rake to monitor the temperature of the leading edge. On RAM C-I, both the thermocouple and electrostatic probes were in line with the water-injection sites to insure similar heating environments. The external configuration of the thermocouple probe fin was the same as that of the electrostatic probe fin and is shown in figure 11. Instead of electrodes, however, three thermocouples were embedded 0.0635 to 0.1016 cm (0.025 to 0.040 in.) from the leading edge of the wedge. The thermocouples were platinum-platinum+13-percent-rhodium and were located 2, 4, and 6 cm (0.79, 1.57, and 2.36 in.) from the payload surface. The useful measurement range of the thermocouples was from 255 to 1977 K (0° to 3100° F).

At elevated temperatures, the insulating properties of the beryllium oxide degraded, and unwanted leakage currents flowed between ion collectors and between ion and electron collectors. The thermocouple probe was used therefore to determine the altitude at which probe heating became significant. The electrical resistivity degradation affected the accuracy of the inferred electron density because the leakage currents added to the measured plasma current and thereby caused a higher than actual electron density to be inferred. In reference 6, the electrostatic probe data were considered to be unusable in an absolute sense once the local probe temperature exceeded 811 K (1000° F). An improved analysis given in reference 4 estimated that the leakage current was on the order of 100 microamperes for a thermocouple temperature of 1366 K (2000° F). For both RAM-C flights the inferred plasma density was greater than 10^{11} electrons/cm³ when the local temperature for a given probe exceeded 1366 K; thus, the error in the inferred density at that point was less than a factor of two. For higher leading-edge temperatures, the leakage current probably exceeded the plasma current; therefore, above 1366 K the data were considered to be degraded for useful plasma-density interpretation purposes.

Retraction of probe rakes. - Although it was desirable to make electrostatic probe measurements over the entire blackout data period from 85.3 to 24.4 km (280 000 to 80 000 ft), certain restrictions were imposed. The high heating rates predicted for the intermediate altitude range from 61.0 to 30.5 km (200 000 to 100 000 ft) would result in structural failure of the probes which could endanger the stability of the payload itself. Therefore, the rakes (electrostatic and thermocouple) were simultaneously retracted into the base region of the payload at a predetermined altitude by programmer action. The RAM C-I rakes were retracted at an altitude of 53.6 km (176 000 ft). RAM C-II probe retraction was initiated simultaneously with the beryllium cap ejection at 56.4 km (185 000 ft), but the effects of retraction on the inferred density were not noted until 55.9 km (183 400 ft).

RAM C-I Water-Injection System

During the RAM C-I flight, water was periodically injected into the flow field from the spacecraft nose to provide for electron density reductions in the peak attenuating layer of the flow field. The water was injected at varying flow rates with specific penetrations over an altitude range of 83.2 to 33.8 km (273 000 to 111 000 ft). The injection locations are shown on the payload sketch in figure 5. Locations and positions of the nozzles are also given in table II. The electrostatic probe rake and two VHF slot antennas were located in line with the injection sites and were the principal diagnostic instrumentation for assessing the plasma alleviation.

The resultant programmed variation of flow rates for the RAM C-I experiment is given in table III, with the altitude shown for the start of each pulse. Typical water flow-rate pulses are shown as a sequence of valve-on times. One complete injection cycle is shown and the cycles were repeated every 4 seconds. The valve-on times were 230 milliseconds and the valves were opened at 0.5-second intervals. A more detailed description of the RAM C-I water-injection system can be found in reference 6.

RAM C-II Microwave Reflectometer System

A four-frequency microwave reflectometer system was used to infer the peak electron density time and altitude histories about the RAM C-II spacecraft. A plasma-density measurement range of three decades (10^{10} to 10^{13} electrons/cm³) was provided by the reflectometer system. The microwave reflectometer technique used the reflectivity of the plasma to infer the electron density and phase measurements to infer the electron density profile shape. Microwave antennas for the four frequencies (L-, S-, X-, and K_a-bands) were located at each of the four body stations (except station 1, L-band excluded), for a total of 15 antennas (fig. 5). Antenna locations are listed in table II. Greater detail on the microwave reflectometer system may be found in reference 7 and in table II.

VHF System

It has been shown that significant pattern changes can occur for plasma-clad cylindrical antennas when the electron density passes through the critical value. (See ref. 10.) These pattern changes are also accompanied by rapid changes in input impedance or input voltage standing wave ratio (VSWR). Received signal strength and onboard antenna VSWR were monitored during the RAM C-I and C-II flights and were used to determine the occurrence of the VHF critical electron density. The antenna VSWR was monitored by onboard directional couplers, and the antenna patterns were reconstructed by use of the signal received from the spinning spacecraft. There were several ground, airborne, and shipborne receiving stations with different look angles; thus, patterns were obtained in several planes. The arrangement of receiving stations for RAM C-II is shown in figure 2(a).

Two types of VHF antennas (cavity-backed slots and circumferential slot arrays) were used for the flights, as shown in figure 5. For the RAM C-I payload, two diametrically opposed, axially oriented, 259.7-MHz cavity-backed slot antennas transmitted the real-time telemetry, and an aft-positioned circumferential slot array (ring) antenna transmitted the delayed-time telemetry. In comparison, on the RAM C-II payload, the real-time and delayed-time telemetry systems utilized a pair of aft-located circumferential slot arrays (ring antennas). The axially oriented slot antennas on RAM C-I were in line with the material-injection orifices and the electrostatic probes. The ring antennas for all payloads were just forward of the electrostatic probes. A more complete description of the VHF antennas on RAM C-I may be found in references 6 and 11 and in table IV.

ELECTROSTATIC PROBE THEORY

The RAM-C electrostatic probe measurements were interpreted by use of a free-molecular cylindrical probe theory modified to account for a directed-ion flux due to the plasma flow. This theory was developed by Scharfman (refs. 12 and 13) based on the works of Hok et al. and Smetana (refs. 14 and 15, respectively) and is summarized in appendix A.

The configuration of the RAM-C probe rake is such that in relation to the flowing plasma, each ion collector appears to be a cylindrical wire 0.0254 cm (0.010 in.) in diameter and 0.5385 cm (0.212 in.) long, which is inclined at an angle of 45° with respect to the plasma flow. Experimental programs were performed at Langley Research Center, Stanford Research Institute, and Cornell Aeronautical Laboratories to verify that the RAM-C electrostatic probe rake could be used to infer accurate localized ambient plasma electron densities. (See refs. 4, 13, 16, and 17.) Typical results from references 13 and 17 are shown in figure 12. The conclusion based on this work is that free-stream electron density can be inferred within ± 20 percent by using the described theory for the

RAM-C flight conditions for plasma densities from 10^{10} to 10^{11} electrons/cm³ and within a factor of two over the 10^9 to 10^{13} electrons/cm³ range.

FLIGHT DATA RESULTS AND DISCUSSION

Measured Electrostatic Probe Ion Currents

Ion currents measured by each of the eight electrostatic probes onboard the RAM C-I and C-II flights are presented as a function of altitude from 85.3 to 53.3 km (280 000 to 175 000 ft) in figures 13 and 14, respectively, and are listed in appendix B. (Altitudes for RAM C-II are too low by 0.3658 km (1200 ft).) In the figures, the measured probe-current data points are represented by the symbols which have been interconnected in order to show small variations clearly. Probes for both flights indicate an initial measurable current at an altitude of about 85.3 km (280 000 ft). Lowest measurable current for the probe electronic systems was about 10^{-7} A. Likewise, system saturation current was 10^{-3} A.

Figures 13(a) to 13(d) show the currents measured by the electrostatic probes aboard RAM C-I. The effects of periodic water injection into the flow field can be seen as respective periods of greatly reduced measured currents for all eight probes. The anomaly period, discussed in an earlier section, occurred between 67.1 and 61.0 km (220 000 and 200 000 ft). The data shown in the figures during the anomaly period are considered to be valid since they were selected only when the onboard calibrates indicated normal amplifier operation. All data are valid after the anomaly period. The probes aboard RAM C-I were retracted at 53.6 km (176 000 ft) from the aft-flow-field region into the payload base region. The probes continued to make measurements after retraction, but the analysis of these data is not presented in this report. Immediately after retraction, the outermost probes still indicated system saturation current because of electrical degradation of the beryllium-oxide probe insulator induced by aerodynamic heating.

Figures 14(a) to 14(d) show the electrostatic-probe-measured ion currents for RAM C-II. Effects of retraction can be seen at about 55.5 km (182 000 ft) in figures 14(a) to 14(c) as a steep dropoff of measured current. Again, the outermost probes of figure 14(d) were still saturated immediately after retraction because of leakage current through the degraded probe insulator.

The small sinusoidal-type variation superimposed on the curves shown in figures 13 and 14 are variations in the plasma density due to spacecraft motion. These variations will be discussed in detail in a later section and in appendix C.

Thermocouple Probe Results

An accurate knowledge of the probe-rake leading-edge temperature during reentry was necessary for valid interpretation of the fixed-bias probe currents because at thermocouple temperatures greater than 1366 K (2000° F), the insulating properties of the dielectric wedge were degraded to the point that the inferred plasma densities were questionable. Therefore, the first task in the data-reduction procedure was to examine the thermocouple data and to identify those probe data for which this threshold had been exceeded.

Measured thermocouple temperatures for both the RAM C-I and C-II reentries are presented in figure 15. Overall, for corresponding thermocouples at identical altitudes, the temperatures of RAM C-I were less than those of RAM C-II most likely because of the cooling effects of water injection which can be seen on the RAM C-I curves. Water-injection cycles for RAM C-I are shown at the top of the figure. The RAM C-I and RAM C-II data are presented in figure 16 as constant-temperature profiles of normal standoff distance y to a given temperature boundary plotted against altitude.

At any altitude, the temperature at any probe location on the leading edge may be determined from the intersection of a horizontal-probe location line, a vertical-altitude line, and a constant-temperature contour. When, for a given probe, this intersection occurs above the 1366 K (2000° F) contour, the interpretation of these data is questionable.

Electron Densities Inferred by Electrostatic Probe

By use of the probe interpretation discussed in appendix A, the collected ion currents given in figures 13 and 14 were converted into respective ion (electron) densities for the two flights. (Flow-field calculations (ref. 9) indicate that positive-ion and electron densities are very nearly equal for the RAM-C trajectory.) The electron densities for RAM C-I are shown in figure 17 and for RAM C-II in figure 18. The electron densities plotted against time and altitude are also tabulated for both flights in appendix B. The RAM C-I and RAM C-II results after probe retraction should be disregarded since no temperature and velocity data are presently available to allow proper interpretation of the ion current.

Flow-field electron-density profiles (electron density plotted against standoff distance y) were determined during both flights. Typical results are shown in figure 19 for selected altitudes during the RAM C-I flight where no water-injection effects were present and in figure 20 for similar altitudes on RAM C-II. The data represent the time-averaged electron density (averaged over one spacecraft revolution) at a given altitude for each probe, and the bars in figure 20 represent the peak-to-peak density change due to body

motions, to be discussed in a later section. The profiles for RAM C-I and RAM C-II flights are similar, although there was a slight difference in the absolute level at the specified altitudes. These differences are also observed in overlays of electron density plotted against altitude for RAM C-I and RAM C-II given in figure 21.

Effects of Ablation Impurities on Electron Density

Since the nose materials for the two RAM spacecraft were different (charring ablator for RAM C-I, nonablating heat sink for RAM C-II), a comparison can be made between contaminated and noncontaminated reentry plasma flow fields. The electron-density histories for RAM C-I and RAM C-II are superimposed for comparison in figure 21. The electron density for RAM C-I is approximately a factor of 2 higher than that for RAM C-II for the altitude range of 85.3 to 73.2 km (280 000 to 240 000 ft). Below this altitude, RAM C-II results are slightly greater than those for RAM C-I, although the RAM C-I anomaly period and the effects of material addition make a quantitative comparison less meaningful. The differences in measured electron density between these flights could be attributed to ablation product contamination effects because the payloads were nearly geometrically identical and they flew nearly identical trajectories. The RAM C-I charring phenolic-graphite nose fed easily ionizable alkali metals (sodium and potassium constituted approximately 1000 to 4000 $\mu\text{g/g}$ in the virgin material) into the flow-field boundary layer, whereas the nonablating beryllium nose cap on RAM C-II did not contaminate the flow. For both spacecraft the teflon afterbody did ablate slightly; however, additional ionization was not probable because here the alkali metal content was kept below 5 ppm of teflon. A detailed discussion of alkali ablation product contamination of the RAM-C flow field is given in reference 9.

Effects of Vehicle Angle-of-Attack Perturbations on Electron Density

An analysis of the accelerometer data (appendix C) revealed that each payload underwent small angle-of-attack oscillations which produced variations in the ion current collected by all probes and variations in the microwave reflectometer measurements (RAM C-II). This effect is more clearly observed in the RAM C-II results (fig. 18) since these results are not disturbed by water injection. Variations in electron density at the probe station were produced because the payload was at an angle of attack (unsymmetrical flow field about payload) while spinning at 18.84 rad/sec (3 rps). When the payload experienced a positive angle of attack (positive normal acceleration), the electrostatic probes were on the windward side of the payload and sensed a compression of the flow field. Conversely, for a negative angle of attack (negative normal acceleration), the probes sensed the leeward (less dense) side of the flow field.

A comparison of the RAM C-II vehicle angle-of-attack motions (determined by accelerometer data) with electron density (inferred from electrostatic probe 1) is shown for the altitude region from 59.4 to 55.8 km (195 000 to 183 000 ft) in figure 22. As seen in the figure, small angle-of-attack motions produced peak-to-peak density fluctuations in the aft part of the flow field approaching a factor of three. The sizable density variations close to the payload for relatively small changes in angle of attack can be one of the reasons that signal-attenuation models do not always accurately predict plasma-caused signal losses when normal zero angle-of-attack plasma profiles are used.

Effects of Water Injection on Electron Density

The effectiveness of water injection as a plasma alleviant in the RAM C-I flow field was assessed by means of two VHF slot antennas and the electrostatic probe rake located in line with the injection sites. The probe measurements provided an excellent means of determining injectant penetration distances as well as the resultant magnitudes of the suppressed plasma.

The amount of plasma suppression due to water injection on the RAM C-I plasma electron density is seen in figure 23. In the upper part of the figure, the water injection pulses are shown with varying magnitude. (Flow rates are given in table III.) Each pulse caused corresponding decreases in measured electron density. Cycle 1 (not shown in the figure) had no flow because of a slow fill rate in the lines. The very low flow rates of cycle 2 produced no detectable plasma alleviation for any of the probes. The larger flow rates of cycle 3, particularly the side-injection flow rates 3 and 4, caused appreciable electron-density reduction for all probes. Electron-density profiles for the various lateral injection flow rates of cycle 3 are shown in figure 24. Here, it is clearly seen that increasing flow rates are more effective in reducing electron density and in penetrating farther out into the flow. The electron-density profiles during stagnation injection (cycle 4, flow rate 5) are shown in figure 25 for selected altitudes over the 593 meter (1947 ft) altitude range.

The probe electronic system anomaly occurred immediately after cycle 4, flow rate 6, and persisted through cycle 4, flow rate 4. For intervals during the periods of water injection, however, the amplifier returned to normal operation and allowed reliable probe measurements.

The effectiveness of the water-injection technique was assessed by comparing density profiles with water injection against those without water for the same altitude range. Alleviation effects of water injection were noted by the ground stations on the signals received from all the onboard radio-frequency systems and good correlation was found between the probe electron-density profile changes and the observed attenuation changes of the signal strengths.

Microwave Reflectometer Measurements

The location and magnitude of the peak electron density inferred by the station 4 microwave reflectometers agree with the electron-density profiles inferred by the electrostatic probes for the RAM C-II flight. This good agreement lends credence to both measurements since both measured and theoretical electron-density gradients along the aft payload surface are small (refs. 7 and 9, respectively).

The microwave phase data (fig. 35 of ref. 7) indicate that there was a strong density gradient between the payload surface and a normal distance into the flow of 1 to 2 cm. Beyond this distance the profile appeared to be nearly uniform for another several centimeters.

The magnitudes of the electron density inferred by the probes and microwaves are also strongly correlated as shown in the longitudinal profiles of peak electron density for constant altitude. (See fig. 26.) In figure 26, the time-averaged peak electron densities as indicated by the reflectometer are plotted against distance along the body, where zero on the abscissa corresponds to the payload nose. Also shown in the figure for purposes of comparison are the time-averaged electron densities (averaged over one body revolution) for probes 1 and 8 (innermost and outermost probes, respectively). The bar on the probe data represents the peak-to-peak density fluctuation due to body motions.

VHF Antenna Measurements

The received VHF signal strengths (recorded at the Bermuda and U.S. Navy Ship (USNS) Twin Falls Victory stations) and the reflected power for the onboard antennas for RAM C-I are presented in figures 27 and 28 and for RAM C-II in figure 29. The Bermuda station was located approximately broadside to the payload during the data period and the Twin Falls Victory station was directly down range. (See fig. 2(a).)

The peak electron density at a given antenna location was inferred from the region where the received signal strength ripple pattern (due to spinning payload) and the onboard antenna reflected power changed abruptly. In reference 10, these changes were shown to occur at the critical electron density; however, since the RAM-C experimental conditions were slightly different than those in reference 10, the peak electron density is estimated to be the critical value within a factor of two uncertainty.

For the RAM C-I records, the time period of interest is from 385 to 394 seconds. In the Bermuda 225.7-MHz record, the pattern ripple is about 30 dB prior to the critical electron-density region (indicated by the arrows) which is in agreement with the measured free-space patterns in the equatorial plane. The ripple structure diminishes markedly in the critical electron-density region and then resumes as attenuation due to an overdense plasma occurs. The same sequential change was also noted by the Bermuda station in the 259.7-MHz antenna pattern ripple structure during a similar time frame.

A related change in the pattern ripple structure was also observed for both antennas in the signal received at the USNS Twin Falls Victory station between 386 and 394 seconds. At 386 seconds, the plasma electron density over the antennas is negligible and the antenna pattern ripple is about ± 2 dB. Also the mean level of the signal received at the two frequencies is different by about 16 to 20 dB in absolute level. Both the magnitude of the pattern ripple and the absolute power levels agree very well with those predicted from the nose-on free-space absolute antenna patterns. During the time period from 390 to 392 seconds, the 225.7-MHz record experiences a 20-dB dip in the received signal level as the plasma goes through critical density. A similar but smaller signal-level dip also occurs at 259.7 MHz. The time of occurrence of these amplitude dips in the received nose-on signal closely correspond to the time period where a significant decrease in pattern ripple was observed from the broadside direction.

The records of reflected power to both the 225.7-MHz and the 259.7-MHz antennas are shown in the lower parts of figures 27 and 28. The sharp rise or increase in reflected power with the simultaneous occurrence of critical electron density over the antenna aperture corresponds to that altitude range where the pattern ripple changes were noted. For RAM C-II, nearly identical antenna effects were observed, as shown in figure 29.

Comparison of Inferred Electron Densities for the RAM-C Flights

The plasma diagnostic results for both flights are shown in figure 30 for the purpose of comparison. They include electron density as a function of altitude inferred from the RAM C-II electrostatic probes, RAM C-II microwave reflectometers, and the RAM C-I and RAM C-II VHF antenna measurements. The data presented for electromagnetic techniques are time-averaged peak electron densities. The probe data represent the envelope of maximum to minimum values for all probes. All inferred densities are corrected for body location and are referred to the probe station by use of the appropriate longitudinal profile in figure 26.

Comparison of Theoretical and Experimental Electron Density Profiles

Calculated electron density profiles for the RAM-C flights were provided by the authors of reference 9. These calculations began with pressure distributions derived from equilibrium inviscid flow-field solutions for sphere-cone shapes. A nonequilibrium streamtube method provided temperature, density, and composition (including electron concentration). Streamline positions were determined by means of mass flow conservation. An equilibrium thin boundary-layer solution was adapted for use with nonequilibrium edge conditions, and the combined viscous-inviscid solution was iterated to account for vorticity and displacement thickness. Inviscid streamline values were discarded upon entry into the boundary layer and were replaced by calculations based on conditions in the

boundary layer. The flow-field solutions described are not valid at altitudes above about 70.1 km (230 000 ft). It should be noted that ambipolar diffusion of the charged particles, which cannot be included in this treatment, was estimated in reference 9 to become an important influence at altitudes higher than 70.1 km (230 000 ft).

For RAM C-II the clean-air assumption should have been valid down to 56.4 km (185 000 ft) where the beryllium nose cap was ejected, but for RAM C-I the flow field was contaminated by ablation products from the phenolic-graphite nose. For both bodies the teflon afterbody did ablate to some extent, but no additional ionization would result because the alkali metal content was kept below 5 ppm in the heat shield. There is, however, an unanswered question concerning the reduction of the electron density due to the electrophilic action of teflon ablation products.

When the measured electron-density profiles shown in figures 19 and 20 were compared with the calculated profiles previously mentioned, the measured profiles were found to be lower and flatter than the calculated ones. Also the measurements appeared to extend to greater distances from the body surface than had been anticipated. A typical comparison is shown in figure 31 with the RAM C-II data bars representing the envelope of probe data (due to body motions). Comparison of the probe data with other available plasma flow-field calculations (ref. 18) also indicates this significant disagreement between experiment and theory in absolute magnitude and in shape of the electron-density profiles.

In an effort to resolve these differences above 71.0 km (233 000 ft), the effects of ambipolar diffusion were considered. Since the analytical model used a streamtube approach, the effects could not be handled directly; rather an ion diffusion correction factor was determined (ref. 9) which accounts for the reduction in the magnitude of the peak electron density. Unfortunately, no theoretical means is available for predicting the spreading of the electron-density profiles; conceptually, however, ambipolar diffusion should decrease the absolute magnitude of density and reduce its gradients.

The theoretical peak electron density and the RAM C-I and RAM C-II envelopes of time-averaged inferred densities from probe 8 are shown in figure 32. The RAM C-II data should provide a better comparison with the "pure air" plasma calculations because the RAM C-II beryllium nose cap minimized flow-field contamination down to an altitude of 56.4 km (185 000 ft). At 85.3 km (280 000 ft) the inviscid calculation of peak electron density must be reduced by approximately two decades because of the ambipolar diffusion correction factor. This correction goes to zero near 70.1 km (230 000 ft), and below this altitude both the inviscid calculations and the inviscid calculations corrected for boundary layer yield identical results and according to reference 9 are believed to be correct. The good agreement between the inviscid calculations corrected for ambipolar diffusion and the experimental measurements above 70.1 km supports the hypothesis that ambipolar

diffusion is a principal mechanism for shaping the high-altitude electron-density profiles. The RAM C-II electron densities from the inviscid calculations corrected for boundary layer, the microwave reflectometer measurements, and the electrostatic probe measurements are given for different body locations in figure 33. Although both the experimental and theoretical curves show a leveling of the electron density below 70.1 km (230 000 ft), the experimental values are greater. The electrostatic probe data envelope shown in the figure includes only those data that are below the 1366 K (2000° F) critical temperature. Although the probe data might be suspect below 70.1 km because of aerodynamic heating, the microwave reflectometer technique does not suffer from this effect.

CONCLUSIONS

Unique high-altitude electrostatic probe measurements have been made on the aft section of two high-velocity reentry spacecraft. Good agreement between the two RAM-C flight probe experiments with strong correlative data from microwave reflectometer and VHF antenna measurements support the following conclusions:

1. High-altitude (above 70 km (230 000 ft) for RAM-C configurations) calculations of electron-density profiles using an inviscid streamtube approach corrected for boundary layer are inadequate and modifications including ambipolar diffusion effects are necessary.
2. Increases in ionization due to phenolic-graphite ablation products in the aft-flow-field boundary layer were no greater than a factor of two over an altitude range of 56.4 to 82.3 km (185 000 to 270 000 ft).
3. Small angle-of-attack motions produce significant peak-to-peak density fluctuations in the aft parts of the flow field. These variations in electron-density profiles can be useful in qualitatively indicating vehicle angle of attack in the high altitudes where accelerometer data are limited.
4. The use of water addition into the flow field as a plasma alleviant is effective in reducing the electron density in the flow field and in alleviating radio blackout.

Langley Research Center,
National Aeronautics and Space Administration,
Hampton, Va., December 20, 1971.

APPENDIX A

ELECTROSTATIC PROBE THEORY

Simplicity makes the electrostatic probe attractive for plasma diagnostics; however, the theoretical interpretation of its current-voltage characteristics is extremely complicated. The difficulty stems from the fact that a probe represents a boundary to a plasma and near this boundary the equations which describe the motion of the charged particles change their character. At the surface of the probe, one polarity of charged particle is collected while the other is repelled; thus, a charge separation region or sheath is created where ion and electron densities differ and hence where large electric fields can be present. A fundamental result of the original theoretical interpretation of probes by Langmuir (ref. 19) is that under many experimental conditions, the sheath may be considered as a thin layer near the probe surface and the plasma appears to be field-free and electrically neutral up to the edge of this well-defined boundary. In recent years considerable progress has been made by the application of computer numerical integration techniques to the analysis of the collection of charged particles in the collisionless case for cylindrical and spherical probes in nonflowing plasmas (refs. 20 to 24). Thus, the artifice of a sheath boundary has been eliminated and the continuous transition from probe surface to ambient plasma is adequately described. Currently, the most realistic collisionless or free-molecular probe theory has been developed by Laframboise (ref. 20) who used the analytical model of Bernstein and Rabinowitz (ref. 21) to calculate the entire probe characteristic for both cylindrical and spherical probes in a Maxwellian plasma at rest. His plasma model consists of positive and negative species of charged particles, each having a Maxwellian velocity distribution with its own characteristic temperature. The analysis was based on the collisionless Boltzmann or Vlasov equations for two species coupled by Poisson's equation for the electric field. These equations are valid for only those conditions where binary collisions are negligible; that is, the collision mean free path is much greater than the probe radius and the plasma Debye length. The electric field, consistent with Poisson's equation, is therefore the dominant influence on the motion of the charged particles.

Flowing Plasmas

The theory for interpreting the response of an electrostatic probe in a plasma with directed flow is considerably more primitive than the classical probe theory just discussed. The available theories for including the effects of flow are oversimplified and their experimental verification are for the most part cursory. Fortunately, positive ion collection with an "infinitely long" cylindrical probe (long enough for end effects to be neglected) aligned parallel to the flow can be interpreted by use of the theory of

APPENDIX A – Continued

Laframboise for nonflowing plasmas. Also, for most experimental conditions, this theory should be applicable for electron collection with any probe orientation because the random velocity of electrons is usually large compared with the directed velocity of the flowing plasma. However, this theory is not applicable for the interpretation of positive ion collection with a cylindrical probe of arbitrary orientation in a flowing plasma. In the following sections, an interpretation for cylindrical probes under these conditions by Scharfman (ref. 12), based on the works of Hok et al. (ref. 14) and Smetana (ref. 15), is presented.

Directed Flow Parallel to Probe

The ion current part of a cylindrical electrostatic probe characteristic has been numerically evaluated by Hok et al. (ref. 14) over a large range of ion densities and electron temperatures for a nonflowing plasma which is also applicable to a plasma with the directed flow parallel to the axis of the probe. For the flowing plasma case, it is advantageous to use this theory because it can easily be modified to account for an arbitrary probe orientation. These results are shown graphically in figure 34 as the variation of the normalized current I_n with the normalized potential difference χ_p between the probe and the plasma for selected values of ratio γ of sheath radius a to probe radius R_p . The normalized current is the ratio of the current I_+ collected by a probe to the random ion current I_r . The random ion current is defined by Hok et al. to be the product of the saturation ion current density and the area of the probe and is given by

$$I_r = \frac{ne v_+}{4} (2\pi R_p L)$$

where

n	electron density or ion density
e	magnitude of electronic charge
R_p	probe radius
L	probe length
v_+	velocity of ions entering sheath

APPENDIX A – Continued

The velocity v_+ is defined to be

$$v_+ = \sqrt{\frac{8kT_e}{\pi M}} \quad (A1)$$

where

k Boltzmann's constant

T_e mean electron temperature

M ion mass

It is to be noted that in equation (A1) the electron temperature T_e is used rather than the ion temperature. This departure from the classical definition for the mean thermal speed is the result of incomplete shielding of the probe sheath. Thus, a total potential drop of order of magnitude kT_e exists in the plasma and accelerates the ions into the probe sheath (ref. 25).

The normalized potential difference χ_p between the probe and the plasma is a dimensionless parameter defined as

$$\chi_p = \frac{e(V - V_\infty)}{kT_e}$$

where

V probe potential

V_∞ plasma potential

Before Hok's results (fig. 34) can be used to interpret experimental probe data, the ratio γ of sheath to probe radii must be known. The ion sheath radius a is defined as

$$a = R_p + d_s$$

where d_s is the sheath thickness. For a planar probe geometry, the sheath thickness varies directly as the probe potential and inversely as the ion density and is given by

$$d_s = \lambda_D \chi_p^{3/4}$$

where λ_D is the Debye length and is defined as

APPENDIX A – Continued

$$\lambda_D = \left(\frac{\epsilon_0 k T_e}{e^2 n} \right)^{1/2}$$

where ϵ_0 is the permittivity of free space.

The approximation of a planar solution for sheath thickness is applicable to cylindrical probes only when the sheath thickness is small compared with the probe radius. When this is not the case, the ratio γ of the sheath to probe radius may be obtained from an inverted form of the Child-Langmuir 3/2-power law for space-charge-limited current flow. This relation has been derived by Hok for cylindrical probes and is plotted in figure 35 as $\gamma - 1$ against Θ where Θ is defined as

$$\Theta = \frac{L}{I_+ R_p} \left(V' + \frac{5kT_e}{e} \right)^{3/2} \left(1 + \frac{2.66}{\sqrt{\chi_p}} \right) \quad (A2)$$

and

I_+ measured probe current

V' absolute magnitude of applied probe bias

To give more physical significance to the current collection curves shown in figure 34, the following asymptotic cases are given:

Case I; thin sheath, $\gamma \approx 1$; $\chi_p < -1$:

$$I_+ = 2\pi R_p L J_i \quad (A3)$$

where J_i is the saturation positive ion current density for a collisionless Maxwellian plasma at rest and is given approximately by Bohm et al. (ref. 26) as

$$J_i = 0.4 n e v_+ \quad (A4)$$

Note that equation (A3) is independent of the applied probe bias.

Case II; moderate to thick sheaths, $\gamma > 1$; large negative probe bias, $\chi_p \ll -\gamma$:

$$I_+ = \gamma 2\pi R_p L J_i \quad (A5)$$

This current varies directly as the applied bias because of γ .

APPENDIX A – Continued

Case III; extremely thick sheaths, $\gamma \gg |\chi_p|$; moderate negative probe bias, $\chi_p < -2$:

$$I_+ = \frac{2}{\sqrt{\pi}} \sqrt{\chi_p + 1} (2\pi R_p L J_i) \quad (A6)$$

In this region the current is approximately proportional to the square root of applied probe bias.

Directed Flow Normal to Probe

The effect of a normally directed ion flux (ions/unit area) on the current collected by free molecular cylindrical probes has been analyzed by several investigators. (See refs. 12, 15, 27, and 28.) If it is assumed that the flow does not distort the form of the ion sheath around the probe, the current density is the result of a superposition of random and directed ion fluxes (ref. 12). This effect is illustrated by figure 36, a curve of the normalized current I_n collected by a cylindrical probe not alined with the flow plotted against the ion speed ratio S . The speed ratio is defined as the normal component v_f of the flow velocity v_{flow} divided by the random thermal velocity v_+

$$S = \frac{v_f}{v_+} \quad (A7)$$

In figure 36 there are two asymptotes shown as dashed lines. The horizontal asymptote represents the value of current collected by a thin-sheathed ($\gamma \approx 1$) probe in a nonflowing plasma and is equal to the random current I_r or to a normalized current of unity. The other asymptote represents the superposition of the random current I_r and a directed current I_d . The directed current is

$$I_d = ne v_f (2R_p L) = \rho v_f A \quad (A8)$$

where

ρ charge density

A projected area of probe

When the normal component of the flow velocity is small ($S \ll 1$), the probe current is approximately that collected in a nonflowing plasma. For larger values of the normal component of flow velocity, that is, $S > 3$, the current collected by the probe approaches the value given in equation (A8).

When the ion sheath is not thin, that is, $\gamma > 1$, the problem is more complicated because the ability of the relatively weak electrostatic potential field around the probe to

APPENDIX A – Continued

capture ions with increased inertial energy due to the flow is reduced. This problem was treated by Smetana (ref. 15) and the results are shown in figure 37.

Scharfman (ref. 12) gives the following qualitative explanation of Smetana's results: For the nonflowing plasma case ($S = 0$) with low values of applied bias ($\chi_p > -1$) and a large sheath thickness ($\gamma \gg 1$), the attraction of the probe's potential field is weak; consequently, most of the ions that enter the sheath orbit past the probe and are not collected. By using simple orbital theory, the radius r_a at which particles will just be collected is

$$r_a = R_p \left(1 + \frac{V}{V_o} \right)^{1/2}$$

where

V probe potential

V_o initial energy of ion entering sheath, kT_e/e

Thus, the current is proportional to the flux (ions/unit area) entering the sheath at the radius r_a and is proportionally given as

$$I_+ \propto nV_o^{1/2} R_p \left(1 + \frac{V}{V_o} \right)^{1/2}$$

In the limit of large applied potential ($\chi_p \ll -1$),

$$I_+ \propto V^{1/2} R_p$$

When a directed velocity is included ($S > 0$), the flux is proportional to $SV_o^{1/2}$ and the capture radius becomes

$$r_a = R_p \left(1 + \frac{V}{S^2 V_o} \right)^{1/2}$$

Thus, the effective capture radius for ions decreases while the flux increases. Therefore,

$$I_+ \propto nSV_o^{1/2} R_p \left(1 + \frac{V}{S^2 V_o} \right)^{1/2}$$

In the limit of large applied potentials ($\chi_p \ll -S^2$), this relationship reduces to the same value as when $S = 0$; that is,

APPENDIX A – Continued

$$I_+ \propto V^{1/2} R_p$$

In the limit of large directed velocity ($S \gg 1$), I_n approaches S in value, and the current I_+ is approximately given by equation (A8).

With this understanding of current collection under directed velocity conditions and with the asymptotic solutions for $S = 0$ and $S \gg 1$, the works of Hok and Smetana can be combined by a transformation of the coordinates of figure 34. This result from Scharfman is replotted in figure 38 as the variation of R with H where

$$R = \frac{I_n}{(1 + S^2)^{1/2}} \quad (A9)$$

$$H = \frac{\chi_p}{1 + S^2} \quad (A10)$$

where

R modified normalized probe current

H ratio of modified potential energy to kinetic energy

The results presented in figure 38 can be readily used to infer positive ion density n by the following algorithm:

- (1) Determine T_e
- (2) Measure the probe current I_+ at V' volts below floating potential
- (3) Calculate the normalized probe to plasma potential

$$\chi_p = \left(\frac{eV'}{kT_e} \right) + 5 \pm 0.5 \quad (A11)$$

- (4) Calculate Θ by use of equation (A2)
- (5) Obtain the appropriate value of γ from figure 35
- (6) Calculate v_+ by using equation (A1)
- (7) Calculate S by using equation (A7)
- (8) Calculate H by using equation (A10)

APPENDIX A – Continued

(9) Obtain the appropriate value of R from figure 38

(10) Calculate the positive ion density from

$$n = \frac{I_+}{\sqrt{1 + S^2 R \sqrt{\pi} e v_+ R_p L}}$$

Interpretation of RAM-C Fixed-Bias Electrostatic Probe Data

The configuration of the RAM-C electrostatic probe is shown in figure 6(b). In relation to the flowing plasma, each ion collector appears to be a cylindrical wire 0.0254 cm (0.010 in.) in diameter and 0.5385 cm (0.212 in.) long, which is inclined at an angle of 45° with respect to the plasma flow. To illustrate the data-reduction procedure, a sample calculation is presented.

Sample Calculation

The following factors are given in the sample calculation:

Altitude, km (ft)	76.2 (250 000)
Ion collector	8
Potential of probe below floating potential, V' , volts	5
Temperature, T , K	7500
Flow velocity, v_{flow} , km/sec (ft/sec)	5160 (16 930)
Angle between flow velocity and probe axis, θ , deg	45
Ion mass (NO^+), M , g	49.88×10^{-24}
Measured current, I_+ , μA	50
Probe length, L , cm (in.)	0.5385 (0.212)
Probe radius, R_p , cm (in.)	0.0127 (0.005)
Boltzmann constant, k , J/K	1.38044×10^{-23}
Electronic charge, e , coulombs	1.5921×10^{-19}

For an altitude of 76.2 km (250 000 ft) and ion collector 8, the temperature was calculated to be 7500 K. The electron temperature is assumed to be equal to the local gas temperature. A plot of gas temperature as a function of altitude for the ion collector locations is shown in figure 39. These temperature data, as well as the flow velocity data given in figure 40, were generated by a nonequilibrium boundary-layer-corrected flow-field analysis of the RAM C-I trajectory.

APPENDIX A – Concluded

The first factor to be calculated is the normalized potential difference between the probe and the plasma by using equation (A11)

$$\chi_p = \frac{eV'}{kT_e} + 5 = 12.69$$

Next, the ratio of ion sheath radius to probe radius γ is estimated by using figure 35 and equation (A2)

$$\Theta = \frac{L}{I_+ R_p} \left(V' + \frac{5kT_e}{e} \right)^{3/2} \left(1 + \frac{2.66}{\sqrt{\chi_p}} \right)$$

For a measured current of $50 \mu A$, the value of Θ is 3.51×10^7 volts^{3/2}/ampere. The corresponding ratio of sheath radius to probe radius γ is 2.61.

The modified normalized probe current R is now determined. Figure 38 is a plot of R as a function of the ratio of modified potential energy to kinetic energy H (eq. (A10)) which is defined as

$$H = \frac{\chi_p}{1 + S^2}$$

The velocity of ions entering the sheath v_+ is calculated (eq. (A1)) to be

$$v_+ = \left(\frac{2kT_e}{M} \right)^{1/2} = 2.037 \times 10^5 \text{ cm/sec}$$

The ion speed ratio S is (from eq. (A7))

$$S = \frac{v_f}{v_+} = \frac{v_{\text{flow}} \sin \theta}{v_+}$$

From equation (A7), $S = 1.791$ and thus the value of H is 3.015. The corresponding value of R is 1.93 from figure 38.

Solving for the density n yields

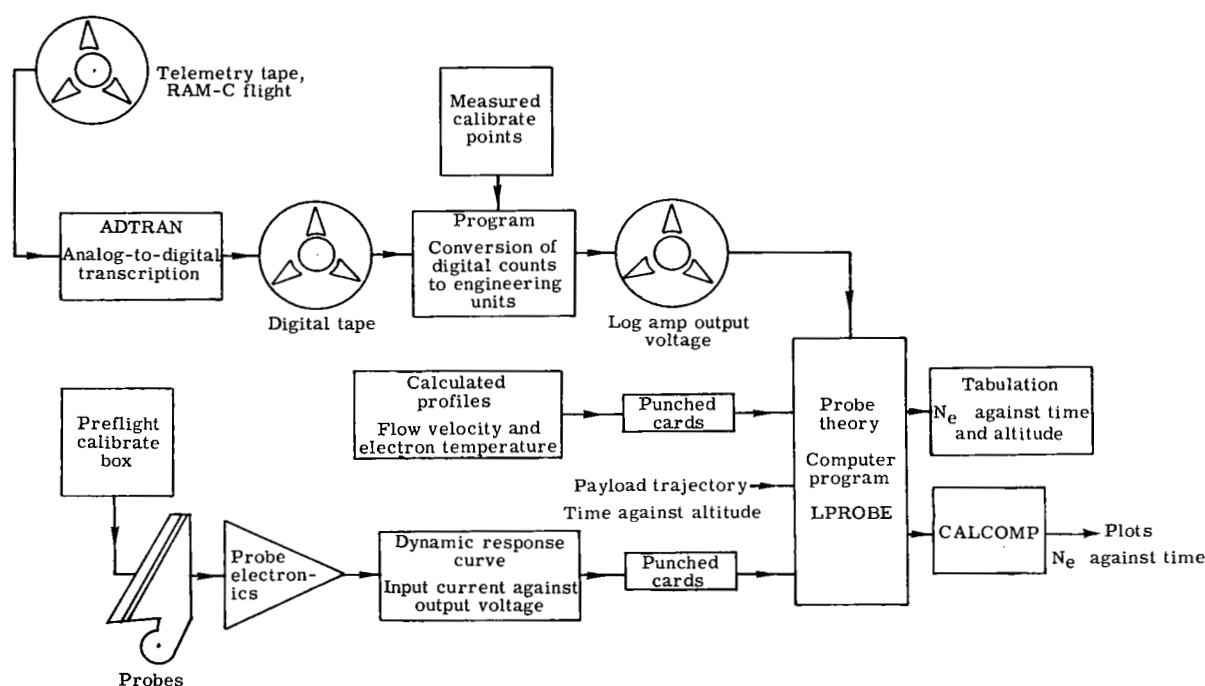
$$n = \frac{I_+}{\sqrt{1 + S^2} R \sqrt{\pi} e v_+ R_p L} = 3.21 \times 10^{10} \text{ cm}^{-3}$$

APPENDIX B

ELECTROSTATIC-PROBE AUTOMATIC DATA REDUCTION PROCEDURE AND LISTINGS

By Lorraine F. Satchell
Langley Research Center

This appendix outlines the method for inferring electron density from telemetry data for the RAM-C flight experiments. The theoretical interpretation used was that of Scharfman (based on the works of Smetana and Hok) as presented in appendix A. A flow chart that illustrates the data-reduction procedure follows:



Telemetry signals containing the electrostatic probe data were recorded by ground receiving stations on magnetic tape. These data were in an analog—frequency-modulation form which consisted of subcarrier oscillator frequency deviations as a function of logarithmic amplifier output voltage. The format for this commutated probe data is given in figure 10. An analog-to-digital transcription made from magnetic telemetry tape data was converted to engineering units to be used as inputs to the probe theory computer program named LPROBE. LPROBE also required, as input data, theoretical flow-field velocities

APPENDIX B – Continued

and electron temperatures for each probe location, as functions of elapsed flight time and altitude, and preflight probe-electronic system calibration. Sufficient points from curves of these input data were tabulated and a second-order interpolation using FTLUP, a table look-up subroutine, provided the desired accuracy.

LPROBE was written in Fortran IV language for the Control Data 6000 series computer. The formats for the program inputs were flight time (FLTIME), delta time (DELTAT), synchronization code (ISYNC), and 24 channels of voltage and 24 channels of current. DNSTY was a subroutine with all tabular data listed internally. LPROBE provided the data in the call sequence and DNSTY computed the electron density. The outputs of LPROBE were CALCOMP plots (figs. 13, 14, 17, and 18) and/or tabulations of electron density (electrons/cm³) as a function of time for each probe.

Presented in this appendix are: a listing of the program, logarithmic amplifier calibrates (output voltage as a function of input current in microamperes) for the two flights, tables of computed gas temperatures (for altitudes in thousands of feet), flow velocity calculations (as a function of time) for each of the probes, and tabulations of computed electron density as a function of time for each of the probes for both RAM C-I and RAM C-II.

```

C          *CALL SEQUENCE FOR SUBROUTINE DNSTY*                                LFS 250
C                                                                                   LFS 260
C  TE=ELECTRON TEMPERATURE,DEGREES KELVIN(COMPUTED FROM TABLES VS. TIME)      LFS 270
C                                                                                   LFS 280
C  TI=ION TEMPERATURE(NOT USED-DUMMY IN CALL STATEMENT)                        LFS 290
C                                                                                   LFS 300
C  PDMILL(DIAMETER OF PROBE)=10.0 MILLS                                         LFS 310
C                                                                                   LFS 320
C  PLMILL(LENGTH OF PROBE)=212.0 MILLS                                         LFS 330
C                                                                                   LFS 340
C  AV  POTENTIAL CC IS MEASURED WITH RESPECT TO PLASMA POTENTIAL.                LFS 350
C                                                                                   LFS 360
C  CC  ION SATURATION CURRENT,MICRCAMPS (COMPUTED VALUES).                     LFS 370
C                                                                                   LFS 380
C  AMU(ION MASS)=28.0 AMU                                                         LFS 390
C                                                                                   LFS 400
C  ANG(ORIENTATION ANGLE OF PROBE)=45.0 DEGREES OR .78539816 RADIANS            LFS 410
C                                                                                   LFS 420
C  FLOVEL(FLOW-VELOCITY) IN M/SEC. (COMPUTED FROM TABLES VS. TIME)             LFS 430
C                                                                                   LFS 440
C  AN(ELECTRON DENSITY) COMPUTED USING SUBROUTINE DNSTY.                        LFS 450
C                                                                                   LFS 460
C  THERE ARE 8 PROBES-EACH SAMPLES THE DATA 3 TIMES PER FLIGHT TIME.           LFS 470
C  SEE FIGURE 11 AND TABLE BELOW.                                              LFS 480
C  DATA(1,09,17) ARE PROBE 1 (FTLUP USES CORRECTED TIME,TEMP1 AND VF 1)        LFS 490
C  DATA(2,10,18) ARE PROBE 2 (FTLUP USES CORRECTED TIME,TEMP2 AND VF 2)        LFS 500
C  DATA(3,11,19) ARE PROBE 3 (FTLUP USES CORRECTED TIME,TEMP3 AND VF 3)        LFS 510
C  DATA(4,12,20) ARE PROBE 4 (FTLUP USES CORRECTED TIME,TEMP4 AND VF 4)        LFS 520
C  DATA(5,13,21) ARE PROBE 5 (FTLUP USES CORRECTED TIME,TEMP5 AND VF 5)        LFS 530
C  DATA(6,14,22) ARE PROBE 6 (FTLUP USES CORRECTED TIME,TEMP6 AND VF 6)        LFS 540
C  DATA(7,15,23) ARE PROBE 7 (FTLUP USES CORRECTED TIME,TEMP7 AND VF 7)        LFS 550
C  DATA(8,16,24) ARE PROBE 8 (FTLUP USES CORRECTED TIME,TEMP8 AND VF 8)        LFS 560
C                                                                                   LFS 570
C          REAL N3(600)                                                           LFS 580
C                                                                                   LFS 590

```

APPENDIX B - Continued

```

DIMENSION VOLTS(50),CUR(50),TIMEA(40),ALTA(40),TEMP(40,8),TIMEB(40,LFS 600
1),ALTB(40),VF(40,8),FLTIME(200),VOLTAGE(200,24),CURRENT(200,24), LFS 610
1ISYNC(200),DELTAT(200),TIME(600),CLRR(600) LFS 620
C LFS 630
EQUIVALENCE (TIMEA,TIMEB),(ALTA,ALTB) LFS 640
C LFS 650
INITIALIZE PLOTTER. LFS 660
CALL CALCCMP LFS 670
C LFS 680
USE PAPER 300 - SET PEN ON RIGHT MARGIN - SET ORIGIN. LFS 690
CALL CALPLT(C.0,I.0,-3) LFS 700
C LFS 710
PRINT CONSTANTS. LFS 720
SIZE=.1 LFS 730
SIZED2=SIZE/2.0 LFS 740
W=(6./7.)*SIZE LFS 750
SIZED=SIZE+SIZED2 LFS 760
C LFS 770
DATA CONSTANTS $ CAYOEP=K/EPSILON LFS 780
PDMILL=1C.0 LFS 790
PLMILL=212.0 LFS 800
AMII=28.00 LFS 810
ANG=.78539816 LFS 820
E=5.0 LFS 830
CAYOEP=.0C0138054/1.60210 LFS 840
C LFS 850
READ,STORE AND WRITE VOLTAGE VS. CURRENT FROM LOG-AMP CURVES(814 LFS 860
C RAM C-I AND 813 RAM C-II)(DYNAMIC INPUT-OUTPUT CURVES) LFS 870
WRITE(6,1) LFS 880
1 FORMAT(*1 VOLTAGE CURRENT LOG-AMP 814*/) LFS 890
CO 10 I=1,50 LFS 900
READ(5,3)VOLTS(I),CUR(I) LFS 910
3 FORMAT(2F10.3) LFS 920
WRITE(6,3)VOLTS(I),CUR(I) LFS 930
10 CONTINUE LFS 940
C LFS 950
READ,STORE AND WRITE TIME AND ALTITUDE VS. TEMPERATURE (1 THRU 8) LFS 960
C (COMPUTED ELECTRON OR GAS TEMPERATURE AS A FUNCTION OF ALTITUDE LFS 970
C FOR ELECTROSTATIC PROBE LOCATIONS ON RAM C-I AND RAM C-II) LFS 980
C LFS 990
WRITE(6,11) LFS 1000
11 FORMAT(*1 TIME ALT TEMP1 TEMP2 TEMP3 TEM LFS 1010
1F4 TEMP6 TEMP7 TEMP8*/) LFS 1020
CO 20 I=1,40 LFS 1030
READ(5,12)TIMEA(I),ALTA(I),(TEMP(I,J),J=1,8) LFS 1040
12 FORMAT(2F8.1,8F8.3) LFS 1050
WRITE(6,13)TIMEA(I),ALTA(I),(TEMP(I,J),J=1,8) LFS 1060
13 FORMAT(2F10.1,8F10.3) LFS 1070
20 CONTINUE LFS 1080
C LFS 1090
READ,STORE AND WRITE TIME AND ALTITUDE VS. FLOW VELOCITY (1 THRU 8) LFS 1100
C (COMPUTED VELOCITY AS A FUNCTION OF ALTITUDE). LFS 1110
WRITE(6,21) LFS 1120
21 FORMAT(*1 TIME ALT VF1 VF2 VF3 VLFS 1130
1F4 VF5 VF6 VF7 VF8*/) LFS 1140
CO 30 I=1,40 LFS 1150
READ(5,12)TIMEB(I),ALTB(I),(VF(I,J),J=1,8) LFS 1160
WRITE(6,13)TIMEB(I),ALTB(I),(VF(I,J),J=1,8) LFS 1170
30 CONTINUE LFS 1180
C LFS 1190
READ AND STORE DATA FROM FLIGHTS (RAM C-I REEL 214009 AND RAM CII LFS 1200
C REEL 314026). LFS 1210
I=1 LFS 1220
60 READ(8)FLTIME(I),ISYNC(I),DELTAT(I),(VOLTAGE(I,J),J=1,24),(CURRENT LFS 1230
1(I,J),J=1,24) LFS 1240
IF(EOF,8)75,65 LFS 1250
65 I=I+1 LFS 1260
GO TO 60 LFS 1270

```

APPENDIX B - Continued

75	REWIND 8	LFS 1280
	CALL EVICT(5LTAPE8)	LFS 1290
	IPTS=1	LFS 1300
C		LFS 1310
C	CCOMPUTE DATA BY PROBES	LFS 1320
	CO 300 IPROBE=1,8	LFS 1330
C		LFS 1340
C	HEADINGS FOR DATA	LFS 1350
	NPTS=0	LFS 1360
	WRITE(6,76)	LFS 1370
76	FORMAT(*1PROBE DIMETER=10 MILS PROBE LENGTH=212 MILS IJN MASL	LFS 1380
	IS=28 AMU ORIENTATION ANGLE=.78539816 RADIANS*/)	LFS 1390
	WRITE(6,77)	LFS 1400
77	FORMAT(*OPROBE FL TIME SYNC VOLTAGE CURRENT ALTITUDE TEMPER	LFS 1410
	LATURE F-VELOCITY AV TIME ELECTRON DNSTY LOG(N3)*)	LFS 1420
	IF(IPROBE.EQ.1)GO TO 81	LFS 1430
	IF(IPROBE.EQ.2)GO TO 82	LFS 1440
	IF(IPROBE.EQ.3)GO TO 83	LFS 1450
	IF(IPROBE.EQ.4)GO TO 84	LFS 1460
	IF(IPROBE.EQ.5)GO TO 85	LFS 1470
	IF(IPROBE.EQ.6)GO TO 86	LFS 1480
	IF(IPROBE.EQ.7)GO TO 87	LFS 1490
	IF(IPROBE.EQ.8)GO TO 88	LFS 1500
81	M1=1	LFS 1510
	M2=17	LFS 1520
	NO=-11	LFS 1530
	GO TO 90	LFS 1540
82	M1=2	LFS 1550
	M2=18	LFS 1560
	NO=-12	LFS 1570
	GO TO 90	LFS 1580
93	M1=3	LFS 1590
	M2=19	LFS 1600
	NO=-13	LFS 1610
	GO TO 90	LFS 1620
84	M1=4	LFS 1630
	M2=20	LFS 1640
	NO=-14	LFS 1650
	GO TO 90	LFS 1660
95	M1=5	LFS 1670
	M2=21	LFS 1680
	NO=-15	LFS 1690
	GO TO 90	LFS 1700
86	M1=6	LFS 1710
	M2=22	LFS 1720
	NO=-16	LFS 1730
	GO TO 90	LFS 1740
87	M1=7	LFS 1750
	M2=23	LFS 1760
	NO=-17	LFS 1770
	GO TO 90	LFS 1780
88	M1=8	LFS 1790
	M2=24	LFS 1800
	NO=-18	LFS 1810
C		LFS 1820
C	TI IS A DUMMY IN CALL STATEMENT TO SUBROUTINE DNSTY.	LFS 1830
90	TI=1.0	LFS 1840
	IS=1	LFS 1850
	CO 100 I=1,IPTS	LFS 1860
	IF(ISYNC(I).EQ.1)GO TO 100	LFS 1870
	IF(ISYNC(I).EQ.2)GO TO 100	LFS 1880
	CO 98 J=M1,M2,8	LFS 1890
	JJ=J	LFS 1900
	IF(VOLTAGE(I,J).LT.(-.C80))GO TO 98	LFS 1910
	IF(VOLTAGE(I,J).GT.(5.264))GO TO 98	LFS 1920

APPENDIX B - Continued

```

IF(CURRENT(I,J).LT.(.100))GO TO 98          LFS 1930
IF(CURRENT(I,J).GT.(1000.))GO TO 98          LFS 1940
IF(LEGVAR(VOLTAGE(I,J)))98,91,98             LFS 1950
91 IF(LEGVAR(CURRENT(I,J)))98,92,98           LFS 1960
92 ATIME=FLTME(I)+(FLOAT(JJ))*DELTAT(I)       LFS 1970
IF(ATIME.GT.(406.000))GO TO 98               LFS 1980
NPTS=NPTS+1                                  LFS 1990
TIME(NPTS)=ATIME                             LFS 2000
CALL FTLUP(ATIME,ALT,2,40,TIMEB,ALTB)         LFS 2010
ALT=ALT*1000.                                LFS 2020
CC=CURRENT(I,J)                              LFS 2030
CURR(NPTS)=CURRENT(I,J)                      LFS 2040
CALL FTLUP(ATIME,TE,2,40,TIMEA,TEMP(1,I,PCBE)) LFS 2050
TE=TE*1000.                                  LFS 2060
AV=E+5.0*CAVQEP*TE                           LFS 2070
CALL FTLUP(ATIME,FLOVEL,2,40,TIMEB,VF(1,I,PROBE)) LFS 2080
FLCVEL=FLCVEL*1000.                          LFS 2090
CALL DNSTY(TE,TI,PD MILL,PLMILL,CC,AV,AMII,ANG,FLOVEL,AN) LFS 2100
N3(NPTS)=ALOG10(AN)                          LFS 2110
WRITE(6,96)I,PROBE,J,FLTME(I),ISYNC(I),VOLTAGE(I,J),CC,ALT,TE, LFS 2120
1 FLOVEL,AV,TIME(NPTS),AN,N3(NPTS)            LFS 2130
96 FORMAT(I2,I4,F9.3,I5,2F10.3,F10.1,2F13.3,F10.3,F8.3,E16.6,F12.6) LFS 2140
KPTS=NPTS                                     LFS 2150
IF(MOD(NPTS,40))98,97,98                     LFS 2160
97 WRITE(6,76)                                LFS 2170
WRITE(6,77)                                  LFS 2180
93 CONTINUE                                  LFS 2190
100 CONTINUE                                  LFS 2200
NPTS=KPTS                                    LFS 2210
C                                             LFS 2220
C SCALE DATA TO BE PLOTTED                  LFS 2230
DO 110 I=1,NPTS                              LFS 2240
TIME(I)=TIME(I)-386.C                         LFS 2250
N3(I)=(N3(I)-7.0)*2.5                         LFS 2260
CURR(I)=(1.0+ALOG10(CURR(I)))*2.5            LFS 2270
110 CONTINUE                                  LFS 2280
C                                             LFS 2290
C PLOT TIME VS. ELECTRON DENSITY (N3) AND TIME VS. CURRENT (CURR). LFS 2300
DO 200 I,PLT=1,2                             LFS 2310
C                                             LFS 2320
C DRAW X-AXIS AND LOGRID                     LFS 2330
CALL AXES(0.0,0.0,0.0,21.0,386.,1.0,1.0,.5,9,HTIME,SEC.,.15,-9) LFS 2340
CALL LOGRID(21.0,2.5,-1.6,0.C,1.0,.5,.2)     LFS 2350
C                                             LFS 2360
C GENERAL IDENTIFICATION OF Y-AXIS           LFS 2370
CALL CALPLT(0.0,15.0,2)                      LFS 2380
CALL CALPLT(0.0,0.0,3)                      LFS 2390
CALL NOTATE(-.3,0.0,SIZE,6HPROBE ,90.0,6)     LFS 2400
NPROBE=I,PROBE                               LFS 2410
XPROBE=NPROBE                                LFS 2420
CALL NUMBER(-.3,(0.0+(5.0*W)),SIZE,XPROBE,90.0,-1) LFS 2430
CALL NCTATE(-.75,0.,SIZE,7HRA C-A,90.0,7)     LFS 2440
IF(I,PLT.EQ.2)GO TO 140                      LFS 2450
CALL NCTATE(-.2,6.5,.15,8HELECTRON,90.0,8)    LFS 2460
CALL NOTATE(-.2,7.7,.15,7HDENSITY,90.0,7)     LFS 2470
C                                             LFS 2480
C TIME VS. N3                                LFS 2490
DO 120 I=1,NPTS                              LFS 2500
CALL FNTPLT(TIME(I),N3(I),NO,IS)              LFS 2510
120 CONTINUE                                  LFS 2520
GO TO 190                                     LFS 2530
C                                             LFS 2540
C TIME VS. CURRENT                          LFS 2550
140 CALL NCTATE(-.2,7.1,.15,7HCURRENT,90.0,7) LFS 2560
DO 180 I=1,NPTS                              LFS 2570
CALL FNTPLT(TIME(I),CURR(I),NO,IS)            LFS 2580
180 CONTINUE                                  LFS 2590
C                                             LFS 2600

```


APPENDIX B - Continued

```

C      MOVE TO NEW PLOTTING AREA                                LFS 2610
190 CALL CALPLT(24.0,C.0,-3)                                    LFS 2620
200 CONTINUE                                                    LFS 2630
C      CLEAR CORE FOR NEXT PRJBE.                                LFS 2640
      DC 250 I=1,NPTS                                           LFS 2650
      TIME(I)=0.0                                               LFS 2660
      N3(I)=0.0                                                 LFS 2670
      CURR(I)=0.0                                               LFS 2680
250 CONTINUE                                                    LFS 2690
300 CONTINUE                                                    LFS 2700
C      RELEASE PLOTTER AND STOP.                                  LFS 2710
C      CALL CALPLT(0.0,C.0,999)                                  LFS 2720
      STOP                                                       LFS 2730
      END                                                         LFS 2740
      SURROUTINE DNSTY(TE,TI,PDMILL,PLMILL,CC,AV,AMII,ANG,FLOVEL,AN) LFS 2750
      DIMENSION R(6),C(6),EIF(9)                                LFS 2760
      DIMENSION D(9),E1P5(9),E2(9),E3(9),E5(9),E1C(9),E2C(9),E5C(9) LFS 2770
      DIMENSION G(6),H(8)                                        LFS 2780
      DATA R/5.2,6.,7.,8.,9.,10./                               LFS 2790
      DATA C/-1.,-.61,-.0926,.463,1.083,1.786/                 LFS 2800
      DATA D/-1.,-.5,C.,.5,1.,1.5,2.,2.5,3./                  LFS 2810
      DATA E1P5/.031,.036,.136,6*.175/                         LFS 2820
      DATA E2/.031,.073,.167,.253,5*.300/                      LFS 2830
      DATA E3/.031,.074,.171,.316,.428,4*.475/                LFS 2840
      DATA E5/.031,.074,.191,.35,.521,.654,3*.7/              LFS 2850
      DATA E1C/.031,.074,.191,.37,.58,.755,.919,.988,1./      LFS 2860
      DATA E2C/.031,.074,.191,.37,.58,.802,1.04,1.19,1.29/    LFS 2870
      DATA E5C/.031,.074,.191,.37,.58,.81,1.05,1.28,1.32/     LFS 2880
      DATA EIF/.031,.074,.191,.37,.58,.81,1.06,1.20,1.55/     LFS 2890
      DATA G/.175,.300,.475,.7,1.,1.3,1.7,10./                LFS 2900
      FL=PLMILL*2.54E-5                                           LFS 2910
1 AC=ARS(CC)*1.E-6                                              LFS 2920
C PR=PDMILL*2.54E-5/2. $AMI=AMII*1.672E-27                     LFS 2930
      PR=.5*PDMILL*2.54E-5 $AMI=AMII*1.672E-27                 LFS 2940
C A=AV*11604./TE                                                LFS 2950
      A=ARS(AV*11604./TE)                                         LFS 2960
      T=PL*AV**1.5*(1.+2.66/SQRT(A))/(PR*AC)                    LFS 2970
      T=ALOG10(T)                                                  LFS 2980
      CALL DISCCT(T,T,B,C,C,-20,6,0,ANS)                          LFS 2990
2 AOR=1.+10.**ANS                                                LFS 3000
3 VP=SQRT(2.*1.38E-23*TE/AMI)                                    LFS 3010
4 S=FLOVEL*SIN(ANG)/VP                                           LFS 3020
      T=A/(1.+S*S)                                                 LFS 3030
      T=ALOG10(T)                                                  LFS 3040
      CALL DISCCT(T,T,D,E1P5,E1P5,-20,9,0,ANS1P5)                LFS 3050
      CALL DISCCT(T,T,D,E2,E2,-20,9,0,ANS2)                       LFS 3060
      CALL DISCCT(T,T,D,E3,E3,-20,9,0,ANS3)                       LFS 3070
      CALL DISCCT(T,T,D,E5,E5,-20,9,0,ANS5)                       LFS 3080
      CALL DISCCT(T,T,D,E1C,E1C,-20,9,0,ANS1C)                    LFS 3090
      CALL DISCCT(T,T,D,E2C,E2C,-20,9,0,ANS2C)                    LFS 3100
      CALL DISCCT(T,T,D,E5C,E5C,-20,9,0,ANS5C)                    LFS 3110
      CALL DISCCT(T,T,D,EIF,EIF,-20,9,0,ANSIF)                    LFS 3120
      F(1)=ANS1P5 $ H(2)=ANS2 $ H(3)=ANS3 $ H(4)=ANS5 $ H(5)=ANS1C LFS 3130
      F(6)=ANS2C $ H(7)=ANS5C $ H(8)=ANSIF                        LFS 3140
      ACR=ALOG10(ACR)                                              LFS 3150
      CALL DISCCT(AOR,AOR,G,H,H,-20,8,0,ANS)                      LFS 3160
      ANS=10.**ANS                                                  LFS 3170
      F=ANS*SQRT(1.+S*S)                                           LFS 3180
      AREA=6.28*PR*PL                                              LFS 3190
5 AN=4.*AC/(AREA*F*1.6E-19*SQRT(8.*1.38E-23*TE/(3.14159*AMI))) LFS 3200
      AN=AN*1.E-6                                                 LFS 3210
      RETURN                                                       LFS 3220
      END                                                         LFS 3230

```

APPENDIX B — Continued

PRE-FLIGHT CALIBRATION OF LOGARITHMIC AMPLIFIERS

RAM C-I Logarithmic amplifier, serial number 814		RAM C-II Logarithmic amplifier, serial number 813	
VOLTAGE	CURRENT	VOLTAGE	CURRENT
-.080	.100	-.136	.100
-.060	.570	0.000	.298
-.040	.695	.090	.370
0.000	.754	.240	.450
.055	.830	.495	.580
.150	.922	.780	.720
.305	1.020	.925	.790
.400	1.085	1.115	.870
.545	1.175	1.375	.990
.700	1.260	1.540	1.090
.850	1.340	1.725	1.240
1.055	1.480	1.825	1.340
1.210	1.625	1.950	1.480
1.300	1.725	2.025	1.600
1.480	1.980	2.140	1.800
1.600	2.185	2.215	2.000
1.710	2.450	2.310	2.300
1.800	2.695	2.375	2.550
1.900	3.030	2.500	3.200
1.990	3.400	2.605	4.000
2.100	3.890	2.651	4.500
2.250	4.810	2.715	5.200
2.300	5.220	2.765	6.000
2.385	6.010	2.810	7.000
2.500	7.640	2.865	8.500
2.635	10.490	2.905	10.000
2.800	13.800	2.940	11.000
3.065	20.700	2.980	12.500
3.200	24.900	3.040	14.500
3.300	28.600	3.130	18.500
3.460	33.400	3.175	21.000
3.600	36.600	3.230	23.500
3.750	49.500	3.330	28.500
3.900	58.900	3.430	34.000
4.000	65.500	3.535	40.000
4.200	80.500	3.725	53.000
4.325	92.700	3.880	65.000
4.400	104.500	4.030	79.000
4.530	133.000	4.110	90.000
4.600	162.500	4.170	100.000
4.700	226.000	4.185	132.000
4.755	274.000	4.190	105.000
4.800	302.000	4.225	120.000
4.900	392.000	4.265	140.000
5.000	505.000	4.330	180.000
5.055	579.000	4.480	277.000
5.100	626.000	4.520	310.000
5.170	717.000	4.615	390.000
5.200	770.000	4.770	550.000
5.264	1000.000	5.023	1000.000

RAM C-I AND C-II COMPUTED GAS TEMPERATURES FOR PROBES 1 - 8

TIME	ALT	TEMP1	TEMP2	TEMP3	TEMP4	TEMP5	TEMP6	TEMP7	TEMP8
386.5	302.6	5.870	7.060	8.530	9.900	10.630	11.160	11.690	12.220
387.0	299.2	5.760	7.030	8.500	9.850	10.570	11.120	11.670	12.220
387.5	295.9	5.660	6.990	8.460	9.760	10.490	11.060	11.630	12.200
388.0	292.6	5.570	6.970	8.400	9.660	10.420	10.990	11.560	12.130
388.5	289.4	5.470	6.920	8.360	9.560	10.340	10.900	11.460	12.020
389.0	286.1	5.380	6.880	8.270	9.450	10.250	10.800	11.350	11.900
389.5	282.8	5.280	6.830	8.200	9.320	10.150	10.680	11.210	11.740
390.0	279.6	5.190	6.780	8.120	9.190	10.030	10.570	11.110	11.650
390.5	276.3	5.100	6.720	8.050	9.060	9.850	10.460	11.070	11.550
391.0	273.0	5.000	6.660	7.940	8.900	9.650	10.250	10.850	11.450
391.5	269.8	4.900	6.580	7.840	8.750	9.440	10.050	10.660	11.270
392.0	266.5	4.810	6.510	7.720	8.590	9.220	9.760	10.300	10.840
392.5	263.3	4.700	6.430	7.620	8.440	9.010	9.470	9.930	9.850
393.0	260.0	4.600	6.330	7.490	8.260	8.770	9.120	9.100	8.920
393.5	256.8	4.510	6.230	7.370	8.070	8.530	8.800	8.610	8.380
394.0	253.5	4.400	6.130	7.230	7.870	8.280	8.470	8.200	7.930
394.5	250.3	4.310	6.030	7.080	7.690	8.050	8.180	7.870	7.580
395.0	247.0	4.200	5.910	6.920	7.480	7.760	7.860	7.540	7.240
395.5	243.7	4.100	5.780	6.750	7.260	7.500	7.540	7.230	6.920
396.0	240.4	4.000	5.660	6.670	7.040	7.220	7.230	6.940	6.630
396.5	237.1	3.890	5.520	6.380	6.810	6.930	6.920	6.670	6.360
397.0	233.9	3.800	5.360	6.180	6.550	6.640	6.630	6.360	6.090
397.5	230.6	3.680	5.200	5.970	6.300	6.340	6.350	6.150	5.840
398.0	227.3	3.580	5.040	5.770	6.050	6.070	6.070	5.920	5.620
398.5	224.1	3.480	4.860	5.530	5.770	5.820	5.820	5.710	5.400
399.0	220.8	3.380	4.660	5.280	5.510	5.550	5.550	5.460	5.160
399.5	217.6	3.270	4.460	5.020	5.230	5.300	5.300	5.240	4.940
400.0	214.3	3.180	4.260	4.760	4.950	5.050	5.020	5.020	4.720
400.5	211.0	3.070	4.020	4.460	4.660	4.770	4.800	4.800	4.500
401.0	207.7	2.970	3.770	4.140	4.370	4.490	4.560	4.560	4.280
401.5	204.7	2.870	3.530	3.830	4.090	4.250	4.320	4.320	4.080
402.0	201.1	2.760	3.250	3.480	3.720	3.980	4.110	4.110	3.860
402.5	197.9	2.660	2.960	3.110	3.500	3.750	3.900	3.900	3.650
403.0	194.6	2.550	2.640	2.730	3.210	3.480	3.690	3.690	3.430
403.5	191.4	2.460	2.350	2.380	2.950	3.270	3.490	3.490	3.270
404.0	188.1	2.350	1.990	1.990	2.660	3.030	3.290	3.290	3.030
404.5	184.9	2.240	1.580	1.580	2.360	2.820	3.100	3.100	2.820
405.0	181.6	2.140	1.250	1.250	2.100	2.610	2.910	2.910	2.590
405.5	178.3	2.040	.920	.920	1.840	2.360	2.750	2.750	2.420
406.0	175.1	1.940	.610	.610	1.600	2.120	2.570	2.570	2.200

RAM C-I AND C-II COMPUTED FLOW VELOCITY FOR PROBES 1 - 8

TIME	ALT	VF1	VF2	VF3	VF4	VF5	VF6	VF7	VF8
386.5	302.6	.850	1.070	1.170	1.240	1.310	1.360	1.420	1.470
387.0	299.2	.845	1.110	1.230	1.340	1.440	1.520	1.640	1.720
387.5	295.9	.840	1.140	1.300	1.450	1.600	1.700	1.850	1.970
388.0	292.6	.830	1.180	1.360	1.560	1.730	1.900	2.060	2.230
388.5	289.4	.825	1.200	1.430	1.660	1.880	2.060	2.275	2.450
389.0	286.1	.820	1.240	1.500	1.770	2.010	2.230	2.470	2.660
389.5	282.8	.818	1.270	1.570	1.870	2.150	2.420	2.710	2.910
390.0	279.6	.815	1.300	1.630	1.980	2.310	2.620	2.920	3.160
390.5	276.3	.810	1.330	1.700	2.080	2.430	2.770	3.120	3.400
391.0	273.0	.808	1.370	1.770	2.190	2.570	2.970	3.350	3.590
391.5	269.8	.805	1.400	1.830	2.300	2.720	3.140	3.560	3.860
392.0	266.5	.804	1.430	1.880	2.400	2.850	3.310	3.750	4.110
392.5	263.3	.810	1.460	1.980	2.500	2.980	3.450	3.940	4.350
393.0	260.0	.830	1.490	2.020	2.570	3.070	3.590	4.120	4.580
393.5	256.8	.850	1.520	2.070	2.630	3.160	3.720	4.300	4.780
394.0	253.5	.880	1.560	2.130	2.710	3.260	3.850	4.490	4.980
394.5	250.3	.910	1.600	2.200	2.790	3.370	3.990	4.660	5.180
395.0	247.0	.950	1.650	2.280	2.880	3.480	4.140	4.830	5.380
395.5	243.7	1.000	1.720	2.370	2.980	3.610	4.280	4.990	5.530
396.0	240.4	1.050	1.790	2.470	3.100	3.730	4.430	5.140	5.680
396.5	237.1	1.120	1.880	2.570	3.220	3.880	4.590	5.300	5.840
397.0	233.9	1.180	1.960	2.690	3.360	4.010	4.740	5.440	5.980
397.5	230.6	1.260	2.070	2.830	3.510	4.180	4.890	5.590	6.120
398.0	227.3	1.320	2.180	2.970	3.670	4.340	5.050	5.730	6.230
398.5	224.1	1.410	2.300	3.130	3.840	4.520	5.210	5.860	6.350
399.0	220.8	1.500	2.440	3.320	4.030	4.720	5.370	5.990	6.460
399.5	217.6	1.600	2.600	3.490	4.230	4.900	5.530	6.120	6.570
400.0	214.3	1.700	2.760	3.700	4.460	5.090	5.700	6.230	6.660
400.5	211.0	1.800	2.950	3.940	4.700	5.310	5.860	6.340	6.750
401.0	207.7	1.930	3.150	4.200	4.970	5.540	6.020	6.450	6.830
401.5	204.4	2.050	3.370	4.480	5.250	5.770	6.190	6.550	6.920
402.0	201.1	2.170	3.630	4.800	5.580	6.020	6.370	6.670	6.980
402.5	197.9	2.290	3.780	5.020	5.760	6.150	6.480	6.750	7.020
403.0	194.6	2.420	3.940	5.230	5.870	6.230	6.570	6.800	7.050
403.5	191.4	2.530	4.050	5.380	5.950	6.290	6.620	6.830	7.070
404.0	188.1	2.640	4.160	5.490	6.030	6.350	6.650	6.870	7.090
404.5	184.9	2.760	4.250	5.570	6.090	6.400	6.680	6.890	7.100
405.0	181.6	2.880	4.330	5.640	6.130	6.440	6.710	6.900	7.110
405.5	178.3	2.990	4.410	5.700	6.170	6.480	6.730	6.910	7.110
406.0	175.1	3.110	4.490	5.740	6.200	6.500	6.750	6.920	7.110

APPENDIX B - Continued

APPENDIX B - Continued

TABULATIONS OF CURRENT AND INFERRED ELECTRON DENSITY RAM C-I, PROBE 1

ELAPSED TIME, SECONDS	ALTITUDE, FEET	CURRENT, MICROAMPS	ELECTRON DENSITY, ELECTRONS PER CUBIC CENTIMETER	ELAPSED TIME, SECONDS	ALTITUDE, FEET	CURRENT, MICROAMPS	ELECTRON DENSITY, ELECTRONS PER CUBIC CENTIMETER	ELAPSED TIME, SECONDS	ALTITUDE, FEET	CURRENT, MICROAMPS	ELECTRON DENSITY, ELECTRONS PER CUBIC CENTIMETER	ELAPSED TIME, SECONDS	ALTITUDE, FEET	CURRENT, MICROAMPS	ELECTRON DENSITY, ELECTRONS PER CUBIC CENTIMETER
386.785	286049	0.443	3.99E+08	393.356	257732	1.920	2.79E+09	396.830	234907	1.016	6.75E+09	402.492	197950	175.000	2.75E+11
389.820	280704	0.443	4.00E+08	393.401	257440	10.153	8.44E+09	396.875	234708	17.430	1.70E+10	402.518	197882	151.500	2.31E+11
389.880	280375	0.443	4.00E+08	393.427	257274	11.361	9.71E+09	396.901	234541	16.359	1.60E+10	402.544	197814	138.000	2.08E+11
389.926	280085	0.443	4.00E+08	393.452	257107	12.331	1.08E+10	396.927	234374	14.791	1.41E+10	402.569	197746	125.000	1.77E+11
389.976	279753	0.443	4.00E+08	393.477	256881	11.086	1.01E+10	396.972	234081	9.817	8.44E+09	402.615	197511	113.000	1.61E+11
390.021	279462	0.443	4.00E+08	393.523	256610	11.348	1.01E+10	397.008	233788	29.343	3.42E+10	402.640	196883	1.120	7.14E+08
390.047	279205	0.443	4.00E+08	393.548	256481	12.438	1.09E+10	397.023	233748	29.343	3.42E+10	402.671	196689	1.190	7.87E+08
390.072	278918	0.443	3.98E+08	393.594	256186	11.902	1.03E+10	397.068	233456	29.343	3.42E+10	402.711	196517	0.980	6.48E+08
390.117	278635	0.443	3.98E+08	393.620	256016	11.578	9.97E+09	397.095	233287	32.913	3.92E+10	402.738	196345	1.710	1.14E+09
390.143	278364	0.443	4.00E+08	393.646	255847	9.819	8.13E+09	397.120	233117	32.323	3.83E+10	402.763	196169	1.420	9.29E+08
390.215	278102	0.443	4.00E+08	393.691	255550	7.754	6.10E+09	397.145	232948	32.323	3.83E+10	402.789	195993	1.230	8.05E+08
390.240	277829	0.443	4.00E+08	393.717	255381	6.819	5.24E+09	397.191	232653	1.147	7.65E+09	402.834	195682	1.370	8.27E+08
390.266	277545	0.443	4.00E+08	393.742	255213	9.472	7.70E+09	397.216	232484	1.215	8.15E+09	402.879	195388	94.000	1.27E+11
390.310	277262	0.443	4.00E+08	393.787	254922	11.252	9.45E+09	397.261	232177	0.942	6.24E+09	402.905	195219	109.000	1.32E+11
390.336	276982	0.443	4.00E+08	393.813	254724	13.074	1.10E+10	397.286	232011	1.033	6.86E+09	402.931	195050	113.320	1.35E+11
390.362	276711	0.443	4.00E+08	393.838	254556	13.180	1.10E+10	397.311	231846	0.942	6.24E+09	402.978	194745	153.500	2.10E+11
390.387	276441	0.443	4.00E+08	393.883	254262	13.848	1.15E+10	397.367	231556	1.463	7.20E+09	403.002	194486	185.200	2.49E+11
390.433	276164	0.443	4.00E+08	393.909	254093	13.301	1.42E+10	397.381	231387	2.522	1.76E+10	403.078	194118	222.000	3.14E+11
390.458	275895	0.443	4.00E+08	393.935	253922	12.651	1.12E+10	397.406	231218	1.453	1.28E+10	403.078	194118	222.000	3.14E+11
390.503	275618	0.443	4.00E+08	393.980	253629	12.883	1.14E+10	397.451	230922	1.483	1.35E+10	403.099	193960	167.500	2.54E+11
390.528	275344	0.443	4.00E+08	394.006	253462	15.301	1.42E+10	397.477	230753	1.170	1.05E+10	403.124	193794	138.000	2.01E+11
390.553	275064	0.443	4.00E+08	394.031	253296	12.648	1.10E+10	397.503	230584	1.170	1.05E+10	403.149	193626	5.220	3.87E+08
390.597	274785	0.443	4.00E+08	394.076	253006	13.180	1.10E+10	397.548	230282	22.000	2.31E+10	403.195	193339	1.330	6.77E+08
390.623	274508	0.443	4.00E+08	394.102	252840	17.067	1.64E+10	397.574	230113	25.403	2.98E+10	403.221	193173	2.420	1.49E+09
390.649	274231	0.443	4.00E+08	394.127	252674	14.756	1.37E+10	397.599	229944	25.403	2.98E+10	403.246	193009	3.470	1.82E+09
390.674	273954	0.443	4.00E+08	394.172	252381	34.159	3.99E+10	397.644	229648	28.503	3.20E+10	403.292	192745	70.000	1.93E+10
390.720	273674	0.443	4.00E+08	394.197	252214	21.492	2.33E+10	397.669	229479	21.492	2.33E+10	403.317	192580	1.170	1.05E+09
390.745	273401	0.443	4.00E+08	394.222	252048	29.588	3.32E+10	397.694	229310	29.588	3.32E+10	403.342	192415	1.170	1.05E+09
390.791	273124	0.443	4.00E+08	394.265	251815	11.200	9.66E+09	397.741	229008	30.003	3.48E+10	403.388	192177	120.000	1.67E+11
390.816	272847	0.443	4.00E+08	394.310	251521	11.200	9.66E+09	397.767	228839	30.253	3.52E+10	403.413	191941	128.000	1.81E+11
390.841	272571	0.443	4.00E+08	394.316	251487	13.000	1.10E+10	397.793	228674	28.503	3.20E+10	403.438	191705	160.000	2.37E+11
390.885	272294	0.443	4.00E+08	394.361	251198	15.600	1.40E+10	397.818	228506	27.250	3.15E+10	403.484	191469	2.590	1.49E+09
390.911	272017	0.443	4.00E+08	394.387	251033	15.848	1.42E+10	397.864	228185	21.492	2.33E+10	403.509	191233	175.000	2.43E+11
390.937	271741	0.443	4.00E+08	394.417	250868	16.000	1.52E+10	397.891	228014	13.003	1.25E+10	403.556	191047	215.000	3.36E+11
390.982	271464	0.443	4.00E+08	394.447	250703	17.200	1.60E+10	397.916	227845	13.003	1.25E+10	403.581	190861	255.000	4.28E+11
391.007	271187	0.443	4.00E+08	394.493	250412	16.700	1.49E+10	397.941	227676	16.700	1.49E+10	403.606	190675	295.000	5.20E+11
391.053	270910	0.443	4.00E+08	394.538	250121	15.400	1.47E+10	397.968	227507	34.076	4.07E+10	403.631	190489	335.000	6.12E+11
391.078	270633	0.443	4.00E+08	394.584	249830	14.400	1.31E+10	397.993	227338	34.076	4.07E+10	403.656	190303	375.000	7.04E+11
391.103	270356	0.443	4.00E+08	394.629	249539	14.400	1.31E+10	398.018	227169	34.076	4.07E+10	403.681	190117	415.000	7.96E+11
391.128	270079	0.443	4.00E+08	394.674	249248	13.000	1.17E+10	398.043	226999	34.076	4.07E+10	403.706	189931	455.000	8.88E+11
391.153	269802	0.443	4.00E+08	394.719	248957	11.400	1.03E+10	398.068	226829	34.076	4.07E+10	403.731	189745	495.000	9.80E+11
391.178	269525	0.443	4.00E+08	394.764	248666	11.400	1.03E+10	398.093	226659	34.076	4.07E+10	403.756	189559	535.000	1.07E+12
391.203	269248	0.443	4.00E+08	394.809	248375	11.400	1.03E+10	398.118	226489	34.076	4.07E+10	403.781	189373	575.000	1.16E+12
391.228	268971	0.443	4.00E+08	394.854	248084	11.400	1.03E+10	398.143	226319	34.076	4.07E+10	403.806	189187	615.000	1.25E+12
391.253	268694	0.443	4.00E+08	394.899	247793	11.400	1.03E+10	398.168	226149	34.076	4.07E+10	403.831	189001	655.000	1.34E+12
391.278	268417	0.443	4.00E+08	394.944	247502	11.400	1.03E+10	398.193	225979	34.076	4.07E+10	403.856	188815	695.000	1.43E+12
391.303	268140	0.443	4.00E+08	394.989	247211	11.400	1.03E+10	398.218	225809	34.076	4.07E+10	403.881	188629	735.000	1.52E+12
391.328	267863	0.443	4.00E+08	395.034	246920	11.400	1.03E+10	398.243	225639	34.076	4.07E+10	403.906	188443	775.000	1.61E+12
391.353	267586	0.443	4.00E+08	395.079	246629	11.400	1.03E+10	398.268	225469	34.076	4.07E+10	403.931	188257	815.000	1.70E+12
391.378	267309	0.443	4.00E+08	395.124	246338	11.400	1.03E+10	398.293	225299	34.076	4.07E+10	403.956	188071	855.000	1.79E+12
391.403	267032	0.443	4.00E+08	395.169	246047	11.400	1.03E+10	398.318	225129	34.076	4.07E+10	403.981	187885	895.000	1.88E+12
391.428	266755	0.443	4.00E+08	395.214	245756	11.400	1.03E+10	398.343	224959	34.076	4.07E+10	404.006	187699	935.000	1.97E+12
391.453	266478	0.443	4.00E+08	395.259	245465	11.400	1.03E+10	398.368	224789	34.076	4.07E+10	404.031	187513	975.000	2.06E+12
391.478	266201	0.443	4.00E+08	395.304	245174	11.400	1.03E+10	398.393	224619	34.076	4.07E+10	404.056	187327	1015.000	2.15E+12
391.503	265924	0.443	4.00E+08	395.349	244883	11.400	1.03E+10	398.418	224449	34.076	4.07E+10	404.081	187141	1055.000	2.24E+12
391.528	265647	0.443	4.00E+08	395.394	244592	11.400	1.03E+10	398.443	224279	34.076	4.07E+10	404.106	186955	1095.000	2.33E+12
391.553	265370	0.443	4.00E+08	395.439	244301	11.400	1.03E+10	398.468	224109	34.076	4.07E+10	404.131	186769	1135.000	2.42E+12
391.578	265093	0.443	4.00E+08	395.484	244010	11.400	1.03E+10	398.493	223939	34.076	4.07E+10	404.156	186583	1175.000	2.51E+12
391.603	264816	0.443	4.00E+08	395.529	243719	11.400	1.03E+10	398.518	223769	34.076	4.07E+10	404.181	186397	1215.000	2.60E+12
391.628	264539	0.443	4.00E+08	395.574	243428	11.400	1.03E+10	398.543	223599	34.076	4.07E+10	404.206	186211	1255.000	2.69E+12
391.653	264262	0.443	4.00E+08	395.619	243137	11.400	1.03E+10	398.568	223429	34.076	4.07E+10	404.231	186025	1295.000	2.78E+12
391.678	263985	0.443	4.00E+08	395.664	242846	11.400	1.03E+10	398.593	223259	34.076	4.07E+10	404.256	185839	1335.000	2.87E+12
391.703	263708	0.443</													

TABULATIONS OF CURRENT AND INFERRED ELECTRON DENSITY FOR
RAM C-I, PROBE 2

1 meter = 0.3048 (ex)

APPENDIX B - Continued

TABULATIONS OF CURRENT AND INFERRED ELECTRON DENSITY FOR RAM C-1, PROBE 3

ELAPSED TIME, SECONDS	ALTITUDE, FEET (a)	CURRENT, MICROAMPS	ELECTRON DENSITY, ELECTRONS PER CUBIC CENTIMETER
389.669	281708	+470	2.43E+08
389.740	281248	+473	3.76E+08
389.736	280848	+640	3.59E+08
389.801	280488	+643	3.59E+08
389.887	280133	+643	3.59E+08
389.922	280044	+473	3.76E+08
389.957	279878	+763	4.24E+08
389.985	279712	+670	3.76E+08
390.028	279620	+703	3.93E+08
390.053	279524	+643	3.59E+08
390.079	279487	+703	3.93E+08
390.124	279392	+722	4.08E+08
390.150	279321	+740	4.13E+08
390.176	279249	+760	4.24E+08
390.221	279150	+783	4.38E+08
390.247	279083	+763	4.24E+08
390.272	279004	+831	4.66E+08
390.317	278911	+863	4.94E+08
390.343	278834	+863	4.94E+08
390.368	278748	+902	5.05E+08
390.414	278671	+823	4.80E+08
390.439	278571	+863	4.94E+08
390.465	278493	+910	5.11E+08
390.490	278407	+983	5.50E+08
390.509	278328	+910	5.11E+08
390.534	278253	+957	5.31E+08
390.560	278167	+940	5.28E+08
390.585	278081	+940	5.28E+08
390.610	277995	+957	5.31E+08
390.635	277909	+922	5.17E+08
390.660	277823	+910	5.11E+08
390.685	277737	+983	5.50E+08
390.710	277651	+1.000	5.62E+08
390.735	277565	+1.017	5.74E+08
390.760	277479	+1.207	6.74E+08
390.785	277393	+1.220	6.85E+08
390.810	277307	+1.220	6.85E+08
390.835	277221	+1.220	6.85E+08
390.860	277135	+1.231	6.97E+08
390.885	277049	+1.204	6.79E+08
390.910	276963	+1.263	7.08E+08
390.935	276877	+1.297	7.29E+08
390.960	276791	+1.283	7.14E+08
390.985	276705	+1.380	7.73E+08
391.010	276619	+1.380	7.73E+08
391.035	276533	+1.380	7.73E+08
391.060	276447	+1.380	7.73E+08
391.085	276361	+1.380	7.73E+08
391.110	276275	+1.380	7.73E+08
391.135	276189	+1.380	7.73E+08
391.160	276103	+1.380	7.73E+08
391.185	276017	+1.380	7.73E+08
391.210	275931	+1.380	7.73E+08
391.235	275845	+1.380	7.73E+08
391.260	275759	+1.380	7.73E+08
391.285	275673	+1.380	7.73E+08
391.310	275587	+1.380	7.73E+08
391.335	275501	+1.380	7.73E+08
391.360	275415	+1.380	7.73E+08
391.385	275329	+1.380	7.73E+08
391.410	275243	+1.380	7.73E+08
391.435	275157	+1.380	7.73E+08
391.460	275071	+1.380	7.73E+08
391.485	274985	+1.380	7.73E+08
391.510	274899	+1.380	7.73E+08
391.535	274813	+1.380	7.73E+08
391.560	274727	+1.380	7.73E+08
391.585	274641	+1.380	7.73E+08
391.610	274555	+1.380	7.73E+08
391.635	274469	+1.380	7.73E+08
391.660	274383	+1.380	7.73E+08
391.685	274297	+1.380	7.73E+08
391.710	274211	+1.380	7.73E+08
391.735	274125	+1.380	7.73E+08
391.760	274039	+1.380	7.73E+08
391.785	273953	+1.380	7.73E+08
391.810	273867	+1.380	7.73E+08
391.835	273781	+1.380	7.73E+08
391.860	273695	+1.380	7.73E+08
391.885	273609	+1.380	7.73E+08
391.910	273523	+1.380	7.73E+08
391.935	273437	+1.380	7.73E+08
391.960	273351	+1.380	7.73E+08
391.985	273265	+1.380	7.73E+08
392.010	273179	+1.380	7.73E+08
392.035	273093	+1.380	7.73E+08
392.060	273007	+1.380	7.73E+08
392.085	272921	+1.380	7.73E+08
392.110	272835	+1.380	7.73E+08
392.135	272749	+1.380	7.73E+08
392.160	272663	+1.380	7.73E+08
392.185	272577	+1.380	7.73E+08
392.210	272491	+1.380	7.73E+08
392.235	272405	+1.380	7.73E+08
392.260	272319	+1.380	7.73E+08
392.285	272233	+1.380	7.73E+08
392.310	272147	+1.380	7.73E+08
392.335	272061	+1.380	7.73E+08
392.360	271975	+1.380	7.73E+08
392.385	271889	+1.380	7.73E+08
392.410	271803	+1.380	7.73E+08
392.435	271717	+1.380	7.73E+08
392.460	271631	+1.380	7.73E+08
392.485	271545	+1.380	7.73E+08
392.510	271459	+1.380	7.73E+08
392.535	271373	+1.380	7.73E+08
392.560	271287	+1.380	7.73E+08
392.585	271201	+1.380	7.73E+08
392.610	271115	+1.380	7.73E+08
392.635	271029	+1.380	7.73E+08
392.660	270943	+1.380	7.73E+08
392.685	270857	+1.380	7.73E+08
392.710	270771	+1.380	7.73E+08
392.735	270685	+1.380	7.73E+08
392.760	270599	+1.380	7.73E+08
392.785	270513	+1.380	7.73E+08
392.810	270427	+1.380	7.73E+08
392.835	270341	+1.380	7.73E+08
392.860	270255	+1.380	7.73E+08
392.885	270169	+1.380	7.73E+08
392.910	270083	+1.380	7.73E+08
392.935	269997	+1.380	7.73E+08
392.960	269911	+1.380	7.73E+08
392.985	269825	+1.380	7.73E+08
393.010	269739	+1.380	7.73E+08
393.035	269653	+1.380	7.73E+08
393.060	269567	+1.380	7.73E+08
393.085	269481	+1.380	7.73E+08
393.110	269395	+1.380	7.73E+08
393.135	269309	+1.380	7.73E+08
393.160	269223	+1.380	7.73E+08
393.185	269137	+1.380	7.73E+08
393.210	269051	+1.380	7.73E+08
393.235	268965	+1.380	7.73E+08
393.260	268879	+1.380	7.73E+08
393.285	268793	+1.380	7.73E+08
393.310	268707	+1.380	7.73E+08
393.335	268621	+1.380	7.73E+08
393.360	268535	+1.380	7.73E+08
393.385	268449	+1.380	7.73E+08
393.410	268363	+1.380	7.73E+08
393.435	268277	+1.380	7.73E+08
393.460	268191	+1.380	7.73E+08
393.485	268105	+1.380	7.73E+08
393.510	268019	+1.380	7.73E+08
393.535	267933	+1.380	7.73E+08
393.560	267847	+1.380	7.73E+08
393.585	267761	+1.380	7.73E+08
393.610	267675	+1.380	7.73E+08
393.635	267589	+1.380	7.73E+08
393.660	267503	+1.380	7.73E+08
393.685	267417	+1.380	7.73E+08
393.710	267331	+1.380	7.73E+08
393.735	267245	+1.380	7.73E+08
393.760	267159	+1.380	7.73E+08
393.785	267073	+1.380	7.73E+08
393.810	266987	+1.380	7.73E+08
393.835	266901	+1.380	7.73E+08
393.860	266815	+1.380	7.73E+08
393.885	266729	+1.380	7.73E+08
393.910	266643	+1.380	7.73E+08
393.935	266557	+1.380	7.73E+08
393.960	266471	+1.380	7.73E+08
393.985	266385	+1.380	7.73E+08
394.010	266299	+1.380	7.73E+08
394.035	266213	+1.380	7.73E+08
394.060	266127	+1.380	7.73E+08
394.085	266041	+1.380	7.73E+08
394.110	265955	+1.380	7.73E+08
394.135	265869	+1.380	7.73E+08
394.160	265783	+1.380	7.73E+08
394.185	265697	+1.380	7.73E+08
394.210	265611	+1.380	7.73E+08
394.235	265525	+1.380	7.73E+08
394.260	265439	+1.380	7.73E+08
394.285	265353	+1.380	7.73E+08
394.310	265267	+1.380	7.73E+08
394.335	265181	+1.380	7.73E+08
394.360	265095	+1.380	7.73E+08
394.385	265009	+1.380	7.73E+08
394.410	264923	+1.380	7.73E+08
394.435	264837	+1.380	7.73E+08
394.460	264751	+1.380	7.73E+08
394.485	264665	+1.380	7.73E+08
394.510	264579	+1.380	7.73E+08
394.535	264493	+1.380	7.73E+08
394.560	264407	+1.380	7.73E+08
394.585	264321	+1.380	7.73E+08
394.610	264235	+1.380	7.73E+08
394.635	264149	+1.380	7.73E+08
394.660	264063	+1.380	7.73E+08
394.685	263977	+1.380	7.73E+08
394.710	263891	+1.380	7.73E+08
394.735	263805	+1.380	7.73E+08
394.760	263719	+1.380	7.73E+08
394.785	263633	+1.380	7.73E+08
394.810	263547	+1.380	7.73E+08
394.835	263461	+1.380	7.73E+08
394.860	263375	+1.380	7.73E+08
394.885	263289	+1.380	7.73E+08
394.910	263203	+1.380	7.73E+08
394.935	263117	+1.380	7.73E+08
394.960	263031	+1.380	7.73E+08
394.985	262945	+1.380	7.73E+08
395.010	262859	+1.380	7.73E+08
395.035	262773	+1.380	7.73E+08
395.060	262687	+1.380	7.73E+08
395.085	262601	+1.380	7.73E+08
395.110	262515	+1.380	7.73E+08
395.135	262429	+1.380	7.73E+08
395.160	262343	+1.380	7.73E+08
395.185	262257	+1.380	7.73E+08
395.210	262171	+1.380	7.73E+08
395.235	262085	+1.380	7.73E+08
395.260	262000	+1.380	7.73E+08
395.285	261914	+1.380	7.73E+08
395.310	261828	+1.380	7.73E+08
395.335	261742	+1.380	7.73E+08
395.360	261656	+1.380	7.73E+08
395.385	261570	+1.380	7.73E+08
395.410	261484	+1.380	7.73E+08
395.435	261398	+1.380	7.73E+08
395.460	261312	+1.380	7.73E+08
395.485	261226	+1.380	7.73E+08
395.510	261140	+1.380	7.73E+08
395.535	261054	+1.380	7.73E+08
395.560	260968	+1.380	7.73E+08
395.585	260882	+1.380	7.73E+08
395.610	260796	+1.380	7.73E+08
395.635	260710	+1.380	7.73E+08
395.660	260624	+1.380	7.73E+08
395.685	260538	+1.380	7.73E+08
395.710	260452	+1.380	7.73E+08
395.735	260366	+1.380	7.73E+08
395.760	260280	+1.380	7.73E+08
395.785	260194	+1.380	7.73E+08
395.810	260108	+1.380	7.73E+08
395.835	260022	+1.380	7.73E+08
395.860	259936	+1.380	7.73E+08
395.885	259850	+1.380	7.

TABULATIONS OF CURRENT AND INFERRED ELECTRON DENSITY FOR
RAM C-I, PROBE 4

1 meter = 0.3048 feet

APPENDIX B - Continued

TABULATIONS OF CURRENT AND INFERRED ELECTRON DENSITY FOR RAM C-I, PROBE 5

ELAPSED TIME, SECONDS	ALTITUDE, FEET (a)	CURRENT, MICROAMPS	ELECTRON DENSITY, ELECTRONS PER CUBIC CENTIMETER
346.649	281834	7.60	4.00E+08
346.675	281866	7.33	3.84E+08
346.702	281858	7.23	3.79E+08
346.727	281820	7.02	3.69E+08
346.752	281071	7.13	3.84E+08
346.777	280908	7.60	4.00E+08
346.802	280622	7.83	4.10E+08
346.826	280557	8.23	4.32E+08
346.851	280292	8.23	4.32E+08
346.876	280002	8.23	4.32E+08
346.901	279836	8.43	4.42E+08
346.926	279670	8.03	4.21E+08
346.951	279519	8.23	4.32E+08
346.976	279212	8.23	4.32E+08
347.001	279045	8.13	4.26E+08
347.026	278744	7.93	4.15E+08
347.051	278478	8.23	4.32E+08
347.076	278266	8.43	4.42E+08
347.101	278104	9.13	4.79E+08
347.126	277925	9.13	4.79E+08
347.151	277762	9.13	4.79E+08
347.176	277607	9.23	4.84E+08
347.201	277452	9.23	4.84E+08
347.226	277297	9.13	4.80E+08
347.251	277142	8.43	4.42E+08
347.276	276987	8.43	4.42E+08
347.301	276832	8.43	4.42E+08
347.326	276677	8.43	4.42E+08
347.351	276522	8.43	4.42E+08
347.376	276367	8.43	4.42E+08
347.401	276212	8.43	4.42E+08
347.426	276057	8.43	4.42E+08
347.451	275902	8.43	4.42E+08
347.476	275747	8.43	4.42E+08
347.501	275592	8.43	4.42E+08
347.526	275437	8.43	4.42E+08
347.551	275282	8.43	4.42E+08
347.576	275127	8.43	4.42E+08
347.601	274972	8.43	4.42E+08
347.626	274817	8.43	4.42E+08
347.651	274662	8.43	4.42E+08
347.676	274507	8.43	4.42E+08
347.701	274352	8.43	4.42E+08
347.726	274197	8.43	4.42E+08
347.751	274042	8.43	4.42E+08
347.776	273887	8.43	4.42E+08
347.801	273732	8.43	4.42E+08
347.826	273577	8.43	4.42E+08
347.851	273422	8.43	4.42E+08
347.876	273267	8.43	4.42E+08
347.901	273112	8.43	4.42E+08
347.926	272957	8.43	4.42E+08
347.951	272802	8.43	4.42E+08
347.976	272647	8.43	4.42E+08
348.001	272492	8.43	4.42E+08
348.026	272337	8.43	4.42E+08
348.051	272182	8.43	4.42E+08
348.076	272027	8.43	4.42E+08
348.101	271872	8.43	4.42E+08
348.126	271717	8.43	4.42E+08
348.151	271562	8.43	4.42E+08
348.176	271407	8.43	4.42E+08
348.201	271252	8.43	4.42E+08
348.226	271097	8.43	4.42E+08
348.251	270942	8.43	4.42E+08
348.276	270787	8.43	4.42E+08
348.301	270632	8.43	4.42E+08
348.326	270477	8.43	4.42E+08
348.351	270322	8.43	4.42E+08
348.376	270167	8.43	4.42E+08
348.401	270012	8.43	4.42E+08
348.426	269857	8.43	4.42E+08
348.451	269702	8.43	4.42E+08
348.476	269547	8.43	4.42E+08
348.501	269392	8.43	4.42E+08
348.526	269237	8.43	4.42E+08
348.551	269082	8.43	4.42E+08
348.576	268927	8.43	4.42E+08
348.601	268772	8.43	4.42E+08
348.626	268617	8.43	4.42E+08
348.651	268462	8.43	4.42E+08
348.676	268307	8.43	4.42E+08
348.701	268152	8.43	4.42E+08
348.726	267997	8.43	4.42E+08
348.751	267842	8.43	4.42E+08
348.776	267687	8.43	4.42E+08
348.801	267532	8.43	4.42E+08
348.826	267377	8.43	4.42E+08
348.851	267222	8.43	4.42E+08
348.876	267067	8.43	4.42E+08
348.901	266912	8.43	4.42E+08
348.926	266757	8.43	4.42E+08
348.951	266602	8.43	4.42E+08
348.976	266447	8.43	4.42E+08
349.001	266292	8.43	4.42E+08
349.026	266137	8.43	4.42E+08
349.051	265982	8.43	4.42E+08
349.076	265827	8.43	4.42E+08
349.101	265672	8.43	4.42E+08
349.126	265517	8.43	4.42E+08
349.151	265362	8.43	4.42E+08
349.176	265207	8.43	4.42E+08
349.201	265052	8.43	4.42E+08
349.226	264897	8.43	4.42E+08
349.251	264742	8.43	4.42E+08
349.276	264587	8.43	4.42E+08
349.301	264432	8.43	4.42E+08
349.326	264277	8.43	4.42E+08
349.351	264122	8.43	4.42E+08
349.376	263967	8.43	4.42E+08
349.401	263812	8.43	4.42E+08
349.426	263657	8.43	4.42E+08
349.451	263502	8.43	4.42E+08
349.476	263347	8.43	4.42E+08
349.501	263192	8.43	4.42E+08
349.526	263037	8.43	4.42E+08
349.551	262882	8.43	4.42E+08
349.576	262727	8.43	4.42E+08
349.601	262572	8.43	4.42E+08
349.626	262417	8.43	4.42E+08
349.651	262262	8.43	4.42E+08
349.676	262107	8.43	4.42E+08
349.701	261952	8.43	4.42E+08
349.726	261797	8.43	4.42E+08
349.751	261642	8.43	4.42E+08
349.776	261487	8.43	4.42E+08
349.801	261332	8.43	4.42E+08
349.826	261177	8.43	4.42E+08
349.851	261022	8.43	4.42E+08
349.876	260867	8.43	4.42E+08
349.901	260712	8.43	4.42E+08
349.926	260557	8.43	4.42E+08
349.951	260402	8.43	4.42E+08
349.976	260247	8.43	4.42E+08
350.001	260092	8.43	4.42E+08
350.026	259937	8.43	4.42E+08
350.051	259782	8.43	4.42E+08
350.076	259627	8.43	4.42E+08
350.101	259472	8.43	4.42E+08
350.126	259317	8.43	4.42E+08
350.151	259162	8.43	4.42E+08
350.176	259007	8.43	4.42E+08
350.201	258852	8.43	4.42E+08
350.226	258697	8.43	4.42E+08
350.251	258542	8.43	4.42E+08
350.276	258387	8.43	4.42E+08
350.301	258232	8.43	4.42E+08
350.326	258077	8.43	4.42E+08
350.351	257922	8.43	4.42E+08
350.376	257767	8.43	4.42E+08
350.401	257612	8.43	4.42E+08
350.426	257457	8.43	4.42E+08
350.451	257302	8.43	4.42E+08
350.476	257147	8.43	4.42E+08
350.501	256992	8.43	4.42E+08
350.526	256837	8.43	4.42E+08
350.551	256682	8.43	4.42E+08
350.576	256527	8.43	4.42E+08
350.601	256372	8.43	4.42E+08
350.626	256217	8.43	4.42E+08
350.651	256062	8.43	4.42E+08
350.676	255907	8.43	4.42E+08
350.701	255752	8.43	4.42E+08
350.726	255597	8.43	4.42E+08
350.751	255442	8.43	4.42E+08
350.776	255287	8.43	4.42E+08
350.801	255132	8.43	4.42E+08
350.826	254977	8.43	4.42E+08
350.851	254822	8.43	4.42E+08
350.876	254667	8.43	4.42E+08
350.901	254512	8.43	4.42E+08
350.926	254357	8.43	4.42E+08
350.951	254202	8.43	4.42E+08
350.976	254047	8.43	4.42E+08
351.001	253892	8.43	4.42E+08
351.026	253737	8.43	4.42E+08
351.051	253582	8.43	4.42E+08
351.076	253427	8.43	4.42E+08
351.101	253272	8.43	4.42E+08
351.126	253117	8.43	4.42E+08
351.151	252962	8.43	4.42E+08
351.176	252807	8.43	4.42E+08
351.201	252652	8.43	4.42E+08
351.226	252497	8.43	4.42E+08
351.251	252342	8.43	4.42E+08
351.276	252187	8.43	4.42E+08
351.301	252032	8.43	4.42E+08
351.326	251877	8.43	4.42E+08
351.351	251722	8.43	4.42E+08
351.376	251567	8.43	4.42E+08
351.401	251412	8.43	4.42E+08
351.426	251257	8.43	4.42E+08
351.451	251102	8.43	4.42E+08
351.476	250947	8.43	4.42E+08
351.501	250792	8.43	4.42E+08
351.526	250637	8.43	4.42E+08
351.551	250482	8.43	4.42E+08
351.576	250327	8.43	4.42E+08
351.601	250172	8.43	4.42E+08
351.626	249917	8.43	4.42E+08
351.651	249762	8.43	4.42E+08
351.676	249607	8.43	4.42E+08
351.701	249452	8.43	4.42E+08
351.726	249297	8.43	4.42E+08
351.751	249142	8.43	4.42E+08
351.776	248987	8.43	4.42E+08
351.801	248832	8.43	4.42E+08
351.826	248677	8.43	4.42E+08
351.851	248522	8.43	4.42E+08
351.876	248367	8.43	4.42E+08
351.901	248212	8.43	4.42E+08
351.926	248057	8.43	4.42E+08
351.951	247902	8.43	4.42E+08
351.976	247747	8.43	4.42E+08
352.001	247592	8.43	4.42E+08
352.026	247437	8.43	4.42E+08
352.051	247282	8.43	4.42E+08
352.076	247127	8.43	4.42E+08
352.101	246972	8.43	4.42E+08
352.126	246817	8.43	4.42E+08
352.151	246662	8.43	4.42E+08
352.176	246507	8.43	4.42E+08
352.201	246352	8.43	4.42E+08
352.226	246197	8.43	4.42E+08
352.251	246042	8.43	4.42E+08
352.276	245887	8.43	4.42E+08
352.301	245732	8.43	4.42E+08
352.326	245577	8.43	4.42E+08
352.351	245422	8.43	4.42E+08
352.376	245267	8.43	4.42E+08
352.401	245112	8.43	4.42E+08
352.426	244957	8.43	4.42E+08
352.451	244802	8.43	4.42E+08
352.476	244647	8.43	4.42E+08
352.501	244492	8.43	4.42E+08
352.526	244337	8.43	4.42E+08
352.551	244182	8.43	4.42E+08
352.576	244027	8.43	4.42E+08
352.601	243872	8.43	4.42E+08
352.626	243717	8.43	4.42E+08
352.651	243562	8.43	4.42E+08
352.676	243407	8.43	4.42E+08
352.701	243252	8.43	4.42E+08
352.726			

APPENDIX B - Continued

TABULATIONS OF CURRENT AND INFERRED ELECTRON DENSITY FOR RAM C-I, PROBE 6

ELAPSED TIME, SECONDS	ALTITUDE, FEET	CURRENT, MICROAMPS	ELECTRON DENSITY, ELECTRONS PER CUBIC CENTIMETER
389.653	281813	+782	4.03E+08
389.679	281845	+703	3.62E+08
389.705	281877	+728	3.72E+08
389.750	281888	+763	3.93E+08
389.775	281905	+832	4.44E+08
389.801	280888	+800	4.13E+08
389.845	280801	+863	4.44E+08
389.871	280871	+902	4.55E+08
389.896	280871	+903	4.55E+08
389.941	279882	+863	4.44E+08
389.967	279818	+863	4.44E+08
389.992	279845	+810	4.18E+08
390.037	279758	+800	4.13E+08
390.063	279791	+843	4.34E+08
390.088	279624	+843	4.34E+08
390.134	278728	+930	4.85E+08
390.160	278557	+893	4.58E+08
390.186	278585	+915	4.70E+08
390.231	278689	+962	4.95E+08
390.256	277908	+963	4.95E+08
390.282	277741	+1.000	5.16E+08
390.326	277446	+962	4.95E+08
390.352	277275	+962	4.95E+08
390.378	277106	+1.002	5.16E+08
390.423	276807	+1.013	5.21E+08
390.449	276638	+1.123	5.72E+08
390.474	276469	+1.075	5.50E+08
390.519	276176	+1.072	5.47E+08
390.545	276011	+1.073	5.47E+08
390.569	275845	+1.093	5.62E+08
390.595	275682	+1.052	5.42E+08
390.620	275510	+1.092	5.58E+08
390.645	275342	+1.132	5.91E+08
390.670	275174	+1.163	6.21E+08
390.696	275006	+1.155	6.18E+08
390.722	274837	+1.223	6.62E+08
390.747	274669	+1.263	6.95E+08
390.773	274500	+1.223	6.62E+08
390.798	274332	+1.263	6.95E+08
390.824	274163	+1.263	6.95E+08
390.849	274000	+1.263	6.95E+08
390.875	273832	+1.263	6.95E+08
390.900	273664	+1.263	6.95E+08
390.926	273500	+1.263	6.95E+08
390.951	273332	+1.263	6.95E+08
390.977	273164	+1.263	6.95E+08
391.002	273000	+1.263	6.95E+08
391.028	272832	+1.263	6.95E+08
391.053	272664	+1.263	6.95E+08
391.079	272500	+1.263	6.95E+08
391.104	272332	+1.263	6.95E+08
391.129	272164	+1.263	6.95E+08
391.155	272000	+1.263	6.95E+08
391.180	271832	+1.263	6.95E+08
391.206	271664	+1.263	6.95E+08
391.231	271500	+1.263	6.95E+08
391.256	271332	+1.263	6.95E+08
391.282	271164	+1.263	6.95E+08
391.307	271000	+1.263	6.95E+08
391.332	270832	+1.263	6.95E+08
391.358	270664	+1.263	6.95E+08
391.383	270500	+1.263	6.95E+08
391.408	270332	+1.263	6.95E+08
391.434	270164	+1.263	6.95E+08
391.459	270000	+1.263	6.95E+08
391.484	269832	+1.263	6.95E+08
391.510	269664	+1.263	6.95E+08
391.535	269500	+1.263	6.95E+08
391.560	269332	+1.263	6.95E+08
391.586	269164	+1.263	6.95E+08
391.611	269000	+1.263	6.95E+08
391.636	268832	+1.263	6.95E+08
391.662	268664	+1.263	6.95E+08
391.687	268500	+1.263	6.95E+08
391.712	268332	+1.263	6.95E+08
391.738	268164	+1.263	6.95E+08
391.763	268000	+1.263	6.95E+08
391.788	267832	+1.263	6.95E+08
391.814	267664	+1.263	6.95E+08
391.839	267500	+1.263	6.95E+08
391.864	267332	+1.263	6.95E+08
391.890	267164	+1.263	6.95E+08
391.915	267000	+1.263	6.95E+08
391.940	266832	+1.263	6.95E+08
391.966	266664	+1.263	6.95E+08
391.991	266500	+1.263	6.95E+08
392.016	266332	+1.263	6.95E+08
392.042	266164	+1.263	6.95E+08
392.067	266000	+1.263	6.95E+08
392.092	265832	+1.263	6.95E+08
392.118	265664	+1.263	6.95E+08
392.143	265500	+1.263	6.95E+08
392.168	265332	+1.263	6.95E+08
392.194	265164	+1.263	6.95E+08
392.219	265000	+1.263	6.95E+08
392.244	264832	+1.263	6.95E+08
392.270	264664	+1.263	6.95E+08
392.295	264500	+1.263	6.95E+08
392.320	264332	+1.263	6.95E+08
392.346	264164	+1.263	6.95E+08
392.371	264000	+1.263	6.95E+08
392.396	263832	+1.263	6.95E+08
392.422	263664	+1.263	6.95E+08
392.447	263500	+1.263	6.95E+08
392.472	263332	+1.263	6.95E+08
392.498	263164	+1.263	6.95E+08
392.523	263000	+1.263	6.95E+08
392.548	262832	+1.263	6.95E+08
392.574	262664	+1.263	6.95E+08
392.599	262500	+1.263	6.95E+08
392.624	262332	+1.263	6.95E+08
392.650	262164	+1.263	6.95E+08
392.675	262000	+1.263	6.95E+08
392.700	261832	+1.263	6.95E+08
392.726	261664	+1.263	6.95E+08
392.751	261500	+1.263	6.95E+08
392.776	261332	+1.263	6.95E+08
392.802	261164	+1.263	6.95E+08
392.827	261000	+1.263	6.95E+08
392.852	260832	+1.263	6.95E+08
392.878	260664	+1.263	6.95E+08
392.903	260500	+1.263	6.95E+08
392.928	260332	+1.263	6.95E+08
392.954	260164	+1.263	6.95E+08
392.979	260000	+1.263	6.95E+08
393.004	259832	+1.263	6.95E+08
393.030	259664	+1.263	6.95E+08
393.055	259500	+1.263	6.95E+08
393.080	259332	+1.263	6.95E+08
393.106	259164	+1.263	6.95E+08
393.131	259000	+1.263	6.95E+08
393.156	258832	+1.263	6.95E+08
393.182	258664	+1.263	6.95E+08
393.207	258500	+1.263	6.95E+08
393.232	258332	+1.263	6.95E+08
393.258	258164	+1.263	6.95E+08
393.283	258000	+1.263	6.95E+08
393.308	257832	+1.263	6.95E+08
393.334	257664	+1.263	6.95E+08
393.359	257500	+1.263	6.95E+08
393.384	257332	+1.263	6.95E+08
393.410	257164	+1.263	6.95E+08
393.435	257000	+1.263	6.95E+08
393.460	256832	+1.263	6.95E+08
393.486	256664	+1.263	6.95E+08
393.511	256500	+1.263	6.95E+08
393.536	256332	+1.263	6.95E+08
393.562	256164	+1.263	6.95E+08
393.587	256000	+1.263	6.95E+08
393.612	255832	+1.263	6.95E+08
393.638	255664	+1.263	6.95E+08
393.663	255500	+1.263	6.95E+08
393.688	255332	+1.263	6.95E+08
393.714	255164	+1.263	6.95E+08
393.739	255000	+1.263	6.95E+08
393.764	254832	+1.263	6.95E+08
393.790	254664	+1.263	6.95E+08
393.815	254500	+1.263	6.95E+08
393.840	254332	+1.263	6.95E+08
393.866	254164	+1.263	6.95E+08
393.891	254000	+1.263	6.95E+08
393.916	253832	+1.263	6.95E+08
393.942	253664	+1.263	6.95E+08
393.967	253500	+1.263	6.95E+08
393.992	253332	+1.263	6.95E+08
394.018	253164	+1.263	6.95E+08
394.043	253000	+1.263	6.95E+08
394.068	252832	+1.263	6.95E+08
394.094	252664	+1.263	6.95E+08
394.119	252500	+1.263	6.95E+08
394.144	252332	+1.263	6.95E+08
394.170	252164	+1.263	6.95E+08
394.195	252000	+1.263	6.95E+08
394.220	251832	+1.263	6.95E+08
394.246	251664	+1.263	6.95E+08
394.271	251500	+1.263	6.95E+08
394.296	251332	+1.263	6.95E+08
394.322	251164	+1.263	6.95E+08
394.347	251000	+1.263	6.95E+08
394.372	250832	+1.263	6.95E+08
394.398	250664	+1.263	6.95E+08
394.423	250500	+1.263	6.95E+08
394.448	250332	+1.263	6.95E+08
394.474	250164	+1.263	6.95E+08
394.499	250000	+1.263	6.95E+08
394.524	249832	+1.263	6.95E+08
394.550	249664	+1.263	6.95E+08
394.575	249500	+1.263	6.95E+08
394.600	249332	+1.263	6.95E+08
394.626	249164	+1.263	6.95E+08
394.651	249000	+1.263	6.95E+08
394.676	248832	+1.263	6.95E+08
394.702	248664	+1.263	6.95E+08
394.727	248500	+1.263	6.95E+08
394.752	248332	+1.263	6.95E+08
394.778	248164	+1.263	6.95E+08
394.803	248000	+1.263	6.95E+08
394.828	247832	+1.263	6.95E+08
394.854	247664	+1.263	6.95E+08
394.879	247500	+1.263	6.95E+08
394.904	247332	+1.263	6.95E+08
394.930	247164	+1.263	6.95E+08
394.955	247000	+1.263	6.95E+08
394.980	246832	+1.263	6.95E+08
395.006	246664	+1.263	6.95E+08
395.031	246500	+1.263	6.95E+08
395.056	246332	+1.263	6.95E+08
395.082	246164	+1.263	6.95E+08
395.107	246000	+1.263	6.95E+08
395.132	245832	+1.263	6.95E+08
395.158	245664	+1.263	6.95E+08
395.183	245500	+1.263	6.95E+08
395.208	245332	+1.263	6.95E+08
395.234	245164	+1.263	6.95E+08
395.259	245000	+1.263	6.95E+08
395.284	244832	+1.263	6.95E+08
395.310	244664	+1.263	6.95E+08
395.335	244500	+1.263	6.95E+08
395.360	244332	+1.263	6.95E+08
395.386	244164	+1.263	6.95E+08
395.411	244000	+1.263	6.95E+08
395.436	243832	+1.263	6.95E+08
395.462	243664	+1.263	6.95E+08
395.487	243500	+1.263	6.95E+08
395.512	243332	+1.263	6.95E+08
395.538	243164	+1.263	6.95E+08
395.563	243000	+1.263	6.95E+08
395.588	242832	+1.263	6.95E+08
395.614	242664	+1.263	6.95E+08
395.639	242500	+1.263	6.95E+08
395.664	242332	+1.263	6.95E+08
395.690	242164	+1.263	6.95E+08
395.715	242000	+1.263	6.95E+08
395.740	241832	+1.263	6.95E+08
395.766	241664	+1.263	6.95E+08
395.791	241500	+1.263	6.95E+08
395.816	241332	+1.263	6.95E+08
395.842	241164	+1.263	6.95E+08
395.867	241000	+1.263	6.95E+08
395.892	240832		

APPENDIX B - Continued

TABULATIONS OF CURRENT AND INFERRED ELECTRON DENSITY FOR RAM C-I, PROBE 7

ELAPSED TIME, SECONDS	ALTITUDE, FEET (a)	CURRENT, MICROAMPS	ELECTRON DENSITY, ELECTRONS PER CUBIC CENTIMETER
339.656	281792	0.643	3.25E+08
339.662	281624	0.643	3.25E+08
339.768	281656	0.643	3.25E+08
339.753	281192	0.752	2.39E+08
339.776	281030	0.703	3.55E+08
339.824	280367	0.733	3.70E+08
339.848	280581	0.663	4.30E+08
339.874	280616	0.702	4.50E+08
339.900	280251	0.703	4.50E+08
339.944	279961	0.693	4.51E+08
339.970	279793	0.663	4.30E+08
339.996	279629	0.643	4.20E+08
340.040	279337	0.652	4.21E+08
340.066	279170	0.670	4.42E+08
340.092	279003	0.693	4.51E+08
340.117	278767	0.713	4.61E+08
340.163	278535	0.752	4.81E+08
340.184	278363	0.782	4.96E+08
340.214	278087	1.022	5.10E+08
340.259	277887	1.043	5.20E+08
340.285	277722	1.272	5.41E+08
340.330	277424	1.130	5.11E+08
340.355	277254	1.182	5.26E+08
340.381	277083	1.203	5.36E+08
340.426	276786	1.223	5.46E+08
340.452	276617	1.283	5.66E+08
340.478	276448	1.283	5.66E+08
340.522	276155	1.313	5.81E+08
340.547	275990	1.363	6.01E+08
340.572	275824	1.463	6.36E+08
340.617	275533	1.223	5.61E+08
340.642	275360	1.223	5.61E+08
340.668	275189	1.283	5.81E+08
340.714	274890	1.483	6.26E+08
340.739	274719	1.483	6.26E+08
340.765	274530	1.753	6.80E+08
340.810	274233	1.753	6.80E+08
340.835	274079	2.083	7.18E+08
340.860	273913	2.123	7.30E+08
340.905	273622	2.123	7.30E+08
340.930	273453	2.273	7.75E+08
340.956	273284	2.463	8.23E+08
341.002	272988	2.463	8.23E+08
341.027	272821	2.273	7.75E+08
341.053	272656	2.273	7.75E+08
341.078	272487	2.613	8.15E+08
341.124	272187	2.257	7.62E+08
341.150	272023	2.257	7.62E+08
341.164	271844	2.423	7.92E+08
341.220	271540	2.463	8.23E+08
341.246	271376	2.463	8.23E+08
341.271	271211	2.423	7.92E+08
341.316	270918	2.423	7.92E+08
341.342	270752	2.273	7.75E+08
341.368	270587	2.223	7.55E+08
341.413	270283	2.123	7.30E+08
341.439	270119	2.423	7.92E+08
341.464	269955	2.423	7.92E+08
341.510	269653	2.423	7.92E+08
341.536	269489	2.183	7.55E+08
341.580	269187	2.463	8.23E+08
341.606	269023	2.463	8.23E+08
341.632	268859	2.463	8.23E+08
341.677	268566	2.223	7.55E+08
341.702	268407	2.463	8.23E+08
341.728	268243	2.253	7.66E+08
341.773	267943	2.153	7.46E+08
341.799	267781	2.183	7.55E+08
341.825	267616	2.463	8.23E+08
341.850	267452	2.463	8.23E+08
341.876	267287	2.463	8.23E+08
341.921	266987	2.123	7.30E+08
341.947	266823	2.123	7.30E+08
341.972	266659	2.463	8.23E+08
342.018	266361	2.463	8.23E+08
342.043	266197	2.463	8.23E+08
342.069	266033	2.463	8.23E+08
342.115	265735	2.463	8.23E+08
342.160	265437	2.463	8.23E+08
342.185	265273	2.463	8.23E+08
342.211	265109	2.463	8.23E+08
342.256	264811	2.463	8.23E+08
342.282	264647	2.463	8.23E+08
342.308	264483	2.463	8.23E+08
342.353	264185	2.463	8.23E+08
342.379	264021	2.463	8.23E+08
342.405	263857	2.463	8.23E+08
342.450	263559	2.463	8.23E+08
342.476	263395	2.463	8.23E+08
342.502	263231	2.463	8.23E+08
342.528	263067	2.463	8.23E+08
342.573	262769	2.463	8.23E+08
342.599	262605	2.463	8.23E+08
342.625	262441	2.463	8.23E+08
342.651	262277	2.463	8.23E+08
342.677	262113	2.463	8.23E+08
342.703	261949	2.463	8.23E+08
342.729	261785	2.463	8.23E+08
342.755	261621	2.463	8.23E+08
342.781	261457	2.463	8.23E+08
342.807	261293	2.463	8.23E+08
342.833	261129	2.463	8.23E+08
342.859	260965	2.463	8.23E+08
342.885	260801	2.463	8.23E+08
342.911	260637	2.463	8.23E+08
342.937	260473	2.463	8.23E+08
342.963	260309	2.463	8.23E+08
342.989	260145	2.463	8.23E+08
343.015	259981	2.463	8.23E+08
343.041	259817	2.463	8.23E+08
343.067	259653	2.463	8.23E+08
343.093	259489	2.463	8.23E+08
343.119	259325	2.463	8.23E+08
343.145	259161	2.463	8.23E+08
343.171	258997	2.463	8.23E+08
343.197	258833	2.463	8.23E+08
343.223	258669	2.463	8.23E+08
343.249	258505	2.463	8.23E+08
343.275	258341	2.463	8.23E+08
343.301	258177	2.463	8.23E+08
343.327	258013	2.463	8.23E+08
343.353	257849	2.463	8.23E+08
343.379	257685	2.463	8.23E+08
343.405	257521	2.463	8.23E+08
343.431	257357	2.463	8.23E+08
343.457	257193	2.463	8.23E+08
343.483	257029	2.463	8.23E+08
343.509	256865	2.463	8.23E+08
343.535	256701	2.463	8.23E+08
343.561	256537	2.463	8.23E+08
343.587	256373	2.463	8.23E+08
343.613	256209	2.463	8.23E+08
343.639	256045	2.463	8.23E+08
343.665	255881	2.463	8.23E+08
343.691	255717	2.463	8.23E+08
343.717	255553	2.463	8.23E+08
343.743	255389	2.463	8.23E+08
343.769	255225	2.463	8.23E+08
343.795	255061	2.463	8.23E+08
343.821	254897	2.463	8.23E+08
343.847	254733	2.463	8.23E+08
343.873	254569	2.463	8.23E+08
343.899	254405	2.463	8.23E+08
343.925	254241	2.463	8.23E+08
343.951	254077	2.463	8.23E+08
343.977	253913	2.463	8.23E+08
344.003	253749	2.463	8.23E+08
344.029	253585	2.463	8.23E+08
344.055	253421	2.463	8.23E+08
344.081	253257	2.463	8.23E+08
344.107	253093	2.463	8.23E+08
344.133	252929	2.463	8.23E+08
344.159	252765	2.463	8.23E+08
344.185	252601	2.463	8.23E+08
344.211	252437	2.463	8.23E+08
344.237	252273	2.463	8.23E+08
344.263	252109	2.463	8.23E+08
344.289	251945	2.463	8.23E+08
344.315	251781	2.463	8.23E+08
344.341	251617	2.463	8.23E+08
344.367	251453	2.463	8.23E+08
344.393	251289	2.463	8.23E+08
344.419	251125	2.463	8.23E+08
344.445	250961	2.463	8.23E+08
344.471	250797	2.463	8.23E+08
344.497	250633	2.463	8.23E+08
344.523	250469	2.463	8.23E+08
344.549	250305	2.463	8.23E+08
344.575	250141	2.463	8.23E+08
344.601	249977	2.463	8.23E+08
344.627	249813	2.463	8.23E+08
344.653	249649	2.463	8.23E+08
344.679	249485	2.463	8.23E+08
344.705	249321	2.463	8.23E+08
344.731	249157	2.463	8.23E+08
344.757	248993	2.463	8.23E+08
344.783	248829	2.463	8.23E+08
344.809	248665	2.463	8.23E+08
344.835	248501	2.463	8.23E+08
344.861	248337	2.463	8.23E+08
344.887	248173	2.463	8.23E+08
344.913	248009	2.463	8.23E+08
344.939	247845	2.463	8.23E+08
344.965	247681	2.463	8.23E+08
344.991	247517	2.463	8.23E+08
345.017	247353	2.463	8.23E+08
345.043	247189	2.463	8.23E+08
345.069	247025	2.463	8.23E+08
345.095	246861	2.463	8.23E+08
345.121	246697	2.463	8.23E+08
345.147	246533	2.463	8.23E+08
345.173	246369	2.463	8.23E+08
345.199	246205	2.463	8.23E+08
345.225	246041	2.463	8.23E+08
345.251	245877	2.463	8.23E+08
345.277	245713	2.463	8.23E+08
345.303	245549	2.463	8.23E+08
345.329	245385	2.463	8.23E+08
345.355	245221	2.463	8.23E+08
345.381	245057	2.463	8.23E+08
345.407	244893	2.463	8.23E+08
345.433	244729	2.463	8.23E+08
345.459	244565	2.463	8.23E+08
345.485	244401	2.463	8.23E+08
345.511	244237	2.463	8.23E+08
345.537	244073	2.463	8.23E+08
345.563	243909	2.463	8.23E+08
345.589	243745	2.463	8.23E+08
345.615	243581	2.463	8.23E+08
345.641	243417	2.463	8.23E+08
345.667	243253	2.463	8.23E+08
345.693	243089	2.463	8.23E+08
345.719	242925	2.463	8.23E+08
345.745	242761	2.463	8.23E+08
345.771	242597	2.463	8.23E+08
345.797	242433	2.463	8.23E+08
345.823	242269	2.463	8.23E+08
345.849	242105	2.463	8.23E+08
345.875	241941	2.463	8.23E+08
345.901	241777	2.463	8.23E+08
345.927	241613	2.463	8.23E+08
345.953	241449	2.463	8.23E+08
345.979	241285	2.463	8.23E+08
346.005	241121	2.463	8.23E+08
346.031	240957	2.463	8.23E+08
346.057	240793	2.463	8.23E+08
346.083	240629	2.463	8.23E+08
346.109	240465	2.463	8.23E+08
346.135	240301	2.463	8.23E+08
346.161	240137	2.463	8.23E+08
346.187	239973	2.463	8.23E+08
346.213	239809	2.463	8.23E+08
346.239	239645	2.463	8.23E+08
346.265	239481	2.463	8.23E+08
346.291	239317	2.463	8.23E+08
346.317	239153	2.463	8.23E+08
346.343	238989	2.463	8.23E+08
346.369	238825	2.463	8.23E+08
346.395	238661		

APPENDIX B - Continued

TABULATIONS OF CURRENT AND INFERRED ELECTRON DENSITY FOR

RAM C-I, PROBE 8

ELAPSED TIME, SECONDS	ALTITUDE, FEET	CURRENT, MICROAMPS	ELECTRON DENSITY, ELECTRONS PER CUBIC CENTIMETER
189.459	281172	4.992	2.45E+08
189.756	281172	4.770	2.35E+08
189.782	281010	4.470	2.34E+08
189.807	280876	4.803	3.09E+08
189.852	280860	4.912	4.54E+08
189.877	280359	9.220	4.25E+08
189.903	280232	9.963	4.48E+08
189.948	279940	9.822	4.38E+08
189.973	279736	9.870	4.37E+08
189.999	279608	9.805	4.28E+08
190.044	279316	9.803	4.48E+08
190.069	279149	9.803	4.48E+08
190.095	278982	9.803	4.48E+08
190.140	278685	1.003	4.18E+08
190.166	278484	1.023	5.07E+08
190.192	278342	1.123	5.67E+08
190.217	278046	1.223	6.06E+08
190.263	277860	1.263	6.26E+08
190.288	277699	1.303	6.46E+08
190.313	277403	1.343	6.66E+08
190.339	277202	1.383	7.06E+08
190.365	276956	1.423	7.46E+08
190.391	276755	1.463	7.86E+08
190.417	276554	1.503	8.26E+08
190.443	276353	1.543	8.66E+08
190.469	276152	1.583	9.06E+08
190.495	275951	1.623	9.46E+08
190.521	275750	1.663	9.86E+08
190.547	275549	1.703	1.02E+09
190.573	275348	1.743	1.06E+09
190.599	275147	1.783	1.10E+09
190.625	274946	1.823	1.14E+09
190.651	274745	1.863	1.18E+09
190.677	274544	1.903	1.22E+09
190.703	274343	1.943	1.26E+09
190.729	274142	1.983	1.30E+09
190.755	273941	2.023	1.34E+09
190.781	273740	2.063	1.38E+09
190.807	273539	2.103	1.42E+09
190.833	273338	2.143	1.46E+09
190.859	273137	2.183	1.50E+09
190.885	272936	2.223	1.54E+09
190.911	272735	2.263	1.58E+09
190.937	272534	2.303	1.62E+09
190.963	272333	2.343	1.66E+09
190.989	272132	2.383	1.70E+09
191.015	271931	2.423	1.74E+09
191.041	271730	2.463	1.78E+09
191.067	271529	2.503	1.82E+09
191.093	271328	2.543	1.86E+09
191.119	271127	2.583	1.90E+09
191.145	270926	2.623	1.94E+09
191.171	270725	2.663	1.98E+09
191.197	270524	2.703	2.02E+09
191.223	270323	2.743	2.06E+09
191.249	270122	2.783	2.10E+09
191.275	269921	2.823	2.14E+09
191.301	269720	2.863	2.18E+09
191.327	269519	2.903	2.22E+09
191.353	269318	2.943	2.26E+09
191.379	269117	2.983	2.30E+09
191.405	268916	3.023	2.34E+09
191.431	268715	3.063	2.38E+09
191.457	268514	3.103	2.42E+09
191.483	268313	3.143	2.46E+09
191.509	268112	3.183	2.50E+09
191.535	267911	3.223	2.54E+09
191.561	267710	3.263	2.58E+09
191.587	267509	3.303	2.62E+09
191.613	267308	3.343	2.66E+09
191.639	267107	3.383	2.70E+09
191.665	266906	3.423	2.74E+09
191.691	266705	3.463	2.78E+09
191.717	266504	3.503	2.82E+09
191.743	266303	3.543	2.86E+09
191.769	266102	3.583	2.90E+09
191.795	265901	3.623	2.94E+09
191.821	265700	3.663	2.98E+09
191.847	265499	3.703	3.02E+09
191.873	265298	3.743	3.06E+09
191.899	265097	3.783	3.10E+09
191.925	264896	3.823	3.14E+09
191.951	264695	3.863	3.18E+09
191.977	264494	3.903	3.22E+09
192.003	264293	3.943	3.26E+09
192.029	264092	3.983	3.30E+09
192.055	263891	4.023	3.34E+09
192.081	263690	4.063	3.38E+09
192.107	263489	4.103	3.42E+09
192.133	263288	4.143	3.46E+09
192.159	263087	4.183	3.50E+09
192.185	262886	4.223	3.54E+09
192.211	262685	4.263	3.58E+09
192.237	262484	4.303	3.62E+09
192.263	262283	4.343	3.66E+09
192.289	262082	4.383	3.70E+09
192.315	261881	4.423	3.74E+09
192.341	261680	4.463	3.78E+09
192.367	261479	4.503	3.82E+09
192.393	261278	4.543	3.86E+09
192.419	261077	4.583	3.90E+09
192.445	260876	4.623	3.94E+09
192.471	260675	4.663	3.98E+09
192.497	260474	4.703	4.02E+09
192.523	260273	4.743	4.06E+09
192.549	260072	4.783	4.10E+09
192.575	259871	4.823	4.14E+09
192.601	259670	4.863	4.18E+09
192.627	259469	4.903	4.22E+09
192.653	259268	4.943	4.26E+09
192.679	259067	4.983	4.30E+09
192.705	258866	5.023	4.34E+09
192.731	258665	5.063	4.38E+09
192.757	258464	5.103	4.42E+09
192.783	258263	5.143	4.46E+09
192.809	258062	5.183	4.50E+09
192.835	257861	5.223	4.54E+09
192.861	257660	5.263	4.58E+09
192.887	257459	5.303	4.62E+09
192.913	257258	5.343	4.66E+09
192.939	257057	5.383	4.70E+09
192.965	256856	5.423	4.74E+09
192.991	256655	5.463	4.78E+09
193.017	256454	5.503	4.82E+09
193.043	256253	5.543	4.86E+09
193.069	256052	5.583	4.90E+09
193.095	255851	5.623	4.94E+09
193.121	255650	5.663	4.98E+09
193.147	255449	5.703	5.02E+09
193.173	255248	5.743	5.06E+09
193.199	255047	5.783	5.10E+09
193.225	254846	5.823	5.14E+09
193.251	254645	5.863	5.18E+09
193.277	254444	5.903	5.22E+09
193.303	254243	5.943	5.26E+09
193.329	254042	5.983	5.30E+09
193.355	253841	6.023	5.34E+09
193.381	253640	6.063	5.38E+09
193.407	253439	6.103	5.42E+09
193.433	253238	6.143	5.46E+09
193.459	253037	6.183	5.50E+09
193.485	252836	6.223	5.54E+09
193.511	252635	6.263	5.58E+09
193.537	252434	6.303	5.62E+09
193.563	252233	6.343	5.66E+09
193.589	252032	6.383	5.70E+09
193.615	251831	6.423	5.74E+09
193.641	251630	6.463	5.78E+09
193.667	251429	6.503	5.82E+09
193.693	251228	6.543	5.86E+09
193.719	251027	6.583	5.90E+09
193.745	250826	6.623	5.94E+09
193.771	250625	6.663	5.98E+09
193.797	250424	6.703	6.02E+09
193.823	250223	6.743	6.06E+09
193.849	250022	6.783	6.10E+09
193.875	249821	6.823	6.14E+09
193.901	249620	6.863	6.18E+09
193.927	249419	6.903	6.22E+09
193.953	249218	6.943	6.26E+09
193.979	249017	6.983	6.30E+09
194.005	248816	7.023	6.34E+09
194.031	248615	7.063	6.38E+09
194.057	248414	7.103	6.42E+09
194.083	248213	7.143	6.46E+09
194.109	248012	7.183	6.50E+09
194.135	247811	7.223	6.54E+09
194.161	247610	7.263	6.58E+09
194.187	247409	7.303	6.62E+09
194.213	247208	7.343	6.66E+09
194.239	247007	7.383	6.70E+09
194.265	246806	7.423	6.74E+09
194.291	246605	7.463	6.78E+09
194.317	246404	7.503	6.82E+09
194.343	246203	7.543	6.86E+09
194.369	246002	7.583	6.90E+09
194.395	245801	7.623	6.94E+09
194.421	245600	7.663	6.98E+09
194.447	245399	7.703	7.02E+09
194.473	245198	7.743	7.06E+09
194.499	244997	7.783	7.10E+09
194.525	244796	7.823	7.14E+09
194.551	244595	7.863	7.18E+09
194.577	244394	7.903	7.22E+09
194.603	244193	7.943	7.26E+09
194.629	243992	7.983	7.30E+09
194.655	243791	8.023	7.34E+09
194.681	243590	8.063	7.38E+09
194.707	243389	8.103	7.42E+09
194.733	243188	8.143	7.46E+09
194.759	242987	8.183	7.50E+09
194.785	242786	8.223	7.54E+09
194.811	242585	8.263	7.58E+09
194.837	242384	8.303	7.62E+09
194.863	242183	8.343	7.66E+09
194.889	241982	8.383	7.70E+09
194.915	241781	8.423	7.74E+09
194.941	241580	8.463	7.78E+09
194.967	241379	8.503	7.82E+09
194.993	241178	8.543	7.86E+09
195.019	240977	8.583	7.90E+09
195.045	240776	8.623	7.94E+09
195.071	240575	8.663	7.98E+09
195.097	240374	8.703	8.02E+09
195.123	240173	8.743	8.06E+09
195.149	239972	8.783	8.10E+09
195.175	239771	8.823	8.14E+09
195.201	239570	8.863	8.18E+09
195.227	239369	8.903	8.22E+09
195.253	239168	8.943	8.26E+09
195.279	238967	8.983	8.30E+09
195.305	238766	9.023	8.34E+09
195.331	238565	9.063	8.38E+09
195.357	238364	9.103	8.42E+09
195.383	238163	9.143	8.46E+09
195.409	237962	9.183	8.50E+09
195.435	237761	9.223	8.54E+09
195.461	237560	9.263	8.58E+09
195.487	237359	9.303	8.62E+09
195.513	237158	9.343	8.66E+09
195.539	236957	9.383	8.70E+09
195.565	236756	9.423	8.74E+09
195.591	236555	9.463	8.78E+09
195.617	236354	9.503	8.82E+09
195.643	236153	9.543	8.86E+09
195.669	235952	9.583	8.90E+09
195.695	235751	9.623	8.94E+09
195.721	235550	9.663	8.98E+09
195.747	235349	9.703	9.02E+09
195.773	235148	9.743	9.06E+09
195.799	234947	9.783	9.10E+09
195.825	234746	9.823	9.14E+09
195.851	234545	9.863	9.18E+09
195.877	234344	9.903	9.22E+09
195.903	234143	9.943	9.26E+09
195.929	233942	9.983	9.30E+09
195.955	233741	10.023	9.34E+09
195.981	233540	10.063	9.38E

APPENDIX B - Continued

TABULATIONS OF CURRENT AND INFERRED ELECTRON DENSITY FOR RAM C-II, PROBE 1

ELAPSED TIME, SECONDS	ALTITUDE, FEET	CURRENT, MICROAMPS	ELECTRON DENSITY, ELECTRONS PER CUBIC CENTIMETER
389.732	281300	+100	6.18E+07
389.760	281151	+100	6.18E+07
389.787	280977	+100	6.18E+07
389.834	280671	+100	6.18E+07
389.862	280484	+100	6.18E+07
389.889	280317	+100	6.18E+07
389.937	280024	+100	6.18E+07
389.992	279628	+100	6.18E+07
390.040	279337	+100	6.18E+07
390.068	279160	+100	6.18E+07
390.095	278982	+100	6.18E+07
390.142	278675	+110	6.18E+07
390.170	278492	+100	6.18E+07
390.197	278313	+100	6.18E+07
390.244	277995	+100	6.20E+07
390.272	277805	+119	7.37E+07
390.375	277124	+100	6.20E+07
390.402	276948	+137	8.51E+07
390.449	276634	+161	1.01E+08
390.477	276452	+129	7.45E+07
390.504	276271	+155	9.01E+07
390.553	275953	+168	1.17E+08
390.581	275767	+119	7.38E+07
390.658	275256	+163	1.02E+08
390.686	275074	+160	1.02E+08
390.710	274914	+211	1.32E+08
390.755	274627	+160	1.07E+08
390.783	274461	+230	1.44E+08
390.810	274290	+190	1.19E+08
390.859	273924	+182	1.17E+08
390.886	273746	+173	1.08E+08
390.913	273568	+120	7.48E+07
390.960	273257	+160	1.02E+08
390.988	273081	+260	1.63E+08
391.015	272904	+260	1.63E+08
391.042	272726	+410	3.44E+08
391.070	272549	+830	5.25E+08
391.117	272244	+75	7.44E+07
391.145	272067	+300	3.65E+08
391.193	271750	+590	3.72E+08
391.220	271581	+378	3.40E+08
391.248	271406	+613	3.85E+08
391.296	271119	+680	4.17E+08
391.324	270937	+860	5.39E+08
391.373	270616	+907	5.00E+08
391.401	270434	+974	5.58E+08
391.428	270256	+874	5.58E+08
391.476	269952	+836	5.31E+08
391.504	269774	+860	5.58E+08
391.531	269595	+876	5.57E+08
391.579	269282	+866	5.38E+08
391.607	269104	+870	5.49E+08
391.634	268927	+871	5.60E+08
391.681	268624	+860	5.28E+08
391.709	268437	+1,087	6.00E+08
391.736	268252	+1,135	7.28E+08
391.784	267941	+1,411	9.13E+08
391.812	267757	+1,117	7.18E+08
391.839	267574	+1,136	7.28E+08
391.887	267273	+989	6.39E+08
391.915	267095	+1,066	6.83E+08
391.942	266917	+1,129	7.28E+08
391.990	266612	+1,302	8.00E+08
392.018	266434	+1,378	8.91E+08
392.045	266256	+1,425	9.58E+08
392.093	265954	+1,551	1.04E+09
392.121	265771	+1,476	9.58E+08
392.148	265594	+1,677	1.20E+09
392.196	265291	+1,261	8.15E+08
392.224	265109	+1,350	8.87E+08
392.251	264924	+1,356	8.75E+08
392.299	264621	+1,339	8.88E+08
392.327	264441	+1,378	9.04E+08
392.354	264265	+1,559	1.02E+09
392.401	263959	+1,332	1.13E+09
392.429	263781	+2,236	1.34E+09
392.456	263602	+2,472	1.60E+09
392.504	263271	+2,229	1.48E+09
392.532	263092	+2,065	1.30E+09
392.560	262911	+2,200	1.32E+09
392.607	262605	+1,832	1.27E+09
392.635	262426	+1,911	1.28E+09
392.682	262124	+2,007	1.30E+09
392.710	261943	+2,009	1.47E+09
392.738	261762	+2,169	1.90E+09
392.785	261454	+2,497	2.83E+09
392.813	261270	+2,555	1.72E+09
392.841	261089	+2,673	1.81E+09
392.888	260785	+3,003	2.14E+09
392.916	260605	+2,722	1.85E+09
392.944	260426	+3,202	2.21E+09
392.971	260246	+3,421	2.38E+09
393.019	259874	+3,746	2.44E+09
393.047	259694	+3,986	2.75E+09
393.074	259514	+4,207	3.01E+09
393.121	259214	+3,321	2.11E+09
393.149	259037	+3,202	2.22E+09
393.176	258860	+3,354	2.34E+09
393.224	258551	+3,672	2.42E+09
393.252	258374	+3,843	2.60E+09
393.279	258194	+3,701	2.41E+09
393.327	257916	+4,488	3.24E+09
393.355	257736	+5,156	3.78E+09
393.382	257556	+5,375	3.88E+09
393.429	257251	+5,073	3.50E+09
393.457	257070	+5,043	3.48E+09
393.484	256892	+4,896	3.38E+09
393.512	256714	+5,131	3.50E+09
393.540	256536	+4,207	3.07E+09
393.587	256231	+4,318	3.18E+09
393.615	256054	+4,431	3.28E+09
393.643	255876	+4,713	3.44E+09
393.690	255571	+4,855	3.58E+09
393.738	255265	+5,223	4.12E+09
393.766	255089	+5,779	4.34E+09
393.793	254912	+5,779	4.34E+09
393.840	254642	+5,672	4.43E+09
393.868	254465	+5,441	4.26E+09

ELAPSED TIME, SECONDS	ALTITUDE, FEET	CURRENT, MICROAMPS	ELECTRON DENSITY, ELECTRONS PER CUBIC CENTIMETER
393.895	254282	+5,872	4.43E+09
393.943	253978	+6,309	4.85E+09
393.971	253799	+6,172	4.49E+09
394.018	253493	+5,279	4.79E+09
394.046	253315	+6,279	4.79E+09
394.074	253137	+5,969	4.52E+09
394.101	252958	+5,808	4.28E+09
394.148	252654	+5,375	4.02E+09
394.176	252476	+4,896	3.61E+09
394.224	252172	+5,166	3.80E+09
394.251	251994	+5,779	4.37E+09
394.279	251816	+5,779	4.37E+09
394.306	251638	+5,217	4.00E+09
394.353	251324	+8,984	7.36E+09
394.381	251146	+8,984	7.36E+09
394.408	250968	+7,758	6.10E+09
394.456	250663	+6,504	5.01E+09
394.484	250485	+5,969	4.54E+09
394.511	250307	+6,172	4.72E+09
394.559	249993	+5,969	4.55E+09
394.587	249815	+6,504	5.02E+09
394.614	249637	+6,995	5.45E+09
394.661	249332	+8,551	6.90E+09
394.689	249154	+9,747	8.18E+09
394.716	248976	+10,439	8.88E+09
394.764	248671	+10,439	8.88E+09
394.792	248493	+10,253	8.72E+09
394.819	248315	+9,586	8.01E+09
394.867	247999	+8,217	6.85E+09
394.895	247821	+8,381	6.82E+09
394.922	247643	+8,551	6.90E+09
394.969	247338	+8,727	7.17E+09
395.000	247160	+9,747	8.22E+09
395.027	246982	+10,439	8.88E+09
395.054	246804	+10,253	8.72E+09
395.081	246626	+9,586	8.01E+09
395.128	246321	+8,217	6.85E+09
395.156	246143	+8,381	6.82E+09
395.183	245965	+8,551	6.90E+09
395.230	245660	+11,307	9.40E+09
395.258	245482	+11,479	9.58E+09
395.285	245304	+11,651	9.76E+09
395.312	245126	+11,823	1.03E+10
395.360	244821	+13,223	1.21E+10
395.387	244643	+14,236	1.32E+10
395.414	244465	+14,574	1.36E+10
395.461	244160	+14,800	1.40E+10
395.489	243982	+14,800	1.40E+10
395.516	243804	+14,800	1.40E+10
395.563	243499	+16,091	1.62E+10
395.591	243321	+16,362	1.66E+10
395.618	243143	+16,633	1.70E+10
395.665	242838	+16,922	1.84E+10
395.693	242660	+17,193	1.88E+10
395.720	242482	+17,464	1.92E+10
395.767	242177	+17,735	1.96E+10
395.795	242000	+18,006	2.00E+10
395.822	241822	+18,277	2.04E+10
395.869	241517	+18,548	2.08E+10
395.897	241339	+18,819	2.12E+10
395.924	241161	+19,090	2.16E+10
395.971	240856	+19,361	2.20E+10
396.000	240678	+19,632	2.24E+10
396.027	240500	+19,903	2.28E+10
396.054	240322	+20,174	2.32E+10
396.081	240144	+20,445	2.36E+10
396.128	239839	+20,716	2.40E+10
396.156	239661	+20,987	2.44E+10
396.183	239483	+21,258	2.48E+10
396.230	239178	+21,529	2.52E+10
396.258	239000	+21,800	2.56E+10
396.285	238822	+22,071	2.60E+10
396.312	238644	+22,342	2.64E+10
396.359	238339	+22,613	2.68E+10
396.387	238161	+22,884	2.72E+10
396.414	237983	+23,155	2.76E+10
396.461	237678	+23,426	2.80E+10
396.489	237500	+23,697	2.84E+10
396.516	237322	+23,968	2.88E+10
396.563	237017	+24,239	2.92E+10
396.591	236839	+24,510	2.96E+10
396.618	236661	+24,781	3.00E+10
396.665	236356	+25,052	3.04E+10
396.693	236178	+25,323	3.08E+10
396.720	236000	+25,594	3.12E+10
396.767	235695	+25,865	3.16E+10
396.795	235517	+26,136	3.20E+10
396.822	235339	+26,407	3.24E+10
396.869	235034	+26,678	3.28E+10
396.897	234856	+26,949	3.32E+10
396.924	234678	+27,220	3.36E+10
396.971	234373	+27,491	3.40E+10
397.000	234195	+27,762	3.44E+10
397.027	234017	+28,033	3.48E+10
397.054	233839	+28,304	3.52E+10
397.101	233534	+28,575	3.56E+10
397.129	233356	+28,846	3.60E+10
397.156	233178	+29,117	3.64E+10
397.203	232873	+29,388	3.68E+10
397.231	232695	+29,659	3.72E+10
397.258	232517	+29,930	3.76E+10
397.305	232212	+30,201	3.80E+10
397.333	232034	+30,472	3.84E+10
397.360	231856	+30,743	3.88E+10
397.407	231551	+31,014	3.92E+10
397.435	231373	+31,285	3.96E+10
397.462	231195	+31,556	4.00E+10
397.509	230890	+31,827	4.04E+10
397.537	230712	+32,098	4.08E+10
397.564	230534	+32,369	4.12E+10
397.611	230229	+32,640	4.16E+10
397.639	230051	+32,911	4.20E+10
397.666	229873	+33,182	4.24E+10
397.713	229568	+33,453	4.28E+10
397.741	229390	+33,724	4.32E+10
397.768	229212	+33,995	4.36E+10
397.815	228907	+34,266	4.40E+10
397.843	228729	+34,537	4.44E+10
397.870	228551	+34,808	4.48E+10

APPENDIX B - Continued

TABULATIONS OF CURRENT AND INFERRED ELECTRON DENSITY FOR RAM C-II, PROBE 2

ELAPSED TIME, SECONDS	ALTITUDE, FEET (a)	CURRENT, MICROAMPS	ELECTRON DENSITY, ELECTRONS PER CUBIC CENTIMETER	ELAPSED TIME, SECONDS	ALTITUDE, FEET (a)	CURRENT, MICROAMPS	ELECTRON DENSITY, ELECTRONS PER CUBIC CENTIMETER	ELAPSED TIME, SECONDS	ALTITUDE, FEET (a)	CURRENT, MICROAMPS	ELECTRON DENSITY, ELECTRONS PER CUBIC CENTIMETER	ELAPSED TIME, SECONDS	ALTITUDE, FEET (a)	CURRENT, MICROAMPS	ELECTRON DENSITY, ELECTRONS PER CUBIC CENTIMETER
389.736	281278	-1.03	5.85E+07	393.844	295420	7.905	5.36E+08	397.857	227970	88.413	9.88E+10	401.967	201315	445.000	5.70E+11
389.763	281129	-1.03	5.85E+07	393.871	295430	7.905	5.36E+08	397.945	227959	88.413	9.88E+10	401.994	201138	445.000	5.70E+11
389.790	280955	-1.03	5.85E+07	393.899	295460	7.905	5.36E+08	397.972	227948	88.413	9.88E+10	402.020	200928	570.000	7.53E+11
389.818	280849	-1.03	5.85E+07	393.927	295490	7.905	5.36E+08	398.000	227937	88.413	9.88E+10	402.047	200718	695.000	8.78E+11
389.845	280742	-1.03	5.85E+07	393.954	295520	7.905	5.36E+08	398.028	226990	94.275	1.07E+11	402.074	200507	770.000	9.01E+11
389.873	280635	-1.03	5.85E+07	394.002	295588	8.551	5.86E+08	398.055	226841	101.426	1.17E+11	402.101	200297	845.000	9.24E+11
389.901	279984	-1.03	5.85E+07	394.050	295377	8.551	5.86E+08	398.102	226638	117.427	1.42E+11	402.128	199992	920.000	9.47E+11
389.928	279808	-1.03	5.85E+07	394.077	295301	8.058	5.46E+08	398.130	226531	134.356	1.66E+11	402.155	199786	995.000	9.70E+11
389.956	279632	-1.03	5.85E+07	394.104	295225	7.558	5.26E+08	398.157	226424	151.285	1.90E+11	402.182	199580	1070.000	9.93E+11
390.004	279315	-1.03	5.85E+07	394.152	295217	7.253	4.87E+08	398.204	225981	124.678	1.49E+11	402.209	199374	1145.000	1.01E+12
390.031	279137	-1.03	5.85E+07	394.179	295241	7.386	4.97E+08	398.232	225703	95.991	1.09E+11	402.236	199168	1220.000	1.03E+12
390.058	278960	-1.03	5.85E+07	394.207	295204	7.386	4.97E+08	398.259	225425	88.413	9.88E+10	402.263	198962	1295.000	1.05E+12
390.146	278648	-1.12	7.03E+07	394.255	295182	8.551	5.87E+08	398.307	225347	83.473	9.22E+10	402.290	198756	1370.000	1.07E+12
390.173	278470	-1.12	7.03E+07	394.282	295107	7.253	4.87E+08	398.355	225050	81.236	8.45E+10	402.317	198550	1445.000	1.09E+12
390.200	278291	-1.12	7.03E+07	394.309	295153	11.680	8.46E+08	398.382	224864	89.788	1.00E+11	402.344	198344	1520.000	1.11E+12
390.248	277977	-1.12	7.03E+07	394.357	295126	12.685	9.32E+08	398.409	224689	100.222	1.14E+11	402.371	198138	1595.000	1.13E+12
390.275	277783	-1.09	6.41E+07	394.384	295104	12.685	9.32E+08	398.436	224514	110.265	1.28E+11	402.398	197932	1670.000	1.15E+12
390.303	277602	-1.03	5.86E+07	394.412	295082	10.796	7.71E+08	398.464	224340	120.308	1.42E+11	402.425	197726	1745.000	1.17E+12
390.351	277185	-1.17	6.96E+07	394.460	295051	8.381	5.75E+08	398.512	224023	134.629	1.56E+11	402.452	197520	1820.000	1.19E+12
390.378	277105	-1.03	5.86E+07	394.487	295032	7.758	5.26E+08	398.560	223711	177.431	2.30E+11	402.479	197314	1895.000	1.21E+12
390.405	276922	-1.10	5.86E+07	394.515	295024	7.617	5.10E+08	398.587	223535	151.473	1.89E+11	402.506	197108	1970.000	1.23E+12
390.453	276611	-1.46	6.35E+07	394.563	294981	7.617	5.10E+08	398.614	223359	137.032	1.67E+11	402.533	196902	2045.000	1.25E+12
390.480	276430	-2.03	1.41E+08	394.590	294913	8.217	5.62E+08	398.662	223043	131.635	1.44E+11	402.560	196696	2120.000	1.27E+12
390.508	276249	-2.03	1.41E+08	394.617	294845	9.586	6.71E+08	398.689	222868	139.393	1.41E+11	402.587	196490	2195.000	1.29E+12
390.556	275936	-2.03	1.41E+08	394.665	294823	11.130	7.81E+08	398.716	222693	129.116	1.55E+11	402.614	196284	2270.000	1.31E+12
390.584	275753	-2.03	1.41E+08	394.692	294802	11.223	7.82E+08	398.764	222346	142.629	1.75E+11	402.641	196078	2345.000	1.33E+12
390.611	275572	-2.03	1.41E+08	394.720	294780	12.685	9.32E+08	398.791	222171	151.473	1.89E+11	402.668	195872	2420.000	1.35E+12
390.638	275391	-2.03	1.41E+08	394.768	294833	12.687	9.32E+08	398.818	221996	144.685	2.07E+11	402.695	195666	2495.000	1.37E+12
390.713	274985	-1.10	1.15E+08	394.795	294853	13.046	9.47E+08	398.866	221675	145.518	1.79E+11	402.722	195460	2570.000	1.39E+12
390.759	274636	-1.10	1.15E+08	394.822	294873	12.687	9.32E+08	398.893	221500	131.712	1.58E+11	402.749	195254	2645.000	1.41E+12
390.786	274459	-1.10	1.15E+08	394.870	294859	12.078	8.83E+08	398.921	221325	131.712	1.58E+11	402.776	195048	2720.000	1.43E+12
390.813	274282	-1.10	1.15E+08	394.918	294840	12.078	8.83E+08	398.948	221150	124.678	1.49E+11	402.803	194842	2795.000	1.45E+12
390.862	273902	-1.23	1.26E+08	394.924	294800	11.876	8.68E+08	398.996	220824	144.283	2.37E+11	402.830	194636	2870.000	1.47E+12
390.889	273724	-1.23	1.26E+08	394.972	294786	12.315	9.04E+08	399.023	220649	151.473	2.08E+11	402.857	194430	2945.000	1.49E+12
390.916	273546	-1.23	1.26E+08	395.000	294764	12.315	9.04E+08	399.050	220474	144.283	2.37E+11	402.884	194224	3020.000	1.51E+12
390.943	273368	-1.23	1.26E+08	395.027	294742	12.685	9.32E+08	399.077	220299	137.032	2.37E+11	402.911	194018	3095.000	1.53E+12
390.970	273190	-1.23	1.26E+08	395.054	294720	13.046	9.47E+08	399.104	220124	129.116	2.37E+11	402.938	193812	3170.000	1.55E+12
391.018	272805	-1.23	1.26E+08	395.102	294707	12.685	9.32E+08	399.131	219949	121.678	2.37E+11	402.965	193606	3245.000	1.57E+12
391.066	272573	-1.23	1.26E+08	395.129	294685	12.078	8.83E+08	399.158	219774	114.283	2.37E+11	402.992	193400	3320.000	1.59E+12
391.093	272395	-1.23	1.26E+08	395.177	294663	12.078	8.83E+08	399.185	219599	106.889	2.37E+11	403.019	193194	3395.000	1.61E+12
391.121	272218	-1.23	1.26E+08	395.204	294641	14.772	1.12E+11	399.212	219424	124.678	1.45E+11	403.046	192988	3470.000	1.63E+12
391.148	272040	-1.23	1.26E+08	395.232	294619	14.772	1.12E+11	399.239	219249	117.427	1.45E+11	403.073	192782	3545.000	1.65E+12
391.175	271862	-1.23	1.26E+08	395.280	294597	14.772	1.12E+11	399.266	219074	110.265	1.45E+11	403.100	192576	3620.000	1.67E+12
391.202	271684	-1.23	1.26E+08	395.307	294575	14.772	1.12E+11	399.293	218899	103.104	1.45E+11	403.127	192370	3695.000	1.69E+12
391.229	271506	-1.23	1.26E+08	395.355	294553	14.772	1.12E+11	399.320	218724	95.991	1.45E+11	403.154	192164	3770.000	1.71E+12
391.256	271328	-1.23	1.26E+08	395.382	294531	14.772	1.12E+11	399.347	218549	88.413	9.88E+10	403.181	191958	3845.000	1.73E+12
391.283	271150	-1.23	1.26E+08	395.430	294509	14.772	1.12E+11	399.374	218374	81.236	8.45E+10	403.208	191752	3920.000	1.75E+12
391.310	270972	-1.23	1.26E+08	395.457	294487	14.772	1.12E+11	399.401	218199	74.059	8.45E+10	403.235	191546	4000.000	1.77E+12
391.337	270794	-1.23	1.26E+08	395.484	294465	14.772	1.12E+11	399.428	218024	66.882	8.45E+10	403.262	191340	4075.000	1.79E+12
391.364	270616	-1.23	1.26E+08	395.511	294443	14.772	1.12E+11	399.455	217849	59.705	8.45E+10	403.289	191134	4150.000	1.81E+12
391.391	270438	-1.23	1.26E+08	395.538	294421	14.772	1.12E+11	399.482	217674	52.528	8.45E+10	403.316	190928	4225.000	1.83E+12
391.418	270260	-1.23	1.26E+08	395.565	294399	14.772	1.12E+11	399.509	217499	45.351	8.45E+10	403.343	190722	4300.000	1.85E+12
391.445	270082	-1.23	1.26E+08	395.592	294377	14.772	1.12E+11	399.536	217324	38.174	8.45E+10	403.370	190516	4375.000	1.87E+12
391.472	269904	-1.23	1.26E+08	395.619	294355	14.772	1.12E+11	399.563	217149	30.997	8.45E+10	403.397	190310	4450.000	1.89E+12
391.499	269726	-1.23	1.26E+08	395.646	294333	14.772	1.12E+11	399.590	216974	23.820	8.45E+10	403.424	190104	4525.000	1.91E+12
391.526	269548	-1.23	1.26E+08	395.673	294311	14.772	1.12E+11	399.617	216799	16.643	8.45E+10	403.451	189898	4600.000	1.93E+12
391.553	269370	-1.23	1.26E+08	395.700	294289	14.772	1.12E+11	399.644	216624	9.466	8.45E+10	403.478	189692	4675.000	1.95E+12
391.580	269192	-1.23	1.26E+08	395.727	294267	14.772	1.12E+11	399.671	216449	2.289	8.45E+10	403.505	189486	4750.000	1.97E+12
391.607	269014	-1.23	1.26E+08	395.754	294245	14.772	1.12E+11	399.698	216274	-5.112	8.45E+10	403.532	189280	4825.000	1.99E+12
391.634	268836	-1.23	1.26E+08	395.781	294223	14.772	1.12E+11	399.725	216099	-12.289	8.45E+10	403.559	189074	4900.000	2.01E+12
391.661	268658	-1.23	1.26E+08	395.808	294201	14.772	1.12E+11	399.752	215924	-19.466	8.45E+10	403.586	188868	4975.000	2.03E+12
391.688	268480	-1.23	1.26E+08	395.835	294179	14.772	1.12E+11	399.779	215749	-26.643	8.45E+10	403.613	188662	50	

APPENDIX B - Continued

TABLATIONS OF CURRENT AND INFERRED ELECTRON DENSITY FOR RAM C-II, PROBE 3

ELAPSED TIME, SECONDS	ALTITUDE, FEET (a)	CURRENT, MICROAMPS PER CUBIC CENTIMETER	ELECTRON DENSITY, ELECTRONS PER CUBIC CENTIMETER
349.730	281257	+103	5.01E+07
349.760	281107	+100	5.01E+07
349.784	280933	+100	5.01E+07
349.841	280627	+100	5.01E+07
349.869	280550	+100	5.01E+07
349.896	280272	+100	5.01E+07
349.944	279981	+100	5.01E+07
349.972	279782	+100	5.01E+07
349.999	279605	+100	5.01E+07
350.027	279263	+100	5.01E+07
350.074	279115	+120	6.73E+07
350.102	278938	+100	5.01E+07
350.148	278626	+110	6.17E+07
350.176	278447	+120	7.18E+07
350.204	278268	+160	8.98E+07
350.251	277947	+100	5.01E+07
350.279	277762	+100	5.01E+07
350.306	277574	+119	6.87E+07
350.334	277382	+100	5.01E+07
350.381	277063	+119	6.87E+07
350.409	276903	+146	8.13E+07
350.456	276588	+100	5.01E+07
350.484	276407	+203	1.14E+08
350.511	276226	+243	1.35E+08
350.560	275907	+155	8.88E+07
350.588	275726	+155	8.88E+07
350.635	275211	+148	8.28E+07
350.663	275042	+148	8.28E+07
350.710	274677	+148	8.28E+07
350.742	274455	+148	8.28E+07
350.770	274325	+220	1.24E+08
350.827	274105	+323	1.80E+08
350.865	273888	+170	1.10E+08
350.892	273732	+153	8.84E+07
350.920	273554	+153	8.84E+07
350.967	273133	+162	9.21E+07
351.004	273036	+145	8.11E+07
351.032	272860	+170	1.21E+08
351.059	272651	+145	8.11E+07
351.087	272473	+145	8.11E+07
351.134	272198	+145	8.11E+07
351.172	271887	+145	8.11E+07
351.200	271732	+145	8.11E+07
351.227	271537	+145	8.11E+07
351.255	271355	+145	8.11E+07
351.303	271074	+145	8.11E+07
351.331	270902	+145	8.11E+07
351.380	270575	+145	8.11E+07
351.408	270398	+145	8.11E+07
351.435	270220	+145	8.11E+07
351.483	269908	+145	8.11E+07
351.511	269730	+145	8.11E+07
351.538	269551	+145	8.11E+07
351.586	269238	+145	8.11E+07
351.613	269060	+145	8.11E+07
351.641	268882	+145	8.11E+07
351.689	268569	+145	8.11E+07
351.716	268395	+145	8.11E+07
351.743	268227	+145	8.11E+07
351.791	267905	+145	8.11E+07
351.819	267728	+145	8.11E+07
351.846	267550	+145	8.11E+07
351.894	267185	+145	8.11E+07
351.922	267011	+145	8.11E+07
351.949	266830	+145	8.11E+07
351.977	266650	+145	8.11E+07
352.025	266339	+145	8.11E+07
352.052	266161	+145	8.11E+07
352.080	265983	+145	8.11E+07
352.108	265807	+145	8.11E+07
352.155	265496	+145	8.11E+07
352.203	265187	+145	8.11E+07
352.231	265011	+145	8.11E+07
352.258	264834	+145	8.11E+07
352.286	264657	+145	8.11E+07
352.333	264347	+145	8.11E+07
352.361	264170	+145	8.11E+07
352.388	263994	+145	8.11E+07
352.436	263683	+145	8.11E+07
352.463	263508	+145	8.11E+07
352.511	263197	+145	8.11E+07
352.538	263024	+145	8.11E+07
352.566	262848	+145	8.11E+07
352.614	262534	+145	8.11E+07
352.642	262357	+145	8.11E+07
352.689	262044	+145	8.11E+07
352.717	261868	+145	8.11E+07
352.745	261693	+145	8.11E+07
352.772	261519	+145	8.11E+07
352.820	261205	+145	8.11E+07
352.848	261028	+145	8.11E+07
352.896	260714	+145	8.11E+07
352.924	260538	+145	8.11E+07
352.952	260362	+145	8.11E+07
352.980	260186	+145	8.11E+07
353.008	259999	+145	8.11E+07
353.036	259823	+145	8.11E+07
353.064	259647	+145	8.11E+07
353.092	259471	+145	8.11E+07
353.120	259295	+145	8.11E+07
353.148	259119	+145	8.11E+07
353.176	258943	+145	8.11E+07
353.204	258767	+145	8.11E+07
353.232	258591	+145	8.11E+07
353.260	258415	+145	8.11E+07
353.288	258239	+145	8.11E+07
353.316	258063	+145	8.11E+07
353.344	257887	+145	8.11E+07
353.372	257711	+145	8.11E+07
353.400	257535	+145	8.11E+07
353.428	257359	+145	8.11E+07
353.456	257183	+145	8.11E+07
353.484	257007	+145	8.11E+07
353.512	256831	+145	8.11E+07
353.540	256655	+145	8.11E+07
353.568	256479	+145	8.11E+07
353.596	256303	+145	8.11E+07
353.624	256127	+145	8.11E+07
353.652	255951	+145	8.11E+07
353.680	255775	+145	8.11E+07
353.708	255599	+145	8.11E+07
353.736	255423	+145	8.11E+07
353.764	255247	+145	8.11E+07
353.792	255071	+145	8.11E+07
353.820	254895	+145	8.11E+07

ELAPSED TIME, SECONDS	ALTITUDE, FEET (a)	CURRENT, MICROAMPS	ELECTRON DENSITY, ELECTRONS PER CUBIC CENTIMETER
353.847	254727	8.094	5.48E+07
353.875	254537	8.084	5.48E+07
353.903	254347	8.185	5.82E+07
353.931	254157	8.084	5.48E+07
353.959	253967	10.420	8.72E+07
353.987	253777	8.084	5.48E+07
354.015	253587	10.253	8.72E+07
354.043	253397	11.680	9.67E+07
354.071	253207	10.253	8.72E+07
354.099	253017	15.181	1.04E+08
354.127	252827	14.075	9.70E+07
354.155	252637	13.138	8.98E+07
354.183	252447	10.618	6.90E+07
354.211	252257	10.618	6.90E+07
354.239	252067	9.379	5.98E+07
354.267	251877	9.379	5.98E+07
354.295	251687	11.307	7.40E+07
354.323	251497	11.307	7.40E+07
354.351	251307	14.972	1.01E+08
354.379	251117	14.972	1.01E+08
354.407	250927	14.974	1.02E+08
354.435	250737	15.391	1.08E+08
354.463	250547	14.974	1.02E+08
354.491	250357	14.974	1.02E+08
354.519	250167	14.974	1.02E+08
354.547	250000	14.974	1.02E+08
354.575	249833	14.974	1.02E+08
354.603	249666	14.974	1.02E+08
354.631	249499	14.974	1.02E+08
354.659	249332	14.974	1.02E+08
354.687	249165	14.974	1.02E+08
354.715	248998	14.974	1.02E+08
354.743	248831	14.974	1.02E+08
354.771	248664	14.974	1.02E+08
354.799	248497	14.974	1.02E+08
354.827	248330	14.974	1.02E+08
354.855	248163	14.974	1.02E+08
354.883	247996	14.974	1.02E+08
354.911	247829	14.974	1.02E+08
354.939	247662	14.974	1.02E+08
354.967	247495	14.974	1.02E+08
354.995	247328	14.974	1.02E+08
355.023	247161	14.974	1.02E+08
355.051	246994	14.974	1.02E+08
355.079	246827	14.974	1.02E+08
355.107	246660	14.974	1.02E+08
355.135	246493	14.974	1.02E+08
355.163	246326	14.974	1.02E+08
355.191	246159	14.974	1.02E+08
355.219	245992	14.974	1.02E+08
355.247	245825	14.974	1.02E+08
355.275	245658	14.974	1.02E+08
355.303	245491	14.974	1.02E+08
355.331	245324	14.974	1.02E+08
355.359	245157	14.974	1.02E+08
355.387	244990	14.974	1.02E+08
355.415	244823	14.974	1.02E+08
355.443	244656	14.974	1.02E+08
355.471	244489	14.974	1.02E+08
355.499	244322	14.974	1.02E+08
355.527	244155	14.974	1.02E+08
355.555	243988	14.974	1.02E+08
355.583	243821	14.974	1.02E+08
355.611	243654	14.974	1.02E+08
355.639	243487	14.974	1.02E+08
355.667	243320	14.974	1.02E+08
355.695	243153	14.974	1.02E+08
355.723	242986	14.974	1.02E+08
355.751	242819	14.974	1.02E+08
355.779	242652	14.974	1.02E+08
355.807	242485	14.974	1.02E+08
355.835	242318	14.974	1.02E+08
355.863	242151	14.974	1.02E+08
355.891	241984	14.974	1.02E+08
355.919	241817	14.974	1.02E+08
355.947	241650	14.974	1.02E+08
355.975	241483	14.974	1.02E+08
356.003	241316	14.974	1.02E+08
356.031	241149	14.974	1.02E+08
356.059	240982	14.974	1.02E+08
356.087	240815	14.974	1.02E+08
356.115	240648	14.974	1.02E+08
356.143	240481	14.974	1.02E+08
356.171	240314	14.974	1.02E+08
356.199	240147	14.974	1.02E+08
356.227	239980	14.974	1.02E+08
356.255	239813	14.974	1.02E+08
356.283	239646	14.974	1.02E+08
356.311	239479	14.974	1.02E+08
356.339	239312	14.974	1.02E+08
356.367	239145	14.974	1.02E+08
356.395	238978	14.974	1.02E+08
356.423	238811	14.974	1.02E+08
356.451	238644	14.974	1.02E+08
356.479	238477	14.974	1.02E+08
356.507	238310	14.974	1.02E+08
356.535	238143	14.974	1.02E+08
356.563	237976	14.974	1.02E+08
356.591	237809	14.974	1.02E+08
356.619	237642	14.974	1.02E+08
356.647	237475	14.974	1.02E+08
356.675	237308	14.974	1.02E+08
356.703	237141	14.974	1.02E+08
356.731	236974	14.974	1.02E+08
356.759	236807	14.974	1.02E+08
356.787	236640	14.974	1.02E+08
356.815	236473	14.974	1.02E+08
356.843	236306	14.974	1.02E+08
356.871	236139	14.974	1.02E+08
356.899	235972	14.974	1.02E+08
356.927	235805	14.974	1.02E+08
356.955	235638	14.974	1.02E+08
356.983	235471	14.974	1.02E+08
357.011	235304	14.974	1.02E+08
357.039	235137	14.974	1.02E+08
357.067	234970	14.974	1.02E+08
357.095	234803	14.974	1.02E+08
357.123	234636	14.974	1.02E+08
357.151	234469	14.974	1.02E+08
357.179	234302	14.974	1.02E+08
357.207	234135	14.974	1.02E+08
357.235	233968	14.974	1.02E+08
357.263	233801	14.974	1.02E+08
357.291	233634	14.974	1.02E+08
357.319	233467	14.974	1.02E+08
357.347	233300	14.974	1.02E+08
357.375	233133	14.974	1.02E+08
357.403	232966	14.974	1.02E+08
357.431	232799	14.974	1.02E+08
357.459	232632	14.974	1.02E+08
357.487	232465	14.974	1.02E+08
357.515	232298	14.974	1.02E+08
357.543	232131	14.974	1.02E+08
357.571	231964	14.974	1.02E+08
357.599	231797	14.974	1.02E+08
357.627	231630	14.974	1.02E+08
357.655	231463	14.974	1.02E+08
357.683	231296	14.974	1.02E+08
357.711	231129	14.974	1.02E+08
357.739	230962	14.974	1.02E+08
357.767	230795	14.974	1.02E+08
357.795	230628	14.974	1.02E+08
357.823	230461	14.974	1.02E+08
357.851	230294	14.974	1.02E+08
357.879	230127	14.974	1.02E+08
357.907	229960	14.974	1.02E+08
357.935	229793	14.974	1.02E+08
357.963	229626	14.974	1.02E+08
357.991	229459	14.974	1.02E+08
358.019	229292	14.974	1.02E+08
358.047	229125	14.974	1.02E+08
358.075	228958	14.974	1.02E+08
358.103	228791	14.974	1.02E+08
358.131	228624	14.974	1.02E+08
358.159	228457	14.974	1.02E+08
358.187	228290	14.974	1.02E+08
358.215	228123	14.974	1.02E+08
358.243	227956	14.974	1.02E+08
358.271	227789	14.974	1.02E+08
358.299	227622	14.974	1.02E+08
358.327	227455	14.974	1.02E+08
358.355	227288	14.974	1.02E+08
358.383	227121	14.974	1.02E+08
358.411	226954	14.974	1.02E+08
358.439	226787	14.974	1.02E+08
358.467	226620	14.974	1.02E+08
358.495	226453	14.974	1.02E+08
358.523	226286	14.974	1.02E+08
358.551	226119	14.974	1.02E+08
358.579	225952	14.974	1.02E+08
358.607	225785	14.974	1.02E+08
358.635	225618	14.974	1.02E+08
358.663	225451	14.974	1.02E+08
358.691	225284	14.974	1.02E+08
358.719	225117	14.974	1.02E+08
358.747	224950	14.974	1.02E+08
358.775	224783	14.974	1.02E+08
358.803	224616	14.974	1.02E+08
358.831	224449	14.974	1.02E+08
358.859	224282	14.974	1.02E+08
358.887	224115	14.974	1.02E+08
358.915	223948	14.974	1.02E+08
358.943	223781	14.974	1.02E+08
358.971	223614	14.974	1.02E+08
359.0	223447	14.974	1.02E+08

APPENDIX B - Continued

TABULATIONS OF CURRENT AND INFERRED ELECTRON DENSITY FOR RAM C-II, PROBE 4

ELAPSED TIME, SECONDS	ALTITUDE, FEET	CURRENT, MICROAMPS	ELECTRON DENSITY, ELECTRONS PER CUBIC CENTIMETER
389.743	254135	1.103	5.42E+07
389.770	254104	1.102	5.40E+07
389.787	254011	1.102	5.40E+07
389.843	254004	1.102	5.40E+07
389.872	254027	1.123	5.41E+07
389.900	254030	1.102	5.41E+07
389.948	254030	1.102	5.41E+07
389.975	254031	1.102	5.42E+07
390.003	254083	1.113	5.42E+07
390.051	254271	1.123	5.42E+07
390.078	254093	1.110	5.42E+07
390.103	254105	1.120	5.43E+07
390.153	254003	1.143	5.43E+07
390.180	254025	1.153	5.43E+07
390.207	254025	1.153	5.43E+07
390.255	254019	1.219	5.43E+07
390.282	254037	1.188	5.43E+07
390.310	254056	1.226	5.43E+07
390.338	254240	1.248	5.43E+07
390.365	254000	1.219	5.43E+07
390.412	254081	1.219	5.43E+07
390.440	254066	1.219	5.43E+07
390.467	254384	1.222	5.43E+07
390.515	254203	1.234	5.43E+07
390.563	254083	1.234	5.43E+07
390.591	254097	1.344	5.43E+07
390.618	254067	1.374	5.43E+07
390.646	254021	1.561	5.43E+07
390.720	254050	1.551	5.43E+07
390.746	254336	1.564	5.43E+07
390.793	254353	1.564	5.43E+07
390.821	254372	1.613	5.44E+07
390.849	254376	1.613	5.44E+07
390.876	254379	1.613	5.44E+07
390.923	254379	1.613	5.44E+07
390.971	254391	1.613	5.44E+07
391.028	254391	1.613	5.44E+07
391.073	254391	1.613	5.44E+07
391.100	254391	1.613	5.44E+07
391.128	254391	1.613	5.44E+07
391.176	254391	1.613	5.44E+07
391.203	254391	1.613	5.44E+07
391.230	254391	1.613	5.44E+07
391.278	254391	1.613	5.44E+07
391.306	254391	1.613	5.44E+07
391.333	254391	1.613	5.44E+07
391.361	254391	1.613	5.44E+07
391.411	254391	1.613	5.44E+07
391.439	254391	1.613	5.44E+07
391.467	254391	1.613	5.44E+07
391.495	254391	1.613	5.44E+07
391.523	254391	1.613	5.44E+07
391.551	254391	1.613	5.44E+07
391.579	254391	1.613	5.44E+07
391.607	254391	1.613	5.44E+07
391.635	254391	1.613	5.44E+07
391.663	254391	1.613	5.44E+07
391.691	254391	1.613	5.44E+07
391.719	254391	1.613	5.44E+07
391.747	254391	1.613	5.44E+07
391.775	254391	1.613	5.44E+07
391.803	254391	1.613	5.44E+07
391.831	254391	1.613	5.44E+07
391.859	254391	1.613	5.44E+07
391.887	254391	1.613	5.44E+07
391.915	254391	1.613	5.44E+07
391.943	254391	1.613	5.44E+07
391.971	254391	1.613	5.44E+07
392.000	254391	1.613	5.44E+07
392.028	254391	1.613	5.44E+07
392.056	254391	1.613	5.44E+07
392.084	254391	1.613	5.44E+07
392.112	254391	1.613	5.44E+07
392.140	254391	1.613	5.44E+07
392.168	254391	1.613	5.44E+07
392.196	254391	1.613	5.44E+07
392.224	254391	1.613	5.44E+07
392.252	254391	1.613	5.44E+07
392.280	254391	1.613	5.44E+07
392.308	254391	1.613	5.44E+07
392.336	254391	1.613	5.44E+07
392.364	254391	1.613	5.44E+07
392.392	254391	1.613	5.44E+07
392.420	254391	1.613	5.44E+07
392.448	254391	1.613	5.44E+07
392.476	254391	1.613	5.44E+07
392.504	254391	1.613	5.44E+07
392.532	254391	1.613	5.44E+07
392.560	254391	1.613	5.44E+07
392.588	254391	1.613	5.44E+07
392.616	254391	1.613	5.44E+07
392.644	254391	1.613	5.44E+07
392.672	254391	1.613	5.44E+07
392.700	254391	1.613	5.44E+07
392.728	254391	1.613	5.44E+07
392.756	254391	1.613	5.44E+07
392.784	254391	1.613	5.44E+07
392.812	254391	1.613	5.44E+07
392.840	254391	1.613	5.44E+07
392.868	254391	1.613	5.44E+07
392.896	254391	1.613	5.44E+07
392.924	254391	1.613	5.44E+07
392.952	254391	1.613	5.44E+07
392.980	254391	1.613	5.44E+07
393.008	254391	1.613	5.44E+07
393.036	254391	1.613	5.44E+07
393.064	254391	1.613	5.44E+07
393.092	254391	1.613	5.44E+07
393.120	254391	1.613	5.44E+07
393.148	254391	1.613	5.44E+07
393.176	254391	1.613	5.44E+07
393.204	254391	1.613	5.44E+07
393.232	254391	1.613	5.44E+07
393.260	254391	1.613	5.44E+07
393.288	254391	1.613	5.44E+07
393.316	254391	1.613	5.44E+07
393.344	254391	1.613	5.44E+07
393.372	254391	1.613	5.44E+07
393.400	254391	1.613	5.44E+07
393.428	254391	1.613	5.44E+07
393.456	254391	1.613	5.44E+07
393.484	254391	1.613	5.44E+07
393.512	254391	1.613	5.44E+07
393.540	254391	1.613	5.44E+07
393.568	254391	1.613	5.44E+07
393.596	254391	1.613	5.44E+07
393.624	254391	1.613	5.44E+07
393.652	254391	1.613	5.44E+07
393.680	254391	1.613	5.44E+07
393.708	254391	1.613	5.44E+07
393.736	254391	1.613	5.44E+07
393.764	254391	1.613	5.44E+07
393.792	254391	1.613	5.44E+07
393.820	254391	1.613	5.44E+07
393.848	254391	1.613	5.44E+07
393.876	254391	1.613	5.44E+07
393.904	254391	1.613	5.44E+07
393.932	254391	1.613	5.44E+07
393.960	254391	1.613	5.44E+07
393.988	254391	1.613	5.44E+07
394.016	254391	1.613	5.44E+07
394.044	254391	1.613	5.44E+07
394.072	254391	1.613	5.44E+07
394.100	254391	1.613	5.44E+07
394.128	254391	1.613	5.44E+07
394.156	254391	1.613	5.44E+07
394.184	254391	1.613	5.44E+07
394.212	254391	1.613	5.44E+07
394.240	254391	1.613	5.44E+07
394.268	254391	1.613	5.44E+07
394.296	254391	1.613	5.44E+07
394.324	254391	1.613	5.44E+07
394.352	254391	1.613	5.44E+07
394.380	254391	1.613	5.44E+07
394.408	254391	1.613	5.44E+07
394.436	254391	1.613	5.44E+07
394.464	254391	1.613	5.44E+07
394.492	254391	1.613	5.44E+07
394.520	254391	1.613	5.44E+07
394.548	254391	1.613	5.44E+07
394.576	254391	1.613	5.44E+07
394.604	254391	1.613	5.44E+07
394.632	254391	1.613	5.44E+07
394.660	254391	1.613	5.44E+07
394.688	254391	1.613	5.44E+07
394.716	254391	1.613	5.44E+07
394.744	254391	1.613	5.44E+07
394.772	254391	1.613	5.44E+07
394.800	254391	1.613	5.44E+07
394.828	254391	1.613	5.44E+07
394.856	254391	1.613	5.44E+07
394.884	254391	1.613	5.44E+07
394.912	254391	1.613	5.44E+07
394.940	254391	1.613	5.44E+07
394.968	254391	1.613	5.44E+07
394.996	254391	1.613	5.44E+07
395.024	254391	1.613	5.44E+07
395.052	254391	1.613	5.44E+07
395.080	254391	1.613	5.44E+07
395.108	254391	1.613	5.44E+07
395.136	254391	1.613	5.44E+07
395.164	254391	1.613	5.44E+07
395.192	254391	1.613	5.44E+07
395.220	254391	1.613	5.44E+07
395.248	254391	1.613	5.44E+07
395.276	254391	1.613	5.44E+07
395.304	254391	1.613	5.44E+07
395.332	254391	1.613	5.44E+07
395.360	254391	1.613	5.44E+07
395.388	254391	1.613	5.44E+07
395.416	254391	1.613	5.44E+07
395.444	254391	1.613	5.44E+07
395.472	254391	1.613	5.44E+07
395.500	254391	1.613	5.44E+07
395.528	254391	1.613	5.44E+07
395.556	254391	1.613	5.44E+07
395.584	254391	1.613	5.44E+07
395.612	254391	1.613	5.44E+07
395.640	254391	1.613	5.44E+07
395.668	254391	1.613	5.44E+07
395.696	254391	1.613	5.44E+07
395.724	254391	1.613	5.44E+07
395.752	254391	1.613	5.44E+07
395.780	254391	1.613	5.44E+07
395.808	254391	1.613	5.44E+07
395.836	254391	1.613	5.44E+07
395.864	254391	1.613	5.44E+07
395.892	254391	1.613	5.44E+07
395.920	254391	1.613	5.44E+07
395.948	254391	1.613	5.44E+07
395.976	254391	1.613	5.44E+07
396.004	254391	1.613	5.44E+07
396.032	254391	1.613	5.44E+07
396.060	254391	1.613	5.44E+07
396.088	254391	1.613	5.44E+07
396.116	254391	1.613	5.44E+07
396.144	254391	1.613	5.44E+07
396.172	254391	1.613	5.44E+07
396.200	254391	1.613	5.44E+07
396.228	254391	1.613	5.44E+07
396.256	254391	1.613	5.44E+07
396.284	254391	1.613	5.44E+07
396.312	254391	1.613	5.44E+07
396.340	254391	1.613	5.44E+07
396.368	254391	1.613	5.44E+07
396.396	254391	1.613	5.44E+07
396.424	254391	1.613	5.44E+07
396.452	254391	1.613	5.44E+07
396.480	254391	1.613	5.44E+07
396.508	254391	1.613	5.44E+07
396.536	254391	1.613	5.44E+07
396.564	254391	1.613	5.44E+07
396.592	254391	1.613	5.44E+07
396.620	254391	1.613	5.44E+07
396.648	254391	1.613	5.44E+07
396.676	254391	1.613	5.44E+07
396.704	254391	1.613	5.44E+07
396.732	254391	1.613	5.44E+07
396.760	254391	1.61	

APPENDIX B - Continued

TABULATIONS OF CURRENT AND INFERRED ELECTRON DENSITY FOR RAM C-II, PROBE 5

ELAPSED TIME, SECONDS	ALTITUDE, FEET	CURRENT, MICROAMPS (a)	ELECTRON DENSITY, ELECTRONS PER CUBIC CENTIMETER
389.746	28121.3	1.22	6.33E+07
389.773	28104.4	1.10	6.33E+07
389.800	28088.4	1.10	6.33E+07
389.848	28058.2	1.10	6.28E+07
389.876	28040.5	1.10	6.28E+07
389.903	28022.6	1.10	6.28E+07
389.951	27991.7	1.10	6.28E+07
389.979	27973.9	1.10	6.28E+07
390.006	27956.4	1.10	6.28E+07
390.054	27924.8	1.10	6.28E+07
390.081	27907.1	1.10	6.28E+07
390.108	27889.3	1.10	6.28E+07
390.156	27858.1	1.10	6.28E+07
390.183	27840.2	1.10	6.28E+07
390.210	27822.4	1.10	6.28E+07
390.238	27804.5	1.10	6.28E+07
390.265	27786.7	1.10	6.28E+07
390.292	27768.8	1.10	6.28E+07
390.319	27751.0	1.10	6.28E+07
390.346	27733.2	1.10	6.28E+07
390.373	27715.4	1.10	6.28E+07
390.400	27697.6	1.10	6.28E+07
390.427	27679.8	1.10	6.28E+07
390.454	27662.0	1.10	6.28E+07
390.481	27644.2	1.10	6.28E+07
390.508	27626.4	1.10	6.28E+07
390.535	27608.6	1.10	6.28E+07
390.562	27590.8	1.10	6.28E+07
390.589	27573.0	1.10	6.28E+07
390.616	27555.2	1.10	6.28E+07
390.643	27537.4	1.10	6.28E+07
390.670	27519.6	1.10	6.28E+07
390.697	27501.8	1.10	6.28E+07
390.724	27484.0	1.10	6.28E+07
390.751	27466.2	1.10	6.28E+07
390.778	27448.4	1.10	6.28E+07
390.805	27430.6	1.10	6.28E+07
390.832	27412.8	1.10	6.28E+07
390.859	27395.0	1.10	6.28E+07
390.886	27377.2	1.10	6.28E+07
390.913	27359.4	1.10	6.28E+07
390.940	27341.6	1.10	6.28E+07
390.967	27323.8	1.10	6.28E+07
390.994	27306.0	1.10	6.28E+07
391.021	27288.2	1.10	6.28E+07
391.048	27270.4	1.10	6.28E+07
391.075	27252.6	1.10	6.28E+07
391.102	27234.8	1.10	6.28E+07
391.129	27217.0	1.10	6.28E+07
391.156	27199.2	1.10	6.28E+07
391.183	27181.4	1.10	6.28E+07
391.210	27163.6	1.10	6.28E+07
391.237	27145.8	1.10	6.28E+07
391.264	27128.0	1.10	6.28E+07
391.291	27110.2	1.10	6.28E+07
391.318	27092.4	1.10	6.28E+07
391.345	27074.6	1.10	6.28E+07
391.372	27056.8	1.10	6.28E+07
391.399	27039.0	1.10	6.28E+07
391.426	27021.2	1.10	6.28E+07
391.453	27003.4	1.10	6.28E+07
391.480	26985.6	1.10	6.28E+07
391.507	26967.8	1.10	6.28E+07
391.534	26950.0	1.10	6.28E+07
391.561	26932.2	1.10	6.28E+07
391.588	26914.4	1.10	6.28E+07
391.615	26896.6	1.10	6.28E+07
391.642	26878.8	1.10	6.28E+07
391.669	26861.0	1.10	6.28E+07
391.696	26843.2	1.10	6.28E+07
391.723	26825.4	1.10	6.28E+07
391.750	26807.6	1.10	6.28E+07
391.777	26789.8	1.10	6.28E+07
391.804	26772.0	1.10	6.28E+07
391.831	26754.2	1.10	6.28E+07
391.858	26736.4	1.10	6.28E+07
391.885	26718.6	1.10	6.28E+07
391.912	26700.8	1.10	6.28E+07
391.939	26683.0	1.10	6.28E+07
391.966	26665.2	1.10	6.28E+07
391.993	26647.4	1.10	6.28E+07
392.020	26629.6	1.10	6.28E+07
392.047	26611.8	1.10	6.28E+07
392.074	26594.0	1.10	6.28E+07
392.101	26576.2	1.10	6.28E+07
392.128	26558.4	1.10	6.28E+07
392.155	26540.6	1.10	6.28E+07
392.182	26522.8	1.10	6.28E+07
392.209	26505.0	1.10	6.28E+07
392.236	26487.2	1.10	6.28E+07
392.263	26469.4	1.10	6.28E+07
392.290	26451.6	1.10	6.28E+07
392.317	26433.8	1.10	6.28E+07
392.344	26416.0	1.10	6.28E+07
392.371	26398.2	1.10	6.28E+07
392.398	26380.4	1.10	6.28E+07
392.425	26362.6	1.10	6.28E+07
392.452	26344.8	1.10	6.28E+07
392.479	26327.0	1.10	6.28E+07
392.506	26309.2	1.10	6.28E+07
392.533	26291.4	1.10	6.28E+07
392.560	26273.6	1.10	6.28E+07
392.587	26255.8	1.10	6.28E+07
392.614	26238.0	1.10	6.28E+07
392.641	26220.2	1.10	6.28E+07
392.668	26202.4	1.10	6.28E+07
392.695	26184.6	1.10	6.28E+07
392.722	26166.8	1.10	6.28E+07
392.749	26149.0	1.10	6.28E+07
392.776	26131.2	1.10	6.28E+07
392.803	26113.4	1.10	6.28E+07
392.830	26095.6	1.10	6.28E+07
392.857	26077.8	1.10	6.28E+07
392.884	26060.0	1.10	6.28E+07
392.911	26042.2	1.10	6.28E+07
392.938	26024.4	1.10	6.28E+07
392.965	26006.6	1.10	6.28E+07
392.992	25988.8	1.10	6.28E+07
393.019	25971.0	1.10	6.28E+07
393.046	25953.2	1.10	6.28E+07
393.073	25935.4	1.10	6.28E+07
393.100	25917.6	1.10	6.28E+07
393.127	25899.8	1.10	6.28E+07
393.154	25882.0	1.10	6.28E+07
393.181	25864.2	1.10	6.28E+07
393.208	25846.4	1.10	6.28E+07
393.235	25828.6	1.10	6.28E+07
393.262	25810.8	1.10	6.28E+07
393.289	25793.0	1.10	6.28E+07
393.316	25775.2	1.10	6.28E+07
393.343	25757.4	1.10	6.28E+07
393.370	25739.6	1.10	6.28E+07
393.397	25721.8	1.10	6.28E+07
393.424	25704.0	1.10	6.28E+07
393.451	25686.2	1.10	6.28E+07
393.478	25668.4	1.10	6.28E+07
393.505	25650.6	1.10	6.28E+07
393.532	25632.8	1.10	6.28E+07
393.559	25615.0	1.10	6.28E+07
393.586	25597.2	1.10	6.28E+07
393.613	25579.4	1.10	6.28E+07
393.640	25561.6	1.10	6.28E+07
393.667	25543.8	1.10	6.28E+07
393.694	25526.0	1.10	6.28E+07
393.721	25508.2	1.10	6.28E+07
393.748	25490.4	1.10	6.28E+07
393.775	25472.6	1.10	6.28E+07
393.802	25454.8	1.10	6.28E+07
393.829	25437.0	1.10	6.28E+07
393.856	25419.2	1.10	6.28E+07
393.883	25401.4	1.10	6.28E+07
393.910	25383.6	1.10	6.28E+07
393.937	25365.8	1.10	6.28E+07
393.964	25348.0	1.10	6.28E+07
393.991	25330.2	1.10	6.28E+07
394.018	25312.4	1.10	6.28E+07
394.045	25294.6	1.10	6.28E+07
394.072	25276.8	1.10	6.28E+07
394.099	25259.0	1.10	6.28E+07
394.126	25241.2	1.10	6.28E+07
394.153	25223.4	1.10	6.28E+07
394.180	25205.6	1.10	6.28E+07
394.207	25187.8	1.10	6.28E+07
394.234	25170.0	1.10	6.28E+07
394.261	25152.2	1.10	6.28E+07
394.288	25134.4	1.10	6.28E+07
394.315	25116.6	1.10	6.28E+07
394.342	25098.8	1.10	6.28E+07
394.369	25081.0	1.10	6.28E+07
394.396	25063.2	1.10	6.28E+07
394.423	25045.4	1.10	6.28E+07
394.450	25027.6	1.10	6.28E+07
394.477	25009.8	1.10	6.28E+07
394.504	24992.0	1.10	6.28E+07
394.531	24974.2	1.10	6.28E+07
394.558	24956.4	1.10	6.28E+07
394.585	24938.6	1.10	6.28E+07
394.612	24920.8	1.10	6.28E+07
394.639	24903.0	1.10	6.28E+07
394.666	24885.2	1.10	6.28E+07
394.693	24867.4	1.10	6.28E+07
394.720	24849.6	1.10	6.28E+07
394.747	24831.8	1.10	6.28E+07
394.774	24814.0	1.10	6.28E+07
394.801	24796.2	1.10	6.28E+07
394.828	24778.4	1.10	6.28E+07
394.855	24760.6	1.10	6.28E+07
394.882	24742.8	1.10	6.28E+07
394.909	24725.0	1.10	6.28E+07
394.936	24707.2	1.10	6.28E+07
394.963	24689.4	1.10	6.28E+07
394.990	24671.6	1.10	6.28E+07
395.017	24653.8	1.10	6.28E+07
395.044	24636.0	1.10	6.28E+07
395.071	24618.2	1.10	6.28E+07
395.098	24600.4	1.10	6.28E+07
395.125	24582.6	1.10	6.28E+07
395.152	24564.8	1.10	6.28E+07
395.179	24547.0	1.10	6.28E+07
395.206	24529.2	1.10	6.28E+07
395.233	24511.4	1.10	6.28E+07
395.260	24493.6	1.10	6.28E+07
395.287	24475.8	1.10	6.28E+07
395.314	24458.0	1.10	6.28E+07
395.341	24440.2	1.10	6.28E+07
395.368	24422.4	1.10	6.28E+07
395.395	24404.6	1.10	6.28E+07
395.422	24386.8	1.10	6.28E+07
395.449	24369.0	1.10	6.28E+07
395.476	24351.2	1.10	6.28E+07
395.503	24333.4	1.10	6.28E+07
395.530	24315.6	1.10	6.28E+07
395.557	24297.8	1.10	6.28E+07
395.584	24280.0	1.10	6.28E+07
395.611	24262.2	1.10	6.28E+07
395.638	24244.4	1.10	6.28E+07
395.665	24226.6	1.10	6.28E+07
395.692	24208.8	1.10	6.28E+07
395.719	24191.0	1.10	6.28E+07
395.746	24173.2	1.10	6.28E+07
395.773	24155.4	1.10	6.28E+07
395.800	24137.6	1.10	6.28E+07
395.827	24119.8	1.10	6.28E+07
395.854	24102.0	1.10	6.28E+07
395.881	24084.2	1.10	6.28E+07
395.908	24066.4	1.10	6.28E+07
395.935	24048.6	1.10	6.28E+07
395.962	24030.8	1.10	6.28E+07
395.989	24013.0	1.10	6.28E+07
396.016	23995.2	1.10	6.28E+07
396.043	23977.4	1.10	6.28E+07
396.070	23959.6	1.10	6.28E+07
396.097	23941.8	1.10	6.28E+07
396.124	23924.0	1.10	6.28E+07
396.151	23906.2	1.10	6.28E+07
396.178	23888.4	1.10	6.28E+07
396.205	23870.6	1.10	6.28E+07
396.232	23852.8	1.10	6.28E+07
396.259	23835.0		

APPENDIX B - Continued

TABULATIONS OF CURRENT AND INFERRED ELECTRON DENSITY FOR RAM C-II, PROBE 6

ELAPSED TIME, SECONDS	ALTITUDE, FEET	CURRENT, MICROAMPS (a)	ELECTRON DENSITY, ELECTRONS PER CUBIC CENTIMETER	ELAPSED TIME, SECONDS	ALTITUDE, FEET	CURRENT, MICROAMPS (a)	ELECTRON DENSITY, ELECTRONS PER CUBIC CENTIMETER	ELAPSED TIME, SECONDS	ALTITUDE, FEET	CURRENT, MICROAMPS (a)	ELECTRON DENSITY, ELECTRONS PER CUBIC CENTIMETER	ELAPSED TIME, SECONDS	ALTITUDE, FEET	CURRENT, MICROAMPS (a)	ELECTRON DENSITY, ELECTRONS PER CUBIC CENTIMETER
389.749	281191	+103	5.18E+07	393.458	254430	109.477	1.17E+10	397.911	227881	207.116	1.63E+11	401.681	202226	1000.000	8.20E+11
389.777	281042	+103	5.18E+07	393.685	254250	109.677	1.17E+10	397.959	227569	206.555	1.47E+11	402.008	201049	1000.000	8.20E+11
389.804	280868	+103	5.18E+07	393.913	254076	110.077	1.17E+10	398.004	227391	206.886	1.47E+11	402.055	200741	1000.000	8.18E+11
389.832	280690	+103	5.18E+07	394.141	253902	110.477	1.17E+10	398.051	227217	207.287	1.47E+11	402.083	200584	1000.000	8.18E+11
389.870	280383	+150	7.77E+07	394.368	253728	110.877	1.17E+10	398.098	227043	207.687	1.47E+11	402.110	200427	1000.000	8.17E+11
389.907	280206	+133	6.73E+07	394.596	253554	111.277	1.17E+10	398.145	226869	208.087	1.47E+11	402.158	200269	1000.000	8.16E+11
389.955	279895	+133	6.73E+07	394.823	253380	111.677	1.17E+10	398.192	226695	208.487	1.47E+11	402.213	199718	1000.000	8.16E+11
389.982	279717	+123	6.21E+07	395.051	253206	112.077	1.17E+10	398.239	226521	208.887	1.47E+11	402.260	199464	1000.000	8.15E+11
390.010	279539	+123	6.21E+07	395.278	253032	112.477	1.17E+10	398.286	226347	209.287	1.47E+11	402.308	199210	1000.000	8.14E+11
390.057	279226	+133	6.73E+07	395.506	252858	112.877	1.17E+10	398.333	226173	209.687	1.47E+11	402.355	198956	1000.000	8.13E+11
390.085	279049	+133	6.73E+07	395.733	252684	113.277	1.17E+10	398.380	226000	210.087	1.47E+11	402.402	198702	1000.000	8.12E+11
390.112	278871	+143	7.25E+07	395.961	252510	113.677	1.17E+10	398.427	225826	210.487	1.47E+11	402.450	198448	1000.000	8.11E+11
390.159	278559	+243	1.24E+08	396.188	252336	114.077	1.17E+10	398.474	225652	210.887	1.47E+11	402.497	198194	1000.000	8.10E+11
390.187	278380	+343	1.80E+08	396.416	252162	114.477	1.17E+10	398.521	225478	211.287	1.47E+11	402.545	197940	1000.000	8.09E+11
390.214	278201	+513	2.43E+08	396.643	251988	114.877	1.17E+10	398.568	225304	211.687	1.47E+11	402.592	197686	1000.000	8.08E+11
390.242	277973	+513	1.71E+08	396.871	251814	115.277	1.17E+10	398.615	225130	212.087	1.47E+11	402.640	197432	1000.000	8.07E+11
390.289	277662	+348	1.80E+08	397.100	251640	115.677	1.17E+10	398.662	224956	212.487	1.47E+11	402.687	197178	1000.000	8.06E+11
390.317	277483	+371	1.92E+08	397.328	251466	116.077	1.17E+10	398.709	224782	212.887	1.47E+11	402.735	196924	1000.000	8.05E+11
390.344	277304	+335	1.73E+08	397.556	251292	116.477	1.17E+10	398.756	224608	213.287	1.47E+11	402.782	196670	1000.000	8.04E+11
390.392	277015	+335	1.73E+08	397.784	251118	116.877	1.17E+10	398.803	224434	213.687	1.47E+11	402.830	196416	1000.000	8.03E+11
390.419	276836	+371	1.92E+08	398.012	250944	117.277	1.17E+10	398.850	224260	214.087	1.47E+11	402.877	196162	1000.000	8.02E+11
390.447	276657	+371	1.92E+08	398.240	250770	117.677	1.17E+10	398.897	224086	214.487	1.47E+11	402.925	195908	1000.000	8.01E+11
390.494	276346	+456	2.35E+08	398.468	250596	118.077	1.17E+10	398.944	223912	214.887	1.47E+11	402.972	195654	1000.000	8.00E+11
390.522	276168	+509	2.40E+08	398.696	250422	118.477	1.17E+10	398.991	223738	215.287	1.47E+11	403.020	195400	1000.000	7.99E+11
390.570	275857	+423	2.19E+08	398.924	250248	118.877	1.17E+10	399.038	223564	215.687	1.47E+11	403.067	195146	1000.000	7.98E+11
390.598	275679	+506	2.62E+08	399.152	250074	119.277	1.17E+10	399.085	223390	216.087	1.47E+11	403.115	194892	1000.000	7.97E+11
390.626	275500	+473	2.48E+08	399.380	249900	119.677	1.17E+10	399.132	223216	216.487	1.47E+11	403.162	194638	1000.000	7.96E+11
390.673	275189	+791	4.49E+08	399.608	249726	120.077	1.17E+10	399.179	223042	216.887	1.47E+11	403.210	194384	1000.000	7.95E+11
390.701	274910	+791	4.49E+08	399.836	249552	120.477	1.17E+10	399.226	222868	217.287	1.47E+11	403.257	194130	1000.000	7.94E+11
390.728	274731	+791	4.49E+08	399.883	249378	120.877	1.17E+10	399.273	222694	217.687	1.47E+11	403.305	193876	1000.000	7.93E+11
390.775	274420	+513	4.70E+08	399.930	249204	121.277	1.17E+10	399.320	222520	218.087	1.47E+11	403.352	193622	1000.000	7.92E+11
390.803	274241	+473	2.48E+08	400.158	249030	121.677	1.17E+10	399.367	222346	218.487	1.47E+11	403.400	193368	1000.000	7.91E+11
390.831	274062	+473	2.48E+08	400.386	248856	122.077	1.17E+10	399.414	222172	218.887	1.47E+11	403.447	193114	1000.000	7.90E+11
390.878	273751	+743	3.82E+08	400.614	248682	122.477	1.17E+10	399.461	222000	219.287	1.47E+11	403.495	192860	1000.000	7.89E+11
390.906	273572	+663	3.31E+08	400.842	248508	122.877	1.17E+10	399.508	221826	219.687	1.47E+11	403.542	192606	1000.000	7.88E+11
390.934	273393	+663	3.31E+08	401.070	248334	123.277	1.17E+10	399.555	221652	220.087	1.47E+11	403.590	192352	1000.000	7.87E+11
390.981	273082	+743	3.82E+08	401.298	248160	123.677	1.17E+10	399.602	221478	220.487	1.47E+11	403.637	192098	1000.000	7.86E+11
391.009	272903	+743	3.82E+08	401.526	247986	124.077	1.17E+10	399.649	221304	220.887	1.47E+11	403.685	191844	1000.000	7.85E+11
391.056	272592	+743	3.82E+08	401.754	247812	124.477	1.17E+10	399.696	221130	221.287	1.47E+11	403.732	191590	1000.000	7.84E+11
391.084	272413	+743	3.82E+08	401.982	247638	124.877	1.17E+10	399.743	220956	221.687	1.47E+11	403.780	191336	1000.000	7.83E+11
391.131	272102	+743	3.82E+08	402.210	247464	125.277	1.17E+10	399.790	220782	222.087	1.47E+11	403.827	191082	1000.000	7.82E+11
391.159	271923	+743	3.82E+08	402.438	247290	125.677	1.17E+10	399.837	220608	222.487	1.47E+11	403.875	190828	1000.000	7.81E+11
391.187	271744	+743	3.82E+08	402.666	247116	126.077	1.17E+10	399.884	220434	222.887	1.47E+11	403.922	190574	1000.000	7.80E+11
391.234	271433	+743	3.82E+08	402.894	246942	126.477	1.17E+10	399.931	220260	223.287	1.47E+11	403.970	190320	1000.000	7.79E+11
391.262	271254	+743	3.82E+08	403.122	246768	126.877	1.17E+10	399.978	220086	223.687	1.47E+11	404.017	190066	1000.000	7.78E+11
391.309	270943	+743	3.82E+08	403.350	246594	127.277	1.17E+10	400.025	219912	224.087	1.47E+11	404.065	189812	1000.000	7.77E+11
391.337	270764	+743	3.82E+08	403.578	246420	127.677	1.17E+10	400.072	219738	224.487	1.47E+11	404.112	189558	1000.000	7.76E+11
391.384	270453	+743	3.82E+08	403.806	246246	128.077	1.17E+10	400.119	219564	224.887	1.47E+11	404.160	189304	1000.000	7.75E+11
391.412	270274	+743	3.82E+08	404.034	246072	128.477	1.17E+10	400.166	219390	225.287	1.47E+11	404.207	189050	1000.000	7.74E+11
391.459	269963	+743	3.82E+08	404.262	245898	128.877	1.17E+10	400.213	219216	225.687	1.47E+11	404.255	188796	1000.000	7.73E+11
391.487	269784	+743	3.82E+08	404.490	245724	129.277	1.17E+10	400.260	219042	226.087	1.47E+11	404.302	188542	1000.000	7.72E+11
391.534	269473	+743	3.82E+08	404.718	245550	129.677	1.17E+10	400.307	218868	226.487	1.47E+11	404.350	188288	1000.000	7.71E+11
391.562	269294	+743	3.82E+08	404.946	245376	130.077	1.17E+10	400.354	218694	226.887	1.47E+11	404.397	188034	1000.000	7.70E+11
391.609	268983	+743	3.82E+08	405.174	245202	130.477	1.17E+10	400.401	218520	227.287	1.47E+11	404.445	187780	1000.000	7.69E+11
391.637	268804	+743	3.82E+08	405.402	245028	130.877	1.17E+10	400.448	218346	227.687	1.47E+11	404.492	187526	1000.000	7.68E+11
391.684	268493	+743	3.82E+08	405.630	244854	131.277	1.17E+10	400.495	218172	228.087	1.47E+11	404.540	187272	1000.000	7.67E+11
391.712	268314	+743	3.82E+08	405.858	244680	131.677	1.17E+10	400.542	218000	228.487	1.47E+11	404.587	187018	1000.000	7.66E+11
391.760	267903	+743	3.82E+08	406.086	244506	132.077	1.17E+10	400.589	217826	228.887	1.47E+11	404.635	186764	1000.000	7.65E+11
391.788	267724	+743	3.82E+08	406.314	244332	132.477	1.17E+10	400.636	217652	229.287	1.47E+11	404.682	186510	1000.000	7.64E+11
391.835	267413	+743	3.82E+08	406.542	244158	132.877	1.17E+10	400.683	217478	229.687	1.47E+11	404.730	186256	1000.000	7.63E+11
391.863	267234	+743	3.82E+08	406.770	243984	133.277	1.17E+10	400.730	217304	230.087	1.47E+11	404.777	186002	1000.000	7.62E+11
391.910	266923	+743	3.82E+08	407.000	243810	133.677	1.17E+10	400.777	21						

APPENDIX B - Continued

TABULATIONS OF CURRENT AND INFERRED ELECTRON DENSITY FOR RAM C-II, PROBE 7

ELAPSED TIME, SECONDS	ALTITUDE, FEET	CURRENT, MICROAMPS	ELECTRON DENSITY, ELECTRONS PER CUBIC CENTIMETER
399.753	261195	+150	7.63E+07
399.780	261320	+180	9.15E+07
399.807	260846	+140	7.12E+07
399.834	260558	+180	9.15E+07
399.862	260161	+200	1.02E+08
399.890	260184	+140	7.12E+07
399.918	270472	+140	7.12E+07
399.946	270604	+120	6.10E+07
399.974	270516	+100	5.08E+07
399.999	270204	+170	8.63E+07
400.028	270402	+170	8.63E+07
400.115	278849	+210	1.17E+08
400.143	278535	+110	2.40E+08
400.170	278358	+500	2.53E+08
400.217	278179	+550	2.79E+08
400.245	277891	+540	2.68E+08
400.272	277609	+370	1.98E+08
400.300	277327	+370	1.98E+08
400.328	277045	+370	1.98E+08
400.356	276763	+370	1.98E+08
400.384	276481	+370	1.98E+08
400.412	276199	+540	2.75E+08
400.440	275917	+440	2.49E+08
400.468	275635	+580	2.97E+08
400.496	275353	+590	2.99E+08
400.524	275071	+580	2.99E+08
400.552	274789	+580	2.99E+08
400.580	274507	+580	2.99E+08
400.608	274225	+580	2.99E+08
400.636	273943	+580	2.99E+08
400.664	273661	+580	2.99E+08
400.692	273379	+580	2.99E+08
400.720	273097	+580	2.99E+08
400.748	272815	+580	2.99E+08
400.776	272533	+580	2.99E+08
400.804	272251	+580	2.99E+08
400.832	271969	+580	2.99E+08
400.860	271687	+580	2.99E+08
400.888	271405	+580	2.99E+08
400.916	271123	+580	2.99E+08
400.944	270841	+580	2.99E+08
400.972	270559	+580	2.99E+08
401.000	270277	+580	2.99E+08
401.028	269995	+580	2.99E+08
401.056	269713	+580	2.99E+08
401.084	269431	+580	2.99E+08
401.112	269149	+580	2.99E+08
401.140	268867	+580	2.99E+08
401.168	268585	+580	2.99E+08
401.196	268303	+580	2.99E+08
401.224	268021	+580	2.99E+08
401.252	267739	+580	2.99E+08
401.280	267457	+580	2.99E+08
401.308	267175	+580	2.99E+08
401.336	266893	+580	2.99E+08
401.364	266611	+580	2.99E+08
401.392	266329	+580	2.99E+08
401.420	266047	+580	2.99E+08
401.448	265765	+580	2.99E+08
401.476	265483	+580	2.99E+08
401.504	265201	+580	2.99E+08
401.532	264919	+580	2.99E+08
401.560	264637	+580	2.99E+08
401.588	264355	+580	2.99E+08
401.616	264073	+580	2.99E+08
401.644	263791	+580	2.99E+08
401.672	263509	+580	2.99E+08
401.700	263227	+580	2.99E+08
401.728	262945	+580	2.99E+08
401.756	262663	+580	2.99E+08
401.784	262381	+580	2.99E+08
401.812	262099	+580	2.99E+08
401.840	261817	+580	2.99E+08
401.868	261535	+580	2.99E+08
401.896	261253	+580	2.99E+08
401.924	260971	+580	2.99E+08
401.952	260689	+580	2.99E+08
401.980	260407	+580	2.99E+08
402.008	260125	+580	2.99E+08
402.036	259843	+580	2.99E+08
402.064	259561	+580	2.99E+08
402.092	259279	+580	2.99E+08
402.120	258997	+580	2.99E+08
402.148	258715	+580	2.99E+08
402.176	258433	+580	2.99E+08
402.204	258151	+580	2.99E+08
402.232	257869	+580	2.99E+08
402.260	257587	+580	2.99E+08
402.288	257305	+580	2.99E+08
402.316	257023	+580	2.99E+08
402.344	256741	+580	2.99E+08
402.372	256459	+580	2.99E+08
402.400	256177	+580	2.99E+08
402.428	255895	+580	2.99E+08
402.456	255613	+580	2.99E+08
402.484	255331	+580	2.99E+08
402.512	255049	+580	2.99E+08
402.540	254767	+580	2.99E+08
402.568	254485	+580	2.99E+08
402.596	254203	+580	2.99E+08
402.624	253921	+580	2.99E+08
402.652	253639	+580	2.99E+08
402.680	253357	+580	2.99E+08
402.708	253075	+580	2.99E+08
402.736	252793	+580	2.99E+08
402.764	252511	+580	2.99E+08
402.792	252229	+580	2.99E+08
402.820	251947	+580	2.99E+08
402.848	251665	+580	2.99E+08
402.876	251383	+580	2.99E+08
402.904	251101	+580	2.99E+08
402.932	250819	+580	2.99E+08
402.960	250537	+580	2.99E+08
402.988	250255	+580	2.99E+08
403.016	249973	+580	2.99E+08
403.044	249691	+580	2.99E+08
403.072	249409	+580	2.99E+08
403.100	249127	+580	2.99E+08
403.128	248845	+580	2.99E+08
403.156	248563	+580	2.99E+08
403.184	248281	+580	2.99E+08
403.212	247999	+580	2.99E+08
403.240	247717	+580	2.99E+08
403.268	247435	+580	2.99E+08
403.296	247153	+580	2.99E+08
403.324	246871	+580	2.99E+08
403.352	246589	+580	2.99E+08
403.380	246307	+580	2.99E+08
403.408	246025	+580	2.99E+08
403.436	245743	+580	2.99E+08
403.464	245461	+580	2.99E+08
403.492	245179	+580	2.99E+08
403.520	244897	+580	2.99E+08
403.548	244615	+580	2.99E+08
403.576	244333	+580	2.99E+08
403.604	244051	+580	2.99E+08
403.632	243769	+580	2.99E+08
403.660	243487	+580	2.99E+08
403.688	243205	+580	2.99E+08
403.716	242923	+580	2.99E+08
403.744	242641	+580	2.99E+08
403.772	242359	+580	2.99E+08
403.800	242077	+580	2.99E+08
403.828	241795	+580	2.99E+08
403.856	241513	+580	2.99E+08
403.884	241231	+580	2.99E+08
403.912	240949	+580	2.99E+08
403.940	240667	+580	2.99E+08
403.968	240385	+580	2.99E+08
403.996	240103	+580	2.99E+08
404.024	239821	+580	2.99E+08
404.052	239539	+580	2.99E+08
404.080	239257	+580	2.99E+08
404.108	238975	+580	2.99E+08
404.136	238693	+580	2.99E+08
404.164	238411	+580	2.99E+08
404.192	238129	+580	2.99E+08
404.220	237847	+580	2.99E+08
404.248	237565	+580	2.99E+08
404.276	237283	+580	2.99E+08
404.304	237001	+580	2.99E+08
404.332	236719	+580	2.99E+08
404.360	236437	+580	2.99E+08
404.388	236155	+580	2.99E+08
404.416	235873	+580	2.99E+08
404.444	235591	+580	2.99E+08
404.472	235309	+580	2.99E+08
404.500	235027	+580	2.99E+08
404.528	234745	+580	2.99E+08
404.556	234463	+580	2.99E+08
404.584	234181	+580	2.99E+08
404.612	233899	+580	2.99E+08
404.640	233617	+580	2.99E+08
404.668	233335	+580	2.99E+08
404.696	233053	+580	2.99E+08
404.724	232771	+580	2.99E+08
404.752	232489	+580	2.99E+08
404.780	232207	+580	2.99E+08
404.808	231925	+580	2.99E+08
404.836	231643	+580	2.99E+08
404.864	231361	+580	2.99E+08
404.892	231079	+580	2.99E+08
404.920	230797	+580	2.99E+08
404.948	230515	+580	2.99E+08
404.976	230233	+580	2.99E+08
405.004	229951	+580	2.99E+08
405.032	229669	+580	2.99E+08
405.060	229387	+580	2.99E+08
405.088	229105	+580	2.99E+08
405.116	228823	+580	2.99E+08
405.144	228541	+580	2.99E+08
405.172	228259	+580	2.99E+08
405.200	227977	+580	2.99E+08
405.228	227695	+580	2.99E+08
405.256	227413	+580	2.99E+08
405.284	227131	+580	2.99E+08
405.312	226849	+580	2.99E+08
405.340	226567	+580	2.99E+08
405.368	226285	+580	2.99E+08
405.396	226003	+580	2.99E+08
405.424	225721	+580	2.99E+08
405.452	225439	+580	2.99E+08
405.480	225157	+580	2.99E+08
405.508	224875	+580	2.99E+08
405.536	224593	+580	2.99E+08
405.564	224311	+580	2.99E+08
405.592	224029	+580	2.99E+08
405.620	223747	+580	2.99E+08
405.648	223465	+580	2.99E+08
405.676	223183	+580	2.99E+08
405.704	222901	+580	2.99E+08
405.732	222619	+580	2.99E+08
405.760	222337	+580	2.99E+08
405.788	222055	+580	2.99E+08
405.816	221773	+580	2.99E+08
405.844	221491	+580	2.99E+08
405.872	221209	+580	2.99E+08
405.900	220927	+580	2.99E+08
405.928	220645	+580	2.99E+08
405.956	220363	+580	2.99E+08
405.984	220081	+580	2.99E+08
406.012	219799	+580	2.99E+08
406.040	219517	+580	2.99E+08
406.068	219235	+580	2.99E+08
406.096	218953	+580	2.99E+08
406.124	218671	+580	2.99E+08
406.152	218389	+580	2.99E+08
406.180	218107	+580	2.99E+08
406.208	217825	+580	2.99E+08
406.236	217543	+580	2.99E+08
406.264	217261	+580	2.99E+08
406.292	216979	+580	2.99E+08
406.320	216697	+580	2.99E+08
406.348	216415	+580	2.99E+08
406.376	216133	+580	2.99E+08
406.404	215851	+580	2.99E+08
406.432	215569	+580	2.99E+08
406.460	215287	+580	2.99E+08
406.488	215005	+580	2.99E+08
406.516	214723	+580	2.99E+08
406.544	214441	+580	2.99E+08
406.572	214159	+580	2.99E+08
406.600	213877	+580	2.99E+08
406.628	213595	+580	2.99E+08
406.656	213313	+580	2.99E+08
406.684	213031	+580	2.99E+08
406.712	212749	+580	2.99E+08
406.740	212467	+580	2.99E+08
406.768	2		

APPENDIX B - Concluded

TABULATIONS OF CURRENT AND INFERRED ELECTRON DENSITY FOR RAM C-II, PROBE 8

ELAPSED TIME, SECONDS	ALTITUDE, FEET (a)	CURRENT, MICROAMPS	ELECTRON DENSITY, ELECTRONS PER CUBIC CENTIMETER
399.756	281173	-103	5.01E+07
399.783	281499	-183	9.00E+07
399.811	280824	-263	1.30E+08
399.838	280516	-223	1.10E+08
399.866	280339	-167	8.00E+07
399.893	280161	-293	1.45E+08
399.921	279984	-113	5.50E+07
399.949	279762	-123	6.00E+07
399.976	279540	-123	6.00E+07
399.004	279182	-143	6.90E+07
399.031	279004	-243	1.20E+08
399.059	278826	-423	2.00E+08
399.086	278648	-543	2.60E+08
399.114	278470	-603	2.90E+08
399.141	278292	-643	3.10E+08
399.169	278114	-643	3.10E+08
399.196	277936	-583	2.70E+08
399.224	277758	-443	2.21E+08
399.251	277580	-503	2.40E+08
399.279	277402	-553	2.60E+08
399.306	277224	-583	2.70E+08
399.334	277046	-603	2.80E+08
399.361	276868	-603	2.80E+08
399.389	276690	-603	2.80E+08
399.416	276512	-603	2.80E+08
399.444	276334	-603	2.80E+08
399.471	276156	-603	2.80E+08
399.499	275978	-603	2.80E+08
399.526	275800	-603	2.80E+08
399.554	275622	-603	2.80E+08
399.581	275444	-603	2.80E+08
399.609	275266	-603	2.80E+08
399.636	275088	-603	2.80E+08
399.664	274910	-603	2.80E+08
399.691	274732	-603	2.80E+08
399.719	274554	-603	2.80E+08
399.746	274376	-603	2.80E+08
399.774	274198	-603	2.80E+08
399.801	274020	-603	2.80E+08
399.829	273842	-603	2.80E+08
399.856	273664	-603	2.80E+08
399.884	273486	-603	2.80E+08
399.911	273308	-603	2.80E+08
399.939	273130	-603	2.80E+08
399.966	272952	-603	2.80E+08
399.994	272774	-603	2.80E+08
400.021	272596	-603	2.80E+08
400.049	272418	-603	2.80E+08
400.076	272240	-603	2.80E+08
400.104	272062	-603	2.80E+08
400.131	271884	-603	2.80E+08
400.159	271706	-603	2.80E+08
400.186	271528	-603	2.80E+08
400.214	271350	-603	2.80E+08
400.241	271172	-603	2.80E+08
400.269	270994	-603	2.80E+08
400.296	270816	-603	2.80E+08
400.324	270638	-603	2.80E+08
400.351	270460	-603	2.80E+08
400.379	270282	-603	2.80E+08
400.406	270104	-603	2.80E+08
400.434	269926	-603	2.80E+08
400.461	269748	-603	2.80E+08
400.489	269570	-603	2.80E+08
400.516	269392	-603	2.80E+08
400.544	269214	-603	2.80E+08
400.571	269036	-603	2.80E+08
400.599	268858	-603	2.80E+08
400.626	268680	-603	2.80E+08
400.654	268502	-603	2.80E+08
400.681	268324	-603	2.80E+08
400.709	268146	-603	2.80E+08
400.736	267968	-603	2.80E+08
400.764	267790	-603	2.80E+08
400.791	267612	-603	2.80E+08
400.819	267434	-603	2.80E+08
400.846	267256	-603	2.80E+08
400.874	267078	-603	2.80E+08
400.901	266900	-603	2.80E+08
400.929	266722	-603	2.80E+08
400.956	266544	-603	2.80E+08
400.984	266366	-603	2.80E+08
401.011	266188	-603	2.80E+08
401.039	266010	-603	2.80E+08
401.066	265832	-603	2.80E+08
401.094	265654	-603	2.80E+08
401.121	265476	-603	2.80E+08
401.149	265298	-603	2.80E+08
401.176	265120	-603	2.80E+08
401.204	264942	-603	2.80E+08
401.231	264764	-603	2.80E+08
401.259	264586	-603	2.80E+08
401.286	264408	-603	2.80E+08
401.314	264230	-603	2.80E+08
401.341	264052	-603	2.80E+08
401.369	263874	-603	2.80E+08
401.396	263696	-603	2.80E+08
401.424	263518	-603	2.80E+08
401.451	263340	-603	2.80E+08
401.479	263162	-603	2.80E+08
401.506	262984	-603	2.80E+08
401.534	262806	-603	2.80E+08
401.561	262628	-603	2.80E+08
401.589	262450	-603	2.80E+08
401.616	262272	-603	2.80E+08
401.644	262094	-603	2.80E+08
401.671	261916	-603	2.80E+08
401.699	261738	-603	2.80E+08
401.726	261560	-603	2.80E+08
401.754	261382	-603	2.80E+08
401.781	261204	-603	2.80E+08
401.809	261026	-603	2.80E+08
401.836	260848	-603	2.80E+08
401.864	260670	-603	2.80E+08
401.891	260492	-603	2.80E+08
401.919	260314	-603	2.80E+08
401.946	260136	-603	2.80E+08
401.974	259958	-603	2.80E+08
402.001	259780	-603	2.80E+08
402.029	259602	-603	2.80E+08
402.056	259424	-603	2.80E+08
402.084	259246	-603	2.80E+08
402.111	259068	-603	2.80E+08
402.139	258890	-603	2.80E+08
402.166	258712	-603	2.80E+08
402.194	258534	-603	2.80E+08
402.221	258356	-603	2.80E+08
402.249	258178	-603	2.80E+08
402.276	257999	-603	2.80E+08
402.304	257821	-603	2.80E+08
402.331	257643	-603	2.80E+08
402.359	257465	-603	2.80E+08
402.386	257286	-603	2.80E+08
402.414	257108	-603	2.80E+08
402.441	256930	-603	2.80E+08
402.469	256752	-603	2.80E+08
402.496	256574	-603	2.80E+08
402.524	256396	-603	2.80E+08
402.551	256218	-603	2.80E+08
402.579	256040	-603	2.80E+08
402.606	255862	-603	2.80E+08
402.634	255684	-603	2.80E+08
402.661	255506	-603	2.80E+08
402.689	255328	-603	2.80E+08
402.716	255150	-603	2.80E+08
402.744	254972	-603	2.80E+08
402.771	254794	-603	2.80E+08
402.799	254616	-603	2.80E+08
402.826	254438	-603	2.80E+08
402.854	254260	-603	2.80E+08
402.881	254082	-603	2.80E+08
402.909	253904	-603	2.80E+08
402.936	253726	-603	2.80E+08
402.964	253548	-603	2.80E+08
402.991	253370	-603	2.80E+08
403.019	253192	-603	2.80E+08
403.046	253014	-603	2.80E+08
403.074	252836	-603	2.80E+08
403.101	252658	-603	2.80E+08
403.129	252480	-603	2.80E+08
403.156	252302	-603	2.80E+08
403.184	252124	-603	2.80E+08
403.211	251946	-603	2.80E+08
403.239	251768	-603	2.80E+08
403.266	251590	-603	2.80E+08
403.294	251412	-603	2.80E+08
403.321	251234	-603	2.80E+08
403.349	251056	-603	2.80E+08
403.376	250878	-603	2.80E+08
403.404	250700	-603	2.80E+08
403.431	250522	-603	2.80E+08
403.459	250344	-603	2.80E+08
403.486	250166	-603	2.80E+08
403.514	250000	-603	2.80E+08
403.541	249822	-603	2.80E+08
403.569	249644	-603	2.80E+08
403.596	249466	-603	2.80E+08
403.624	249288	-603	2.80E+08
403.651	249110	-603	2.80E+08
403.679	248932	-603	2.80E+08
403.706	248754	-603	2.80E+08
403.734	248576	-603	2.80E+08
403.761	248398	-603	2.80E+08
403.789	248220	-603	2.80E+08
403.816	248042	-603	2.80E+08
403.844	247864	-603	2.80E+08
403.871	247686	-603	2.80E+08
403.899	247508	-603	2.80E+08
403.926	247330	-603	2.80E+08
403.954	247152	-603	2.80E+08
403.981	246974	-603	2.80E+08
404.009	246796	-603	2.80E+08
404.036	246618	-603	2.80E+08
404.064	246440	-603	2.80E+08
404.091	246262	-603	2.80E+08
404.119	246084	-603	2.80E+08
404.146	245906	-603	2.80E+08
404.174	245728	-603	2.80E+08
404.201	245550	-603	2.80E+08
404.229	245372	-603	2.80E+08
404.256	245194	-603	2.80E+08
404.284	245016	-603	2.80E+08
404.311	244838	-603	2.80E+08
404.339	244660	-603	2.80E+08
404.366	244482	-603	2.80E+08
404.394	244304	-603	2.80E+08
404.421	244126	-603	2.80E+08
404.449	243948	-603	2.80E+08
404.476	243770	-603	2.80E+08
404.504	243592	-603	2.80E+08
404.531	243414	-603	2.80E+08
404.559	243236	-603	2.80E+08
404.586	243058	-603	2.80E+08
404.614	242880	-603	2.80E+08
404.641	242702	-603	2.80E+08
404.669	242524	-603	2.80E+08
404.696	242346	-603	2.80E+08
404.724	242168	-603	2.80E+08
404.751	241990	-603	2.80E+08
404.779	241812	-603	2.80E+08
404.806	241634	-603	2.80E+08
404.834	241456	-603	2.80E+08
404.861	241278	-603	2.80E+08
404.889	241100	-603	2.80E+08
404.916	240922	-603	2.80E+08
404.944	240744	-603	2.80E+08
404.971	240566	-603	2.80E+08
405.000	240388	-603	2.80E+08
405.027	240210	-603	2.80E+08
405.055	240032	-603	2.80E+08
405.082	239854	-603	2.80E+08
405.110	239676	-603	2.80E+08
405.137	239498	-603	2.80E+08
405.165	239320	-603	2.80E+08
405.192	239142	-603	2.80E+08
405.220	238964	-603	2.80E+08
405.247	238786	-603	2.80E+08
405.275	238608	-603	2.80E+08
405.302	238430	-603	2.80E+08
405.330	238252	-603	2.80E+08
405.357	238074	-603	2.80E+08
405.385	237896	-603	2.80E+08
405.412	237718	-603	2.80E+08
405.440	237540	-603	2.80E+08
405.467	237362	-603	2.80E+08
405.495	237184	-603	2.80E+08
405.522	237006	-603	2.80E+08
405.550	236828	-603	2.80E+08
405.577</			

APPENDIX C

ANALYSIS OF SPACECRAFT MOTIONS AND WIND ANGLES

By William L. Weaver
Langley Research Center

The spacecraft axis system employed and its relation to the wind axis are illustrated in figure 41.

The rate gyro data show coning of the RAM C-I and C-II spacecraft after separation of the expended fourth-stage motors, but the very low dynamic pressures and resulting low accelerations did not permit accurate determinations of the spacecraft wind angles from accelerometer data. Coning of the spacecraft was also indicated by the cyclic variations in the electrostatic probe-measured electron densities observed during both flights. Figure 42 shows the correlation of measured normal aerodynamic acceleration with variations in electron densities measured by probe 1 on RAM C-II during the last few seconds before probe-rake retraction. Figure 43 shows that the electrostatic probe rake was in the same plane as the measured normal acceleration, and thus the correlation of figure 42 suggests that the cyclic variations in measured electron densities were due to displacements of the probe rake from the wind axis in the angle-of-attack (α) plane. The variations were generally symmetrical; this symmetry further suggests that the average value of the electron densities corresponded to the zero-angle-of-attack case.

Determination of Wind Angles

Prior to separation of the fourth-stage motors, the RAM C-I and C-II spacecraft had roll momenta only with the X-axes fixed in direction. The separation impulses produced uniform coning (precession) of the X-axes about the total angular momentum vectors. The motion is illustrated in figure 44, and the equations which describe it are

$$L = I_l \omega_l \tag{C1}$$

$$\tan \theta = \frac{I_l \omega_l}{I_{Xp}} \tag{C2}$$

$$\nu_H = \frac{I_{Xp}}{I_l \cos \theta} \frac{1}{2\pi} \tag{C3}$$

$$\nu_b = \frac{I_X - I_l}{I_l} \frac{p}{2\pi} \tag{C4}$$

APPENDIX C – Continued

Values computed by these equations for both flights are given in table V. The preflight-measured moments of inertia and the flight-measured rotation rates are given in table VI. It can be seen from figures 41 and 44 that for the case of $\eta_0 = 0$ (X-axes initially aligned with velocity vectors), the total wind angles will describe the cones of half-angle θ . Thus the absolute change in the total wind angle ($|\Delta\eta|$) is given by 2θ .

To study the spacecraft motions further, a computer-programed set of equations for the angular motions of a rigid body was employed. At about 380 seconds, short-duration (0.01 second) angular impulses were applied; these impulses produced matchups of the gyro-measured lateral rotation rates. Total wind angle was set to zero ($\eta_0 = 0$). Figure 45 shows the comparisons of the measured and program-computed spacecraft rotation rates. The required impulses were

$$L = 3.93 \text{ N-m-sec (2.9 lb-ft-sec)} \quad (\text{RAM C-I})$$

$$L = 3.25 \text{ N-m-sec (2.4 lb-ft-sec)} \quad (\text{RAM C-II})$$

These values are in good agreement with the impulses computed by equation (C1). (See table V.) Figure 45 shows that both the magnitudes and frequencies of the rotation rates are closely matched. The frequencies are identical with the values of ν_b given in table V.

Figure 46 shows the histories of the program-computed values of the wind angles for the computer runs which produced the matchup in rotation rates. These values are not the actual histories of the in-flight wind angles. They do represent the characteristic trends, and the frequencies and absolute variations in the angles should closely approximate those in flight. Note that the maximum values of η are twice the values of the cone angles θ in table V and that the frequencies of η are identical to those listed for ν_H in table V. The component wind angles (α, β) are seen to have variations approximately equal to $\pm 2\theta$ because the spacecraft is rolling on the surface of the precession cone as illustrated in figure 44. If it is assumed that the velocity vectors were aligned with the spacecraft X-axes at stage separations, the variations in η were

$$0 \leq \eta \leq 5^\circ \quad (\text{for RAM C-I})$$

$$0 \leq \eta \leq 4^\circ \quad (\text{for RAM C-II})$$

and the peak-to-peak variations in the component wind angles were

$$\alpha, \beta = \pm 5^\circ \quad (\text{for RAM C-I})$$

$$\alpha, \beta = \pm 4^\circ \quad (\text{for RAM C-II})$$

APPENDIX C – Concluded

Summary of Wind-Angle Analysis

Cyclic changes in the measured electron densities were shown to be due to the displacements of the electrostatic probe from the wind axis in the angle-of-attack (α) plane. Peak-to-peak variations in the densities were produced by variations in angle of attack of $\alpha = \pm 5^\circ$ (for RAM C-I) and $\alpha = \pm 4^\circ$ (for RAM C-II). The symmetry of the density variation suggests that the average values corresponded to the case where $\alpha = 0$.

REFERENCES

1. Bachynski, M. P.: Electromagnetic Wave Penetration of Reentry Plasma Sheaths. Radio Sci., J. Res. NBS, vol. 69D, no. 2, Feb. 1965, pp. 147-154.
2. Anon.: Proceedings of the NASA Conference on Communicating Through Plasmas of Atmospheric Entry and Rocket Exhaust. NASA SP-52, 1964.
3. Akey, Norman D.: Overview of RAM Reentry Measurement Program. The Entry Plasma Sheath and Its Effects on Space Vehicle Electromagnetic Systems, Vol. I, NASA SP-252, 1970, pp. 19-31.
4. Jones, William Linwood, Jr.: Probe Measurements of Electron Density Profiles During a Blunt-Body Reentry. Ph. D. Thesis, Virginia Polytechnic Inst. & State Univ., June 1971.
5. Jones, W. Linwood, Jr.; and Cross, Aubrey E.: Electrostatic Probe Measurements of Plasma Surrounding Three 25 000 Foot Per Second Reentry Flight Experiments. The Entry Plasma Sheath and Its Effects on Space Vehicle Electromagnetic Systems, Vol. I, NASA SP-252, 1970, pp. 109-136.
6. Akey, Norman D.; and Cross, Aubrey E. (With appendix A by Thomas G. Campbell; appendix B by Fred B. Beck; and appendix C by W. Linwood Jones, Jr.): Radio Blackout Alleviation and Plasma Diagnostic Results From a 25 000 Foot Per Second Blunt-Body Reentry. NASA TN D-5615, 1970.
7. Grantham, William L.: Flight Results of a 25 000-Foot-Per-Second Reentry Experiment Using Microwave Reflectometers To Measure Plasma Electron Density and Standoff Distance. NASA TN D-6062, 1970.
8. Sutton, Kenneth; Zoby, Ernest V.; and Butler, David H.: An Evaluation Test of a Full-Scale Replica of the RAM-CA Flight Heat Shield in a Rocket-Engine Exhaust. NASA TM X-1841, 1969.
9. Schexnayder, Charles J., Jr.; Huber, Paul W.; and Evans, John S.: Calculation of Electron Concentration for a Blunt Body at Orbital Speeds and Comparison With Experimental Data. NASA TN D-6294, 1971.
10. Swift, C. T.; Gooderum, P. B.; and Castellow, S. L., Jr.: Experimental Investigation of a Plasma Covered, Axially Slotted Cylinder Antenna. IEEE Trans. Antennas Propagation, vol. AP-17, no. 5, Sept. 1969, pp. 598-605.
11. Croswell, William F.; and Jones, W. Linwood, Jr.: Effects of Reentry Plasma on RAM C-I VHF Telemetry Antennas. The Entry Plasma Sheath and Its Effects on Space Vehicle Electromagnetic Systems, Vol. I, NASA SP-252, 1970, pp. 183-201.

12. Scharfman, W. E.: The Use of Langmuir Probes To Determine the Electron Density Surrounding Re-Entry Vehicles. SRI Project 5034 (Contract NAS 1-3942), Stanford Res. Inst., June 1965.
13. Scharfman, W. E.; and Bredfeldt, H. R.: Use of the Langmuir Probe To Determine the Electron Density and Temperature Surrounding Re-Entry Vehicles. SRI Project 5771 (Contract NAS 1-4872), Stanford Res. Inst., Dec. 1966. (Available as NASA CR-66275.)
14. Hok, Gunnar; Spencer, N. W.; Reifman, A.; and Dow, W. G.: Dynamic Probe Measurements in the Ionosphere. AFCRC TN-58-616, U.S. Air Force, Nov. 1958.
15. Smetana, Frederick O.: On the Current Collected by a Charged Circular Cylinder Immersed in a Two-Dimensional Rarefied Plasma Stream. Rarefied Gas Dynamics, Vol. II, J. A. Laurmann, ed., Academic Press, Inc., 1963, pp. 65-91.
16. Dunn, Michael G.: Laboratory Measurements of Electron Density and Electron Temperature With RAM Flight Probes. The Entry Plasma Sheath and Its Effect on Space Vehicle Electromagnetic Systems, Vol. I, NASA SP-252, 1970, pp. 261-276.
17. Dunn, Michael G.: Experimental Plasma Studies. NASA CR-1958, 1972.
18. Webb, H., Jr.; Dresser, H.; Korkan, K.; and Raparelli, R.: Theoretical Flow Field Calculations for Project RAM. NASA CR-1308, 1969.
19. Suits, C. Guy; and Way, Harold E., eds.: The Collected Works of Irving Langmuir. Vol. 4 - Electrical Discharge. Pergamon Press, Inc., c.1961.
20. Laframboise, James G.: Theory of Spherical and Cylindrical Langmuir Probes in a Collisionless, Maxwellian Plasma at Rest. Rep. No. 100, Inst. Aerosp. Studies, Univ. of Toronto, June 1966. (Available from DDC as AD 634 596.)
21. Bernstein, Ira B.; and Rabinowitz, Irving N.: Theory of Electrostatic Probes in a Low-Density Plasma. Phys. Fluids, vol. 2, no. 2, Mar.-Apr. 1959, pp. 112-121.
22. Allen, J. E.; Boyd, R. L. F.; and Reynolds, P.: The Collection of Positive Ions by a Probe Immersed in a Plasma. Proc. Phys. Soc., vol. 70, pt. 3, no. 447B, Mar. 1, 1957, pp. 297-304.
23. Lam, S. H.: The Langmuir Probe in a Collisionless Plasma. AFOSR 64-0353, U.S. Air Force, Mar. 1964. (Available from DDC as AD 434 342.)
24. Chen, Francis F.: Numerical Computations for Ion Probe Characteristics in a Collisionless Plasma. MATT-252 (Contract AT(30-1)-1238), Plasma Phys. Lab., Princeton Univ., Feb. 1964.
25. Chen, Francis F.: Electric Probes. Plasma Diagnostic Techniques, Richard H. Huddleston and Stanley L. Leonard, eds., Academic Press, 1965, pp. 113-200.

26. Bohm, David.; Burhop, E. H. S.; and Massey, H. S. W.: The Use of Probes for Plasma Exploration in Strong Magnetic Fields. The Characteristics of Electrical Discharges in Magnetic Fields, A. Guthrie and R. K. Wakerling, eds., McGraw-Hill Book Co., Inc., 1949, pp. 13-76.
27. Sonin, A. A.: The Behaviour of Free Molecular Cylindrical Langmuir Probes in Supersonic Flows, and Their Application to the Study of the Blunt Body Stagnation Layer. UTIAS Rep. No. 109, Univ. of Toronto, Aug. 1965.
28. Hoegy, W. R.; and Brace, L. H.: The Dumbbell Electrostatic Ionosphere Probe: Theoretical Aspects. Rep. JS-1 (Contracts AF 19(604)6124, DA-20-018-509-ORD-103, and NASw-139), College Eng., Univ. Michigan, Sept. 1961.

TABLE I.- ALTITUDE, VELOCITY, AND TIME OF RAM C-I AND RAM C-II* REENTRY TRAJECTORIES

Altitude		Velocity		Time from lift-off, sec	Altitude		Velocity		Time from lift-off, sec
km	ft	m/sec	ft/sec		km	ft	m/sec	ft/sec	
152.4	500 × 10 ³	7012	23 004	355.98	77.7	255 × 10 ³	7657	25 121	393.77
150.9	495	7095	23 279	356.83	76.2	250	7661	25 135	394.54
149.4	490	7183	23 567	357.64	74.7	245	7670	25 164	395.30
147.8	485	7277	23 875	358.42	73.2	240	7664	25 143	396.07
146.3	480	7366	24 166	359.19	71.6	235	7660	25 131	396.83
144.8	475	7460	24 476	359.98	70.1	230	7662	25 139	397.59
143.2	470	7527	24 696	360.77	68.6	225	7665	25 148	398.36
141.7	465	7564	24 816	361.57	67.0	220	7670	25 165	399.13
140.2	460	7580	24 872	362.34	65.5	215	7668	25 156	399.89
138.7	455	7579	24 866	363.11	64.0	210	7664	25 145	400.65
137.2	450	7578	24 863	363.87	62.5	205	7657	25 123	401.41
135.6	445	7580	24 872	364.64	61.0	200	7651	25 102	402.18
134.1	440	7587	24 892	365.40	59.4	195	7655	25 115	402.94
132.6	435	7590	24 902	366.18	57.9	190	7653	25 108	403.71
131.1	430	7596	24 920	366.95	56.4	185	7643	25 076	404.48
129.5	425	7597	24 926	367.73	54.9	180	7640	25 064	405.25
128.0	420	7594	24 916	368.49	53.3	175	7630	25 034	406.02
126.5	415	7594	24 914	369.25	51.8	170	7623	25 009	406.79
125.0	410	7597	24 924	370.00	50.3	165	7610	24 967	407.56
123.4	405	7602	24 941	370.75	48.8	160	7596	24 923	408.32
121.9	400	7609	24 965	371.52	47.2	155	7568	24 829	409.09
120.4	395	7614	24 982	372.30	45.7	150	7544	24 752	409.86
118.9	390	7611	24 971	373.08	44.2	145	7517	24 663	410.64
117.3	385	7610	24 967	373.85	42.7	140	7477	24 532	411.42
115.8	380	7610	24 969	374.61	41.4	135	7432	24 384	412.20
114.3	375	7612	24 973	375.37	39.6	130	7363	24 157	412.99
112.8	370	7616	24 986	376.14	38.1	125	7279	23 882	413.80
111.2	365	7617	24 991	376.92	36.6	120	7182	23 563	414.61
109.7	360	7619	24 996	377.70	35.0	115	7072	23 202	415.43
108.2	355	7622	25 008	378.47	33.5	110	6938	22 763	416.26
106.7	350	7626	25 019	379.23	32.0	105	6759	22 176	417.12
105.2	345	7629	25 029	379.99	30.5	100	6539	21 455	418.00
103.6	340	7627	25 024	380.75	29.0	95	6232	20 446	418.91
102.1	335	7629	25 031	381.52	27.4	90	5938	19 483	419.87
100.6	330	7631	25 037	382.29	25.9	85	5555	18 226	420.87
99.1	325	7628	25 026	383.07	24.4	80	5089	16 697	421.96
97.5	320	7628	25 025	383.86	22.9	75	4552	14 935	423.16
96.0	315	7633	25 042	384.63	21.3	70	3945	12 942	424.51
94.5	310	7640	25 065	385.39	19.8	65	3238	10 624	426.12
93.0	305	7650	25 098	386.14	18.3	60	2438	8 000	428.22
91.4	300	7649	25 094	386.88	16.8	55	1739	5 706	430.88
89.9	295	7646	25 087	387.64	15.2	50	1049	3 441	434.69
88.4	290	7642	25 074	388.40	13.7	45	581	1 906	440.26
86.9	285	7645	25 082	389.17	12.2	40	271	890	448.98
85.3	280	7649	25 095	389.93	10.7	35	220	721	459.34
83.8	275	7651	25 103	390.70	9.1	30	239	785	467.88
82.3	270	7649	25 094	391.46	7.6	25	227	744	475.40
80.8	265	7649	25 096	392.23	6.1	20	276	907	484.45
79.2	260	7654	25 113	393.00					

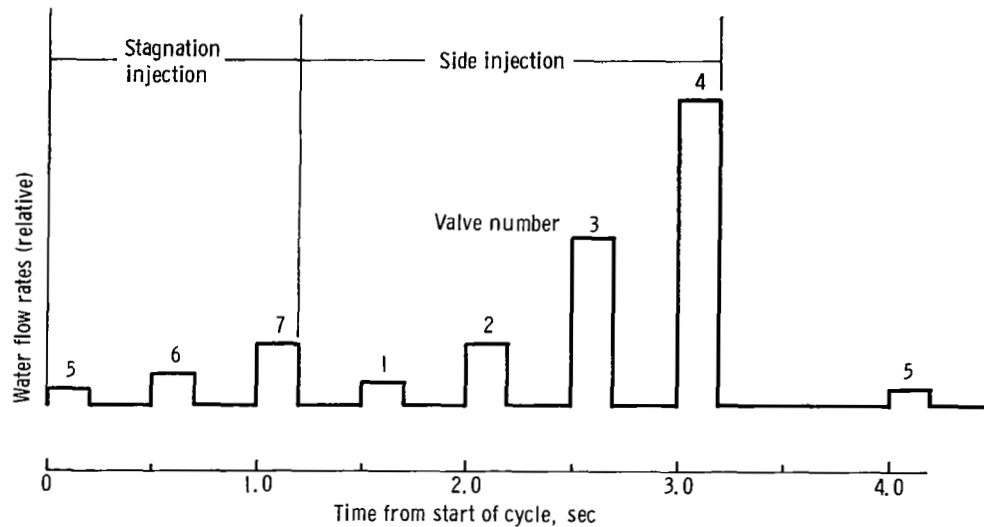
*For time correlation purposes, between the times of 386.88 and 406.79 seconds, the C-II spacecraft was 365.8 m (1200 ft) higher in altitude than listed in the table with a velocity of approximately 18 m/sec (60 ft/sec) greater than the value listed.

TABLE II. - POSITION OF FUNCTIONAL PARTS ON THE RAM C-I AND C-II PAYLOADS

Payload	Part and function	x		ϕ , deg (a)	x/D (b)
		cm (a)	in. (a)		
Water-injection nozzle					
RAM C-I	Stagnation	0	0	---	0
	Lateral	15.2	6.0	0	.48
	Lateral	15.2	6.0	180	.48
Antenna					
RAM C-II	S-band open-ended guide (3344 MHz)	4.6	1.8	90	0.15
	X-band conical horn (10 044 MHz)	4.6	1.8	330	.15
	K _a -band conical horn (35 000 MHz)	4.6	1.8	210	.15
	L-band open-ended guide (1116 MHz)	23.1	9.1	195	.76
	S-band open-ended guide (3344 MHz)	23.1	9.1	15	.76
	X-band conical horn (10 044 MHz)	23.1	9.1	285	.76
	K _a -band conical horn (35 000 MHz)	23.1	9.1	227	.76
	L-band open-ended guide (1116 MHz)	70.1	27.6	195	2.30
	S-band open-ended guide (3344 MHz)	70.1	27.6	15	2.30
	X-band conical horn (10 044 MHz)	70.1	27.6	285	2.30
K _a -band conical horn (35 000 MHz)	70.1	27.6	105	2.30	
RAM C-I	VHF axial cavity-backed slot (259.7 MHz)	75.2	29.6	0	2.36
	VHF axial cavity-backed slot (259.7 MHz)	75.2	29.6	180	2.36
RAM C-I	X-band rectangular horn (9210 MHz)	82.8	32.6	60	2.60
	X-band rectangular horn (9210 MHz)	82.8	32.6	150	2.60
	X-band rectangular horn (9210 MHz)	82.8	32.6	240	2.60
	X-band rectangular horn (9210 MHz)	82.8	32.6	330	2.60
RAM C-II	X-band rectangular horn (9210 MHz)	80.5	31.7	15	2.65
	X-band rectangular horn (9210 MHz)	80.5	31.7	105	2.65
	X-band rectangular horn (9210 MHz)	80.5	31.7	195	2.65
	X-band rectangular horn (9210 MHz)	80.5	31.7	285	2.65
RAM C-II	VHF circumferential-slot array (259.7 MHz)	97.5	38.4	---	3.20
RAM C-I	VHF circumferential-slot array (225.7 MHz)	109.2	43.0	---	3.42
RAM C-II	L-band open-ended guide (1116 MHz)	106.2	41.8	195	3.48
	S-band open-ended guide (3344 MHz)	106.2	41.8	15	3.48
	X-band conical horn (10 044 MHz)	106.2	41.8	285	3.48
	K _a -band conical horn (35 000 MHz)	106.2	41.8	105	3.48
RAM C-II	C-band rectangular horn (5800 MHz)	106.7	42.0	32	3.50
RAM C-I	C-band rectangular horn (5700 MHz)	118.4	46.6	30	3.71
RAM C-II	VHF circumferential-slot array (225.7 MHz)	114.8	45.2	---	3.76
Probe rake					
RAM C-I	Electrostatic	123.4	48.6	0	3.87
	Thermocouple	123.4	48.6	180	3.87
RAM C-II	Electrostatic	123.4	48.6	0	4.05
	Thermocouple	123.4	48.6	180	4.05

^a Center-line location of parts.^b Nose diameter D is 31.90 cm (12.56 in.) for RAM C-I; nose diameter D is 30.48 cm (12.00 in.) for RAM C-II.

TABLE III.- RAM C-I TYPICAL INJECTION CYCLE AND FLOW RATE HISTORY



Cycle	Valve for -		Flow rate		Altitude		Cycle	Valve for -		Flow rate		Altitude	
	Stagnation injection	Side injection	kg/sec	lb/sec	km	ft		Stagnation injection	Side injection	kg/sec	lb/sec	km	ft
1	5		0	0			5	5		0.023	0.05	61.1	200 490
	6		0	0				6		.068	.15	60.1	197 236
	7		0	0				7		.127	.28	59.1	193 982
		1	0	0					1	.045	.10	58.1	190 724
		2	0	0					2	.109	.24	57.1	187 462
2	5		0	0	85.0	278 908	6	5		0.027	0.06	53.2	174 451
	6		0	0	84.0	275 639		6		.082	.18	52.2	171 212
	7		.014	.03	83.2	273 027		7		.163	.36	51.2	167 968
		1	.004	.01	82.0	269 115			1	.059	.13	50.2	164 722
		2	.018	.04	81.0	265 866			2	.145	.32	49.2	161 466
3	5		0.009	0.02	77.1	252 861	7	5		0.032	0.07	45.2	148 484
	6		.032	.07	76.1	249 598		6		.104	.23	44.3	145 267
	7		.064	.14	75.1	246 328		7		.195	.43	43.3	142 058
		1	.027	.06	74.1	243 048			1	.068	.15	42.3	138 864
		2	.064	.14	73.1	239 771			2	.159	.35	41.4	135 684
4	5		0.018	0.04	69.1	226 690	8	5		0.036	0.08	37.5	123 137
	6		.054	.12	68.1	223 442		6		.109	.24	36.6	120 058
	7		.109	.24	67.1	220 185		7		.195	.43	35.7	117 010
		1	.036	.08	66.1	216 915			1	.068	.15	34.7	113 987
		2	.095	.21	65.1	213 635			2	.159	.35	33.8	110 986
		3	.249	.55	64.1	210 348			3	0	0		
		4	.404	.89	63.1	207 054			4	0	0		

TABLE IV. - RAM C-I AND RAM C-II RADIO-FREQUENCY SYSTEMS

Payload	Purpose	Frequency		Antenna type	Transmitter		Body location, x/D	Remarks
		Band	MHz		Approximate RF power, watts	Modulation		
RAM C-I	Real-time telemetry	VHF	259.7	Axial cavity-backed slots	5	FM	2.36	Two slots, diametrically opposed -----
RAM C-II		VHF	259.7	Circumferential-slot array	5	FM	3.20	
RAM C-I	Delayed-time telemetry	VHF	225.7	Circumferential-slot array	5	FM	3.42	Same data as real-time telemetry, but delayed by onboard tape loop for approximately 45 sec
RAM C-II		VHF	225.7	Circumferential-slot array	5	FM	3.76	
RAM C-I	Radar beacon	C	5 700	Rectangular horn	900 peak	Pulse	3.71	-----
RAM C-II		C	5 800	Rectangular horn	800 peak	Pulse	3.50	-----
RAM C-I	Real-time telemetry	X	9 210	Rectangular-horn array	500 peak	PPM	2.60	Four horns, 90° spacing
RAM C-II		X	9 210	Rectangular horn	500 peak	PPM	2.65	Four horns, 90° spacing
RAM C-II	Reflectometer experiment	L	1 116	T-fed slot	0.1	CW	---, 0.76, 2.30, and 3.48	Station number 1; x/D of 0.15
		S	3 344	Open-ended waveguide	.1	CW	0.15, 0.76, 2.30, and 3.48	Station number 2; x/D of 0.76
		X	10 044	Conical horn	.1	CW	0.15, 0.76, 2.30, and 3.48	Station number 3; x/D of 2.30
		K _a	35 000	Conical horn	.1	CW	0.15, 0.76, 2.30, and 3.48	Station number 4; x/D of 3.48

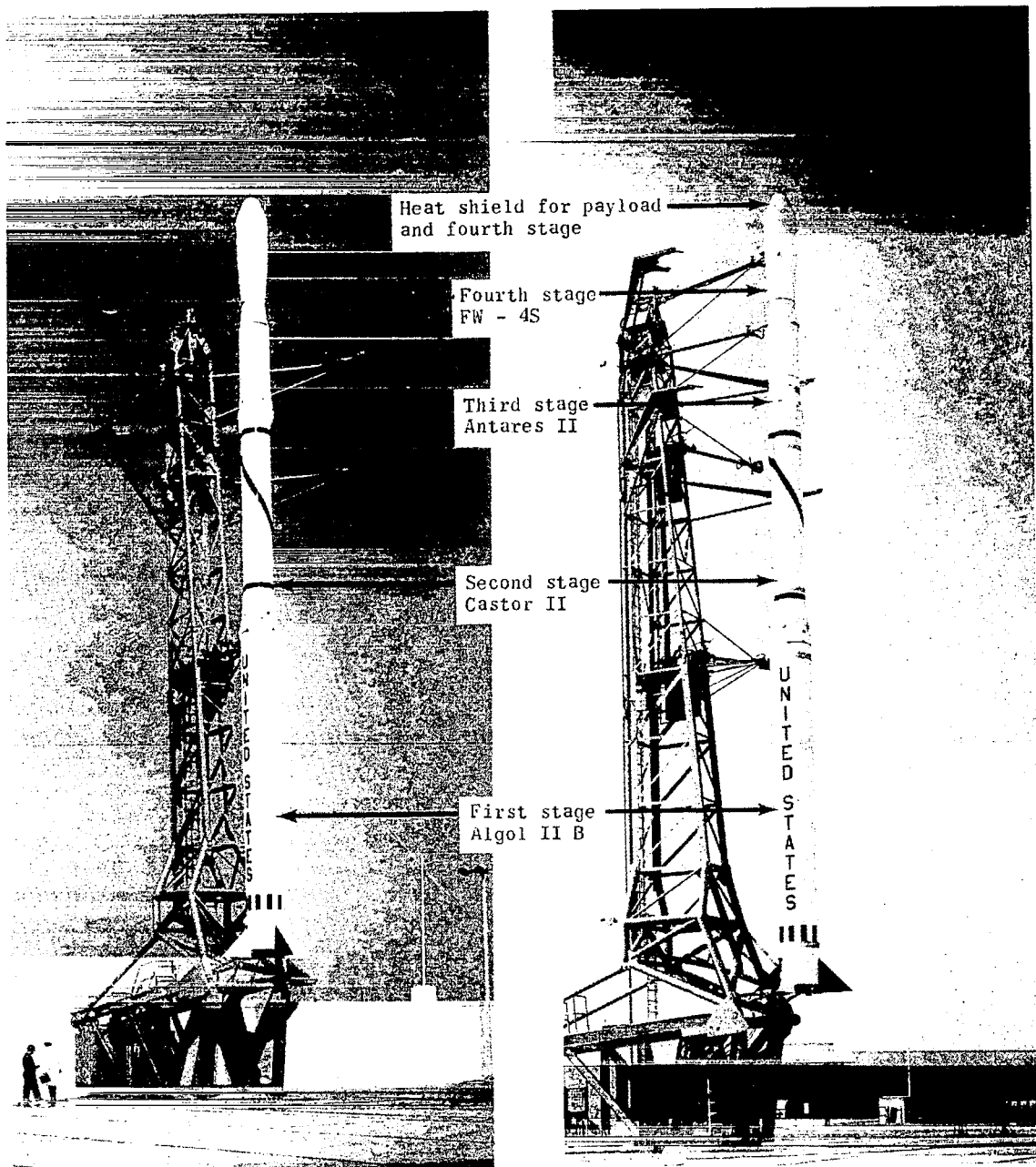
TABLE V.- COMPUTED VALUES OF IMPULSE, PRECESSION CONE ANGLE, AND
PRECESSION FREQUENCIES (EQS. (C1) TO (C4))

Flight	L		θ , deg	$\nu_{\mathbf{H}}$, Hz	$\nu_{\mathbf{b}}$, Hz
	N-m-sec	lb-ft-sec			
C-I	3.7	2.7	2.48	0.704	2.25
C-II	3.2	2.3	2.00	.800	2.25

TABLE VI.- PREFLIGHT-MEASURED SPACECRAFT MOMENTS OF INERTIA*
AND FLIGHT-MEASURED ROTATION RATES

Flight	$I_{\mathbf{X}}$		$I_{\mathbf{Y}}$		$I_{\mathbf{Z}}$		p, rad/sec	$\omega_{\mathbf{I}}$, rad/sec
	kg-m ²	slug-ft ²	kg-m ²	slug-ft ²	kg-m ²	slug-ft ²		
C-I	4.62	3.41	19.31	14.24	19.66	14.50	18.5	0.190
C-II	4.68	3.45	18.06	13.32	17.92	13.22	19.1	.175

* Moments of inertia constant during data period.

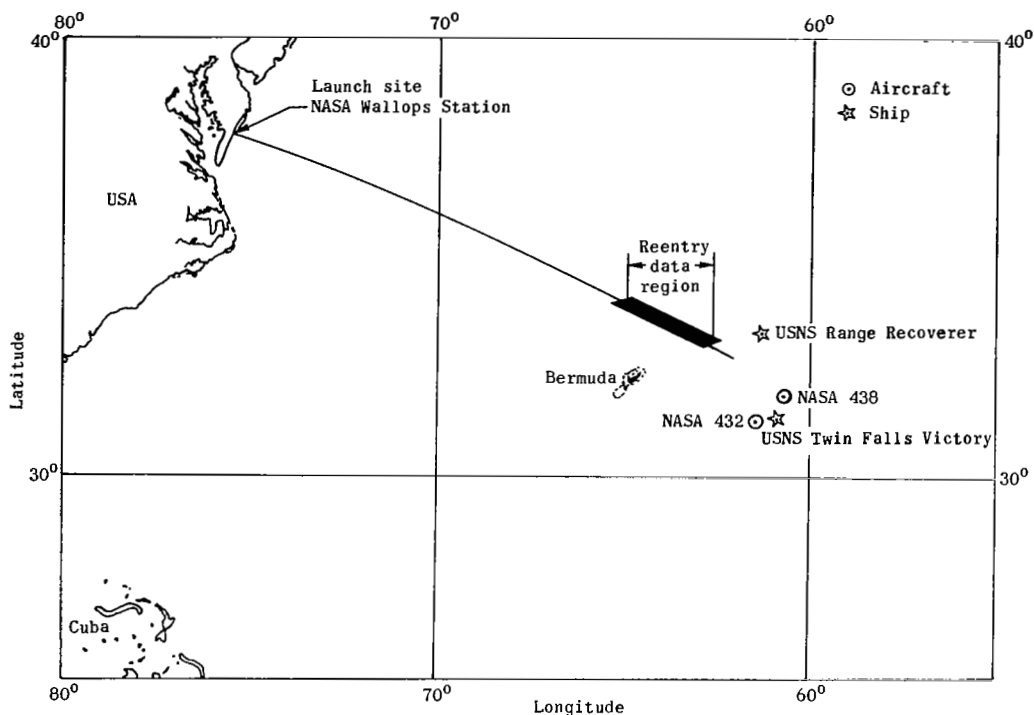


L-71-7172

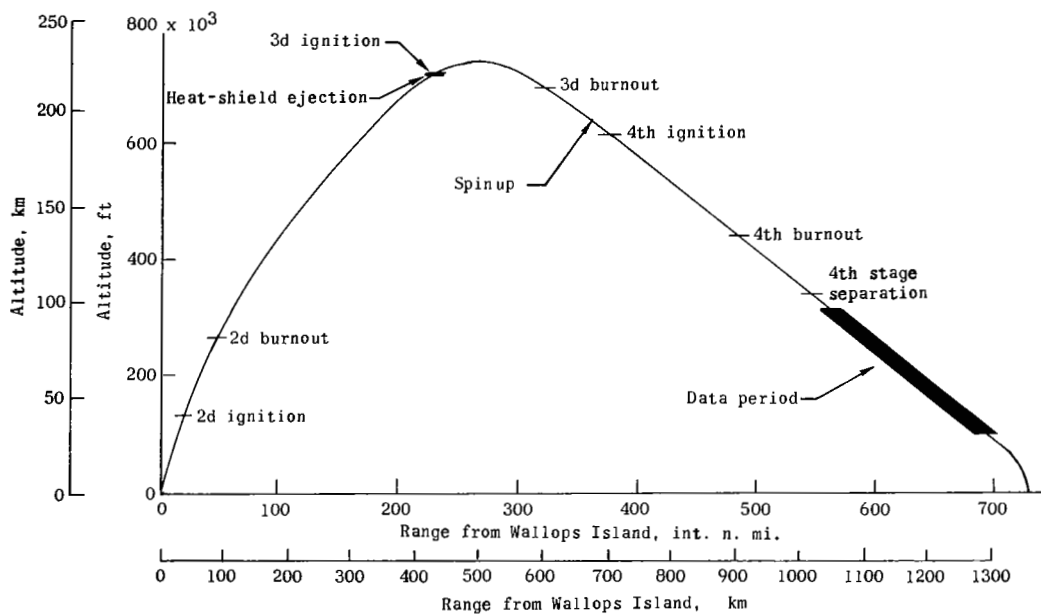
(a) S-159; RAM C-I.

(b) S-168; RAM C-II.

Figure 1.- Launch vehicles.



(a) RAM C-II ground track.



(b) RAM C-I and C-II flight events.

Figure 2.- Ground track and flight events.

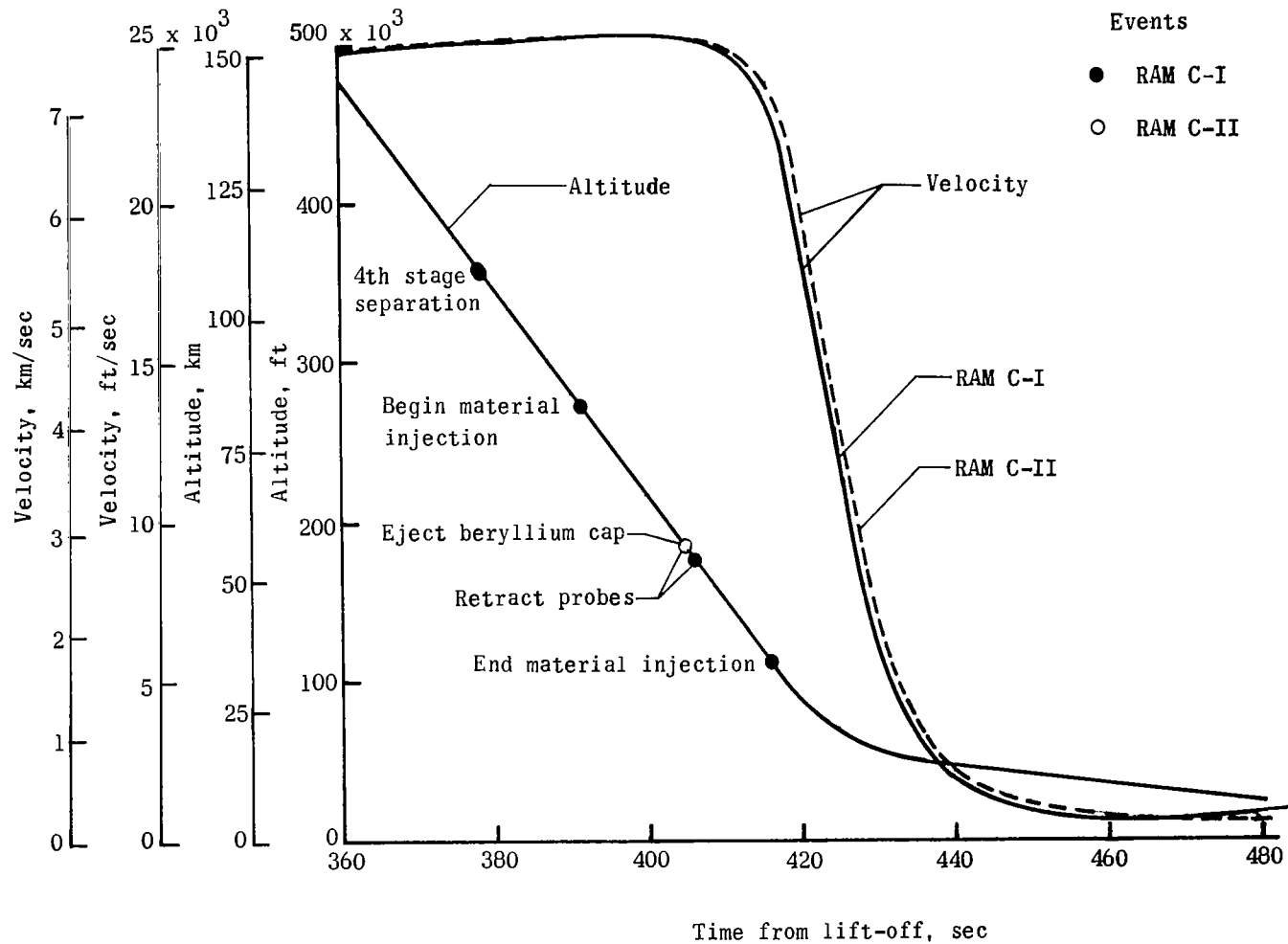
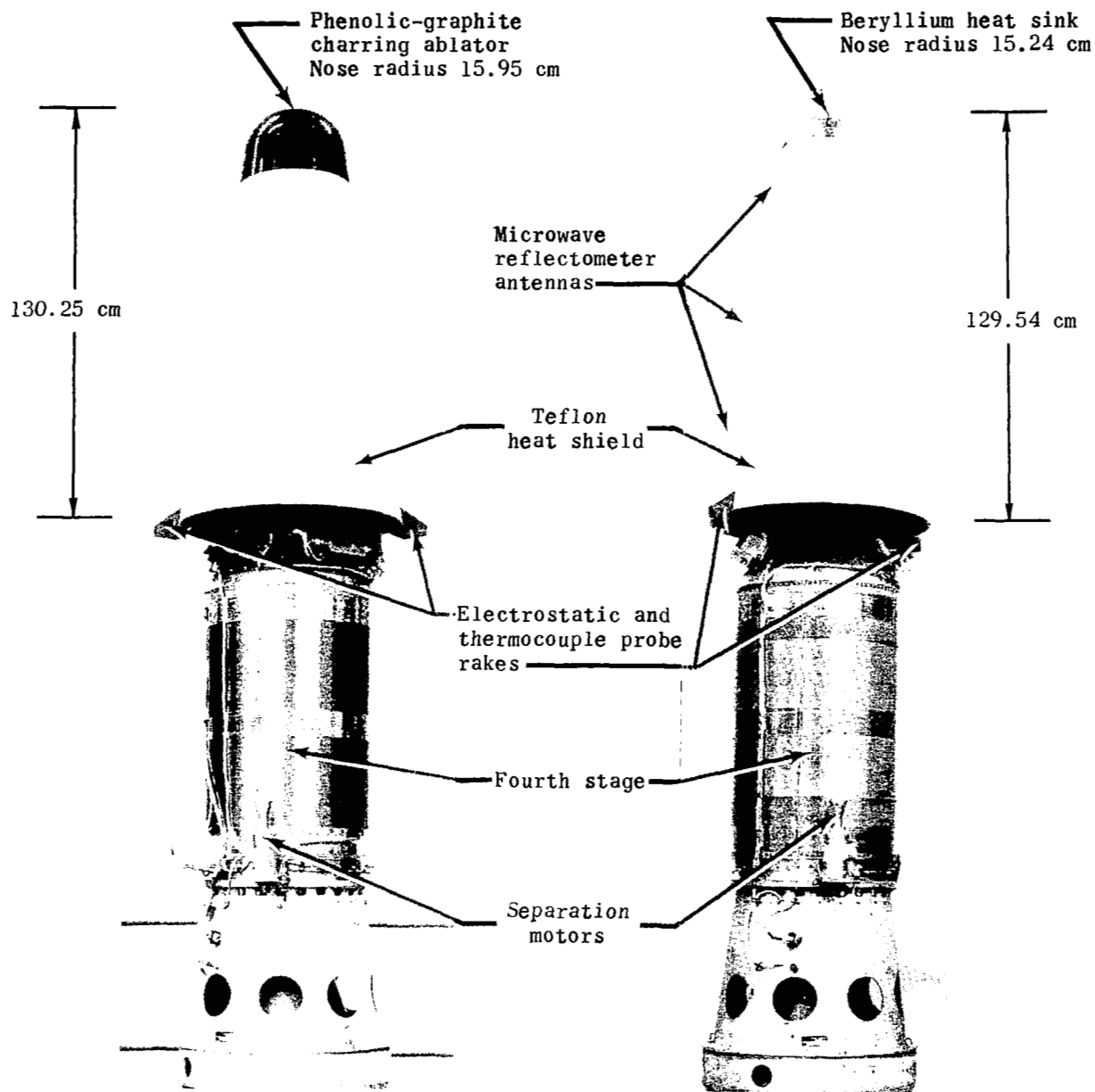


Figure 3.- Reentry trajectories.

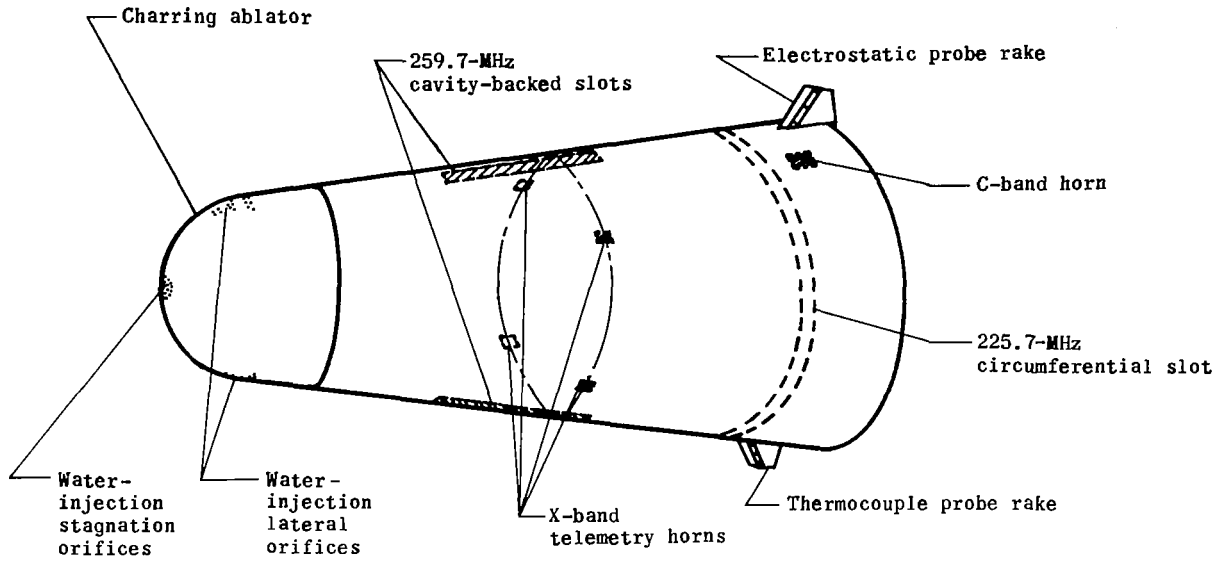


(a) RAM C-I.

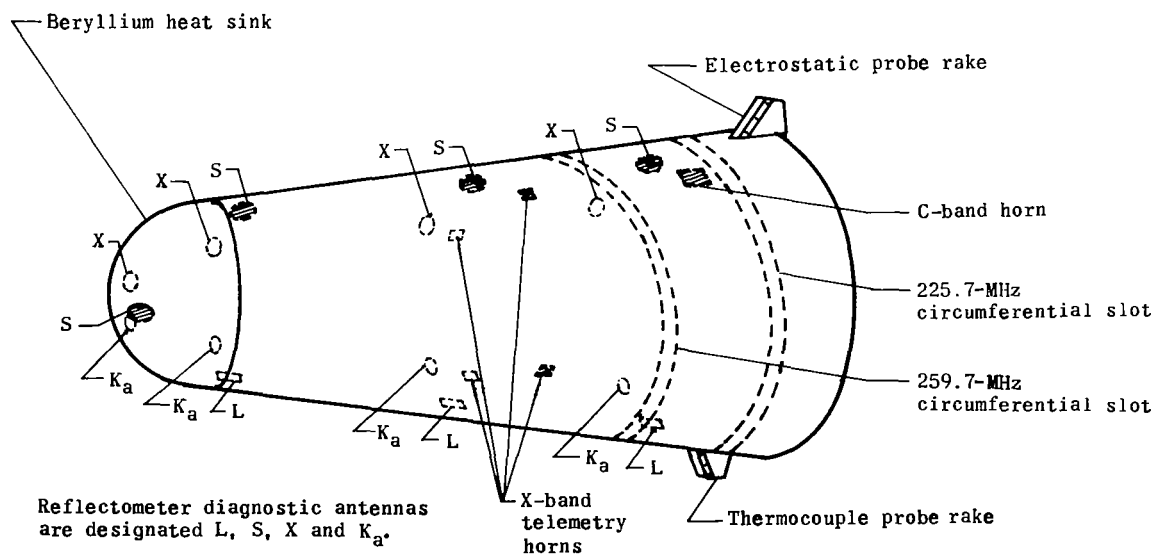
(b) RAM C-II.

L-71-7173

Figure 4.- Payload configurations shown with fourth-stage engines and separation motors.

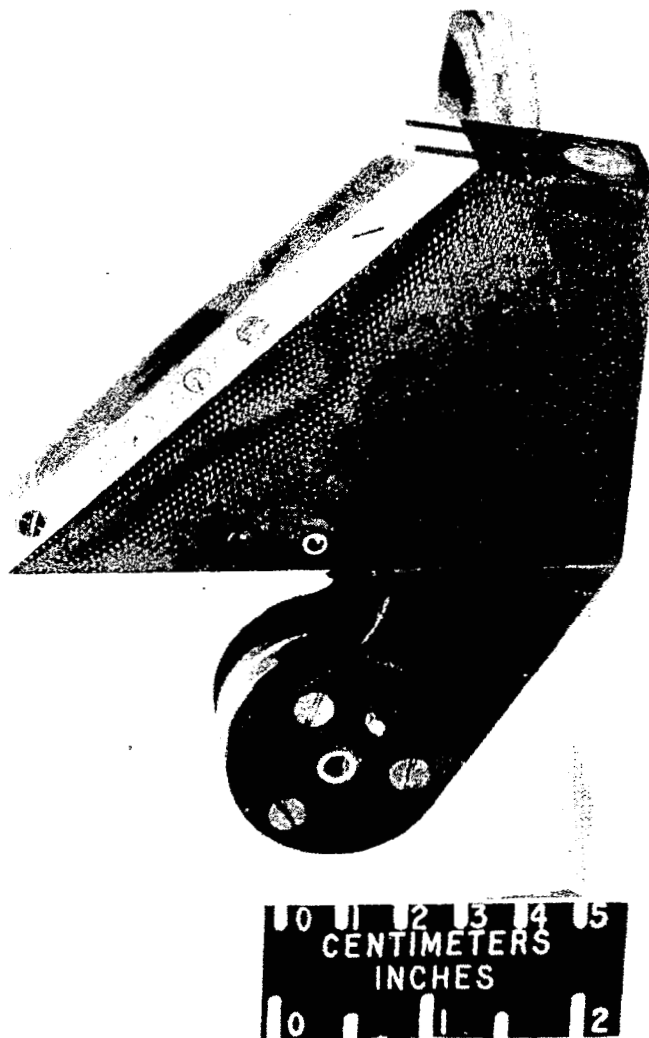


(a) RAM C-I.



(b) RAM C-II.

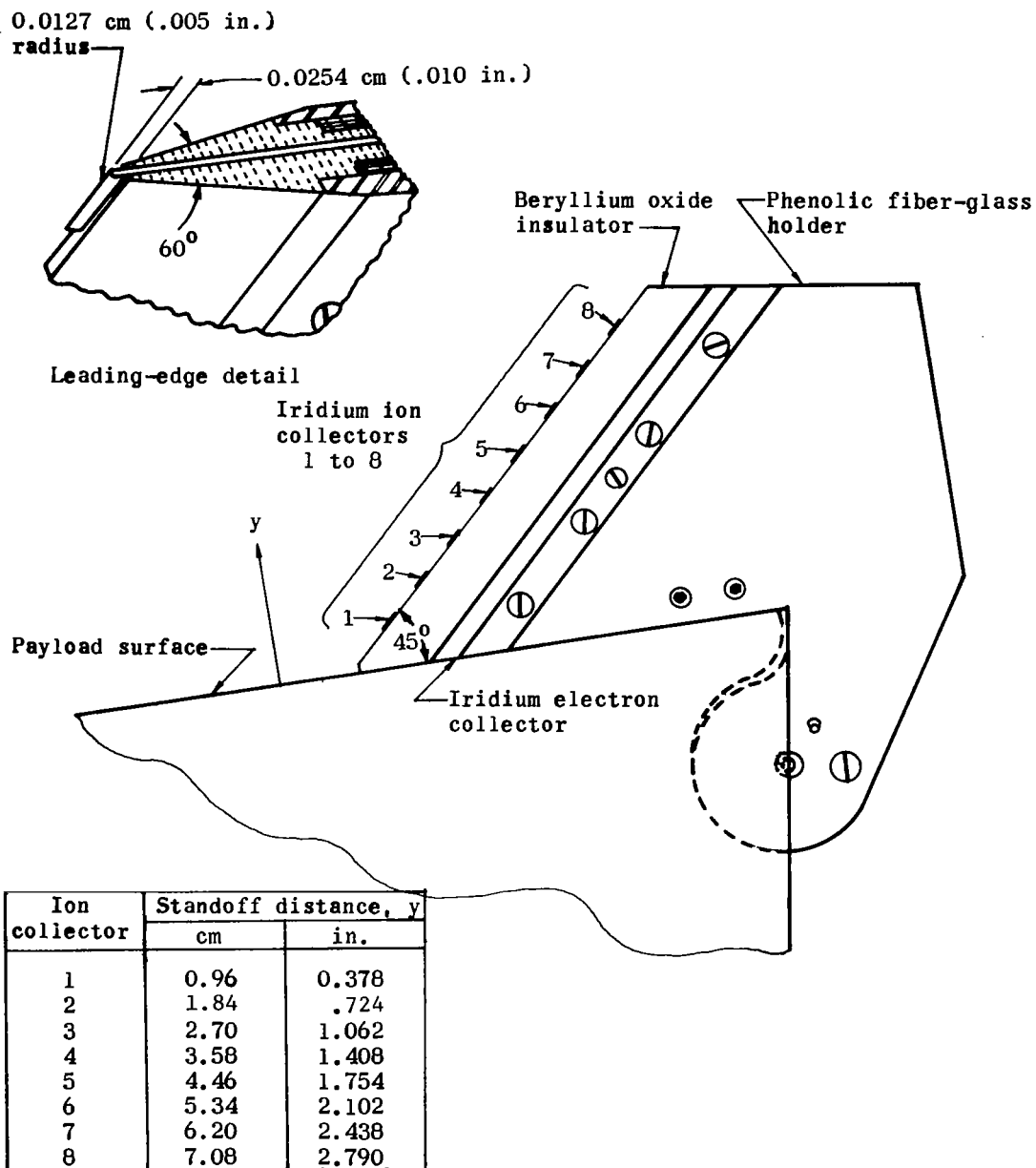
Figure 5.- Electrostatic probe and radio-frequency antenna locations.



L-67-5814

(a) Photograph of rake.

Figure 6.- Electrostatic probe rake.



(b) Detail sketch of rake. Collection area of each ion collector was 0.0420 cm^2 (0.006 in^2).

Figure 6.- Concluded.

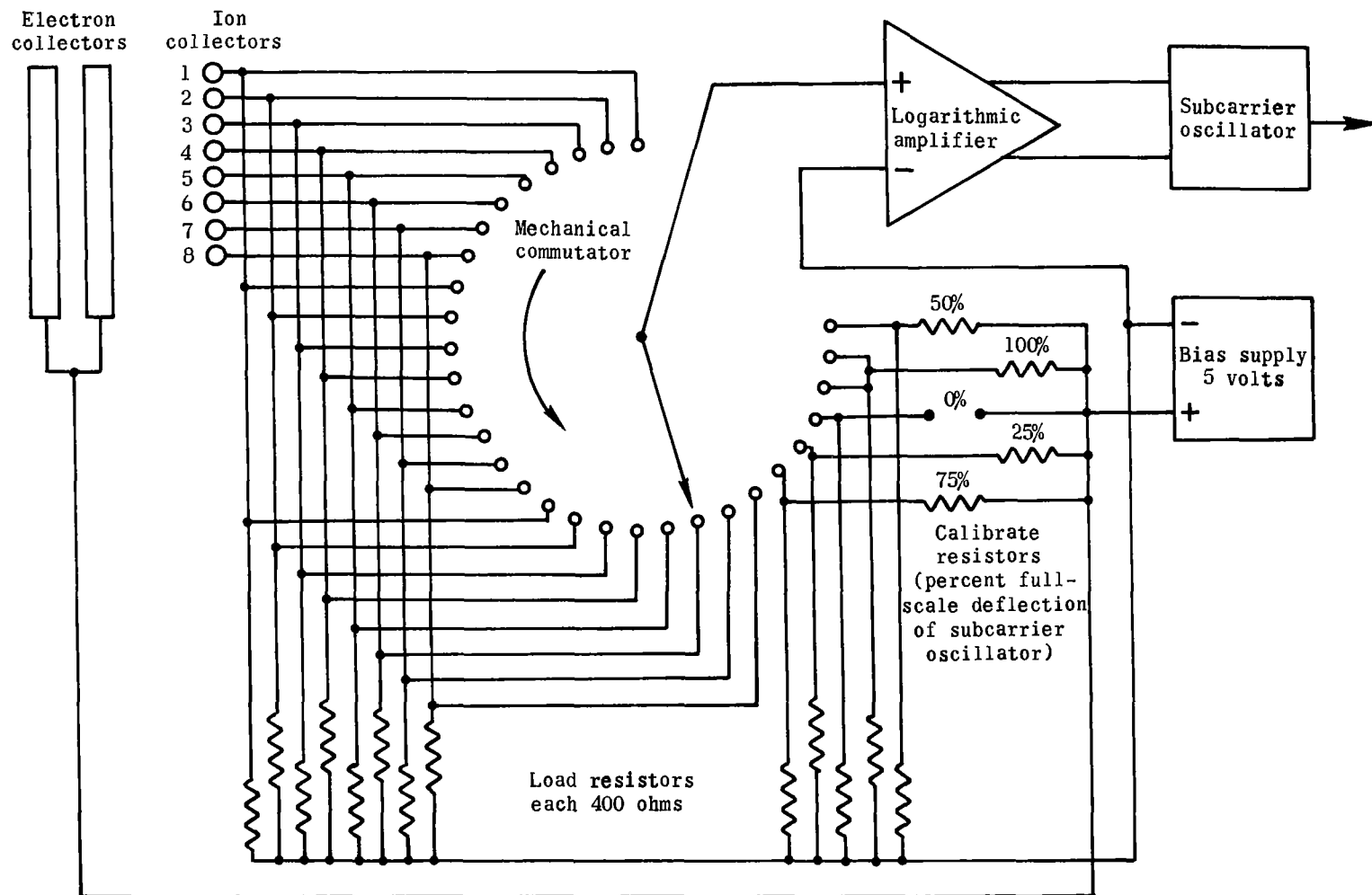
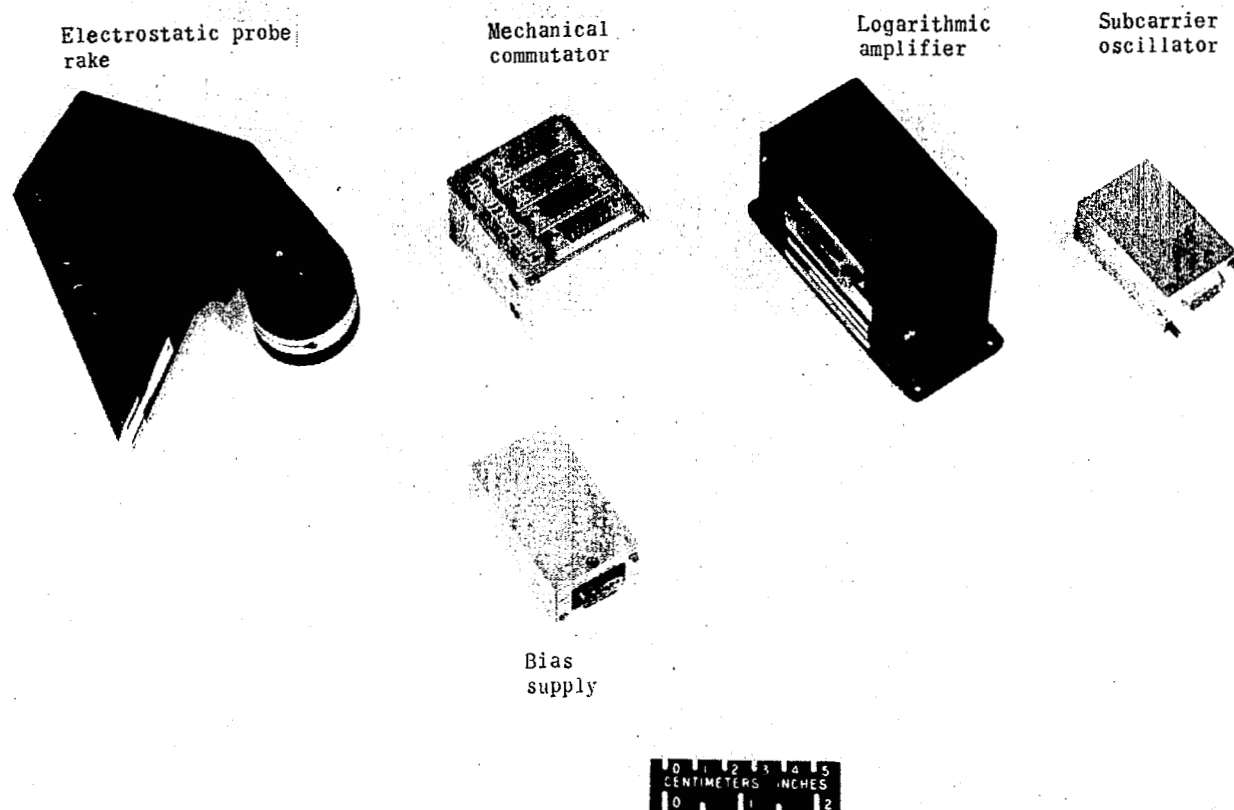
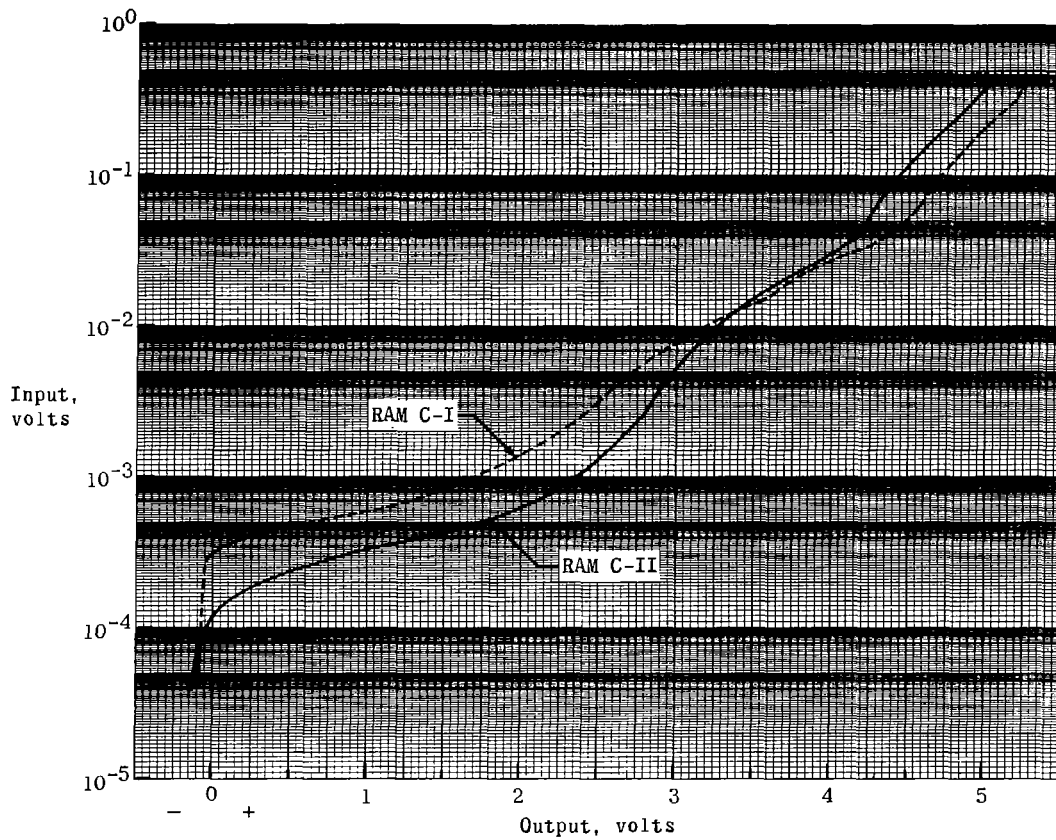


Figure 7.- Circuit diagram for electrostatic probe system.

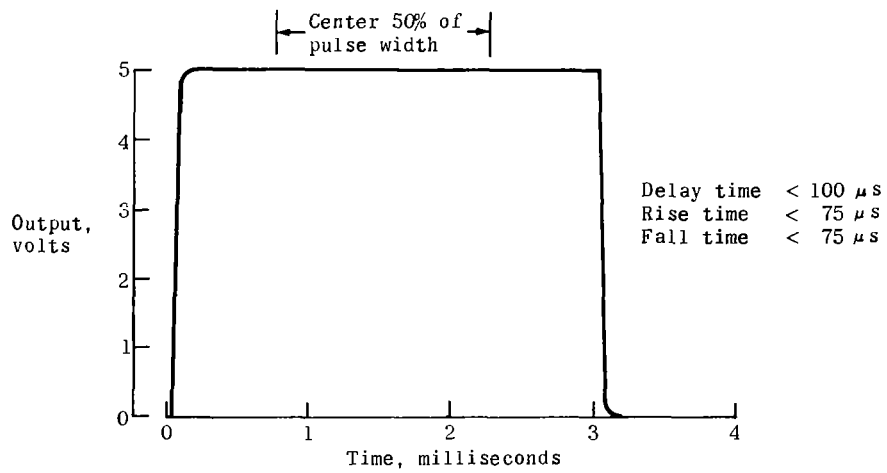


L-70-8365.1

Figure 8.- Major components of electrostatic probe system.



(a) Dynamic input-output curves.



(b) Typical pulse-response curve.

Figure 9.- Electrical characteristics of logarithmic amplifiers.

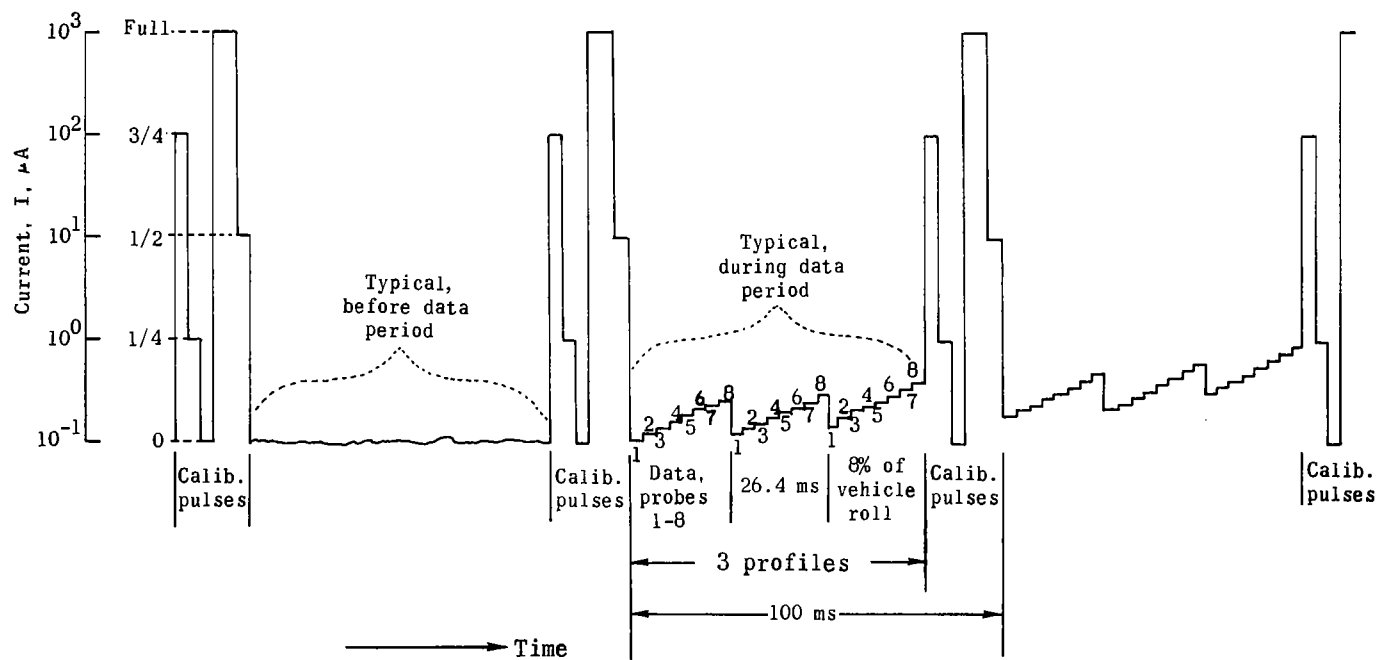
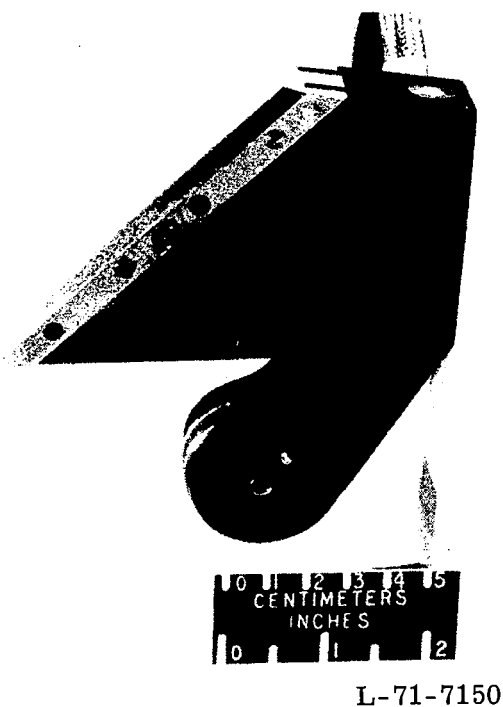
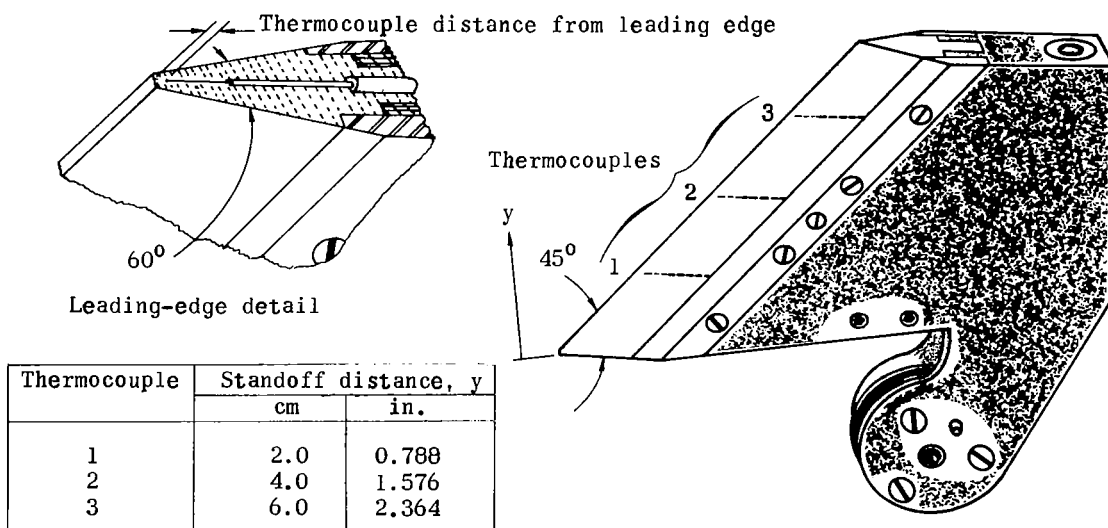


Figure 10.- Electrostatic probe data format.



L-71-7150

(a) Photograph of rake.



(b) Rake configuration. Thermocouple distance from leading edge for RAM C-I was 0.0635 cm (0.025 in.) and for RAM C-II, the distance was 0.1016 cm (0.040 in.).

Figure 11.- Thermocouple probe rake.

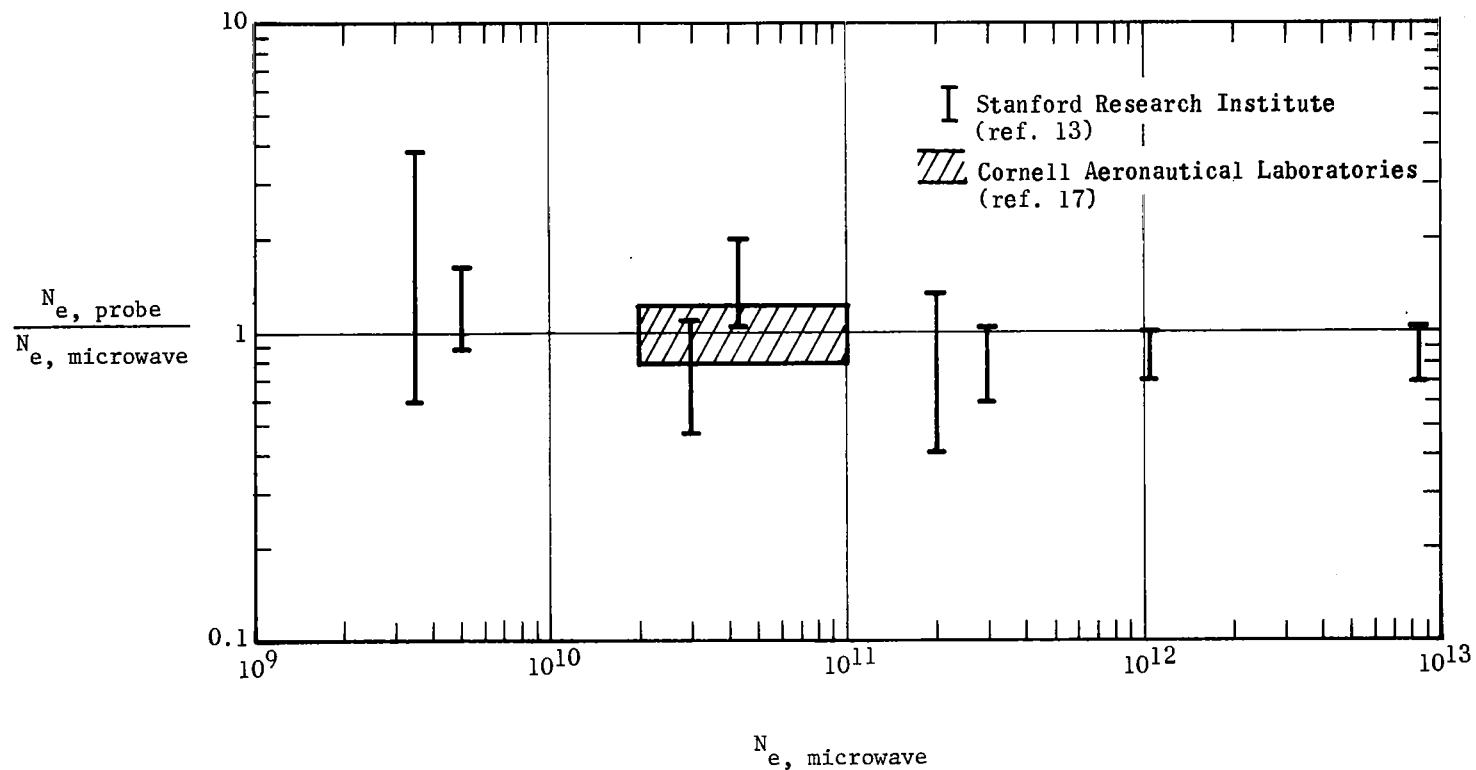
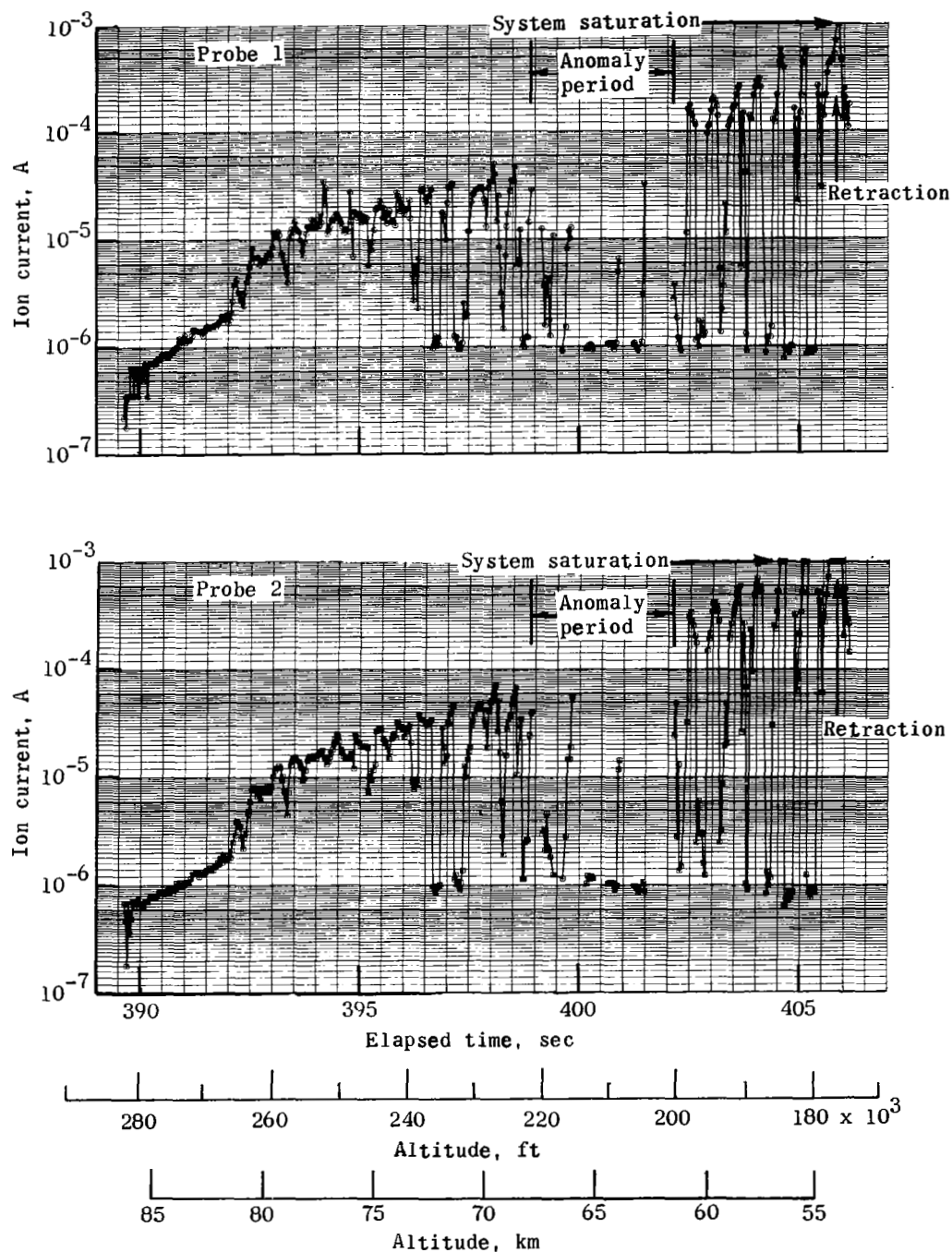
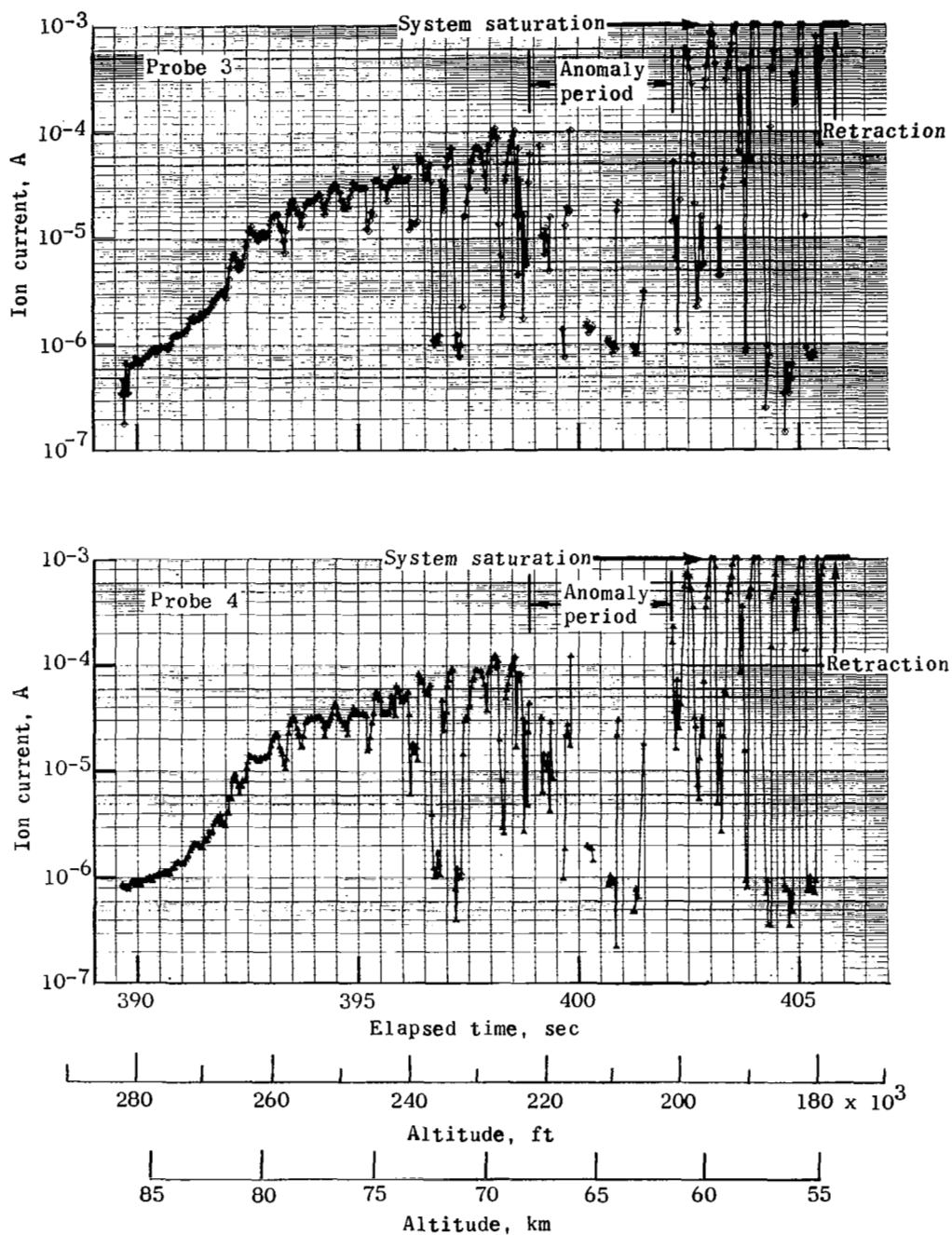


Figure 12.- Ratio of electron densities inferred from probes and from microwave data as a function of electron density inferred from microwave data.



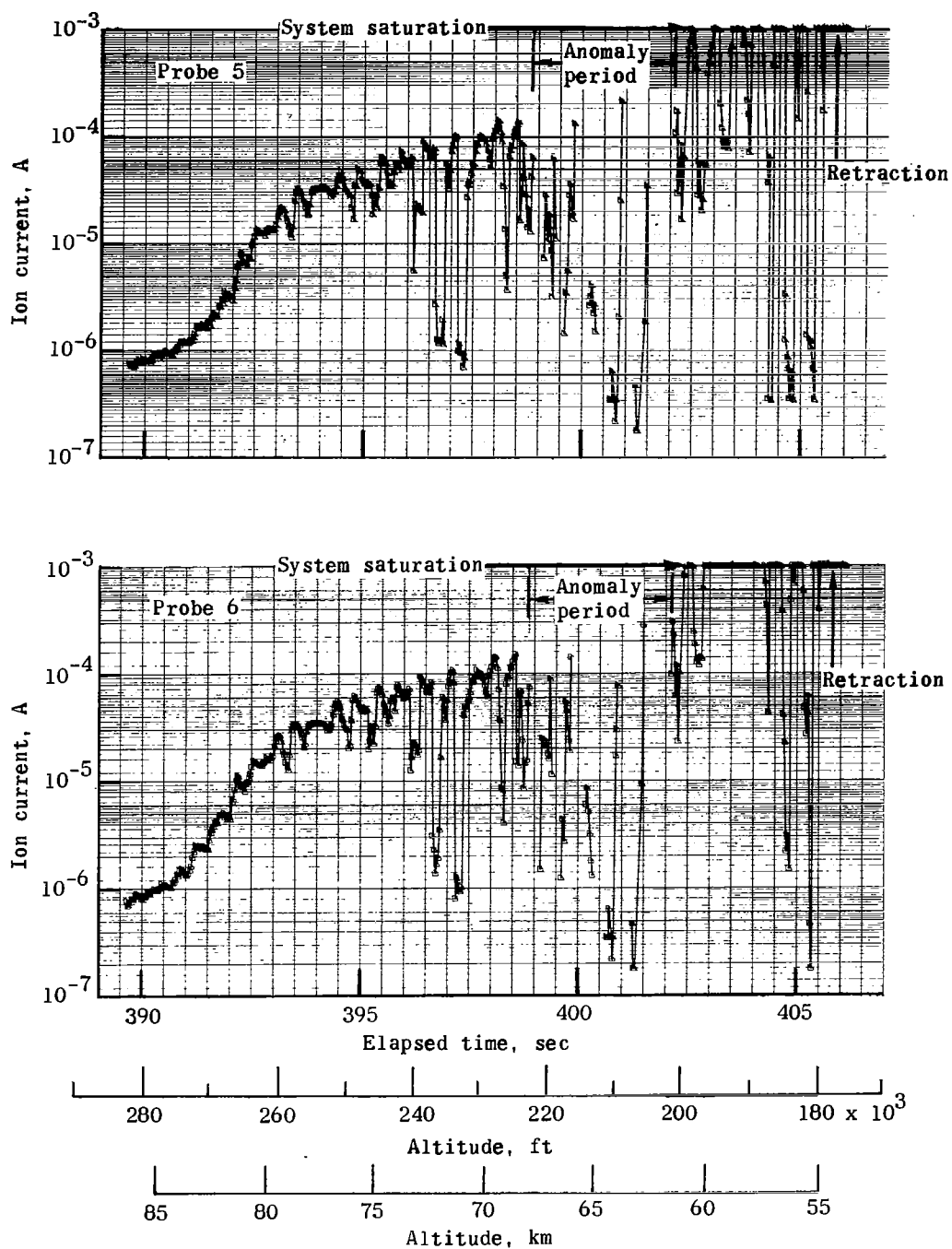
(a) Electrostatic probes 1 and 2.

Figure 13.- Ion current measurements from electrostatic probes on RAM C-I flight experiment.



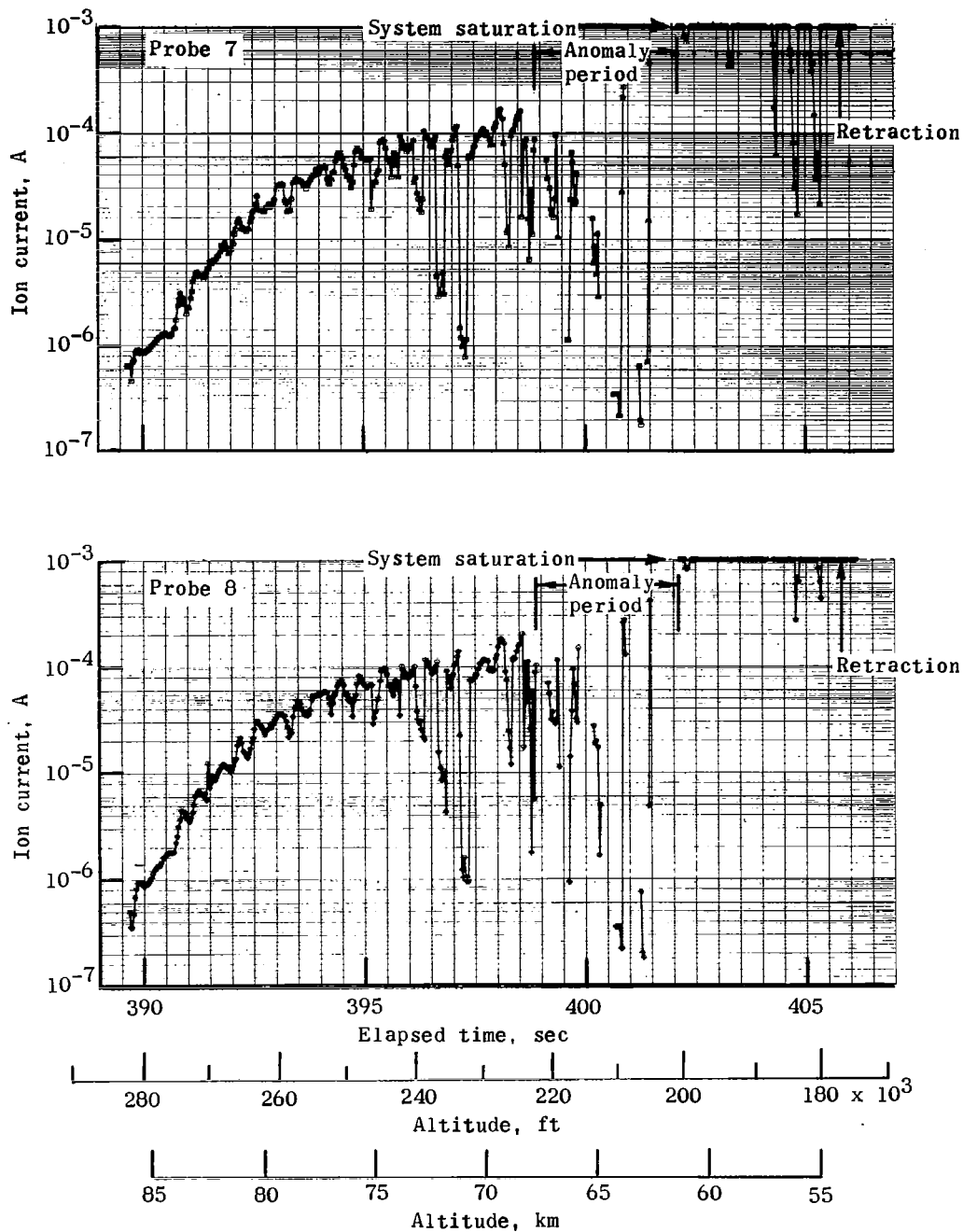
(b) Electrostatic probes 3 and 4.

Figure 13.- Continued.



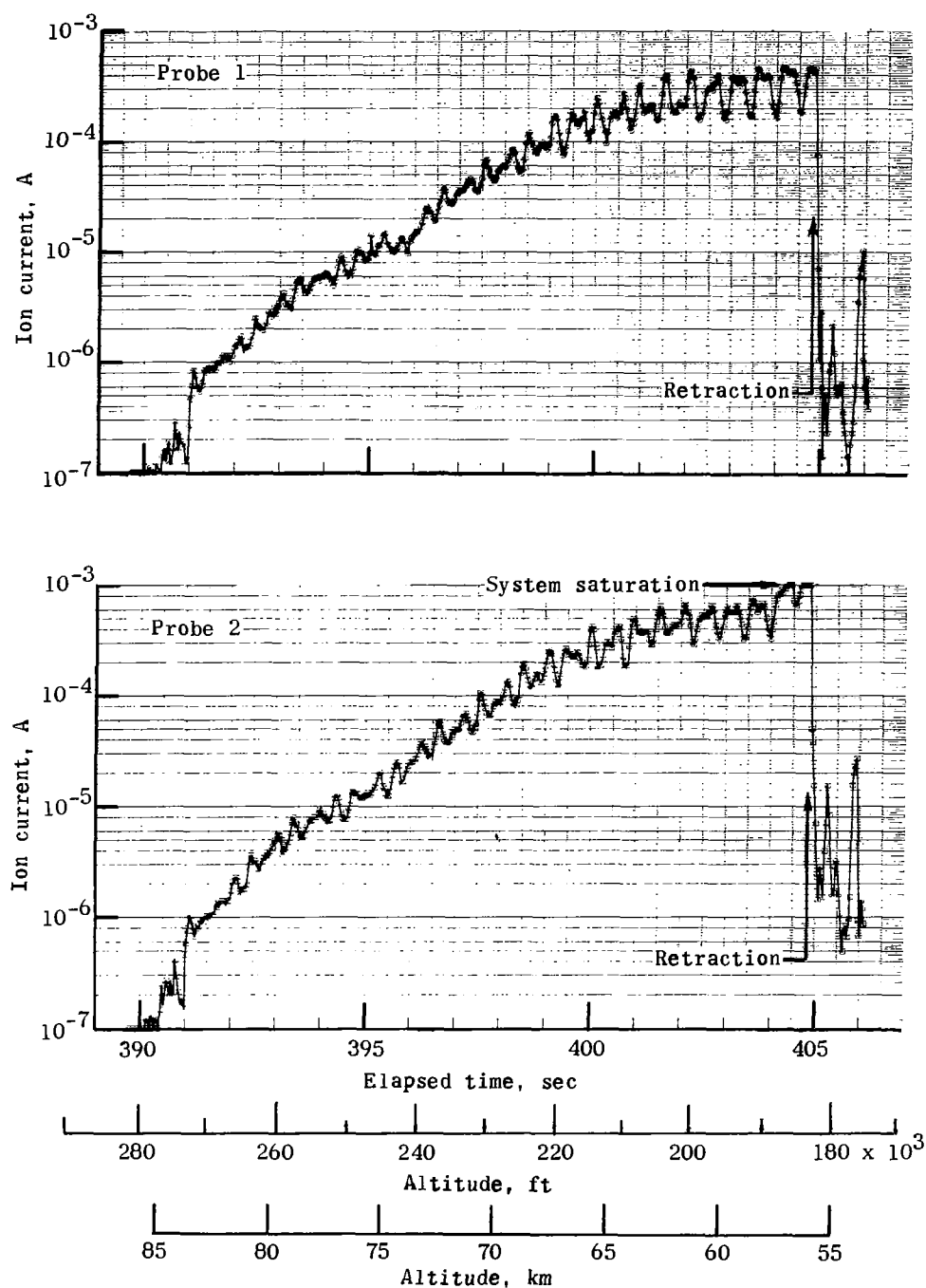
(c) Electrostatic probes 5 and 6.

Figure 13.- Continued.



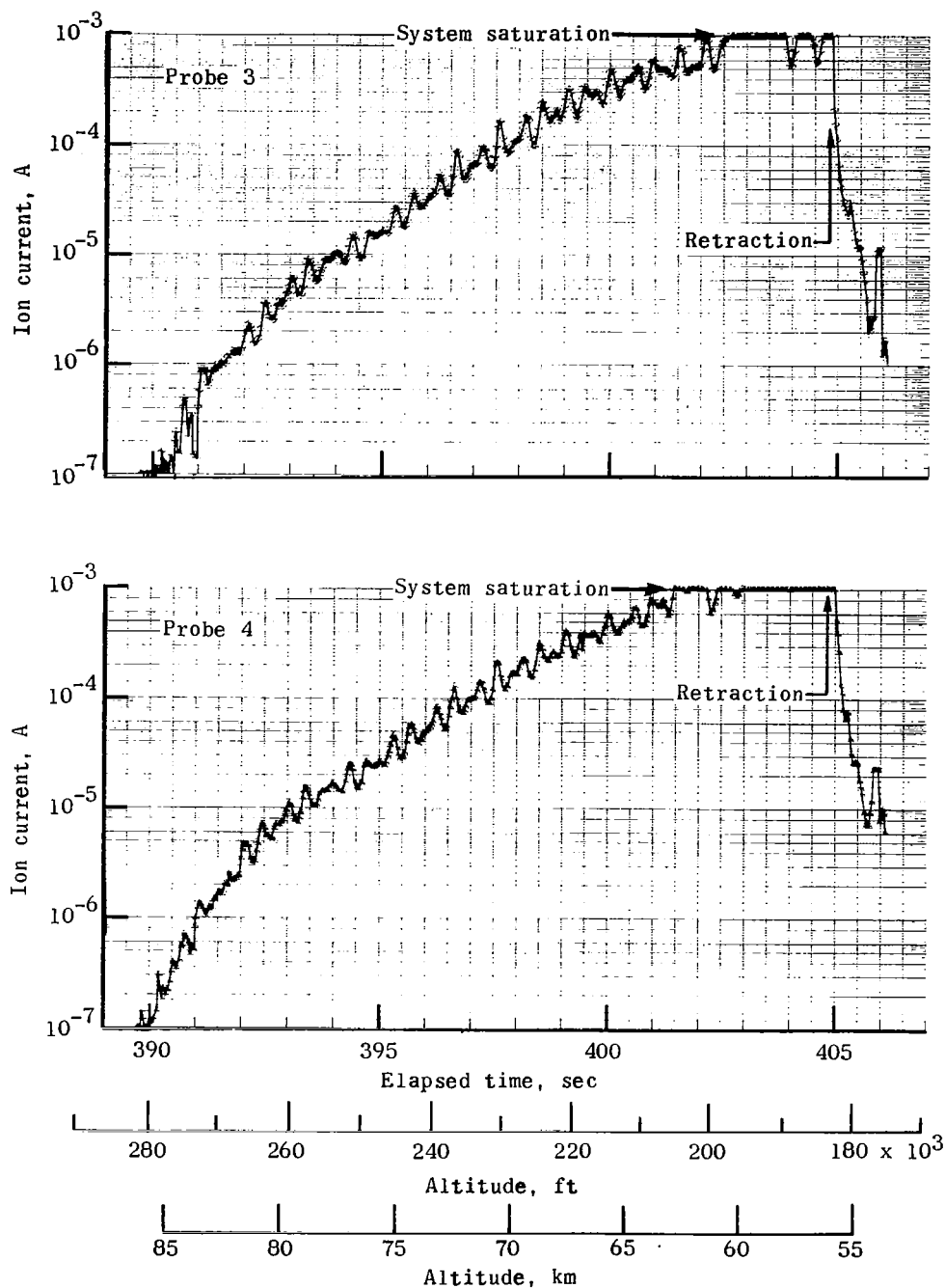
(d) Electrostatic probes 7 and 8.

Figure 13.- Concluded.



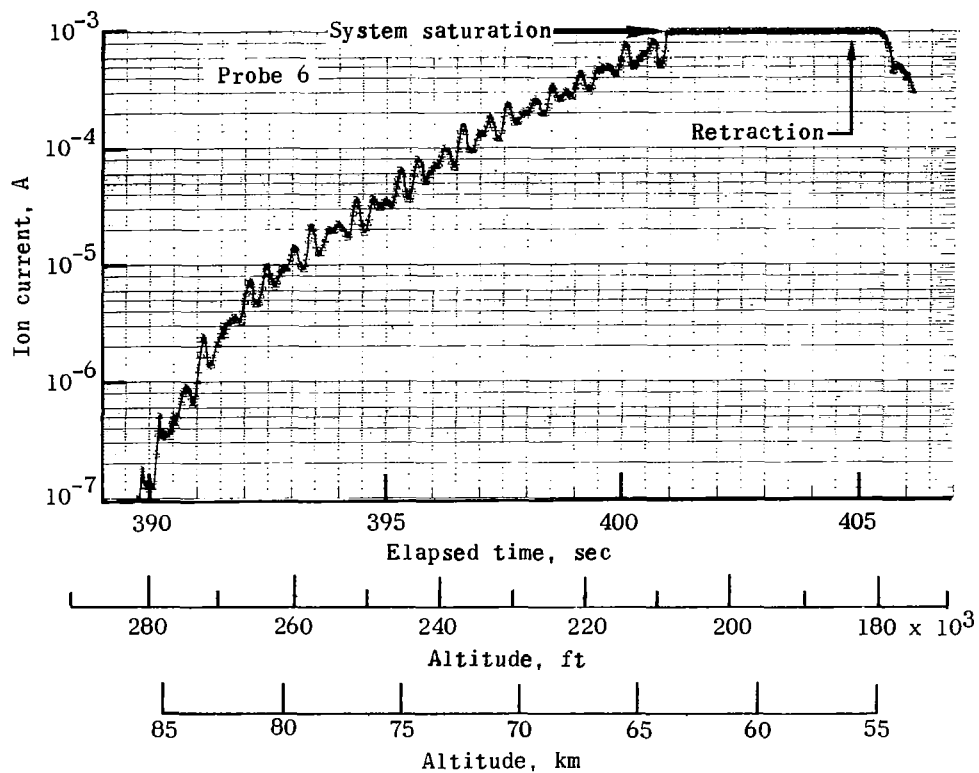
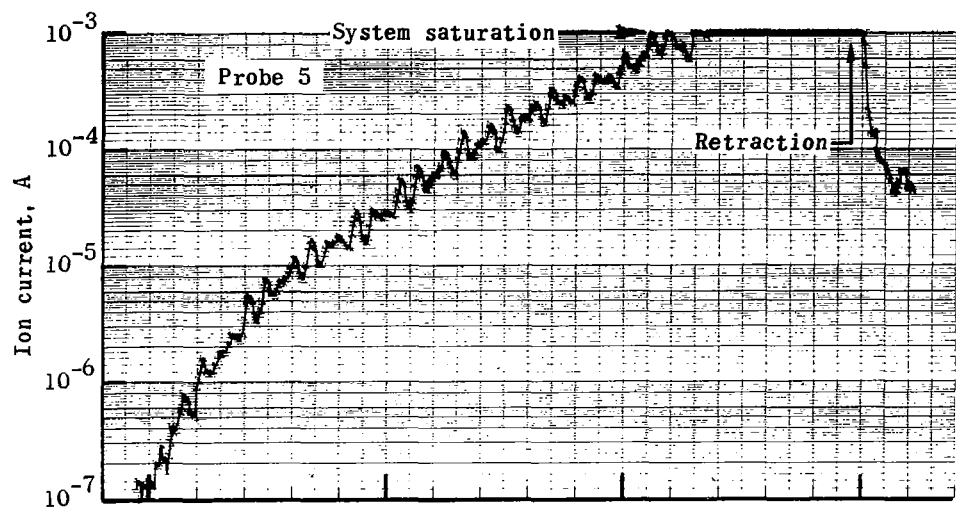
(a) Electrostatic probes 1 and 2.

Figure 14.- Ion current measurements from electrostatic probes on RAM C-II flight experiment. Altitudes shown are 0.3658 km (1200 ft) too low because of use of RAM C-I trajectory.



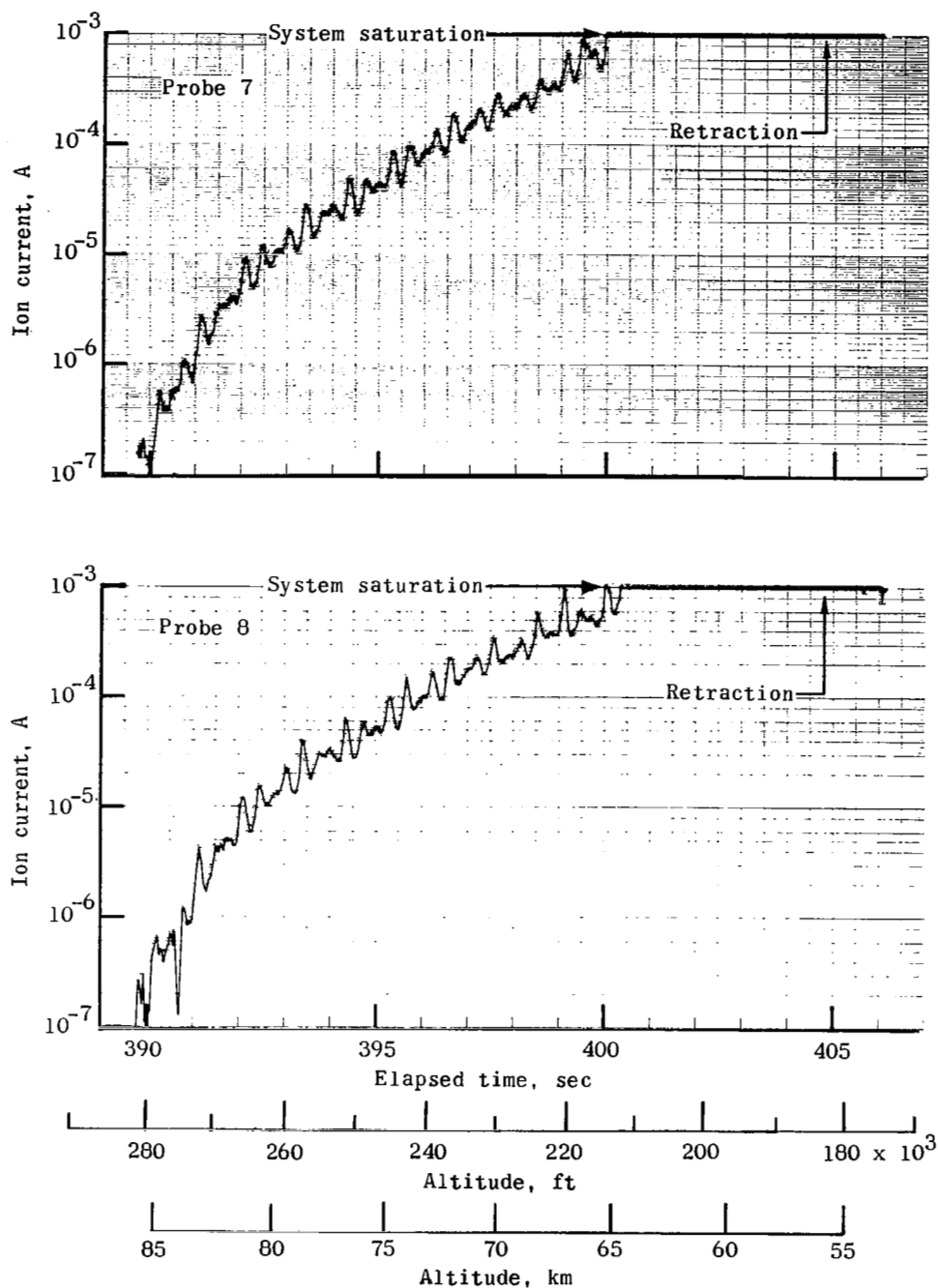
(b) Electrostatic probes 3 and 4.

Figure 14.- Continued.



(c) Electrostatic probes 5 and 6.

Figure 14.- Continued.



(d) Electrostatic probes 7 and 8.

Figure 14.- Concluded.

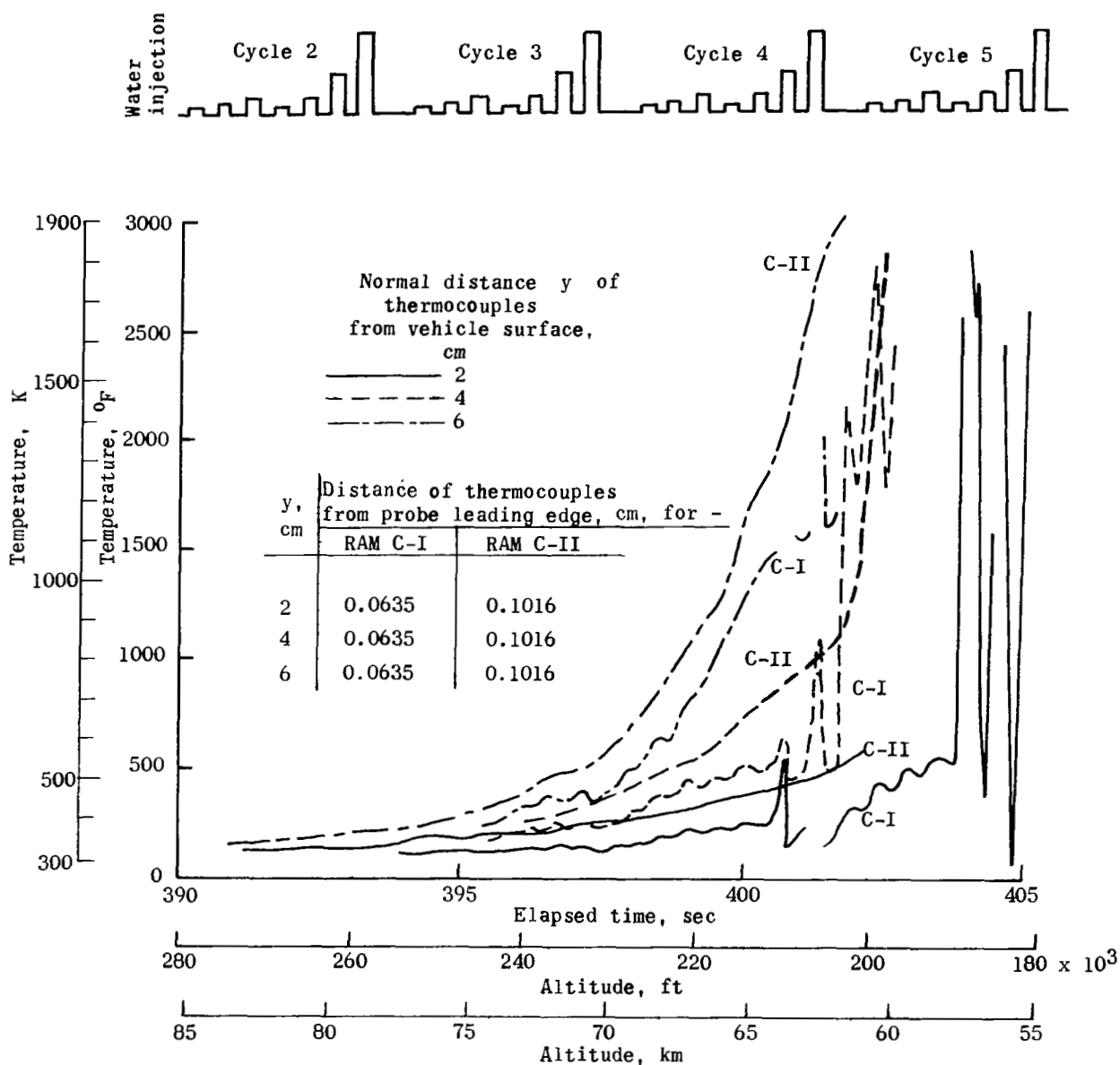


Figure 15.- Comparison of thermocouple-rake leading-edge temperatures.

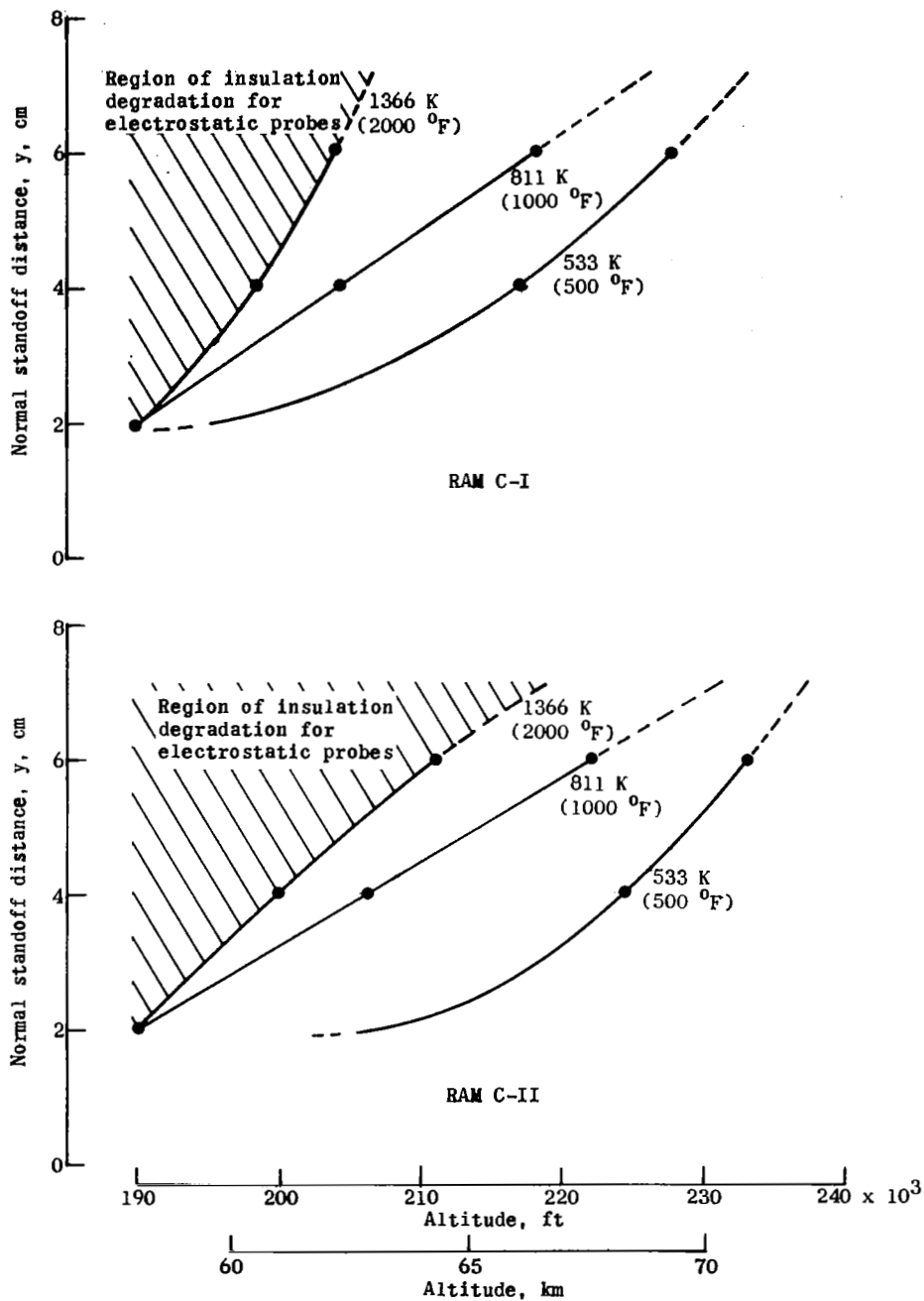
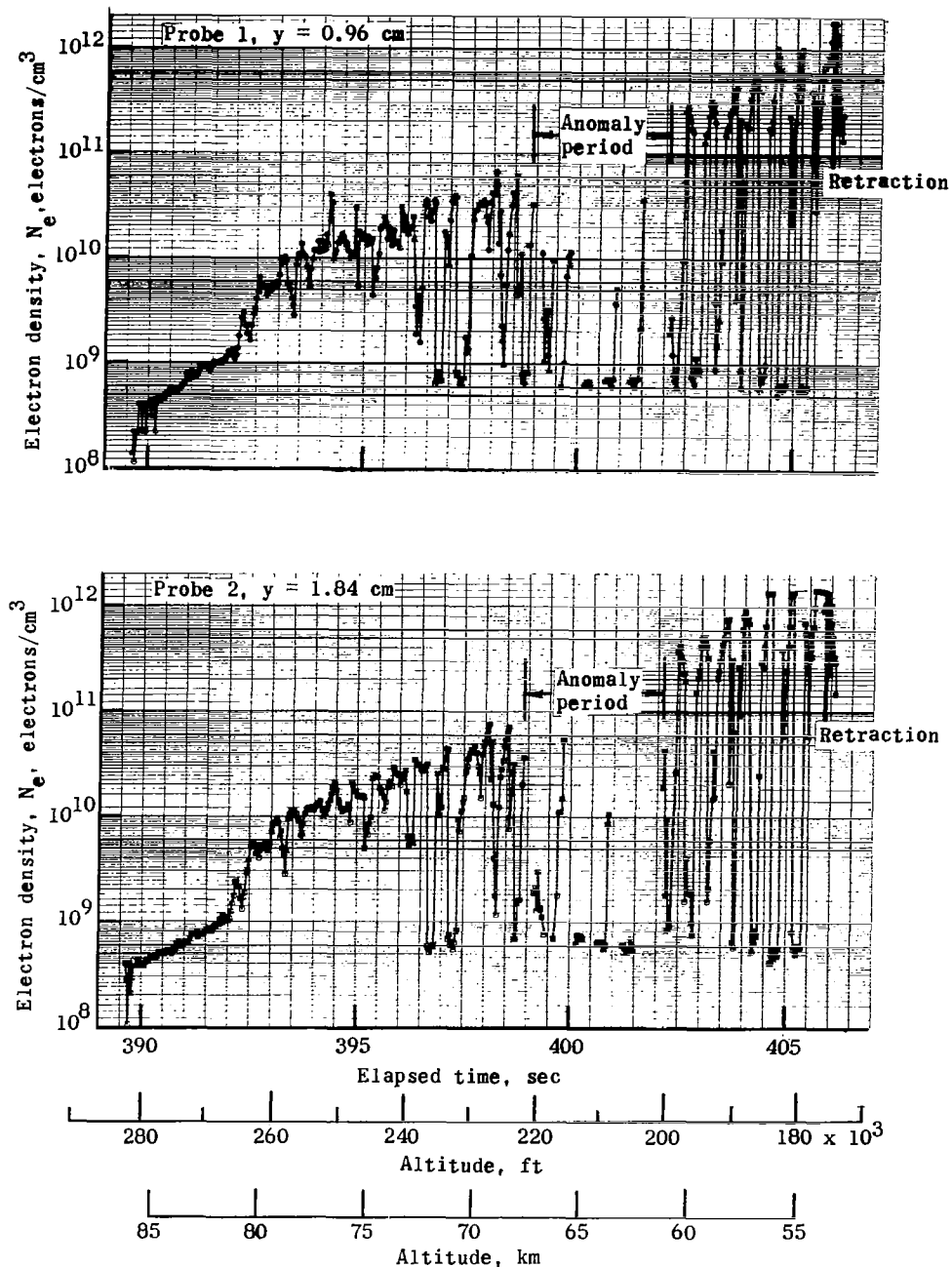
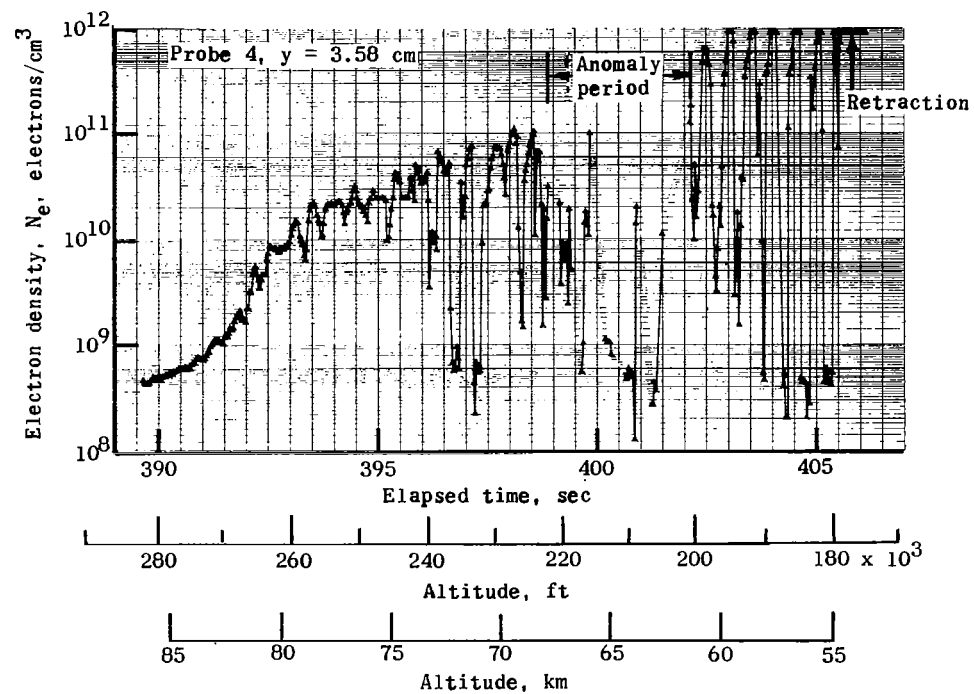
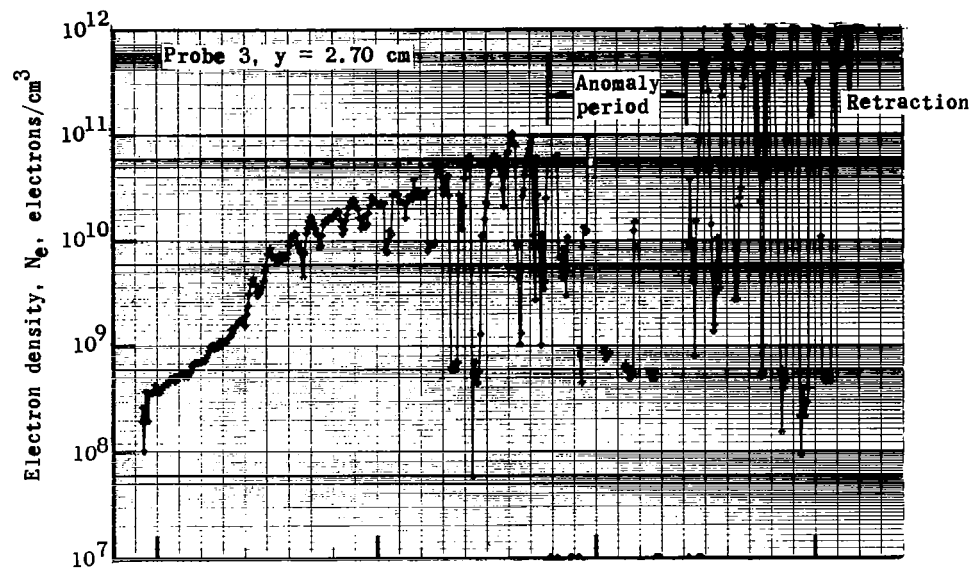


Figure 16.- Constant-temperature profiles from thermocouple measurements.



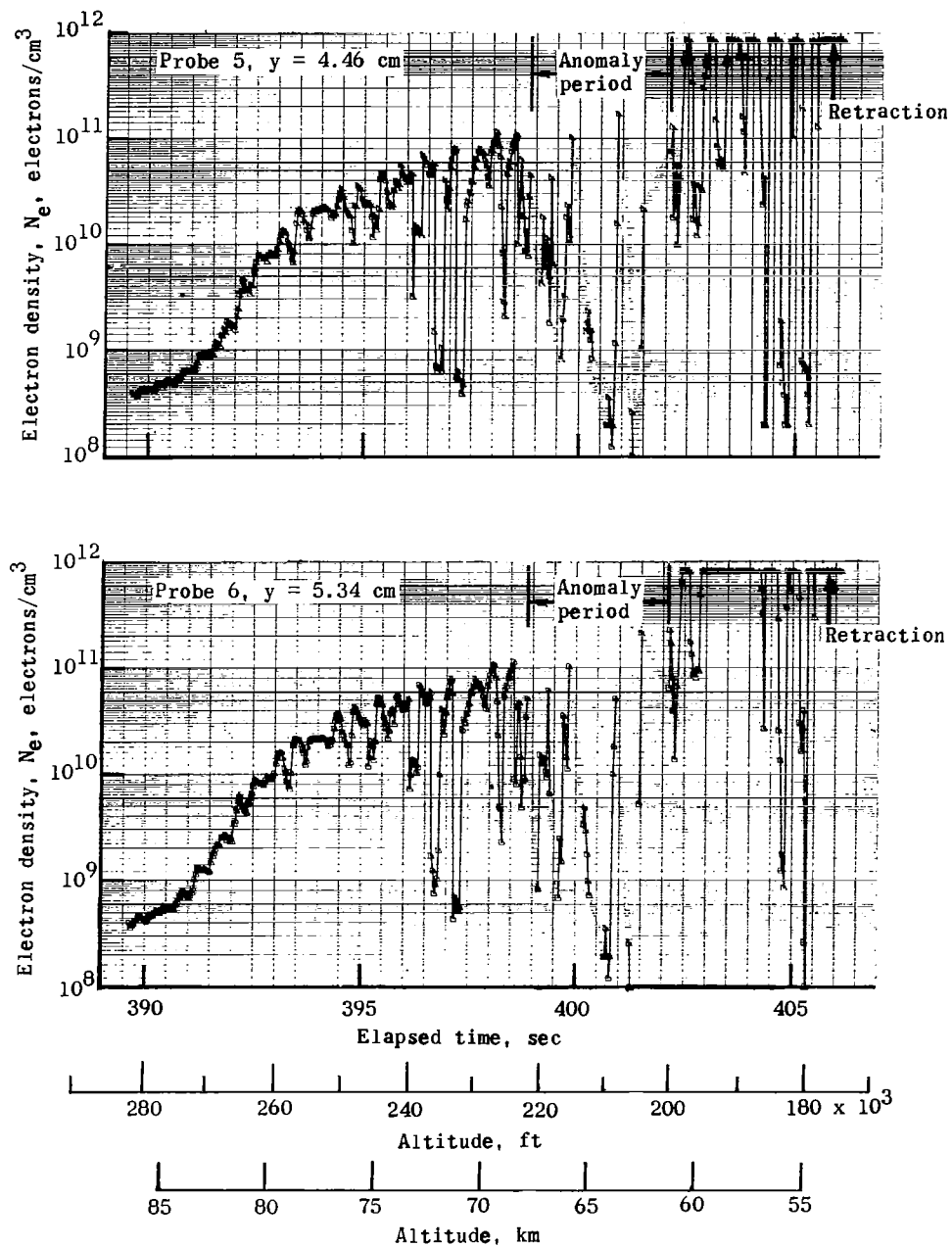
(a) Electrostatic probes 1 and 2.

Figure 17.- Electron density of RAM C-I flow field at standoff distances y ranging between 1 and 7 cm as inferred from electrostatic probe measurements.



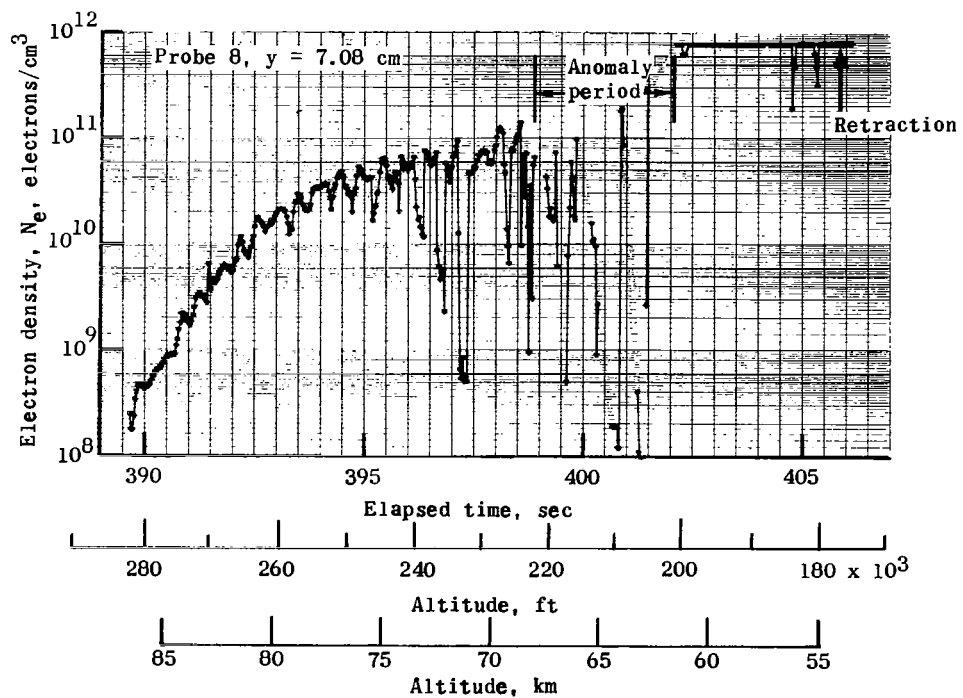
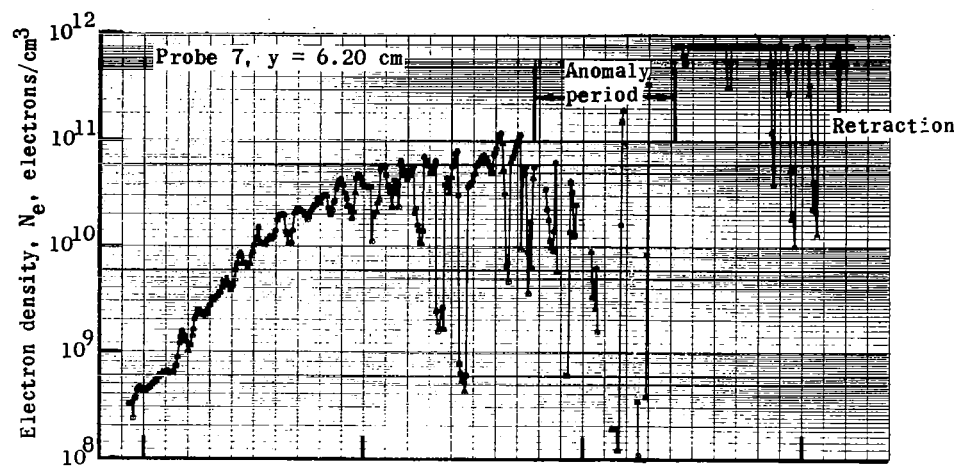
(b) Electrostatic probes 3 and 4.

Figure 17.- Continued.



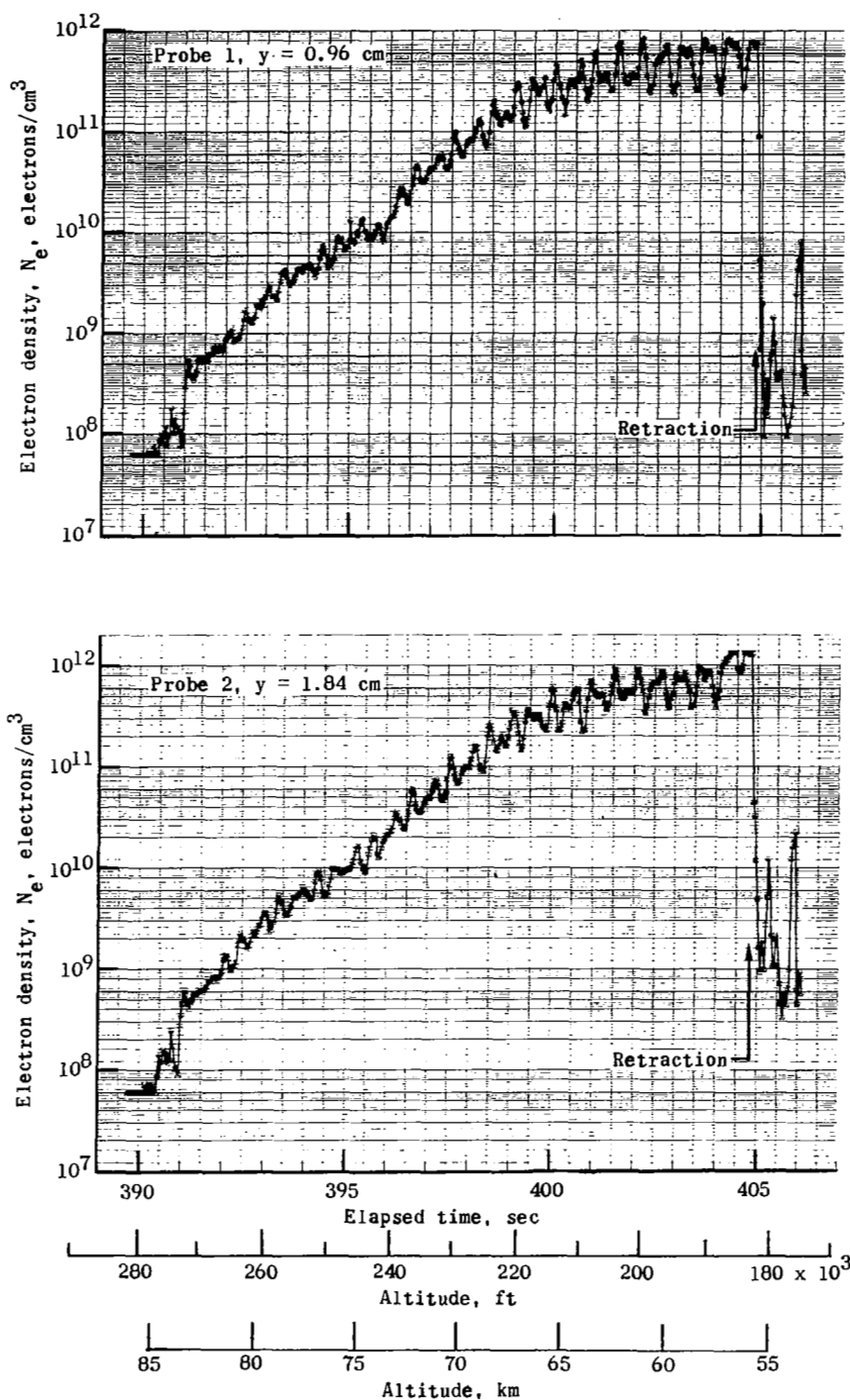
(c) Electrostatic probes 5 and 6.

Figure 17.- Continued.



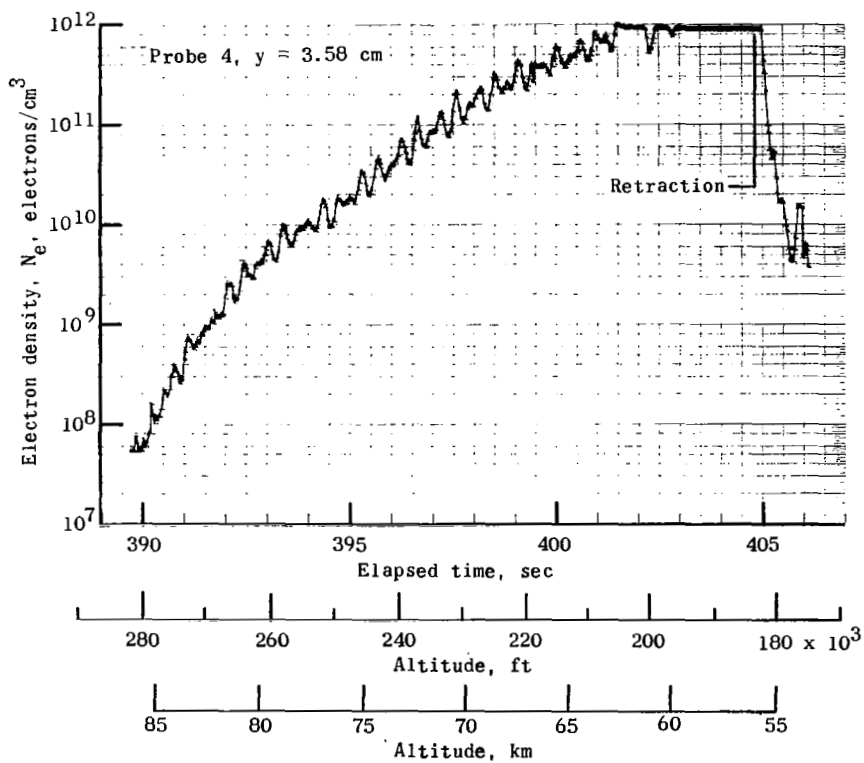
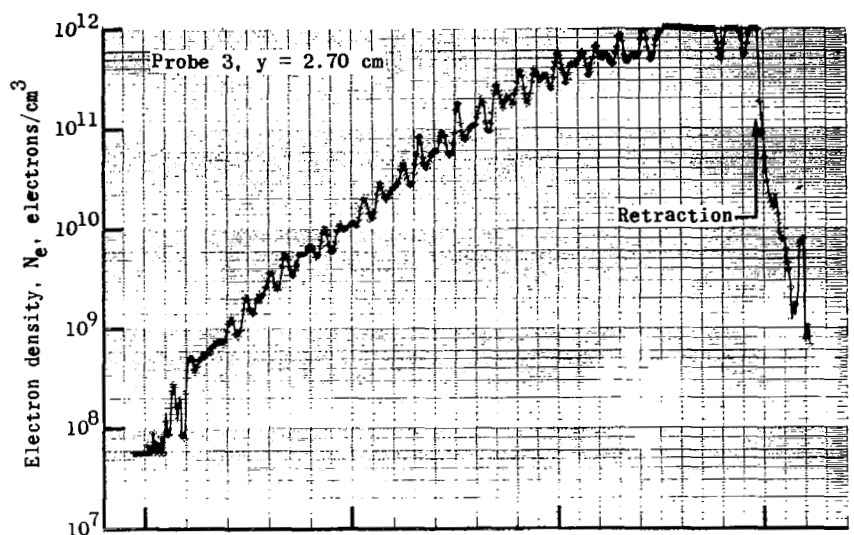
(d) Electrostatic probes 7 and 8.

Figure 17.- Concluded.



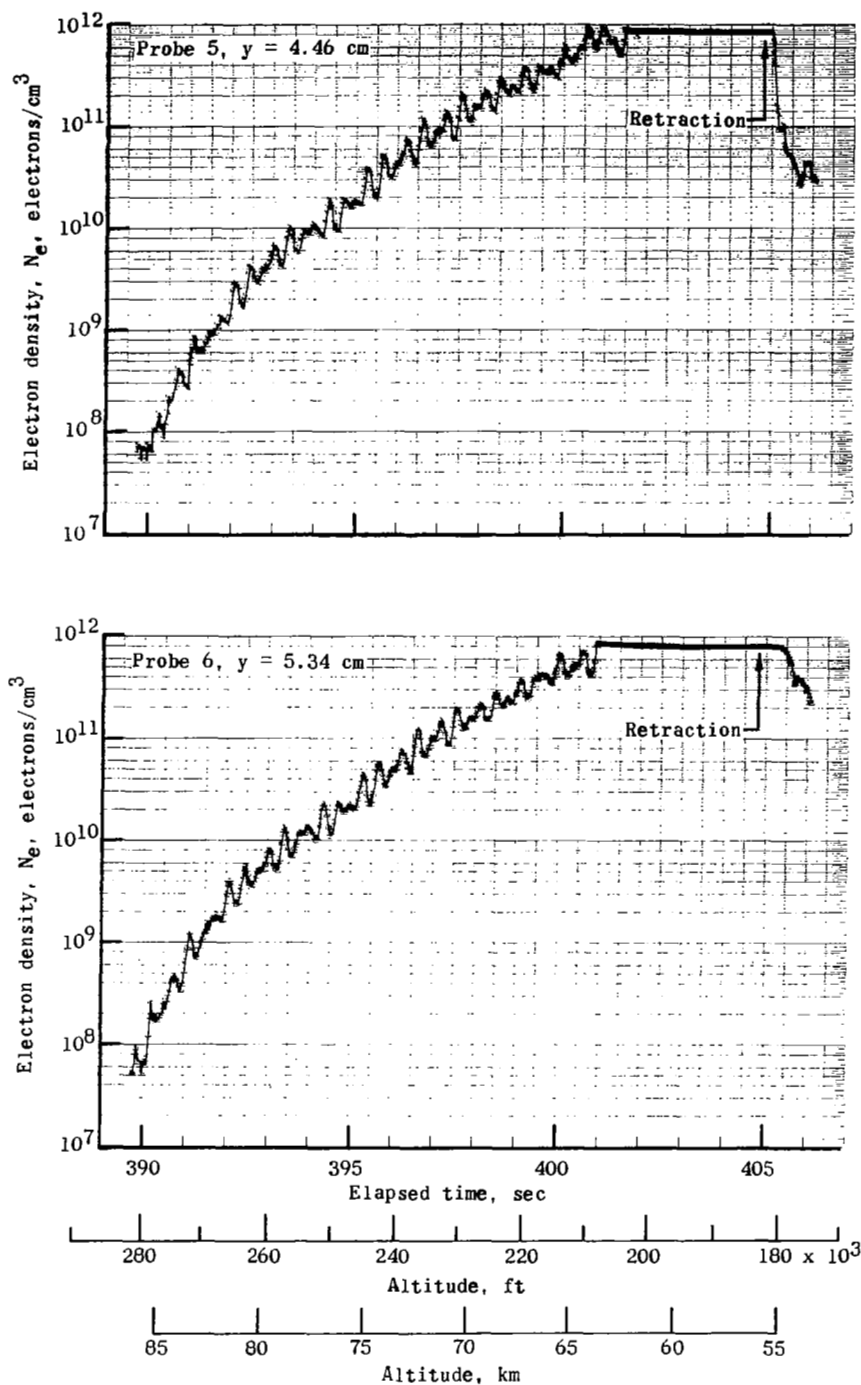
(a) Electrostatic probes 1 and 2.

Figure 18.- Electron density of RAM C-II flow field at standoff distances y ranging between 1 and 7 cm as inferred from electrostatic probe measurements. Altitudes shown are 0.3658 km (1200 ft) too low because of use of RAM C-I trajectory.



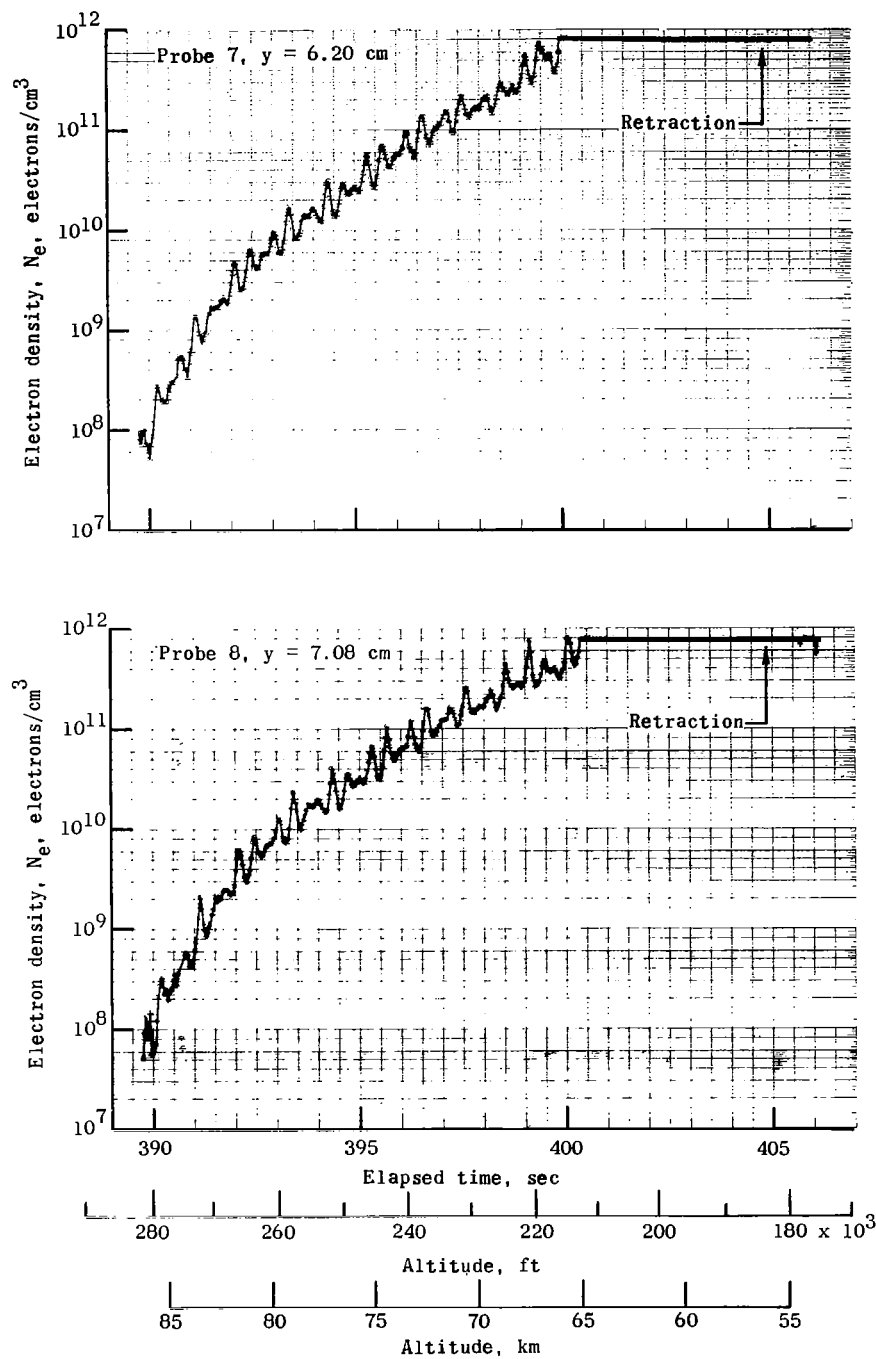
(b) Electrostatic probes 3 and 4.

Figure 18.- Continued.



(c) Electrostatic probes 5 and 6.

Figure 18.- Continued.



(d) Electrostatic probes 7 and 8.

Figure 18.- Concluded.

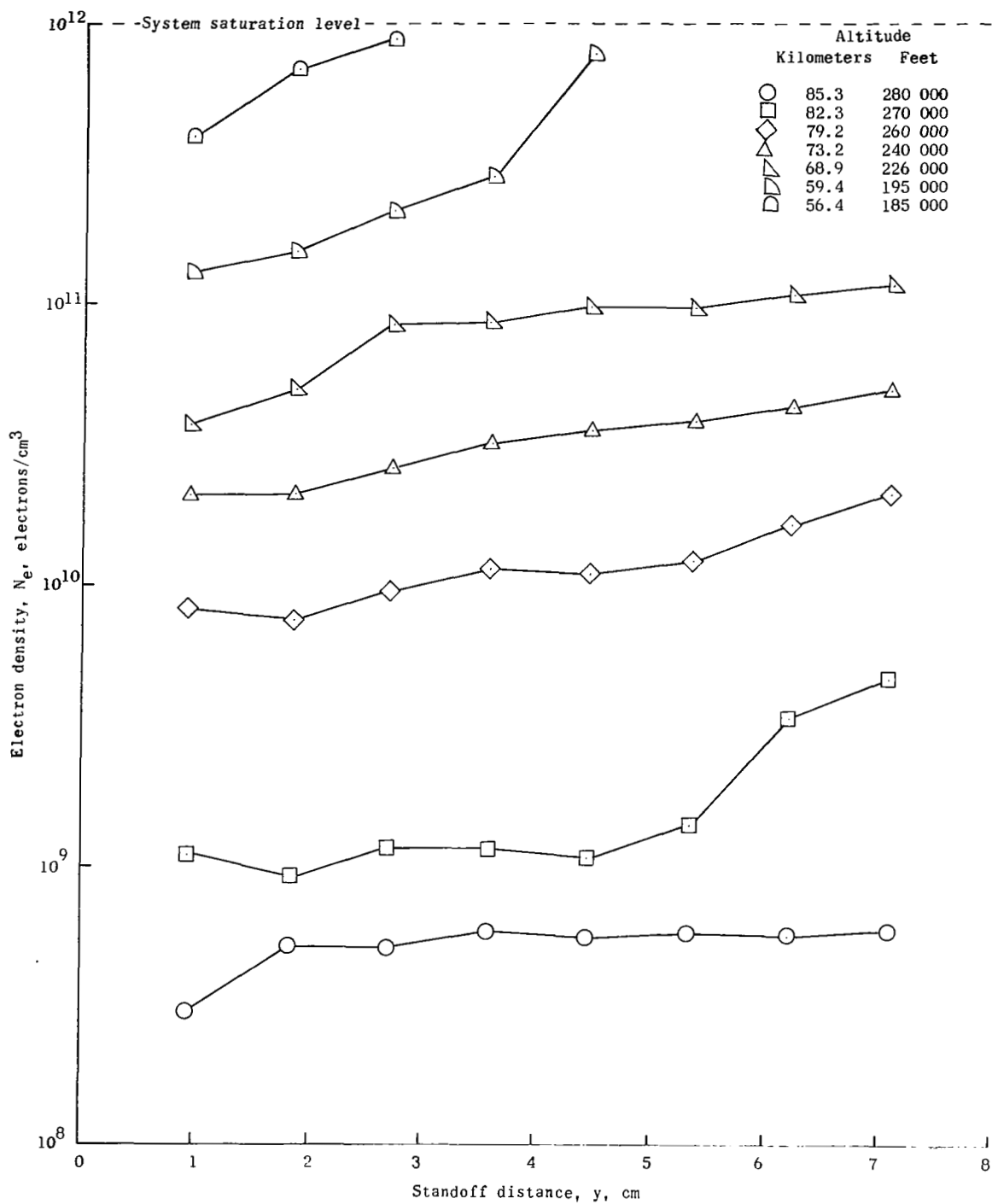


Figure 19.- Measured time-average electron density profiles for RAM C-I at selected altitudes during no water injection.

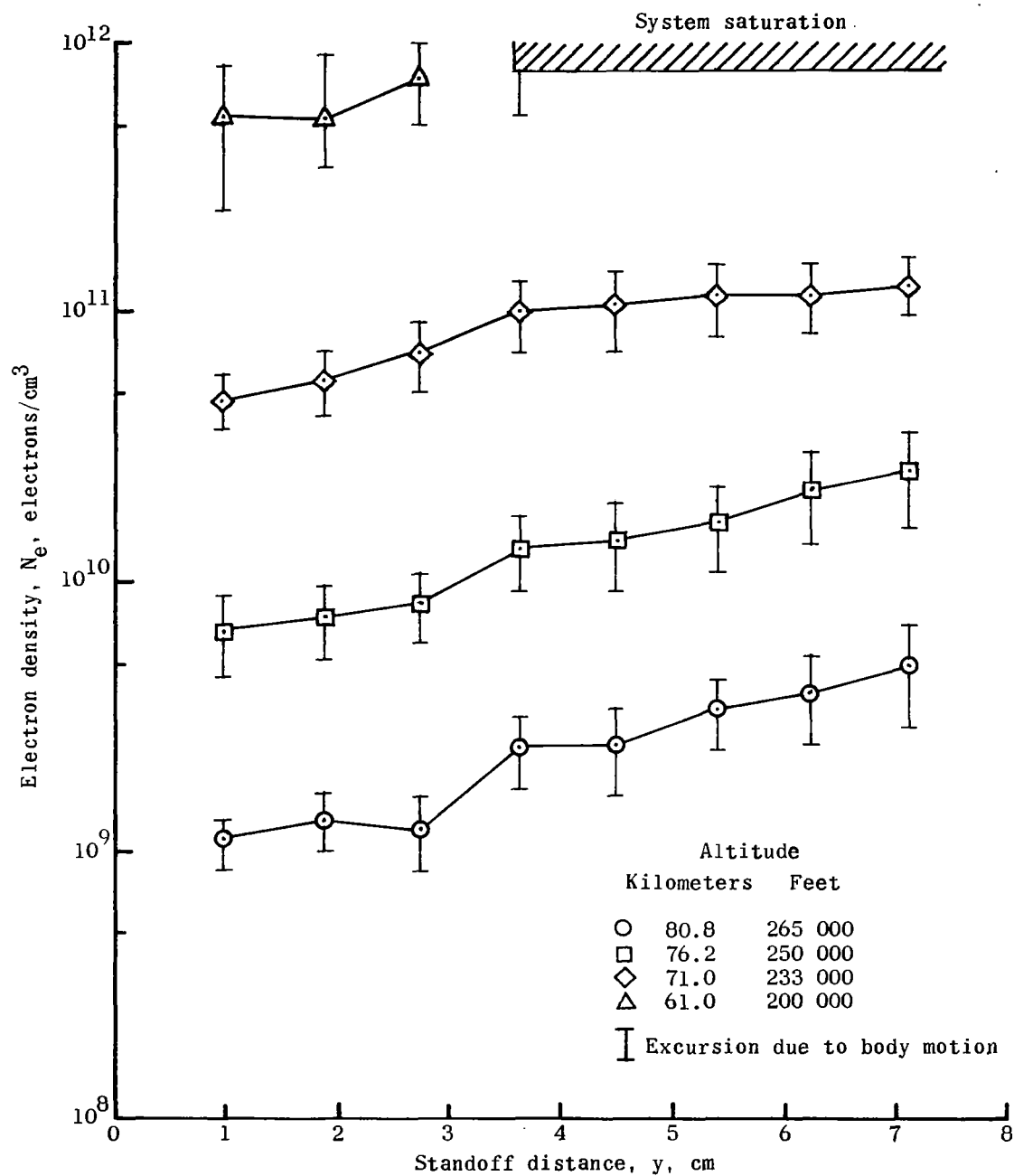
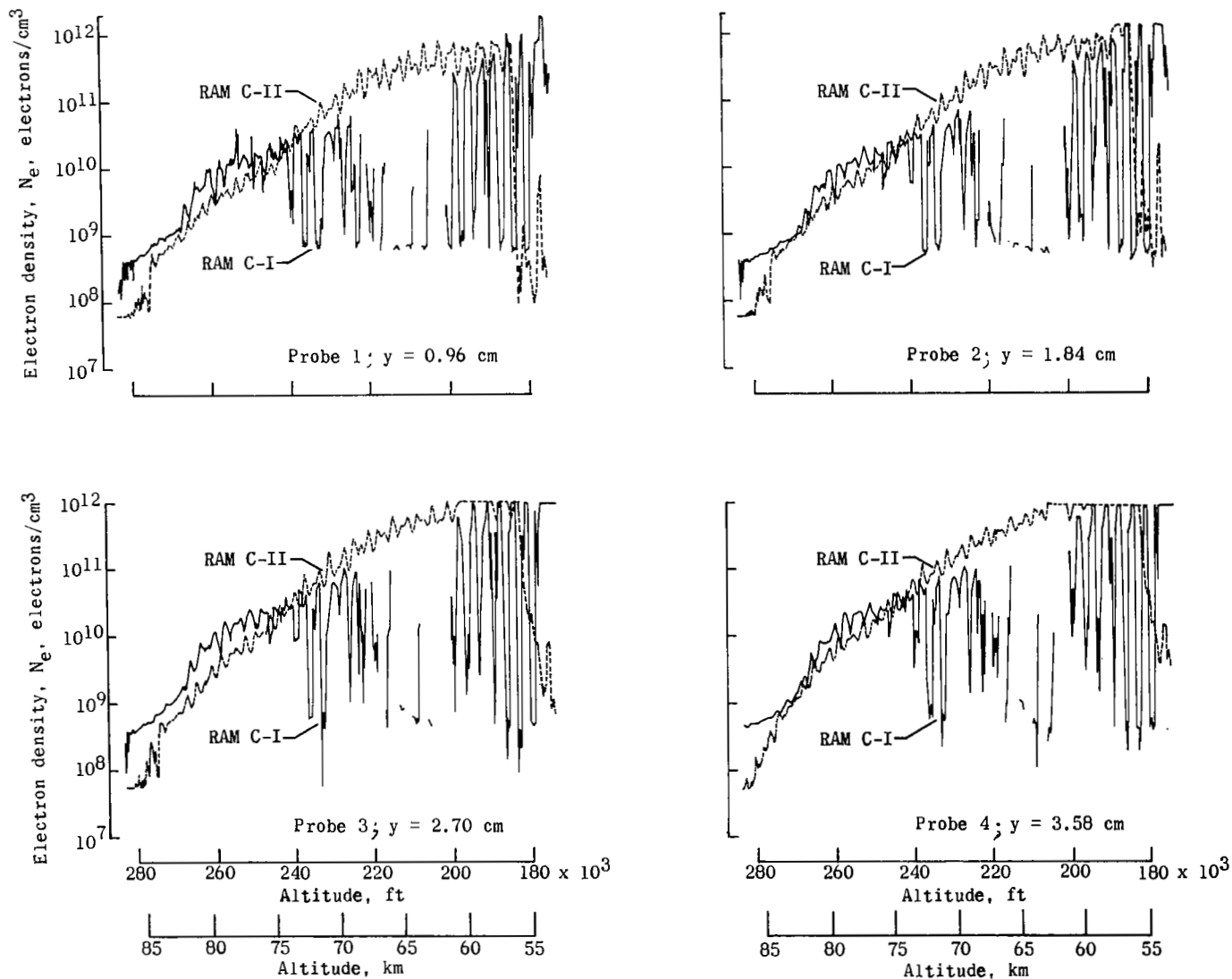
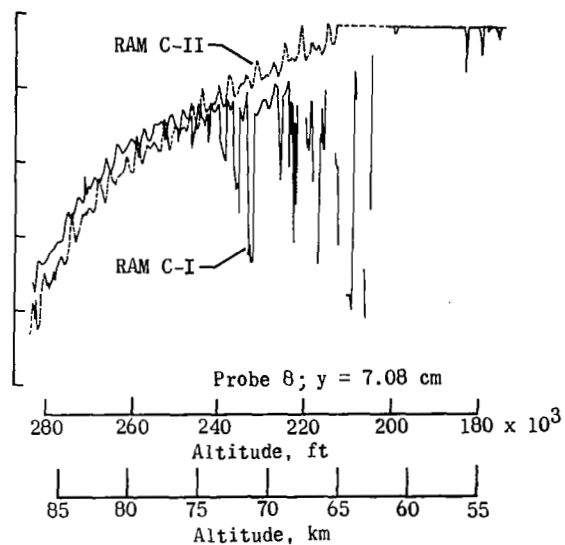
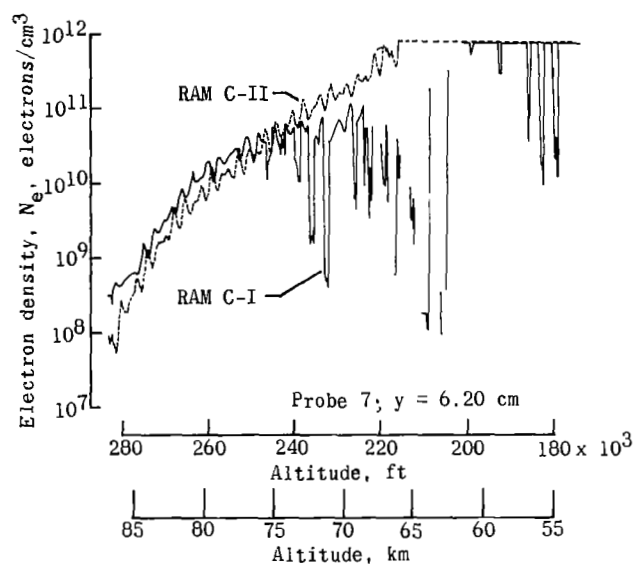
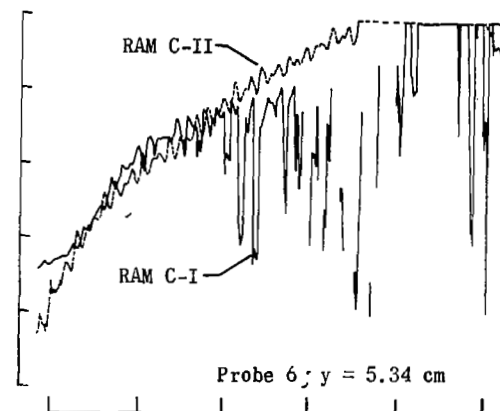
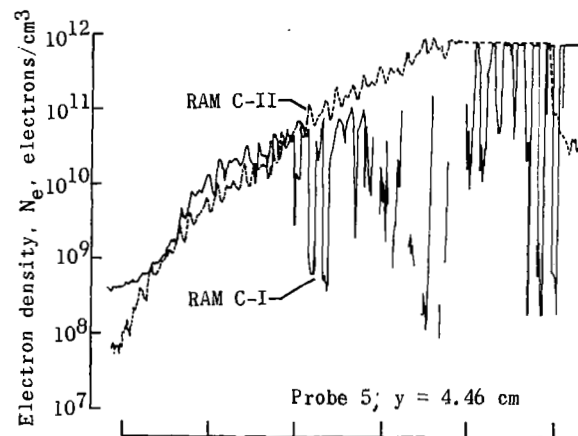


Figure 20.- Measured time-average electron density profiles for RAM C-II at four altitudes.



(a) Probes 1 to 4.

Figure 21.- Comparison of measured electron densities for individual probes on RAM C-I and C-II. Altitudes for RAM C-II data are 0.3658 km (1200 ft) too low because of use of RAM C-I trajectory.



(b) Probes 5 to 8.

Figure 21.- Concluded.

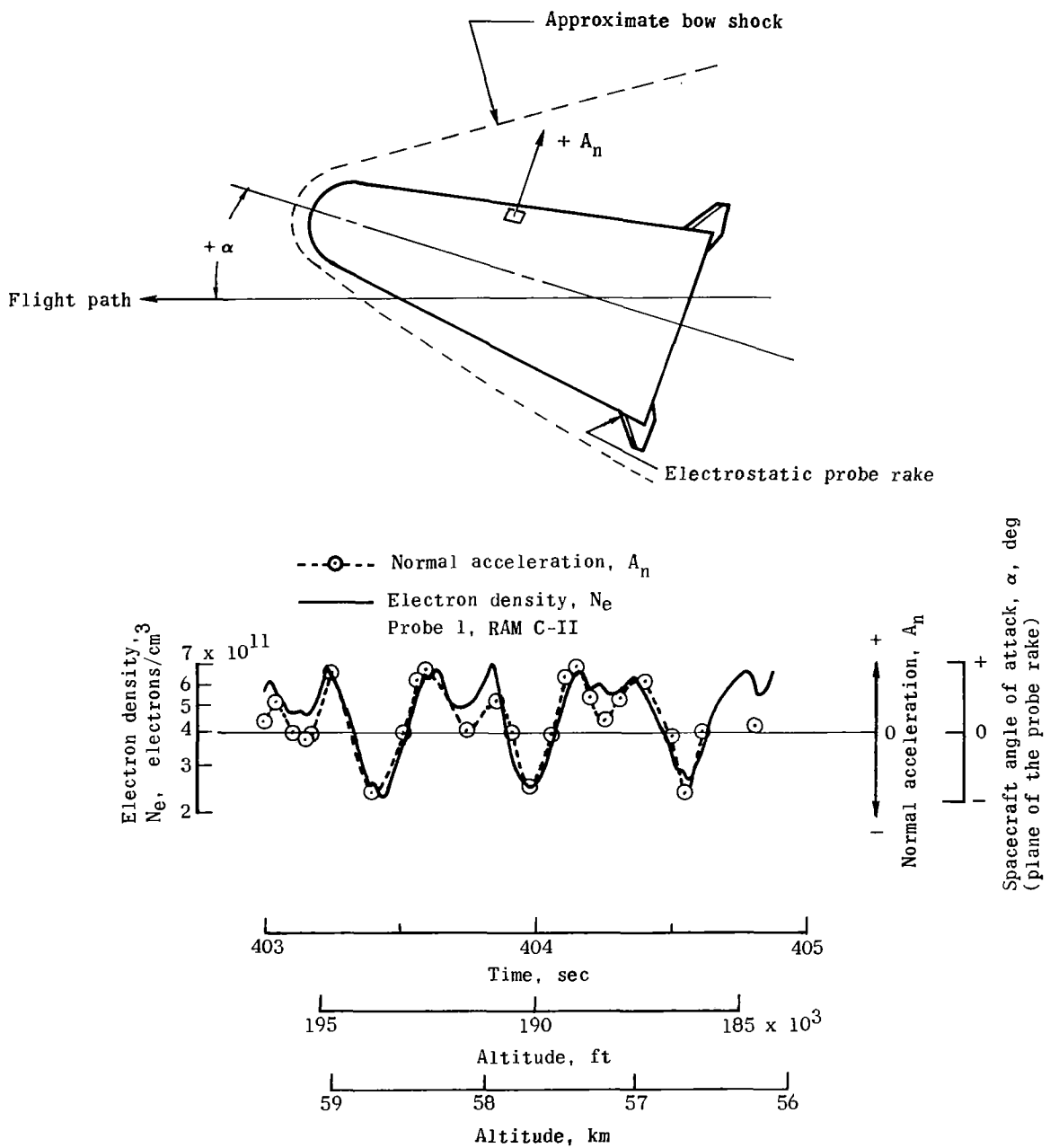


Figure 22.- Correlation of RAM C-II fixed-bias electrostatic probe measurements with spacecraft angle-of-attack motions.

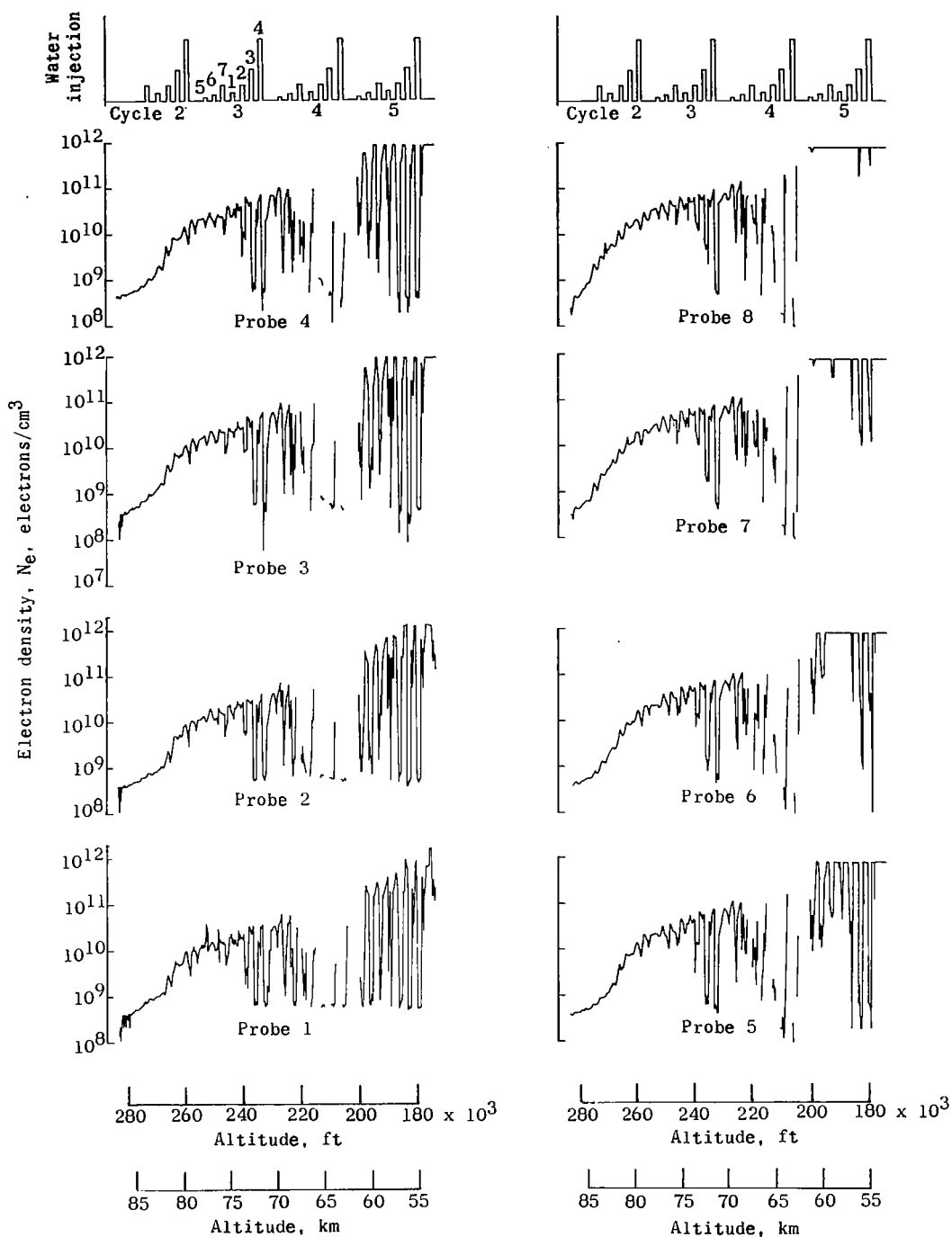


Figure 23.- Effects of water injection on electron density as inferred by RAM C-I electrostatic probes.

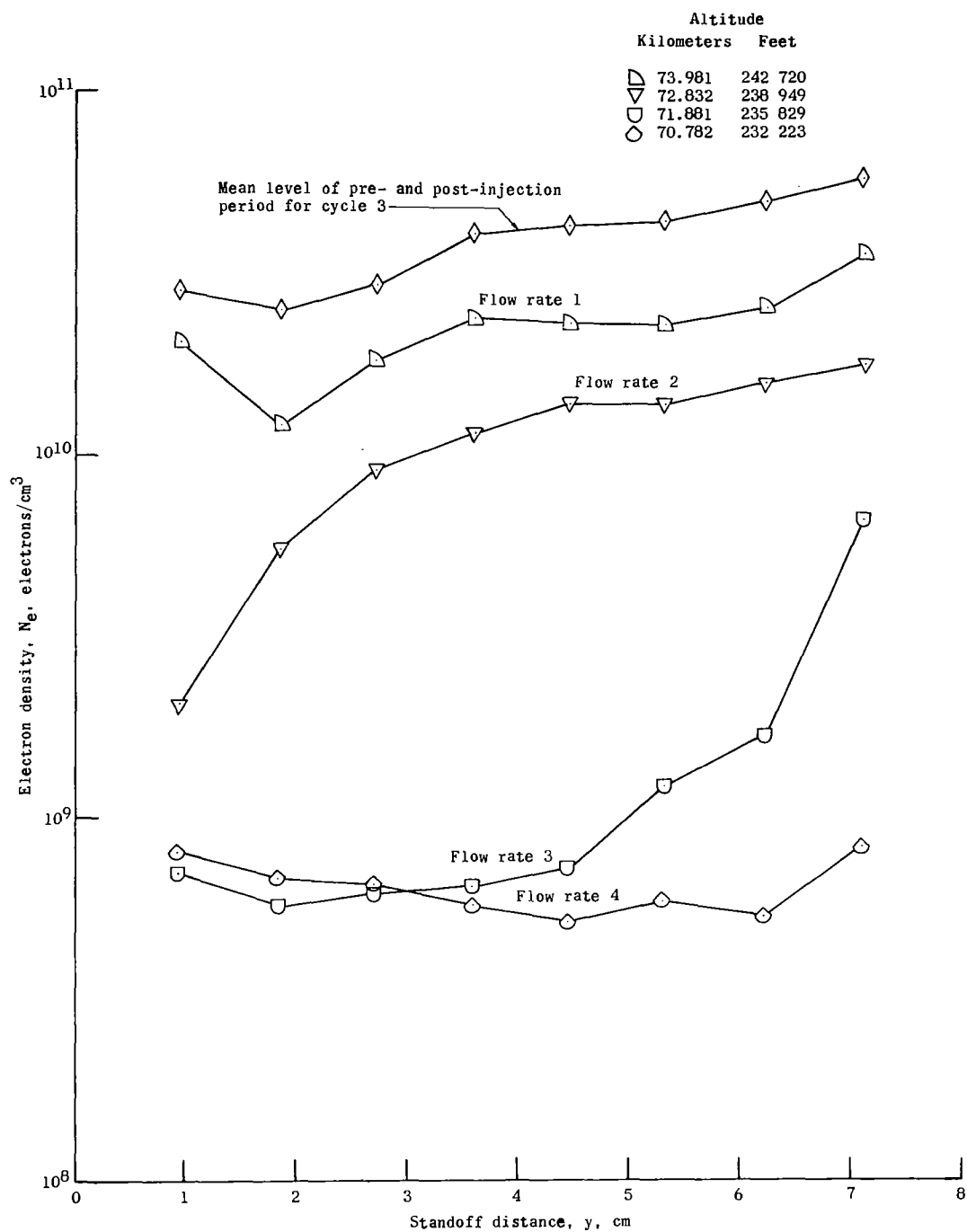


Figure 24.- RAM C-I electron-density distribution profiles during side injection portion of cycle 3.

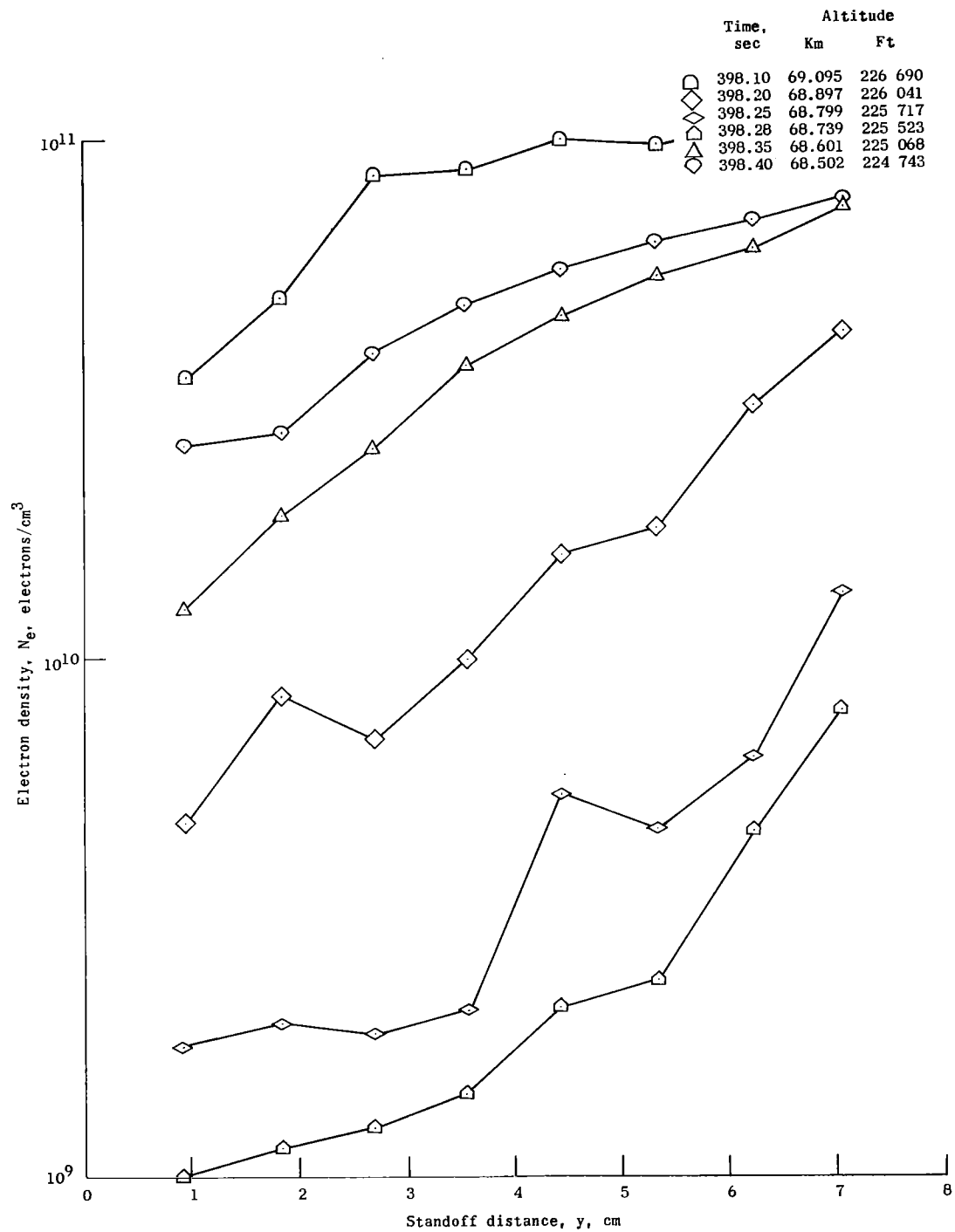


Figure 25.- Effect of stagnation injection at flow rate 5 of cycle 4 on RAM C-I electron density distribution profiles at various altitudes.

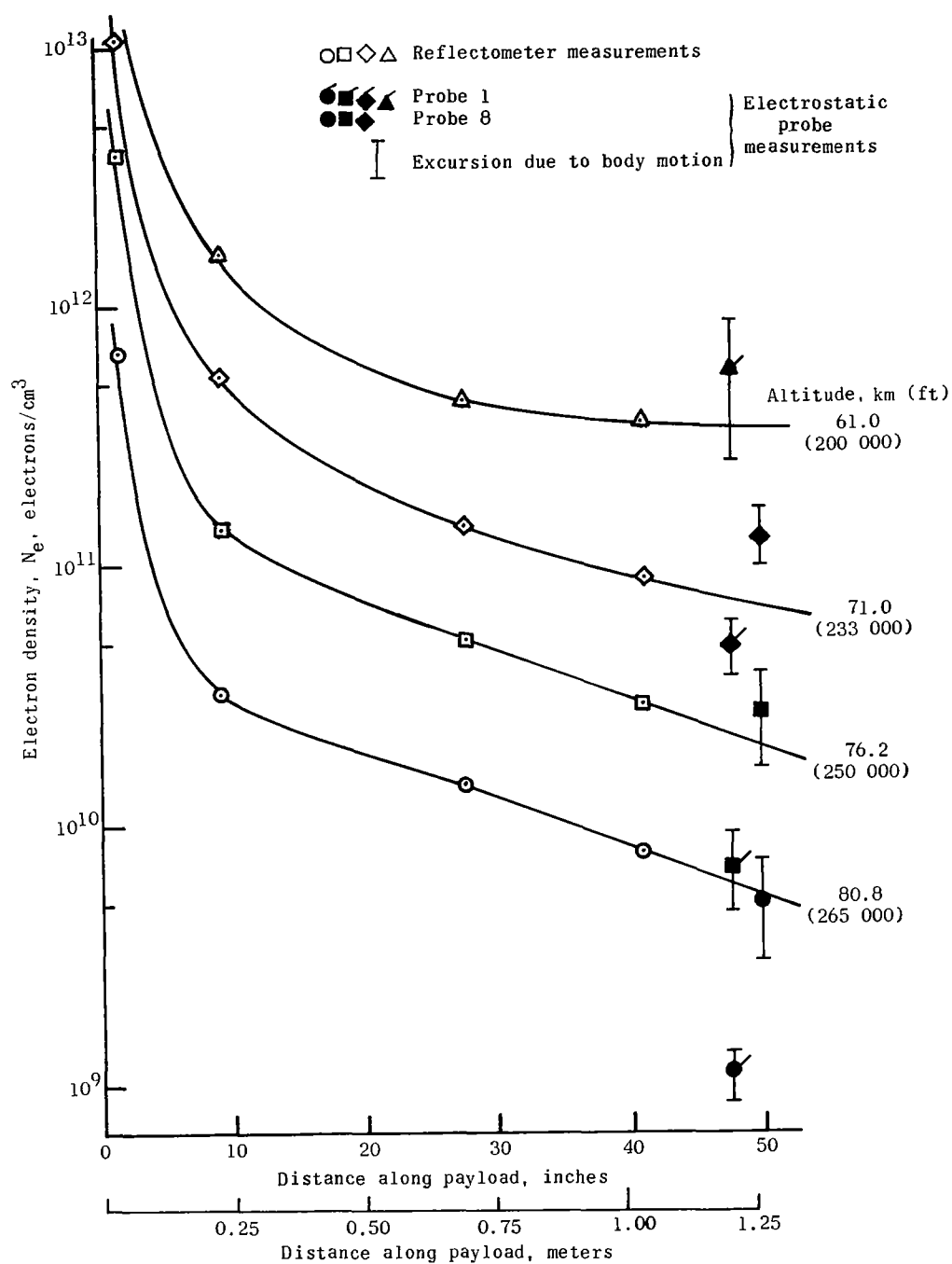


Figure 26.- RAM C-II longitudinal profiles of inferred peak electron density for constant altitudes.

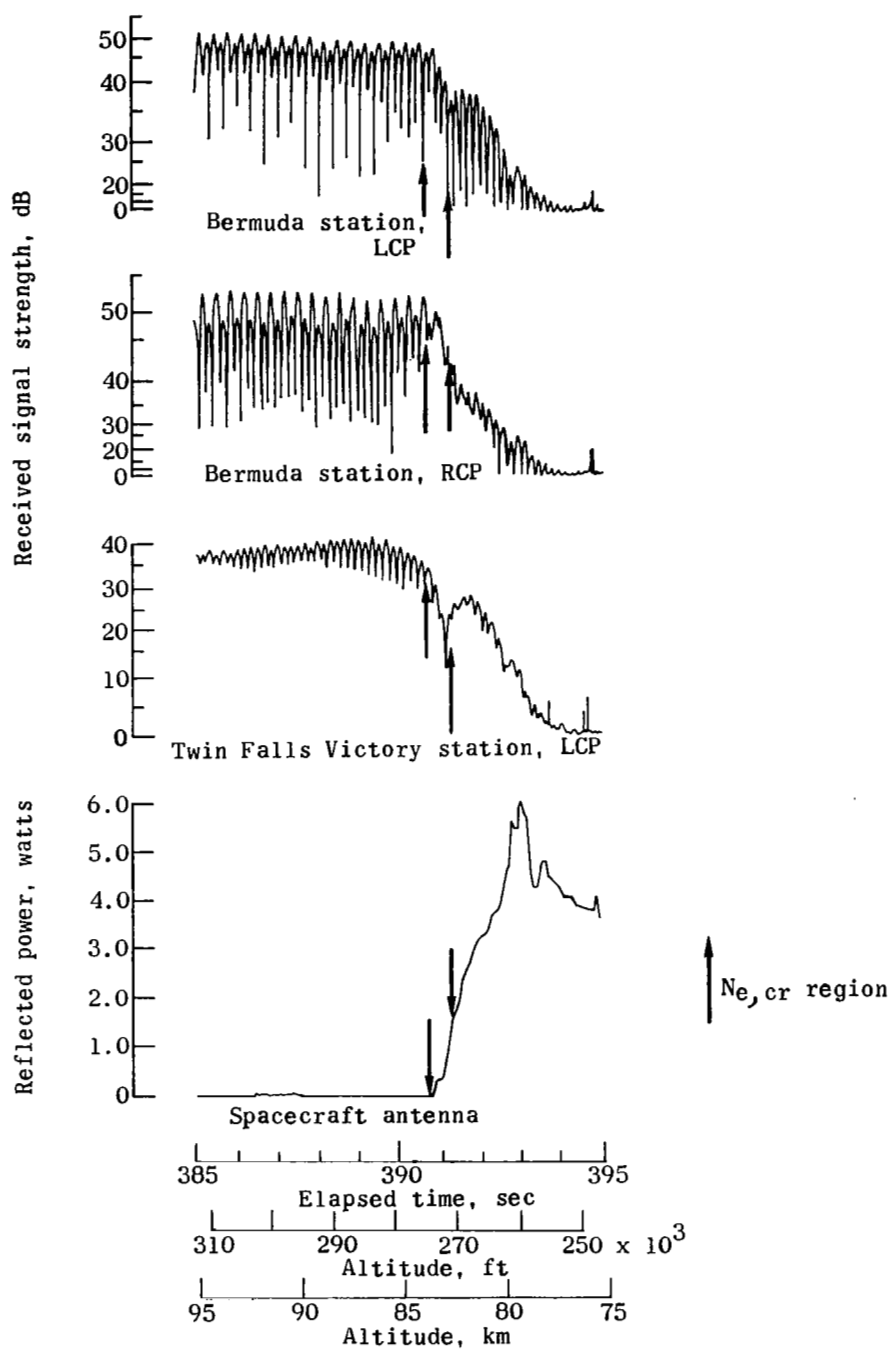


Figure 27.- Effects of RAM C-I reentry plasma on 225.7 MHz telemetry antenna. LCP, left circular polarization; RCP, right circular polarization.

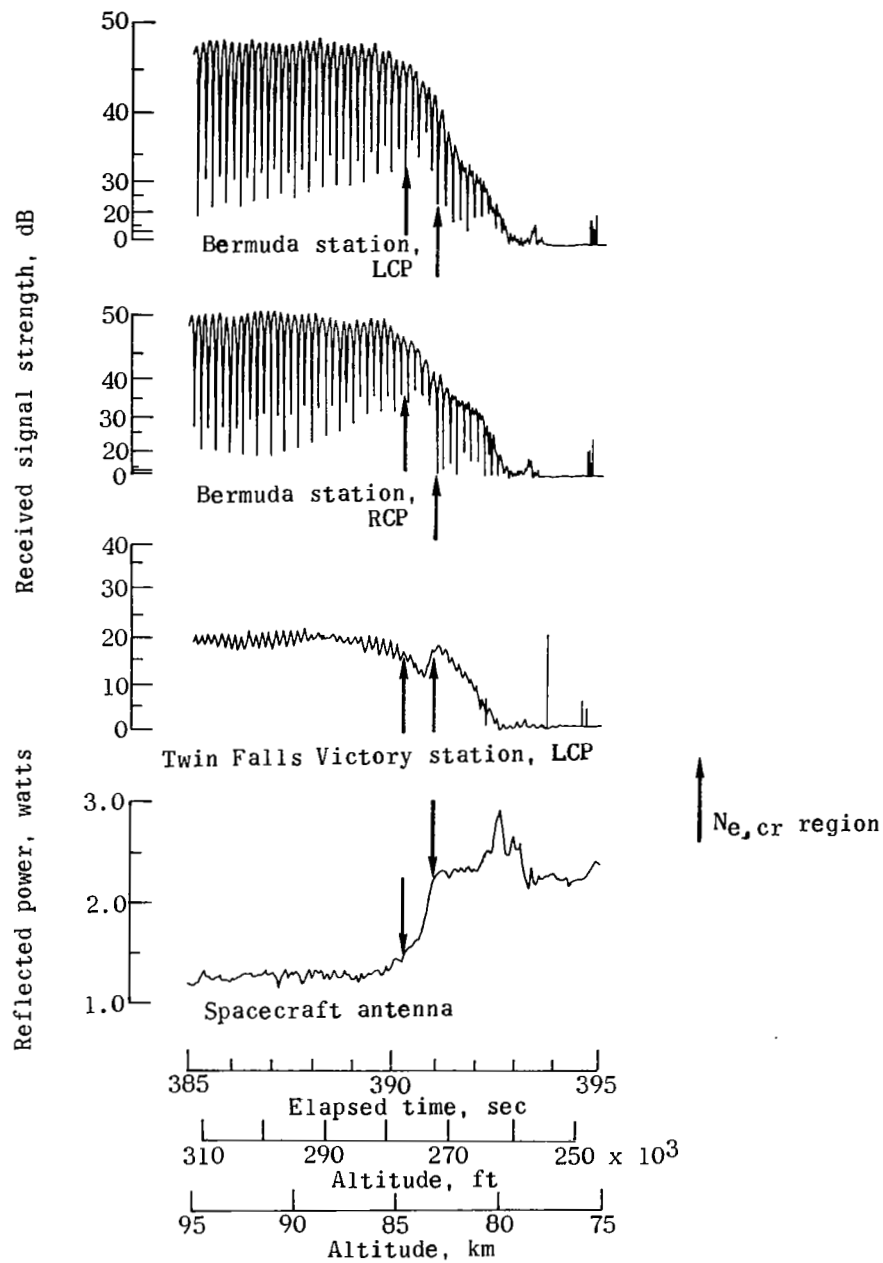


Figure 28.- Effects of RAM C-I reentry plasma on 259.7 MHz telemetry antenna. LCP, left circular polarization; RCP, right circular polarization.

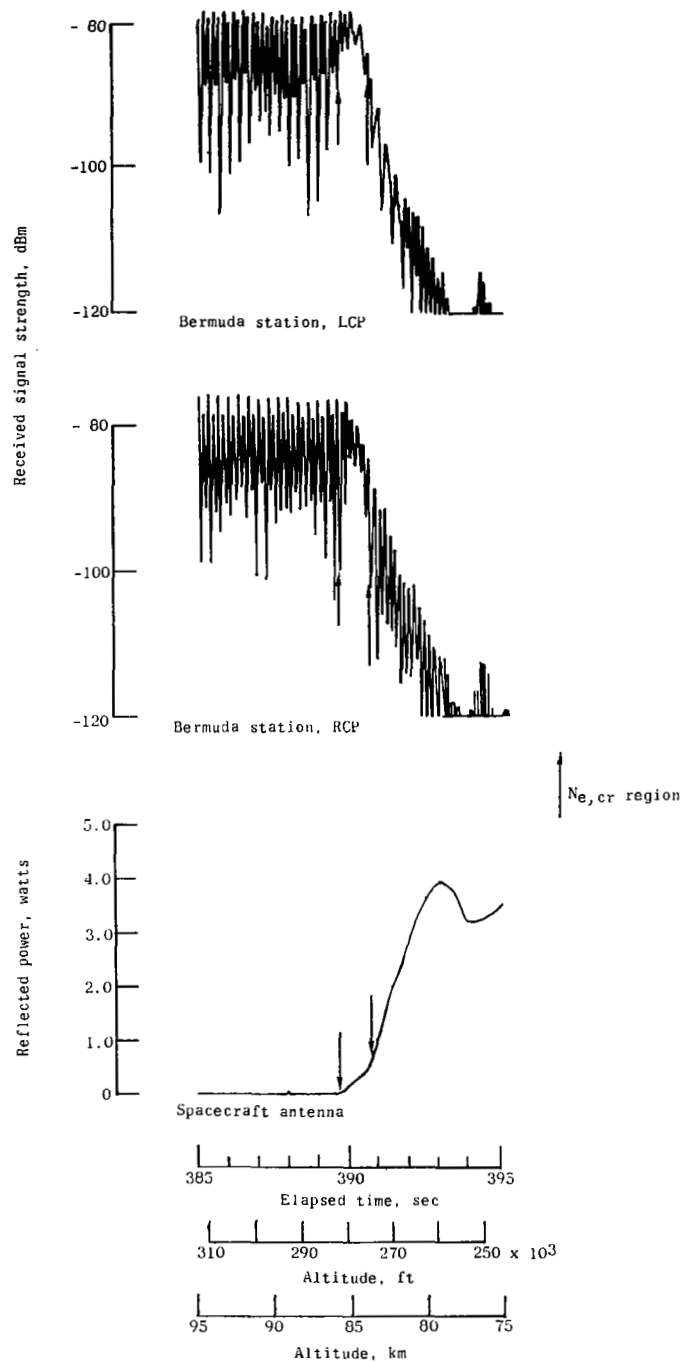


Figure 29.- Effects of RAM C-II reentry plasma on 225.7 MHz telemetry antenna. LCP, left circular polarization; RCP, right circular polarization.

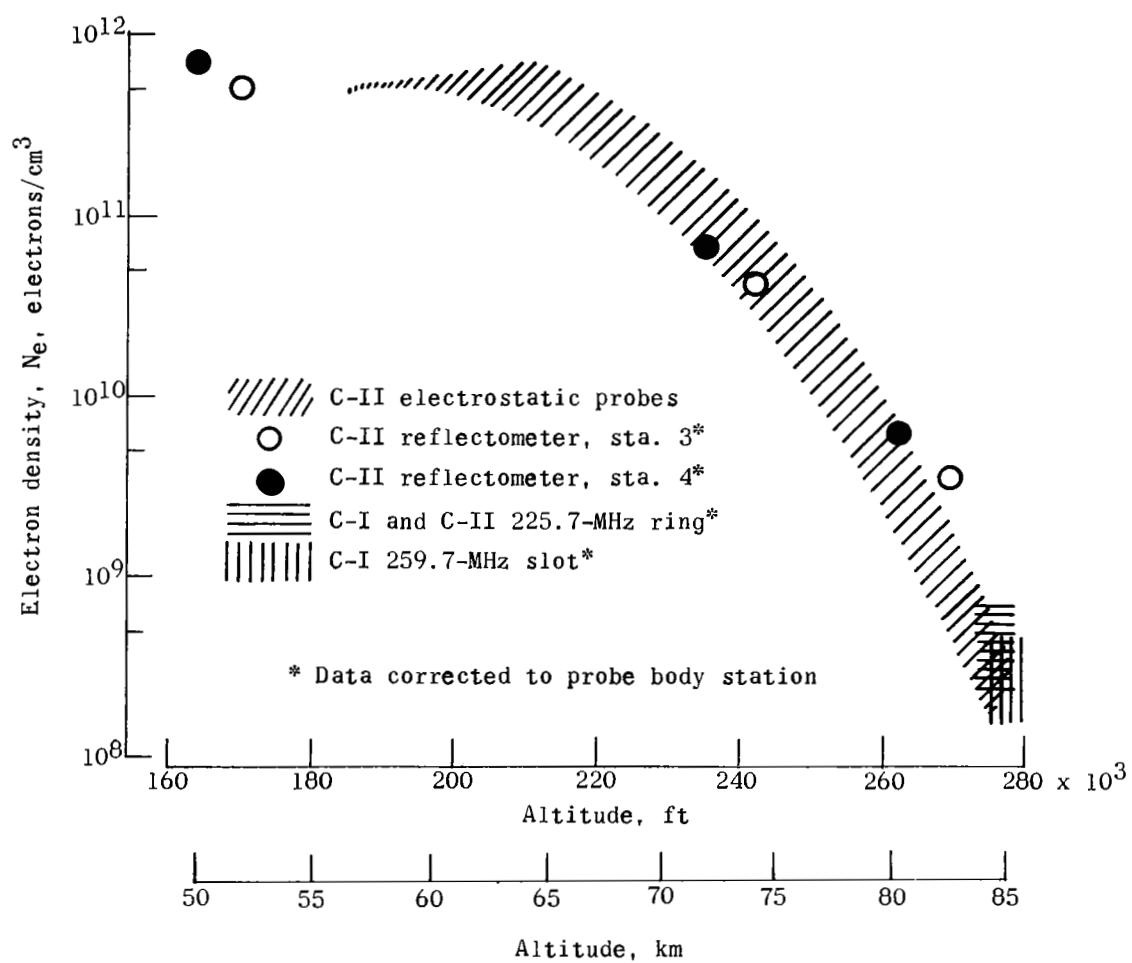


Figure 30.- Comparison of inferred electron densities.

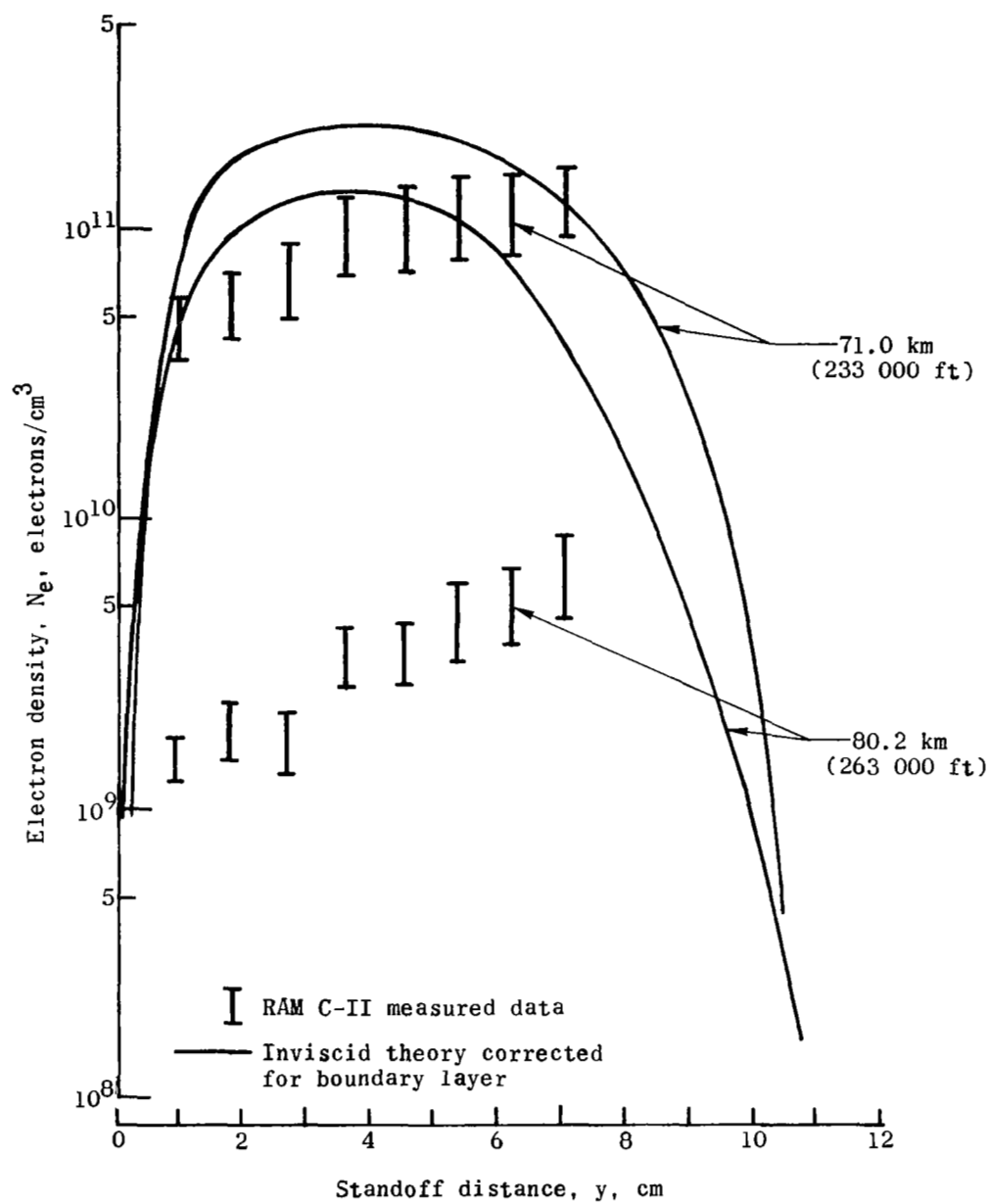


Figure 31.- Comparison of RAM C-II electrostatic probe measured data with theoretical electron density profiles.

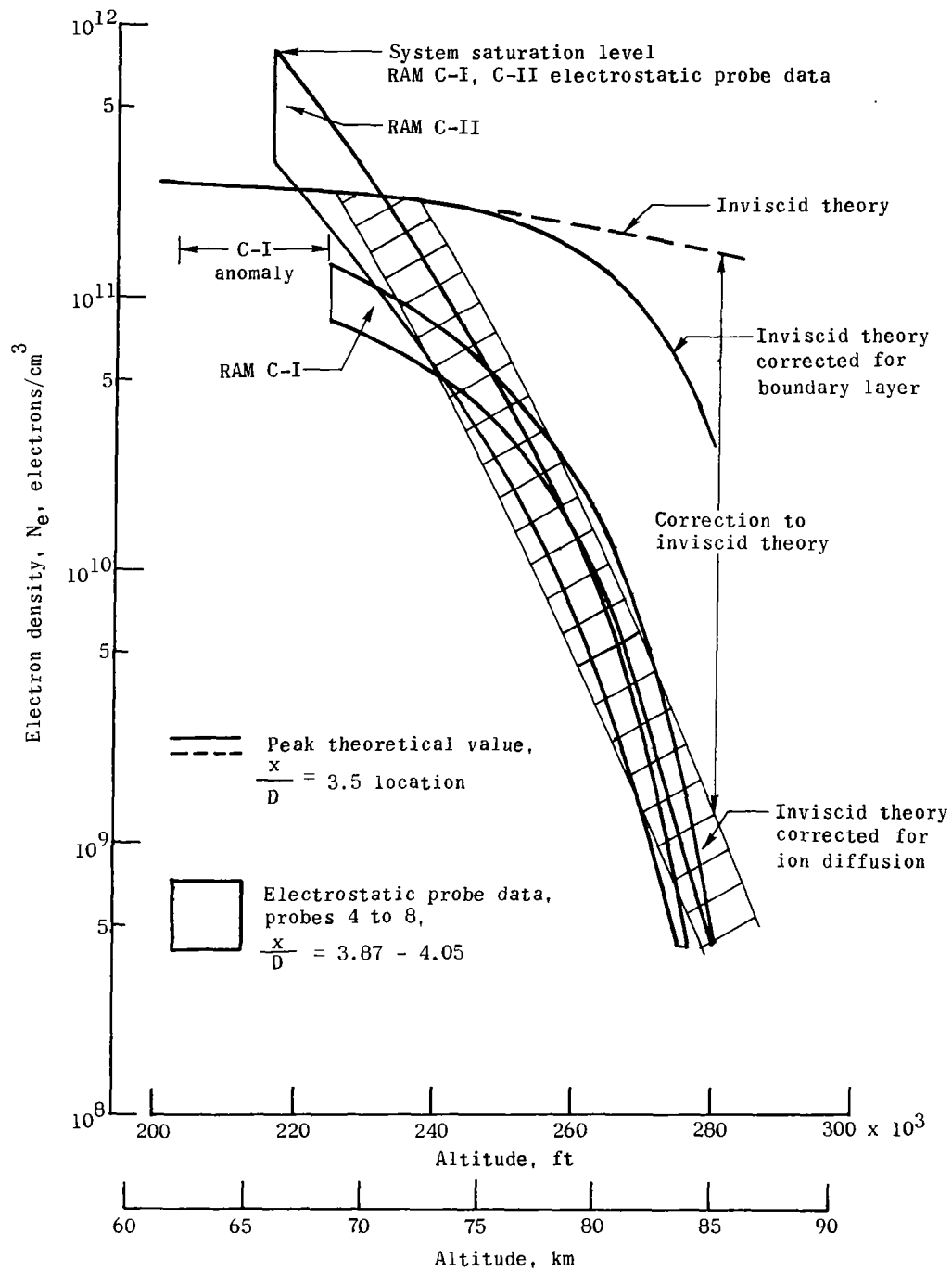


Figure 32.- Comparison of high-altitude electron density at aft body station.

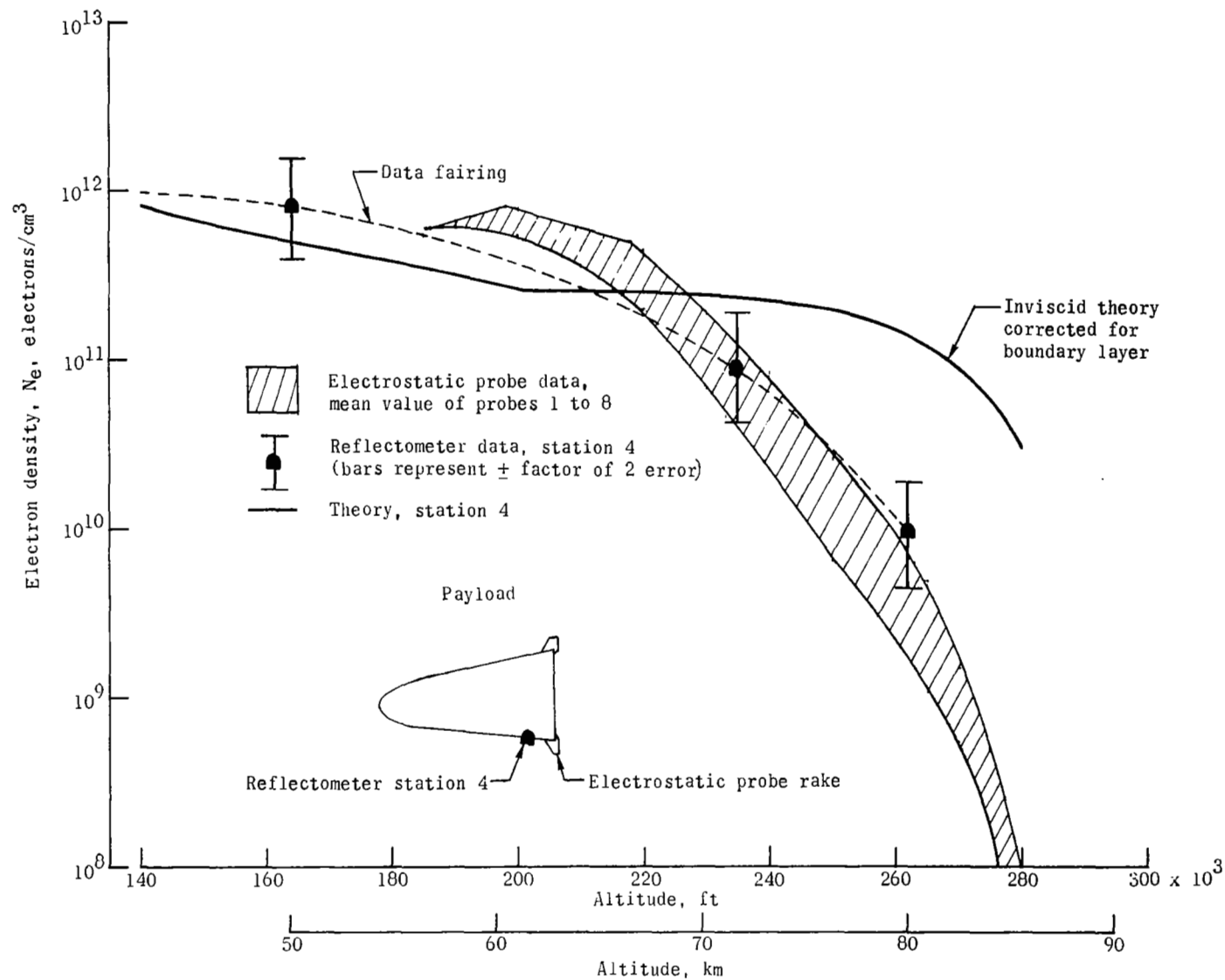


Figure 33.- Comparison of RAM C-II plasma diagnostic measurements with theoretical calculations.

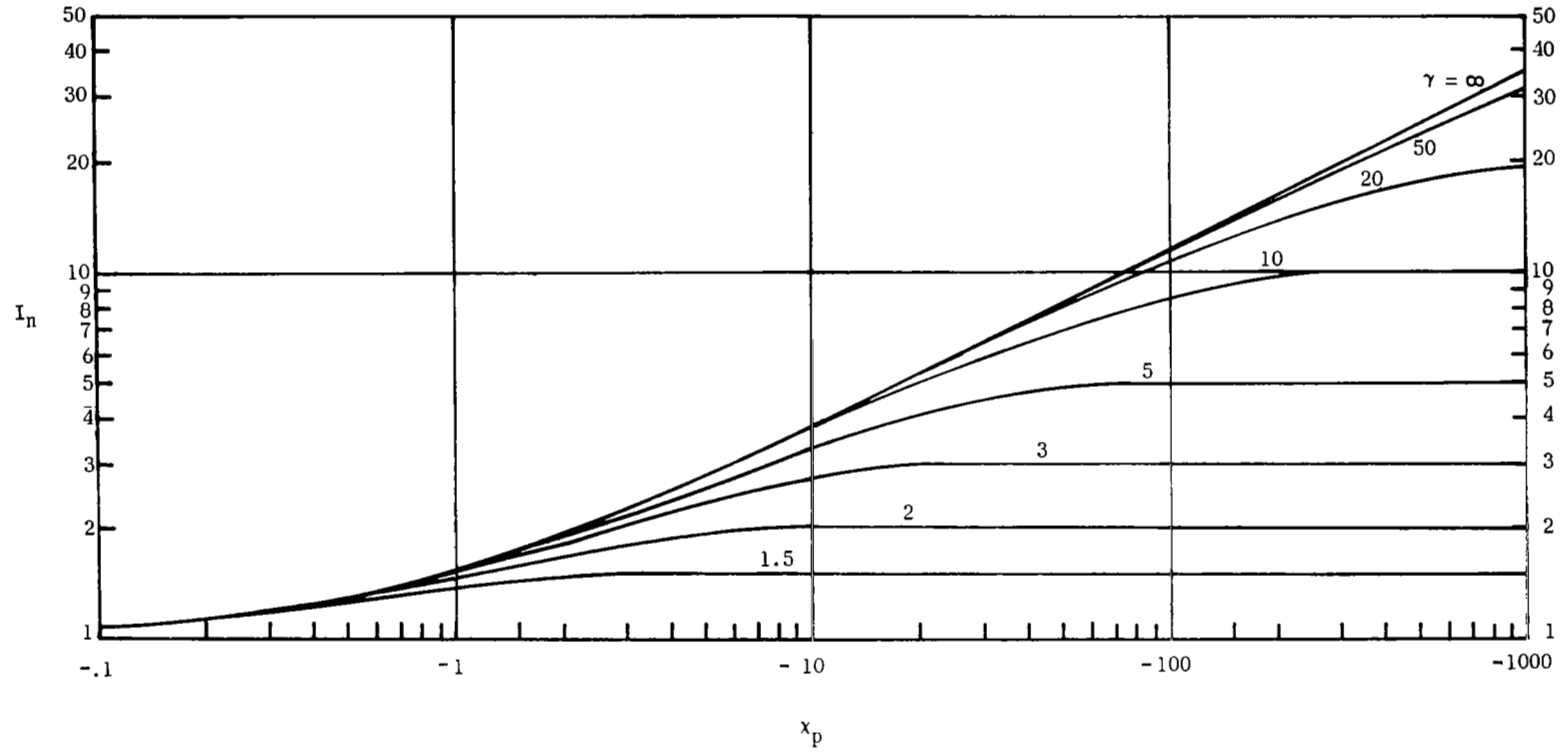


Figure 34.- Variation of normalized probe current with normalized potential difference between probe and plasma for range of γ .

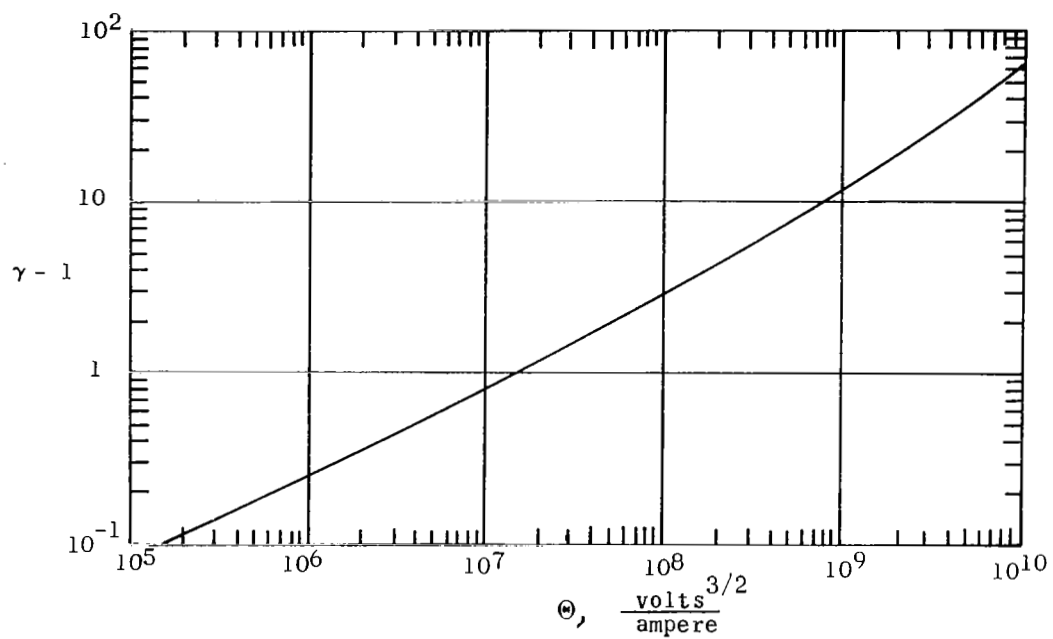


Figure 35.- Inverted form of space-charge-limited diode equation.

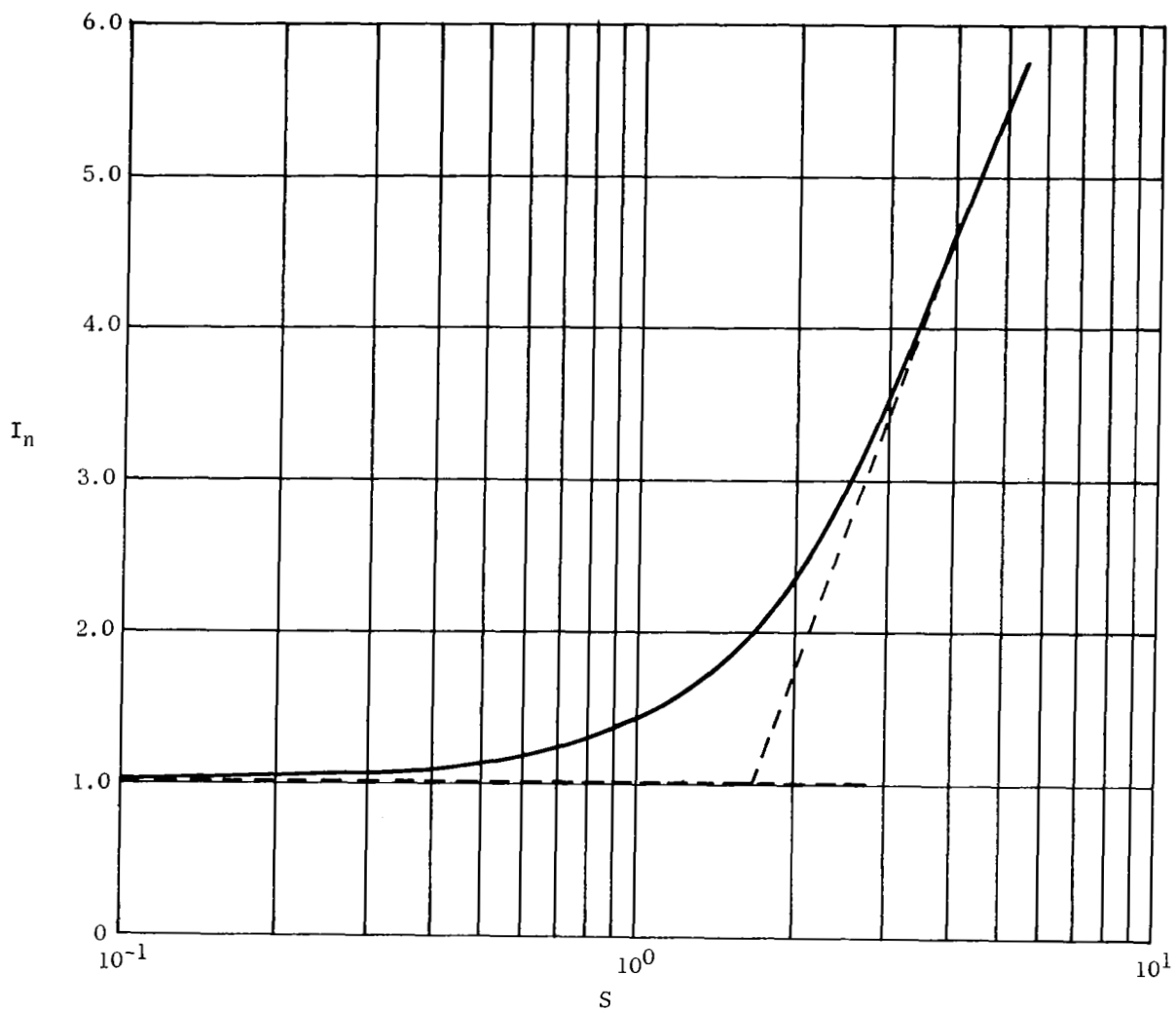


Figure 36.- Normalized current I_n collected by a probe perpendicular to the directed velocity as a function of the ratio S of directed to random velocity. Dashed lines indicate asymptotes.

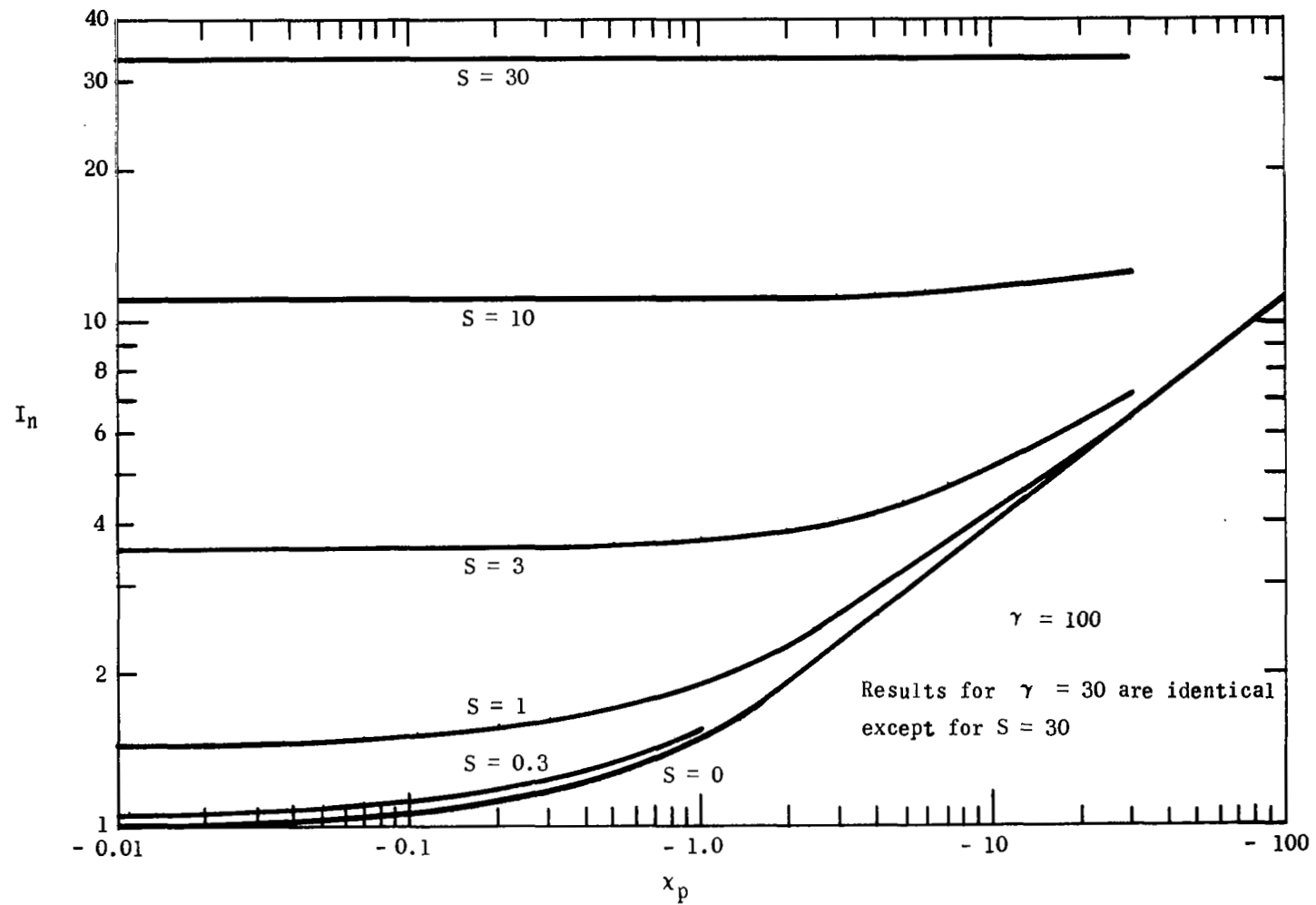


Figure 37.- Variation of normalized current with dimensionless probe potential for various speed ratios at $\gamma = 100$.

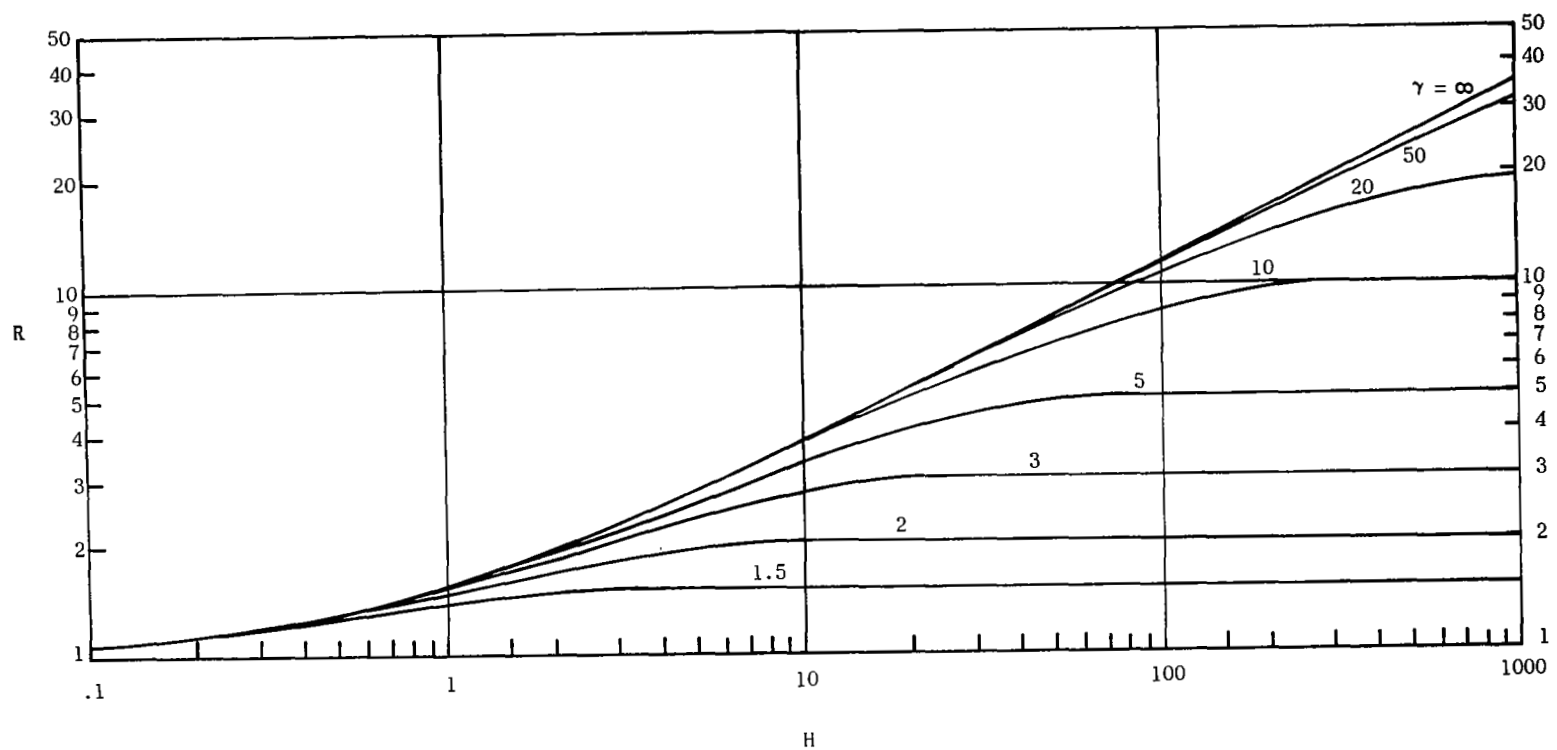


Figure 38.- Normalized probe current R as a function of the ratio of modified potential energy to the kinetic energy H for various values of γ .

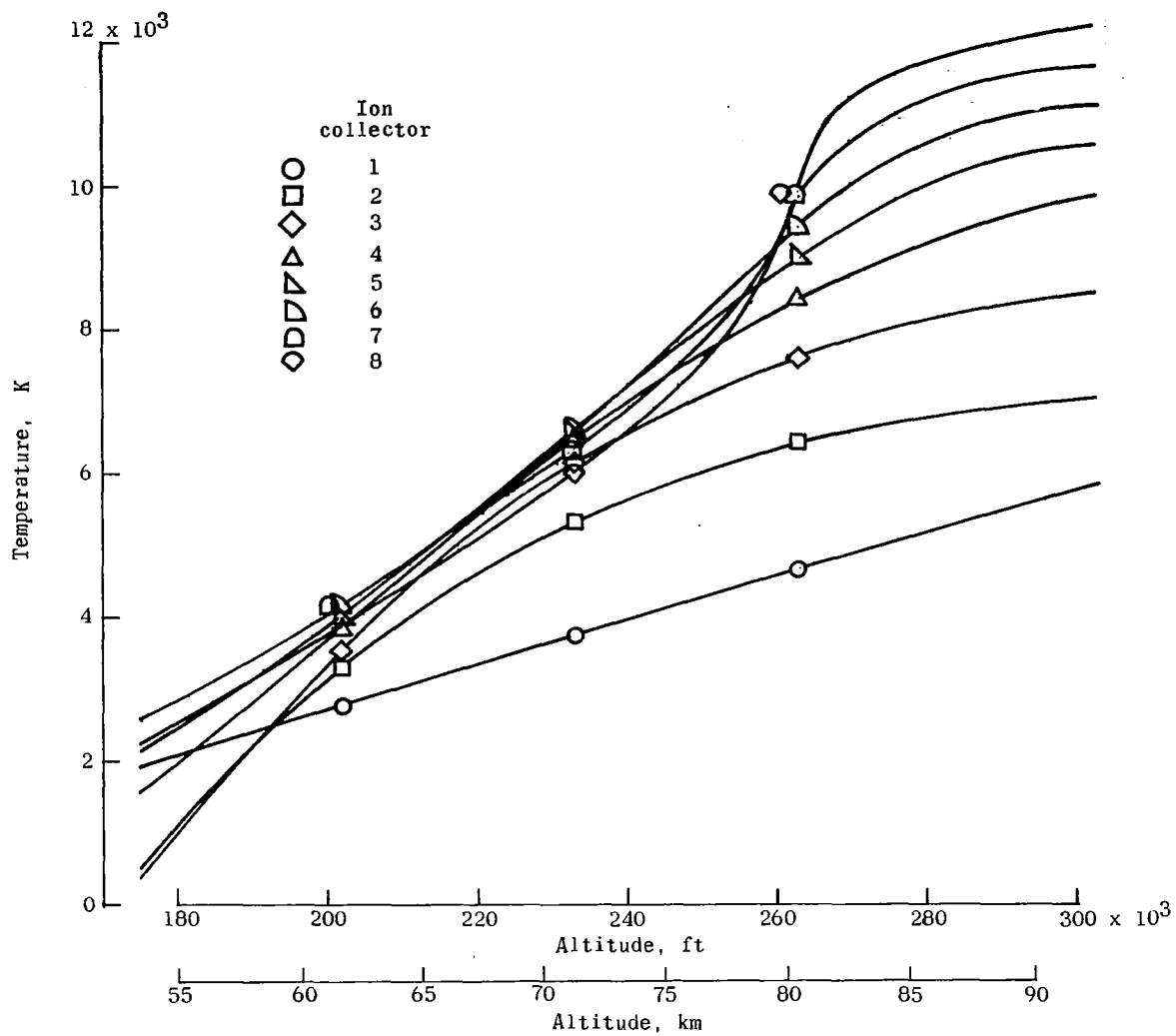


Figure 39. - Computed gas temperature as a function of altitude for electrostatic probe locations.

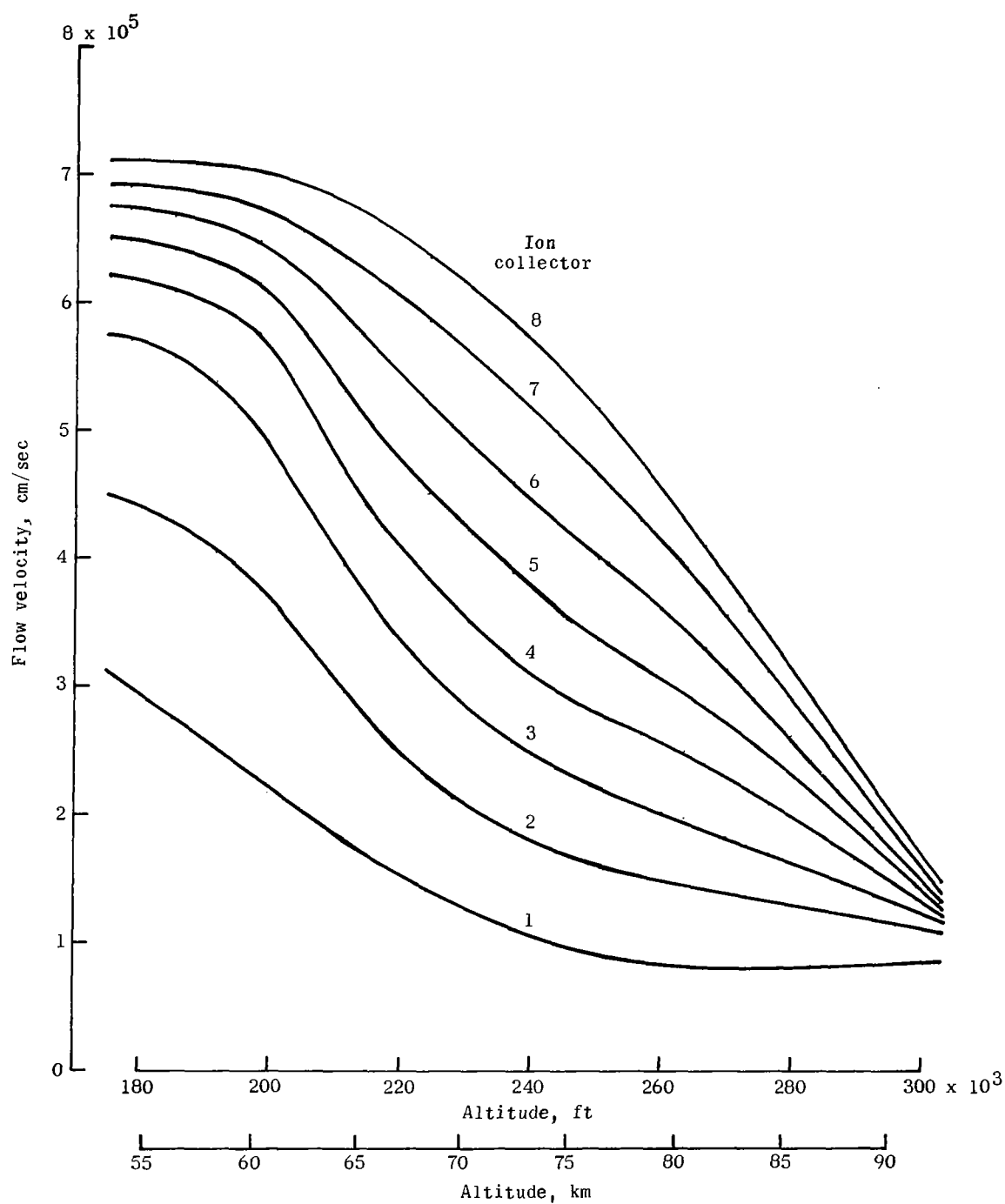
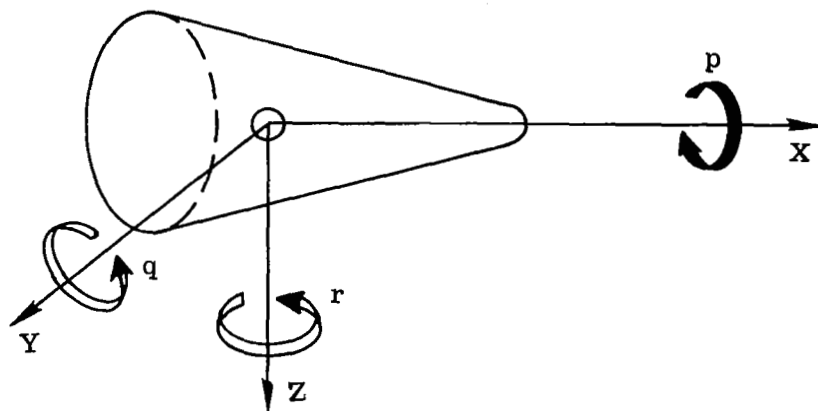
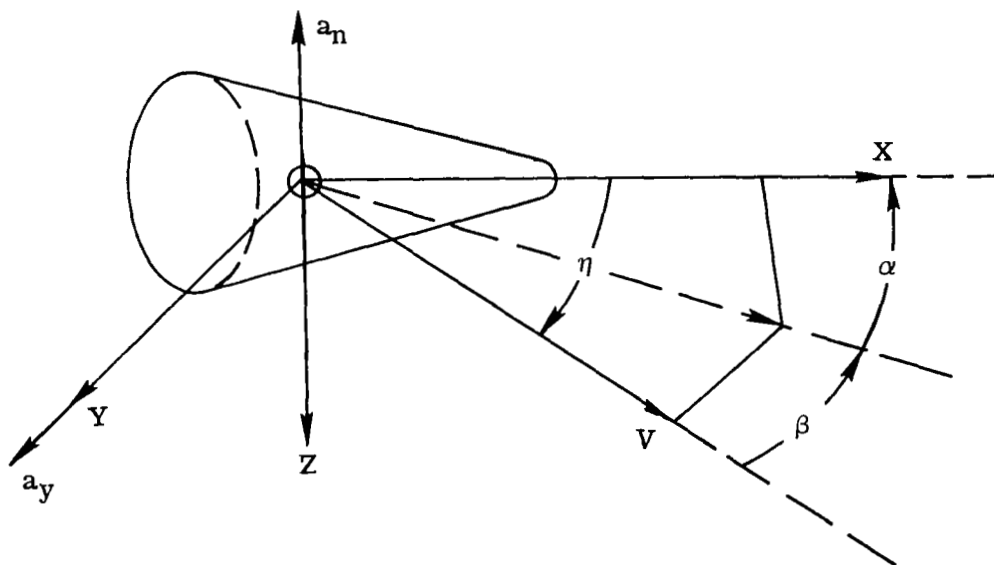


Figure 40.- Computed flow velocity as a function of altitude for electrostatic probe locations.



(a) Illustration of body rotations.



(b) Illustration of orientation with wind axis.

Figure 41.- Spacecraft axis system.

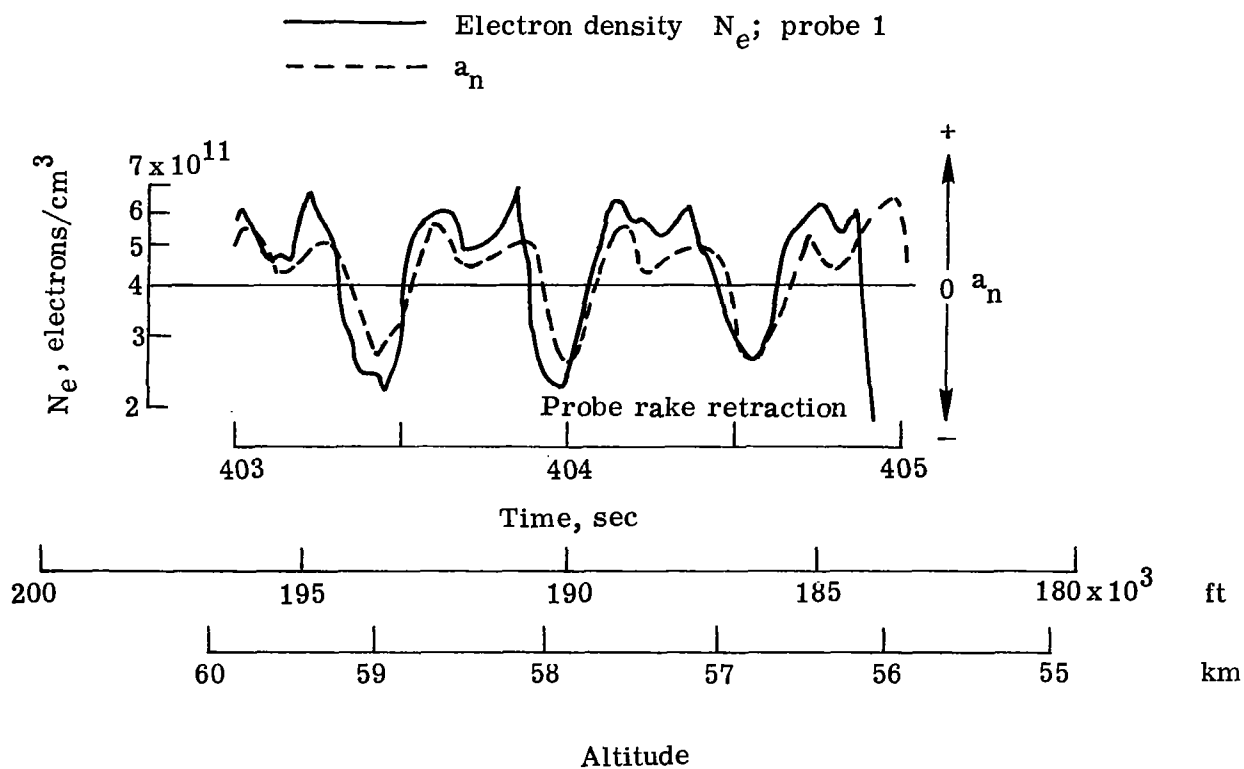


Figure 42.- Correlation of measured electron densities with measured normal acceleration on RAM C-II.

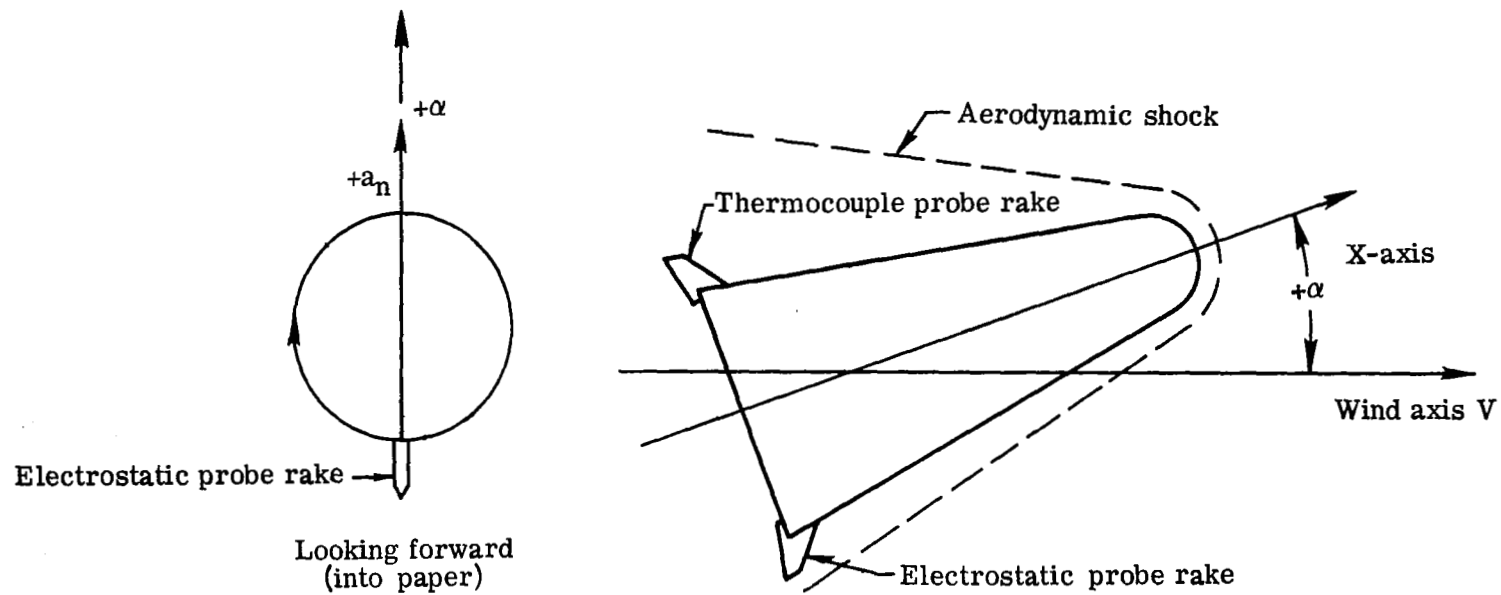


Figure 43.- Locations of probe rakes relative to axes systems.

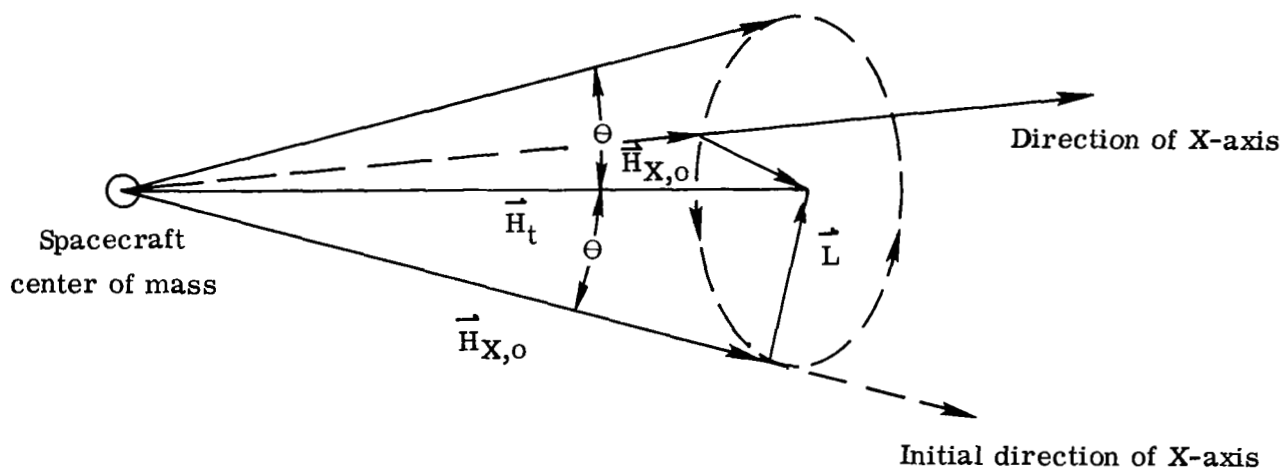
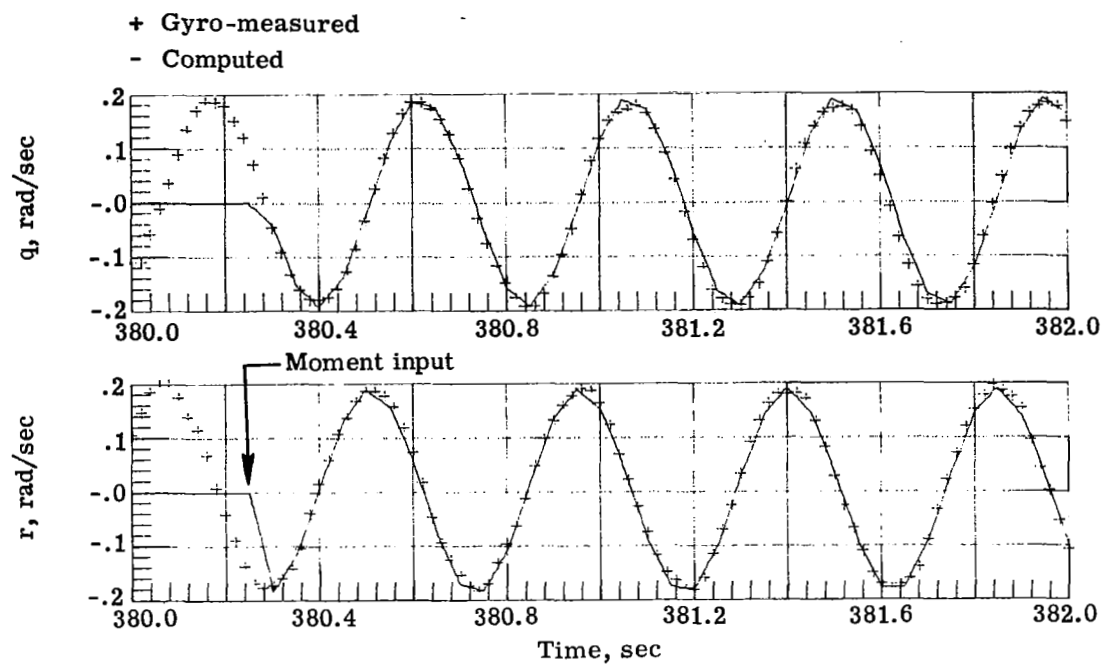
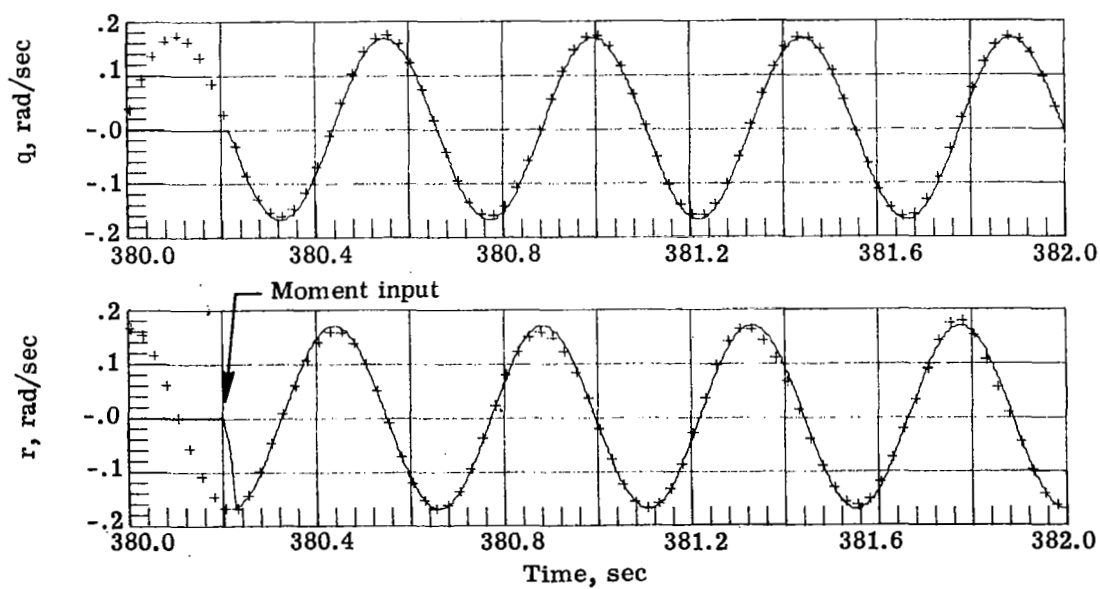


Figure 44.- Spacecraft precession in force-free space.

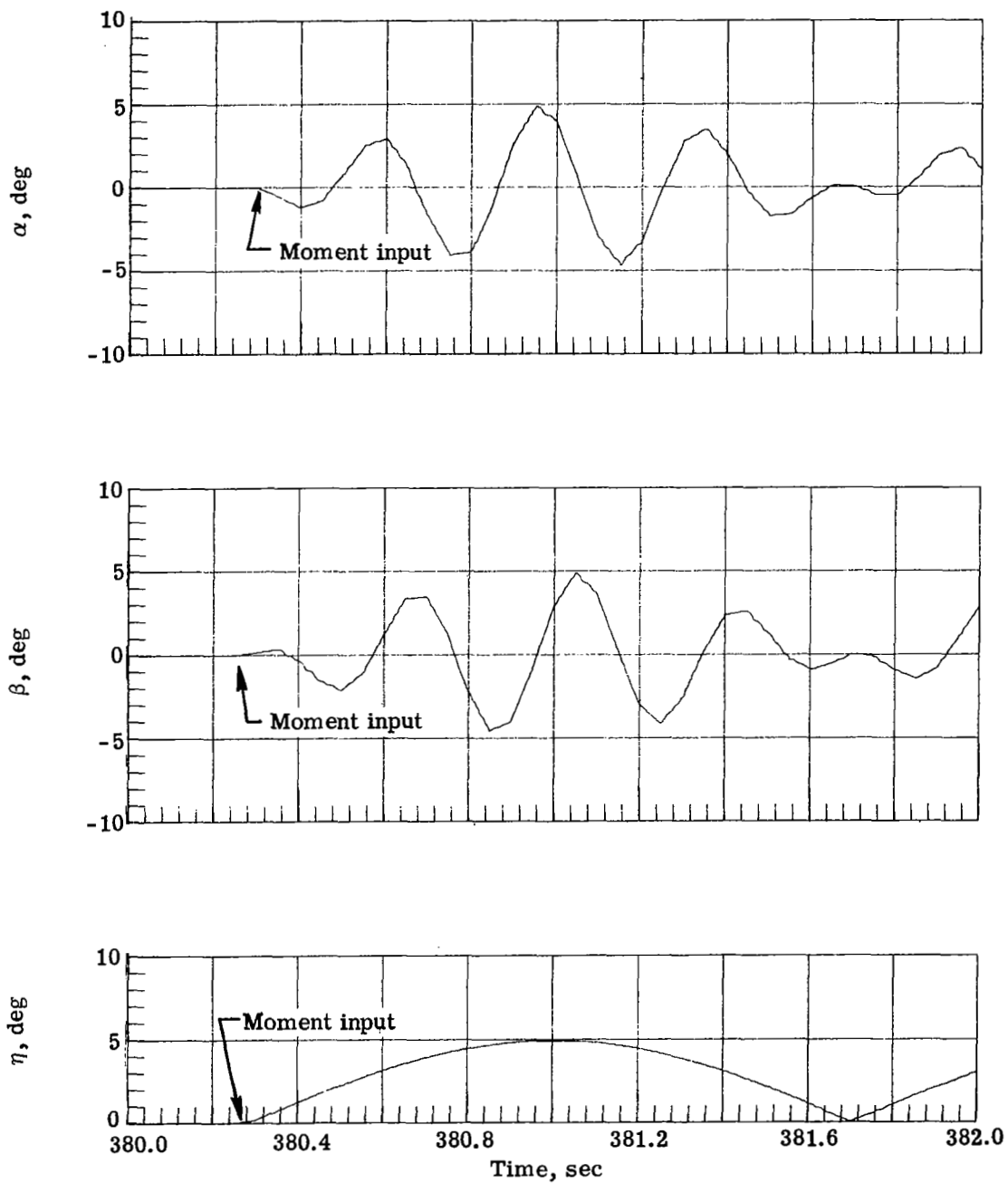


(a) RAM C-I.



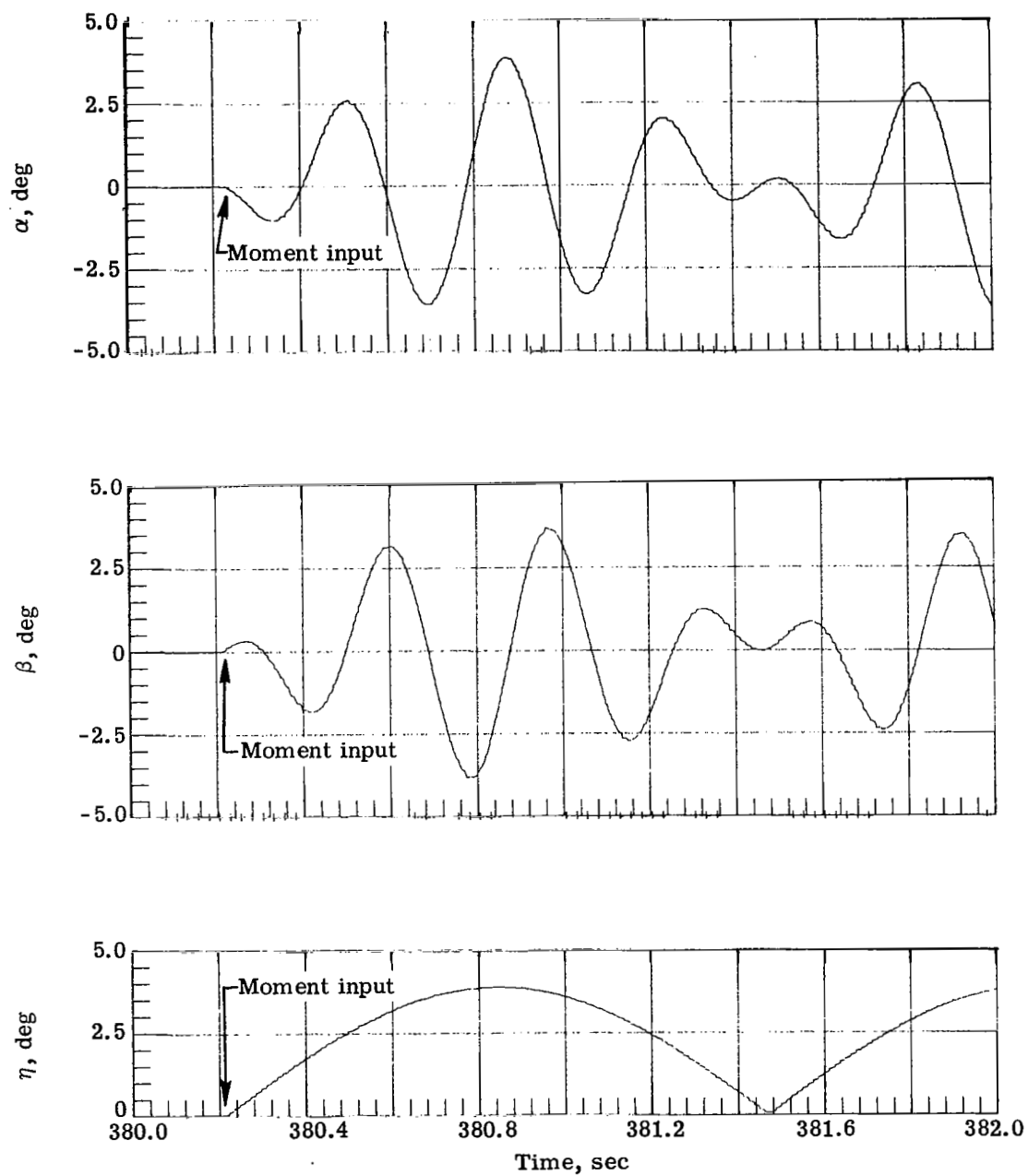
(b) RAM C-II.

Figure 45.- Comparisons of gyro-measured spacecraft rotation rates with computed rotation rates.



(a) RAM C-I.

Figure 46.- Computed characteristic wind angles.



(b) RAM C-II.

Figure 46.- Concluded.